

**WestminsterResearch**

<http://www.westminster.ac.uk/westminsterresearch>

**Interaction of skin cells with skin microbiota**

**Moinipoor, Zeynab**

This is a PhD thesis awarded by the University of Westminster.

© Mrs Zeynab Moinipoor, 2023.

<https://doi.org/10.34737/w41z3>

The WestminsterResearch online digital archive at the University of Westminster aims to make the research output of the University available to a wider audience. Copyright and Moral Rights remain with the authors and/or copyright owners.

# Interaction of Skin Microbiota with Skin Cells

Zeynab Moinipoor

A thesis submitted in the partial fulfilment of the  
requirements of the University of Westminster for the  
degree of Doctor of Philosophy

December 2022

# Abstract

The interaction between skin cells and skin microbiota is complicated and not fully understood. A diverse community of microbes resides on the skin that participates in shaping its physiology. Skin microbiota can modulate skin immunity and barrier, thus, contributing to skin health. Also, the microbiota's imbalance and dysbiosis can cause skin disorders. Yet the mechanisms of function of skin microbiota on skin health and disease are only beginning to be discovered. *Pseudomonas aeruginosa* is one of the leading opportunistic pathogens in chronic wound infections. Biofilm formation of *P. aeruginosa* in the wound area following its attachment to the keratinocytes has a deleterious impact on wound healing. On the other hand, *Staphylococcus epidermidis*, as a skin commensal, has been shown to protect the skin against pathogens. Therefore, this study aims to investigate the effect of skin commensal bacteria on the skin cells and the opportunistic bacteria inhabiting the skin.

The effect of *S. epidermidis* NCTC 11047 supernatant on the biofilm formation, virulence factors production, and quorum sensing network of *P. aeruginosa* strains NCTC 10662 and PAO1 was investigated using a range of colorimetric assays and RT-qPCR. Also, the effect of *S. epidermidis* supernatant on the viability, migration, and proliferation of the human skin keratinocytes (HaCaT cell line) was investigated using scratch and MTT assays. Furthermore, the protective impact of *S. epidermidis* and its supernatant on the skin cells against *P. aeruginosa* infection was explored by co-culturing keratinocytes with the bacterial cells. The co-culture of *S. epidermidis* and *P. aeruginosa* in planktonic and biofilm states was also investigated in order to investigate the interaction of commensal and opportunistic microbes.

*S. epidermidis* supernatant diminished biofilm formation by 68% in NCTC 10662 and 34% in PAO1 ( $P=0.0001$  and  $P=0.002$ , respectively). It also diminished the virulence factor production of *P. aeruginosa* (such as elastase production  $P=0.02$ ) without any impact on its growth through the modulation of the *P. aeruginosa* quorum sensing network. Furthermore, the *S. epidermidis* supernatant improved proliferation of keratinocytes ( $P=0.001$ ). It also increased the re-epithelisation rate of an *in vitro* scratch model wound on a monolayer of keratinocytes in 24 hours ( $P=0.01$ ). *S. epidermidis* in co-culture with *P. aeruginosa* decreased the adhesion of NCTC 10662 ( $P=0.02$ ) and PAO1 ( $P=0.02$ ) to the abiotic surface. However, *S. epidermidis*, during the co-culture formed on keratinocytes, was unable to decrease the adhesion of *P. aeruginosa* to the keratinocytes (biotic surface). With increase in the prevalence of multi-drug resistant pathogens, the discovery and application of molecules from the supernatant of commensals offering anti-virulence properties may be a promising alternative therapy for the healing of infected wounds.

# List of contents

<b>Abstract</b> .....	<b>ii</b>
<b>List of figures</b> .....	<b>vi</b>
<b>List of tables</b> .....	<b>viii</b>
<b>Acknowledgement</b> .....	<b>ix</b>
<b>Author's declaration</b> .....	<b>x</b>
<b>List of abbreviations</b> .....	<b>xi</b>
<b>Chapter 1 Introduction</b> .....	<b>1</b>
<b>1.1 Human skin</b> .....	<b>1</b>
1.1.1 Human skin structure .....	1
1.1.2 Epidermal appendages .....	4
<b>1.2 Skin immune system</b> .....	<b>6</b>
<b>1.3 Skin microbiota</b> .....	<b>9</b>
1.3.1 Host-microbe interaction.....	12
1.3.2 <i>Staphylococcus epidermidis</i> .....	13
<b>1.4 Wound healing</b> .....	<b>17</b>
1.4.1 Stages of wound healing.....	17
1.4.2 Types of wounds .....	22
1.4.2.1 Acute wound .....	22
1.4.2.2 Chronic wound.....	22
1.4.3 The role of growth factors, cytokines, and chemokines in wound healing .....	23
<b>1.5 Wound microbiota</b> .....	<b>25</b>
1.5.1 <i>Pseudomonas aeruginosa</i> .....	27
1.5.1.1 Biofilm formation of <i>P. aeruginosa</i> .....	28
1.5.1.2 Virulence factors in <i>P. aeruginosa</i> .....	32
1.5.1.3 Antibiotics and resistance in <i>P. aeruginosa</i> .....	35
1.5.1.4 Antibiotic resistance mechanisms in <i>P. aeruginosa</i> .....	37
1.5.1.5 Quorum sensing network in <i>P. aeruginosa</i> .....	39
<b>1.6 Key factors involved in the study of wound healing</b> .....	<b>42</b>
1.6.1 Microbial cells.....	42
1.6.2 Human cells .....	43
1.6.3 Extracellular matrix proteins (ECM proteins) .....	44
1.6.4 Chemicals.....	45
<b>Aim and objectives</b> .....	<b>47</b>
<b>Chapter 2 Material and Methods</b> .....	<b>48</b>
<b>2.1 Materials</b> .....	<b>48</b>
2.1.1 Bacterial strains .....	48
2.1.2 Mammalian cell line.....	48
<b>2.2 Bacterial cell culture methods</b> .....	<b>49</b>
2.2.1 Media preparation.....	49
2.2.2 Bacterial culture conditions and inoculum preparation .....	49
2.2.3 Growth curve .....	50
2.2.4 Preparation of <i>S. epidermidis</i> supernatant (SES) .....	51

2.2.5 Protein assay on the SES.....	52
2.2.6 Crystal violet biofilm formation assay .....	53
2.2.7 Extraction of extracellular polymeric substances (EPS) from <i>P. aeruginosa</i> biofilm .....	54
2.2.7.1 Carbohydrate assay on EPS.....	54
2.2.7.2 Protein assay on EPS .....	55
2.2.7.3 eDNA quantification in EPS.....	56
2.2.8 Assessment of <i>P. aeruginosa</i> virulence factors .....	56
2.2.8.1 Pyocyanin quantification .....	56
2.2.8.2 Pyoverdine quantification.....	57
2.2.8.3 Assessment of elastase activity.....	57
2.2.8.4 Motility assay .....	58
2.2.9 Evaluating antibiotics susceptibility in <i>P. aeruginosa</i> .....	58
2.2.10 Evaluating the combined activity of antibiotics and SES on preformed biofilm of <i>P. aeruginosa</i> .....	59
2.2.10.1 Crystal violet assay on preformed biofilm .....	60
2.2.10.2 MTT assay on preformed biofilm .....	60
2.2.11 Accumulation assay .....	60
2.2.12 Planktonic co-culture growth curve.....	61
2.2.13 Biofilm co-culture model set up .....	63
2.2.14 Quantitative Reverse Transcription Polymerase Chain Reaction (RT-qPCR) .....	65
2.2.14.1 RNA extraction and purification.....	65
2.2.14.2 Reverse transcription.....	66
2.2.14.3 Quantitative real-time PCR .....	66
<b>2.3 Mammalian cell culture methods .....</b>	<b>68</b>
2.3.1 Mammalian cell culture conditions and maintenance .....	68
2.3.2 Trypan blue exclusion assay .....	69
2.3.3 Microscopy .....	70
2.3.4 Scratch wound healing assay.....	70
2.3.5 Keratinocytes proliferation assay .....	71
2.3.6 Human cytokine array.....	71
2.3.7 Co-culture of keratinocytes with bacterial cells .....	74
2.3.7.1 Preparation of bacterial cells for co-culture with keratinocytes .....	74
2.3.7.2 Assessment of keratinocytes viability after infection with bacterial cells .....	74
2.3.7.3 Assessment of bacterial cells' adhesion to the keratinocytes .....	75
<b>2.4 Statistical analysis .....</b>	<b>75</b>
<b>Chapter 3 The effect of <i>S. epidermidis</i> supernatant on the biofilm formation and virulence factors of <i>P. aeruginosa</i> .....</b>	<b>76</b>
<b>3.1 Introduction .....</b>	<b>76</b>
<b>3.2 Results .....</b>	<b>77</b>
3.2.1 <i>S. epidermidis</i> growth curve .....	77
3.2.2 Protein concentration in the <i>S. epidermidis</i> supernatant (SES).....	79
3.2.3 Biofilm formation of <i>P. aeruginosa</i> in the presence of SES .....	79
3.2.4 Growth curve of <i>P. aeruginosa</i> in the presence of SES.....	81
3.2.5 The effect of SES on extracellular polymeric substances (EPS) of <i>P. aeruginosa</i> biofilm .....	83
3.2.6 The effect of SES on the virulence factors production of <i>P. aeruginosa</i> .....	85
3.2.6.1 The impact on motility of <i>P. aeruginosa</i> .....	85
3.2.6.2 The impact on the enzyme, toxin, and pigment production of <i>P. aeruginosa</i> .....	89
3.2.7 Antibiotic susceptibility of <i>P. aeruginosa</i> in the presence of SES .....	92
3.2.7.1 Evaluating the combined activity of antibiotics and SES on preformed biofilm of <i>P. aeruginosa</i> .....	94
3.2.7.2 Evaluating the effect of SES on the efflux pumps activity of <i>P. aeruginosa</i> .....	99
3.2.8 Evaluating the effect of SES on the expression of quorum sensing genes in <i>P. aeruginosa</i> .....	100
<b>3.3 Discussion .....</b>	<b>103</b>

<b>Chapter 4 Investigation of <i>P. aeruginosa</i> and <i>S. epidermidis</i> co-culture in planktonic and biofilm state .....</b>	<b>109</b>
<b>4.1 Introduction .....</b>	<b>109</b>
<b>4.2 Results .....</b>	<b>110</b>
4.2.1 Co-culture of <i>P. aeruginosa</i> and <i>S. epidermidis</i> in the planktonic state .....	110
4.2.2 Co-culture of <i>P. aeruginosa</i> and <i>S. epidermidis</i> in biofilm state .....	117
4.2.3 Antibiotic susceptibility of <i>P. aeruginosa</i> when is co-cultivated with <i>S. epidermidis</i> .....	126
4.2.3.1 Evaluating <i>P. aeruginosa</i> efflux pumps activity in the co-culture of <i>P. aeruginosa</i> and <i>S. epidermidis</i> .....	130
<b>4.3 Discussion .....</b>	<b>131</b>
<b>Chapter 5 Investigation of the effect of <i>S. epidermidis</i> and its supernatant on protecting keratinocytes against <i>P. aeruginosa</i> infection .....</b>	<b>136</b>
<b>5.1 Introduction .....</b>	<b>136</b>
<b>5.2 Results .....</b>	<b>137</b>
5.2.1 Investigation of the effect of SES on keratinocytes .....	137
5.2.1.1 Viability of keratinocytes .....	137
5.2.1.2 Morphology assessment by microscopy .....	138
5.2.1.3 The effect of SES on keratinocyte wound healing .....	139
5.2.1.4 The effect of SES on keratinocytes proliferation .....	141
5.2.1.5 The effect of SES on the cytokine production of keratinocytes .....	142
5.2.2 Investigation of the protective effect of <i>S. epidermidis</i> and its supernatant on keratinocytes against <i>P. aeruginosa</i> infections .....	145
<b>5.3 Discussion .....</b>	<b>154</b>
<b>Chapter 6 Overall discussion .....</b>	<b>159</b>
<b>Chapter 7 Conclusion and future work .....</b>	<b>164</b>
<b>7.1 Conclusion.....</b>	<b>164</b>
<b>7.2 Future work.....</b>	<b>166</b>
<b>References .....</b>	<b>168</b>

# List of figures

<b>Figure 1.1</b> Representation of different layers of the epidermis (Kabashima <i>et al.</i> , 2019)...	4
<b>Figure 1.2</b> The phylogenetic tree from a metagenomic approach gives a comprehensive detail of the microbial community (Taken from Chen and Tsao, 2013).....	11
<b>Figure 1.3</b> Wound healing phases in normal skin.....	21
<b>Figure 1.4</b> Biofilm formation in the chronic wound.....	31
<b>Figure 1.5</b> Virulence mechanisms in <i>P. aeruginosa</i> (Taken from Lee and Zang, 2015).....	34
<b>Figure 1.6</b> Quorum sensing system in <i>P. aeruginosa</i> and regulation of virulence factors.	41
<b>Figure 2.1</b> Protein standard curve to measure protein concentration in SES sample. ....	53
<b>Figure 2.2</b> Glucose standard curve to measure carbohydrate concentration in EPS sample. .....	55
<b>Figure 2.3</b> Protein standard curve to measure protein concentration in EPS sample. ....	56
<b>Figure 2.4</b> Schematic illustration of biofilm co-culture set-up.....	64
<b>Figure 2.5</b> Schematic picture for coordination of cytokines on the nitrocellulose membrane of Human Cytokine Array kit.....	73
<b>Figure 3.1</b> Growth curve of <i>S. epidermidis</i> in TSB. <i>S. epidermidis</i> was grown in 50 ml TSB in a 250 ml shaking flask at 37°C and 180 rpm for 24 hours. ....	78
<b>Figure 3.2</b> Correlation between the number of viable bacterial cells (CFU/ml) in the culture of <i>S. epidermidis</i> and the OD of the culture measured at 600 nm.....	78
<b>Figure 3.3</b> Biofilm formation of <i>P. aeruginosa</i> NCTC 10662 (A), and <i>P. aeruginosa</i> PAO1 (B) in the presence and absence of SES.....	80
<b>Figure 3.4</b> Growth curve of <i>P. aeruginosa</i> NCTC 10662 (A), and <i>P. aeruginosa</i> PAO1 (B) in the presence and absence of SES.....	82
<b>Figure 3.5</b> Quantification of EPS components, eDNA (A), protein (B), and carbohydrate (C) in the presence and absence of SES in two strains of <i>P. aeruginosa</i> PAO1 and NCTC 10662. .....	84
<b>Figure 3.6</b> The impact of SES on swarming, swimming, and twitching motility of <i>P. aeruginosa</i> NCTC 10662.....	86
<b>Figure 3.7</b> The impact of SES on swarming, swimming, and twitching motility of <i>P. aeruginosa</i> PAO1.....	87
<b>Figure 3.8</b> Motility of <i>P. aeruginosa</i> PAO1 and NCTC 10662 in the absence and presence of SES.....	88
<b>Figure 3.9</b> Quantification of virulence factors released from <i>P. aeruginosa</i> NCTC 10662 and PAO1 in the presence and absence (control) of SES.....	90
<b>Figure 3.10</b> Virulence factors gene expression of <i>P. aeruginosa</i> in the presence and absence of SES.....	91
<b>Figure 3.11</b> The effect of SES on antibiotic susceptibility of the established biofilm of <i>P. aeruginosa</i> NCTC 10662.....	95
<b>Figure 3.12</b> The effect of SES on antibiotic susceptibility of established biofilm of <i>P. aeruginosa</i> PAO1.....	97
<b>Figure 3.13</b> Fluorometric accumulation assay of <i>P. aeruginosa</i> NCTC 10662 (A) and PAO1 (B) in the presence of SES, compared to the untreated control.....	100
<b>Figure 3.14</b> Quorum sensing gene expression in <i>P. aeruginosa</i> NCTC 10662 in the absence and presence of SES. ....	101

<b>Figure 3.15</b> Quorum sensing gene expression in <i>P. aeruginosa</i> PAO1 in the absence and presence of SES. ....	102
<b>Figure 4.1</b> Planktonic growth of <i>P. aeruginosa</i> NCTC 10662 and <i>S. epidermidis</i> in mono- and co-culture. ....	111
<b>Figure 4.2</b> Competition growth profile between <i>P. aeruginosa</i> NCTC 10662 and <i>S. epidermidis</i> in co-culture. ....	113
<b>Figure 4.3</b> Planktonic growth of <i>P. aeruginosa</i> PAO1 and <i>S. epidermidis</i> in mono- and co-culture. ....	114
<b>Figure 4.4</b> Competition growth profile between <i>P. aeruginosa</i> PAO1 and <i>S. epidermidis</i> in co-culture. ....	116
<b>Figure 4.5</b> Biofilm growth of <i>P. aeruginosa</i> NCTC 10662 in co-culture with <i>S. epidermidis</i> (SE) when NCTC 10662 was added to the 24-hour preformed biofilm of <i>S. epidermidis</i> . ....	119
<b>Figure 4.6</b> Biofilm growth of <i>P. aeruginosa</i> NCTC 10662 in co-culture with <i>S. epidermidis</i> (SE) when <i>S. epidermidis</i> was added to the 24-hour preformed biofilm of NCTC 10662. ....	120
<b>Figure 4.7</b> Biofilm growth of <i>P. aeruginosa</i> NCTC 10662 in co-culture with <i>S. epidermidis</i> (SE) when NCTC 10662 and <i>S. epidermidis</i> were co-cultivated at the same time. ....	121
<b>Figure 4.8</b> Biofilm growth of <i>P. aeruginosa</i> PAO1 in co-culture with <i>S. epidermidis</i> (SE) when PAO1 was added to the 24-hour preformed biofilm of <i>S. epidermidis</i> . ....	123
<b>Figure 4.9</b> Biofilm growth of <i>P. aeruginosa</i> PAO1 in co-culture with <i>S. epidermidis</i> (SE) when <i>S. epidermidis</i> was added to the 24-hour preformed biofilm of PAO1. ....	124
<b>Figure 4.10</b> Biofilm growth of <i>P. aeruginosa</i> PAO1 in co-culture with <i>S. epidermidis</i> (SE) when PAO1 and <i>S. epidermidis</i> were co-cultivated at the same time. ....	125
<b>Figure 4.11</b> Fluorometric accumulation assay of <i>P. aeruginosa</i> NCTC 10662 (A) and PAO1 (B) in their mono-culture and co-culture with <i>S. epidermidis</i> . ....	130
<b>Figure 5.1</b> The viability of keratinocytes in the absence and presence of SES. ....	137
<b>Figure 5.2</b> The morphology of the keratinocytes was assessed using an EVOS microscope. ....	138
<b>Figure 5.3</b> Keratinocytes' re-epithelisation during wound healing in the presence and absence of bacterial cultures supernatants. ....	140
<b>Figure 5.4</b> Proliferation of keratinocytes in the presence and absence of SES. ....	141
<b>Figure 5.5</b> Representative image of nitrocellulose membranes of Human Cytokine Array and the detected cytokines and chemokines present in the keratinocyte's supernatant. ....	143
<b>Figure 5.6</b> Cytokines and chemokines detected in the supernatant of keratinocytes treated or untreated with SES, spotted by Proteome Profiler™ Human Cytokine Array. ....	144
<b>Figure 5.7</b> Infection of keratinocytes with <i>P. aeruginosa</i> NCTC 10662. ....	146
<b>Figure 5.8</b> Infection of keratinocytes with <i>P. aeruginosa</i> NCTC 10662. ....	148
<b>Figure 5.9</b> Infection of keratinocytes with <i>P. aeruginosa</i> NCTC 10662. ....	149
<b>Figure 5.10</b> Infection of keratinocytes with <i>P. aeruginosa</i> PAO1. ....	150
<b>Figure 5.11</b> Infection of keratinocytes with <i>P. aeruginosa</i> PAO1. ....	151
<b>Figure 5.12</b> Infection of keratinocytes with <i>P. aeruginosa</i> PAO1. ....	152



# List of tables

<b>Table 1.1</b> Toll-like receptors as pattern recognition receptors and their ligands. TLR10 ligand is unknown. ....	8
<b>Table 1.2</b> Antibiotics that have been used to treat <i>P. aeruginosa</i> infections .....	36
<b>Table 2.1</b> Media and their components used in this study. ....	50
<b>Table 2.2</b> Standard protein solution used to make a standard curve. ....	52
<b>Table 2.3</b> Reverse transcription master mix composition.....	66
<b>Table 2.4</b> The primers that were used in this study (Kalgudi <i>et al.</i> , 2021).....	67
<b>Table 2.5</b> Cell culture media and reagents used in this study.....	68
<b>Table 2.6</b> List of detectable cytokines using Human Cytokine Array kit and their coordination on the nitrocellulose membrane.....	73
<b>Table 3.1</b> Protein concentration in each SES sample at different stages of growth. ....	79
<b>Table 3.2</b> Susceptibility of <i>P. aeruginosa</i> to antibiotics tetracycline, gentamicin, and ciprofloxacin alone and in combination with SES. ....	93
<b>Table 4.1</b> Antibiotic susceptibility of <i>P. aeruginosa</i> NCTC 10662 and <i>S. epidermidis</i> in a co-culture. ....	127
<b>Table 4.2</b> Antibiotic susceptibility of <i>P. aeruginosa</i> PAO1 and <i>S. epidermidis</i> in a co-culture. ....	129
<b>Table 5.1</b> The summary of the protective impact of <i>S. epidermidis</i> and its supernatant on <i>P. aeruginosa</i> infected keratinocytes.....	153

# Acknowledgement

Firstly, I would like to express my sincere appreciation to my Director of Studies, Prof. Tajalli Keshavarz, for his incredible support and supervision throughout my studies. His experience, patience and guidance helped me enormously to overcome the challenges I faced during my PhD. It was an honour to be part of his team. I would also like to thank Dr. John Murphy and Prof. Mohammed Gulrez Zariwala, my second supervisors, for their invaluable insights and encouragement.

I would like to thank all my friends and colleagues in the lab and office at the University of Westminster, whose advice and support encouraged me every day. I'm also grateful to the technical team at the School of Life Sciences for being immensely kind and supportive.

I am deeply grateful to my parents for their presence, love, and compassion and to my brothers and their families for helping me to find confidence in myself. And most importantly, to my husband for his unconditional support and love and for believing in me when I needed it the most.

I couldn't have gone through the four years of PhD without your kind and loving presence.

To women all over the world, especially Iranian women, who their resilience inspire me to be brave, strong, and proud of being a woman.

# Author's declaration

I, Zeynab Moinipoor, declare that the work presented in this thesis is my own and was carried out in accordance with the guidelines and regulations of the University of Westminster. I confirm where information has been obtained from other sources, it is indicated in this thesis.

Zeynab Moinipoor

December 2022

## List of abbreviations

3-oxo-C12-HSL	N-3-oxo-dodecanoyl-homoserine lactone
6-HAP	6-N-hydroxyaminopurine
ABC	ATP binding cassette
AHL	acyl homoserine lactone
AI	autoinducer
AIDS	acquired immune deficiency syndrome
AMP	antimicrobial peptide
ANOVA	analysis of variance
AP	alkaline protease
AP-1	activator protein 1
ATCC	American type culture collection
AtIE	autolysin proteins
ATP	adenosine triphosphate
BSA	bovine serum albumin
C4-HSL	N-butanoyl-homoserine lactone
cDNA	complementary DNA
CFU	colony forming units
CI	competitive index
CoNS	coagulase-negative staphylococci
COVID-19	coronavirus disease 2019
CXCL	C-X-C chemokine ligand
CXCR	C-X-C chemokine receptor
DAMP	damage-associated molecular patterns
DMEM	Dulbecco's modified eagle medium
DMSO	dimethyl sulfoxide
DNA	deoxyribonucleic acid
DNase	deoxyribonuclease
DPBS	Dulbecco's phosphate buffered saline
ECR	elastin Congo red
ECM	extracellular matrix
eDNA	extracellular DNA
EDTA	ethylenediaminetetraacetic acid
eEF-2	eukaryotic elongation factor-2
EGF	epidermal growth factor
ELISA	enzyme-linked immunosorbent assay
EPS	extracellular polymeric substances
ESCMID	European Society of Clinical Microbiology and Infectious Diseases
EUCAST	European Committee for Antimicrobial Susceptibility Testing
FBS	foetal bovine serum

FGF	fibroblast growth factor
FISH	fluorescence in situ hybridisation
HaCaT	human immortalised keratinocyte
HBD	human $\beta$ -defensin
HCN	hydrogen cyanide
HHQ	4-hydroxy-2-heptylquinoline
HMGB	high-mobility group protein box 1
HQNO	2-heptyl-4-quinolone N-oxide
HRP	horseradish peroxidase
ICAM-1	intercellular adhesion molecule 1
IFN	Interferon
IGF	insulin growth factor
IL	interleukin
ILC	innate lymphoid cells
IQS	integrated quorum sensing
IRF	interferon regulatory factor
l	litre
LB	Luria Bertani
LPS	lipopolysaccharides
LTA	lipoteichoic acid
MAPK	mitogen-activated protein kinase
MATE	multidrug and toxic efflux
MBC	minimum bactericidal concentration
MF	major facilitator
mg	milligram
MHA	Muller Hinton agar
MHB	Muller Hinton broth
MIC	minimum inhibitory concentration
MIF	macrophage migration inhibitory factor
ml	millilitre
mM	millimolar
MMP	metalloproteinase
MOI	multiplicity of infection
MTT	3-(4, 5-dimethylthiazol-2-yl)-2, 5-diphenyltetrazolium bromide
NA	nutrient agar
NB	nutrient broth
NCTC	national collection of type cultures
NF- $\kappa$ B	nuclear factor-kappa B
NLR	NOD-like receptors
nm	nanometre
NOD	nucleotide oligomerization domain

OD	optical density
P IV	Protease IV
PAAP	<i>P. aeruginosa</i> aminopeptidase
PAI-1	plasminogen activator inhibitor-1
PAMP	pathogens-associated molecular patterns
PBS	phosphate buffer saline
PCR	Polymerase Chain Reaction
PDGF	platelet-derived growth factor
PIA	Polysaccharide intercellular adhesin
PNAG	poly- $\beta$ (1-6)-N-acetylglucosamine
PQS	<i>Pseudomonas</i> quinolone signal
PRR	pattern recognition receptors
PSM	phenol soluble modulins
RIR	relative increase ratio
RNA	ribonucleic acid
RNase-7	ribonuclease 7
RND	resistance-nodulation-division
ROS	reactive oxygen species
rpm	revolutions per minutes
RPMI	Roswell Park Memorial Institute
rRNA	ribosomal RNA
RT-qPCR	quantitative reverse transcription polymerase chain reaction
SCV	small colony variant
SE	<i>S. epidermidis</i>
SEM	standard error of the mean
SES	<i>S. epidermidis</i> supernatant
SMR	small multidrug resistance
SSP	staphylococcal surface proteins
TA	teichoic acid
TGF	transforming growth factor
TGF	transforming growth factors
TLR	toll-like receptors
TNF	tumour necrosis factors
TRI	total RNA isolation
T <sub>RM</sub>	resident memory T cells
TSA	tryptone soy agar
TSB	tryptone soy broth
UV	ultraviolet
VEGF	vascular endothelial growth factor
$\mu$	micro

# Chapter 1 Introduction

## 1.1 Human skin

The skin is a complex and dynamic organ with a unique structure, and it has the capacity to grow and restore itself. One of the important roles of the skin is to protect the inner body from external assaults such as ultraviolet radiation, dehydration, chemical agents, and pathogen invasion. The skin controls body temperature and moisture by regulating water evaporation through sweat glands, which also acidify the skin, making conditions unfavourable for the growth of certain pathogens (Kolarsick *et al.*, 2011). Among the essential roles of the skin is the synthesis of vitamin D from sunlight, which is necessary for the normal growth of bones and the normal function of the immune system (Fitzpatrick *et al.*, 2012). Alongside the chemical and physical barrier that the skin makes for the body is the immune barrier, which is comprised of both adaptive and innate immune cells residing in the skin. The immune defence is distributed throughout the skin and is in constant connection with other epithelial cells to orchestrate the cutaneous behaviour and homeostasis. A well-balanced cutaneous barrier is a prerequisite to the maintenance of body integrity and health. The importance of this function can be observed in people with defective skin, like in burn victims who are most at risk of infection (Proksch *et al.*, 2008).

### 1.1.1 Human skin structure

The skin is one of the largest organs of the body, constituting 15% of the body weight. It has three major layers, which from outside to inside, are: the epidermis, the dermis, and the hypodermis or subcutaneous tissue. The thickness of the skin varies throughout the body, and based on the geographical location, it can change between 0.05 mm thick (eyelid) to 1.5 mm (palms) approximately (Fitzpatrick *et al.*, 2012).

The hypodermis or subcutaneous tissue is the innermost layer of the skin. It mostly consists of adipocytes packed with lipids and fatty acids, which protects the underlying layers from

external shock and provides an energy reservoir for the body. It also contains a large number of blood vessels and nerves that supply vascular networks in the dermis (Kolarsick *et al.*, 2011).

The dermis mostly consists of connective and fibrous tissue, supports the epidermal layer, and provides structure and resilience to the skin. In the dermis, the main type of cells are fibroblasts, which secrete collagen and elastin fibres that form a dense extracellular matrix (ECM). The ECM provides a scaffold for immune cell migration. It also provides a network for the distribution of blood and lymph vasculatures and neurons. Blood capillaries irrigate the dermis while lymph fluid is drained through lymphatic vessels to lymph nodes (Fitzpatrick *et al.*, 2012). In addition to fibroblast, other resident cell types are present in the dermis, including innate immune cells (such as dendritic cells, macrophages, and mast cells), innate lymphoid cells (ILCs),  $\gamma\delta$  T cells, and a large number of adaptive resident lymphocytes such as CD8<sup>+</sup> T cells (Kabashima *et al.*, 2019).

As the epidermis is the most superficial layer of the skin, it plays an important role in the skin's barrier function. This layer does not have blood vessels, but it is thin enough to be nourished by underlying layers. The epidermis is mainly composed of keratinocytes, but other types of cells such as melanocytes (produce melanin pigment), Merkle cells (a type of sensory cell), dendritic cells (a type of antigen-presenting cells), Langerhans cells (a unique type of tissue-resident macrophages), and resident memory T cells ( $T_{RM}$ ) also reside in there (Kabashima *et al.*, 2019). The epidermis is a multi-layered structure with the ability to renew itself through cell division. Constant division and differentiation of keratinocytes rise to make the four layers of the epidermis (Figure 1.1). These four distinct layers of the epidermis are identified by the maturity and morphology of the keratinocytes, the pattern of proteins, and the expression of lipids (Kolarsick *et al.*, 2011).

The stratum basale (basal layer) is the deepest layer of the epidermis, which is located on top of the dermis. Basal keratinocytes are attached to the basement membrane via  $\alpha$  and  $\beta$  integrins, which provide a connection to the underlying ECM. There is a single layer of epidermal stem cells and transit-amplifying cells in this part that differentiate into keratinocytes (Koster and Roop, 2007). Keratinocytes' morphology in this layer is cuboidal,



and they can be distinguished from other cells by the expression of keratin 5 and 14 (Simpson *et al.*, 2011). Epidermal keratinocytes constantly migrate from the base of the epidermis to the upper layer, and as they migrate, they proliferate and differentiate to regenerate the epidermis.

As the cells in the basal layer continue to divide asymmetrically, they leave the stratum basale and form the stratum spinosum. This layer comprises 8-10 layers of keratinocytes. In the lower layers, cells are polyhedral in shape with rounded nuclei, whereas in the upper layers, they become flattened and contain lamellar granules. Lamellar granules produce lipids, fibrillar proteins, and hydrolytic enzymes. Lipids produced by keratinocytes in this layer are essential for water retention (Fitzpatrick *et al.*, 2012). Fibrillar proteins such as keratins eventually aggregate together and make desmosomes. The desmosomal network is responsible for cell connection, which promotes intercellular connection and resistance to mechanical stress. Keratinocytes in this layer express keratin 1 and 10, which are specific to these cells. As the cells move into the stratum granulosum, they flatten and develop keratohyalin granules, which are composed of filaggrin, keratin filaments, loricrin, and involucrin. All these proteins are responsible for the hydration of the stratum corneum and filtration of ultraviolet (UV) radiation. Also, by binding to the desmosomal structure and underlying plasma membrane, loricrin forms the cornified cell envelope, which is important for the construction of the epidermis (Simpson *et al.*, 2011). The last stage of keratinocytes differentiation is self-destruction, which in this process, they destroy almost all their cellular components except keratin filaments and filaggrin matrix. Several layers of these flattened and cornified cells form the stratum corneum, the uppermost layer of the skin (Proksch *et al.*, 2008). Corneocytes in this layer are filled with proteins and are surrounded by an extracellular lipid matrix. This combination is known as the 'bricks' (corneocytes) and 'mortar' (extracellular lipids). Regulation of permeability, desquamation, antimicrobial peptide activity, and selective chemical absorption are all primary functions of the extracellular lipid matrix.

On the other hand, corneocytes are responsible for mechanical support, skin hydration, cytokine production, and protection from UV radiation (Fitzpatrick *et al.*, 2012).

Keratinocytes, sebocytes, and commensal microbes are the producer of lipids in the skin. Ceramides are produced by epidermal cells; cholesterol, triglycerides, and free fatty acids are often produced by microbes; and squalene and wax ester are produced by sebaceous glands (Chen *et al.*, 2018).

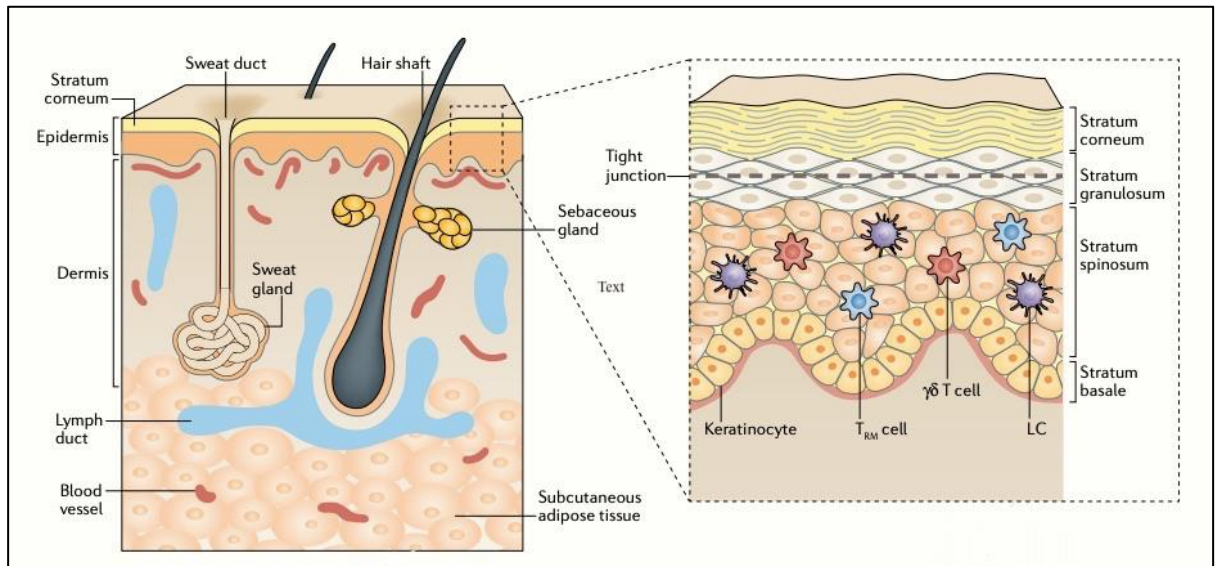


**Figure 1.1** Representation of different layers of the epidermis (Kabashima *et al.*, 2019).

### 1.1.2 Epidermal appendages

In addition to the epidermis layers, the appendages are also present throughout the epidermis. These appendages are important in thermo-regulation, waterproofing, skin flexibility, and pH control. These appendages include sebaceous glands, sweat glands, and hair follicles (Kolarsick *et al.*, 2011) (Figure 1.1)

Sebaceous glands produce and secrete sebum, lipid-rich substances, to the different layers of the skin to improve flexibility. Some of these glands are also connected to the hair follicles, which together form pilosebaceous units to lubricate hair growth. The pilosebaceous unit can be a suitable environment for bacterial growth. The by-product of bacterial metabolism from sebum, which is hydrolysing triglycerides into free fatty acids, builds the acidic pH of the skin (Fitzpatrick *et al.*, 2012). Sebaceous glands are distributed all over the body but are mostly present in the face and scalp. Hormones and

age control the sebum production by these glands; specifically, in puberty, the sebum production is elevated (SanMiguel and Grice, 2015).

There are two types of sweat glands: apocrine sweat glands and eccrine sweat glands. Apocrine sweat glands are mainly restricted to the axillae, perineum, and hairy region in the body. They mostly secrete oily substances to the hair follicle and are not open to the skin surface. Apocrine glands are involved in thermoregulation and scent release, which is essential in sexual attractants (Grice and Segre, 2011).

Eccrine sweat glands are dispersed throughout the body, predominantly present in the palms, soles, and forehead. These are the only glands that are open to the skin's surface. The hypotonic solutions of the sweat are essential for thermoregulation, pH maintenance, and skin hydration (SanMiguel and Grice, 2015).

The other appendage in the skin is the hair follicle, which has an important function in heat loss, protection against UV radiation, and scratches to the skin. At the base of the hair follicle, there is a hair bulb, and living cells in the hair bulb differentiate and keratinise to form the hair shaft. Blood vessels, nerves, and sebaceous glands are connected to the hair follicle to nourish the follicle and control hair growth (Fitzpatrick *et al.*, 2012).

Epidermal appendages have an essential role in human skin activity. They provide moisture, nutrients, and balanced pH in different sites of the skin, and make the skin a unique environment for the growth of a diverse microbial community. Also, there are no corneocytes (dead cells) around the appendages; the microbiota coexists with living keratinocytes in these areas, which results in skin appendages being an immunologically unique spot. So, it is important to investigate the contribution of the epidermis and epidermal appendages to the skin microbiome.

## 1.2 Skin immune system

The epidermis, which mostly consists of keratinocytes, makes the first defence barrier in the skin. The primary function of keratinocytes is to maintain the physical barrier of the skin, but this is not the only role. They are also a component of the innate immune system and the mainline of immune response by the production of a range of cytokines, chemokines, and antimicrobial peptides (AMPs) (Nestle *et al.*, 2009). Cytokines are small proteins released by different types of cells, mostly immune cells and epithelial cells, that affect the behaviour of nearby cells that bear appropriate receptors. Chemokines, a particular subgroup of cytokines that act as a chemoattractant, attract cells bearing chemokine receptors such as neutrophils. The release of cytokines and chemokines in the skin, which are responsible for cellular communications, activates a complex network of signalling with several different results. For example, they can result in attracting immune cells from the adaptive immune system to the skin. They are also essential for the proliferation, differentiation, and balanced physiology of keratinocytes (Hanel *et al.*, 2013).

Keratinocytes recognise pathogens and other stimuli in the skin through multiple receptors known as pattern recognition receptors (PRRs). These receptors are expressed on the cell surface or within the cells. Toll-like receptors (TLRs) are one of the PRRs which recognise a distinct set of molecular patterns that are called pathogens-associated molecular patterns (PAMPs) or damage-associated molecular patterns (DAMPs). PAMPs are a general component of both pathogenic and non-pathogenic microbes that usually have repetitive structures, such as bacterial lipopolysaccharides (LPS) and viral double-stranded (ds) ribonucleic acid (RNA). DAMPs are endogenous danger signals from stressed, damaged, and necrotic cells such as reactive oxygen species (ROS), high-mobility group protein box 1 (HMGB1), heat shock proteins, uric acids, and adenosine triphosphate (ATP) (Hornef and Bogdan, 2005; Nguyen and Soulika, 2019).

TLRs are transmembrane receptors located on the cell surface or the surface of endosomal organelles. There are 10 TLRs recognised in the human body, and each of them is specific in recognition of a distinct PAMP and DAMP (Table 1.1). For example, TLR4 recognises bacterial LPS, and TLR5 recognises bacterial flagella. Among 10 different types of TLRs, all

of them are expressed in keratinocytes except TLR7 and TLR8 (Lebre *et al.*, 2007). Recognition of dangers by TLRs activates different transcription factors such as nuclear factor-kappa B (NF- $\kappa$ B), interferon regulatory factor (IRF), activator protein 1 (AP-1), and mitogen-activated protein kinase (MAPKs). The ability of TLRs to activate NF- $\kappa$ B and other transcription factors is crucial to enable the adaptive immune response and initiate the expression of cytokines, chemokines, AMP, and co-stimulatory molecules (Fitzpatrick *et al.*, 2012).

Cytokines and chemokines production activated by TLR signalling include Interleukins (IL-1 $\alpha$ , IL-1 $\beta$ , IL-6, IL-8, IL-10), Interferons (IFN- $\alpha$ , IFN- $\beta$ ), growth factors, tumour necrosis factors (TNF- $\alpha$ ), and transforming growth factors (TGF- $\alpha$ , TGF $\beta$ ) (Williams and Kupper, 1996). IL-1 $\alpha$ , IL-1 $\beta$ , IL-6, IL-8, and TNF- $\alpha$ , key pro-inflammatory cytokines expressed by keratinocytes, can induce mechanisms that trigger local inflammation. In the presence of environmental dangers such as bacterial LPS and UV radiation, the production of IL-1 and TNF- $\alpha$  increases. IL-1 and TNF- $\alpha$  are primary cytokines that modulate the production of other cytokines. In response to primary cytokines, the release of IL-6 (enhance B cell growth and differentiation) and IL-8 (or CXCL8, which is a potent chemoattractant for neutrophils) significantly rise. These processes cause immediate elimination of infection, repair of damaged tissue, and activation of the adaptive immune response for further action (Kupper, 1990; Gröne, 2002; Nguyen and Soulika, 2019).

On the other hand, anti-inflammatory cytokines, which are immunosuppressive proteins, inhibit the function of pro-inflammatory cytokines. IL-10 is one of the important anti-inflammatory cytokines produced by keratinocytes that can inhibit T cell proliferation. A balanced release of anti and pro-inflammatory cytokines is essential in the regulation of immune response (Gröne, 2002; Hanel *et al.*, 2013).

The other receptors from the PRRs family that can detect both PAMPs and DAMPs are nucleotide oligomerisation domain (NOD)-like receptors (NLRs). NLRs are exclusively cytoplasmic receptors and have different subtypes (Nestle *et al.*, 2009). Activation of some NLRs mediates the formation of the inflammasome complex, which is a large multiprotein consisting of NLR, adaptor protein ASC (an apoptosis-associated speck-like protein

containing a caspase recruitment domain), and pro-caspase1. The inflammasome assembly activates caspase1, which cleaves pro-IL-1  $\beta$  to its active form (Martinon, 2009).

**Table 1.1** Toll-like receptors as pattern recognition receptors and their ligands. TLR10 ligand is unknown.

PRRS	PAMP
Cytoplasmic TLR	
TLR3	Viral ds RNA
TLR7, TLR8	Viral ss RNA
TLR9	Bacterial unmethylated CpG deoxyribonucleic acid (DNA)
Cell membrane	
TLR1/2 or TLR2/6 (TLR2 can form a heterodimer with either TLR1 or TLR6)	Bacterial lipoprotein/peptides
TLR4	Bacterial LPS
TLR5	Bacterial flagellin
TLR2, TLR4	HMGB1 (DAMP)

The other tool of keratinocytes to defend the skin and fight microbes is the production of antimicrobial peptides. Antimicrobial peptides are one of the essential components of the innate immune system that disrupt microbial membranes and assist in the resolution of infection. They are 10 – 150 amino acids long and cationic amphipathic peptides that are produced by different cell types, including neutrophils, mast cells, and keratinocytes (Schauber and Gallo, 2007). The most abundant antimicrobial peptides produced by human keratinocytes are the human  $\beta$ -defensin 1 (HBD-1), HBD-2, HBD-3, cathelicidin (such as LL-37), and ribonuclease 7 (RNase-7). The expression of antimicrobial peptides is either regularly at a low level or is stimulated by inflammatory triggers (Schauber and Gallo, 2008). For instance, HBD-1 is produced continuously while the secretion of other antimicrobial peptides is induced by other stimuli such as cytokines (TNF- $\alpha$  and IL-1  $\beta$ ) and microbial products (LPS and lipoteichoic acids) (Kolls *et al.*, 2008). This is not the only function of antimicrobial peptides; they also contribute to activating and attracting adaptive immune cells and inducing the production of anti and pro-inflammatory cytokines through TLRs at the site of infection (Nguyen and Soulika, 2019).

The skin is the first line of defence in our bodies, and it ensures protection through physical, chemical, and immune barriers. However, there is another important line that contributes to the defence and homeostasis of the skin, and this is a microbiome barrier.

## 1.3 Skin microbiota

The skin is colonized by millions of bacteria, fungi, and viruses that compose the skin microbiota. The skin microbiota with their genetic information, metabolites, structural elements, and host interactions, build the human skin microbiome (Grice and Serge, 2011; Byrd *et al.*, 2018; Carmona-Cruz *et al.*, 2022). Characterising the microbial community living on the different sites of the skin is important to understanding the role of the skin microbiota in health and disease. Historically, the skin microbiota was identified by their cultivation from swabs of the skin surface. This approach selects microorganisms that grow in artificial cultures, so it underestimates the diversity of the microbial community since most skin microbes are unculturable. In 2007, the National Institutes of Health started the Human Microbiome Project to study the microbial community in different parts of the human body, including the human skin using molecular gene sequencing techniques (Turnbaugh *et al.*, 2007; Peterson *et al.*, 2009). There are conserved taxonomic gene sequences as molecular fingerprints in the bacterial and fungal genome that are specific to bacterial and fungal organisms and are not found in other organisms. These sequences are the 16S ribosomal RNA (rRNA) gene in bacteria and the internal transcribed spacer 1 region in fungi. Sequencing these regions provides genus identification; however, species-specific sequences are usually found adjacent to 16S rRNA and can be used to identify bacteria at the species level (Grice *et al.*, 2008; Grice *et al.*, 2009; Costello *et al.*, 2009). Researchers first amplify the specific region using designed primers. After sequencing the amplified region, they compare the raw data with the known bacterial sequences database library to identify the bacteria. This method is also known as amplicon sequencing, as it just targets a specific amplicon. The other method that has been used is shotgun metagenomic sequencing, in which the whole genetic material in the sample is sequenced without targeting specific regions. Since shotgun metagenomics amplifies all genetic material, it

allows us to study the community composition at the species and strain level (Oh *et al.*, 2014; Oh *et al.*, 2016; Byrd *et al.*, 2018). The result of these studies at different skin sites of healthy individuals showed that the majority of the skin bacteria are categorised into four phyla of *Actinobacteria*, *Firmicutes*, *Bacteroidetes*, and *Proteobacteria* (Figure 1.2). However, the diversity and dominance of bacterial species vary based on the different physiological sites of the skin.

The distribution of sweat glands, hair follicles, and sebaceous glands is not uniform throughout the skin. Based on the secretion of the glands, each site of the skin has different physiology and characteristics. The physiology of the skin can be categorised as moist, dry, and oily or sebaceous, influenced by appendages present in these sites (SanMiguel and Grice, 2015). These physiological features of skin provide a suitable microenvironment for the growth of specific microorganisms. Several other factors specify the composition of the microbial community living on each individual's skin. These include climatic conditions, hygiene frequency, use of antibiotics, and other environmental factors (Prescott *et al.*, 2017).

Furthermore, the skin microbiome can change in the lifetime of each individual. For example, the microbial community in a new-born baby can be determined based on the mode of delivery and exposure of the new-borns to others and the specific environment. Another example is the change in the skin microbiome during puberty; changes in hormone levels and sebaceous secretion can change the skin microbiome noticeably (Kong, 2011; Kong and Segre, 2017).

A comprehensive analysis of skin microbiota has revealed that in sebaceous sites of the skin, like the face and the upper back, *Cutibacterium*, a lipophilic bacterium, is dominant. This bacterium tends to hydrolyse sebum found in the skin and produce free fatty acids, which acidify the sebaceous areas as a result (Grice *et al.*, 2009; Costello *et al.*, 2009). *Cutibacterium acne* (formerly known as *Propionibacterium acnes* (*P. acnes*)) is one of the species that colonise oily parts of the skin, especially the face, and it can cause acne vulgaris in some cases. Acne vulgaris is a common skin disorder that causes comedones, papules, and nodules on the skin because of the inflammation of pilosebaceous units. However, it



has been shown that *P. acnes* species are commensal microbes in those with and without acne, but some certain strains are related to acne vulgaris (Xu and Li, 2019).

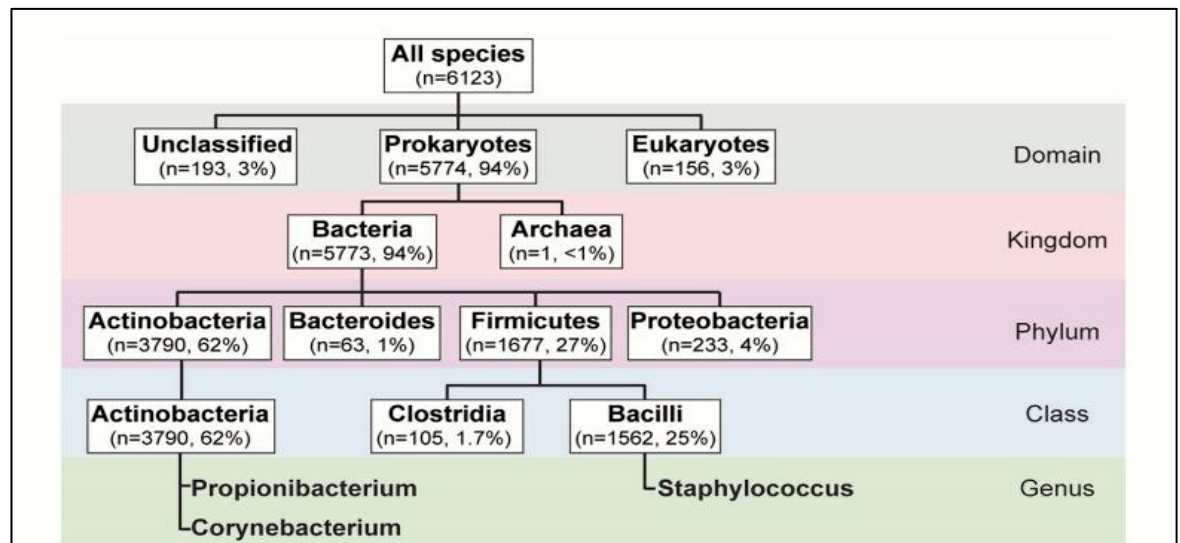


**Figure 1.2** The phylogenetic tree from a metagenomic approach gives a comprehensive detail of the microbial community (Taken from Chen and Tsao, 2013).

*Staphylococcus* and *Corynebacterium* are predominant organisms in moist skin zones like the axilla and inner elbow. It has been shown that *Corynebacterium*'s metabolization of sweat glands' secretions in the axilla area is related to the production of odorous compounds that are responsible for the smell of sweat. Staphylococci inhabit the aerobic area and utilise the urea in sweat as a nitrogen source (Costello *et al.*, 2009; Grice and Serge, 2011). Atopic dermatitis (eczema) is a chronic skin disorder in moist areas, which despite being non-infectious, it is related to skin microbiota dysbiosis (an imbalance of skin microorganisms). The 16S rRNA sequencing has revealed an increase in the colonisation of *Staphylococcus aureus* (*S. aureus*) in atopic dermatitis flares and a decrease in bacterial diversity. Although there is no clear evidence of pathogenicity of *S. aureus*, it seems there is an immune response to the staphylococcal protein A, secreted in the site of atopic dermatitis, which might intensify eczema symptoms (Kong *et al.*, 2012; De Vuyst *et al.*, 2017).

Despite the sebaceous and moist area of the skin, dry zones have greater bacterial diversity with a lower bacterial load. *Proteobacteria* and *Bacteroidetes* are dominant in dry regions like the elbow, knee, forearm, and leg (Grice *et al.*, 2009; Costello *et al.*, 2009). The common

skin disease in dry parts of the skin is psoriasis vulgaris, which is caused by chronic inflammation and over division of keratinocytes because of excessive production of inflammatory factors. It has been shown that there is a significant increase in the number of *Corynebacterium*, *Cutibacterium*, *Staphylococcus*, and *Streptococcus* at the site of psoriasis plaque. However, the exact mechanism of inflammation and the microbiota's roles are still unclear (Fyhrquist *et al.*, 2019).

Microbial diversity is not limited to the bacterial cells; fungal species also play an essential role in the skin microbiome and human health and disease (Findley *et al.*, 2013). Foot sites and toenails have a notable fungal diversity; however, the other sites of the skin are dominated by *Malassezia*. *Malassezia* species are dominant fungal species in sebaceous areas. The two major species are *M. globosa* and *M. restricta*, which might cause seborrheic dermatitis (dandruff). The diversity of both bacterial and fungal species in sebaceous habitats is limited (Grice and Dawson, 2017). The other players in skin microbiota are viruses, with bacteriophages being predominant. The lytic bacteriophages that replicate inside bacterial cells may modulate bacterial populations in the skin through preying and genetic exchange (Hannigan *et al.*, 2015; Liu *et al.*, 2015).

### 1.3.1 Host-microbe interaction

The physical and immunological barriers are not the only defence mechanism in the skin. The microbial barrier is an essential component of defending the skin against pathogens' colonisation. Although the skin's chemistry drives its microbial composition, the interaction of the microbial community with local immune cells and keratinocytes is an essential factor contributing to the homeostasis of the skin.

Keratinocytes and other immune cells that reside in the skin continuously recognise microbes through their PRPs and react accordingly to maintain the healthy balance of the skin. Skin microbes also contribute to the immunity of the skin through their influence on the function of skin cells (Byrd *et al.*, 2018). For example, researchers in 2012, showed that commensal microbes affect IL-1 signalling in T cells. They concluded that the defect in T cell signalling might be a result of an impaired dialogue between skin commensals and immune cells (Naik *et al.*, 2012). Several studies support the influence of *Staphylococcus epidermidis*

(*S. epidermidis*) and other commensal bacteria on the skin (Chehoud *et al.*, 2013; Naik *et al.*, 2015; Nakatsuji *et al.*, 2018; Williams *et al.*, 2019). This is supported by the evidence that the imbalance of microbial community can cause skin disorders such as atopic dermatitis, psoriasis, and non-healing wounds (Kong *et al.*, 2012; Fry *et al.*, 2013; Gardner *et al.*, 2013; Fahlen *et al.*, 2018). Although increasing studies indicate dysbiosis in numerous pathogenesises, it is still unclear if the dysbiosis causes skin disorders or if immune dysregulation triggers the dysbiosis.

### 1.3.2 *Staphylococcus epidermidis*

One of the most abundant skin colonisers is coagulase-negative staphylococci (CoNS). Staphylococcal species are Gram-positive round shape bacteria that form grape-like clusters under the microscope. All species in the genus of *Staphylococcus*, with a few exceptions, are catalase-positive, which differs them from *Streptococcus*, and they are all facultative anaerobes. Most staphylococci, under unfavourable conditions such as presence of antibiotics, tend to select for small colony variants (SCVs) in their population. SCVs are a slow-growing subpopulation of bacteria which form very small colonies on agar compared to the wild-type subpopulation. The slow growth in SCVs is attributed to the deficiency in the electron transport chain, which can cause metabolic alterations in bacteria. SCVs are usually persistent inside host cells (Proctor *et al.*, 2006; Melter and Radojevic, 2010). Staphylococci can be divided into coagulase-positive and coagulase-negative groups based on their ability to convert the fibrinogen in plasma to fibrin using the enzyme coagulase. *S. aureus* is a famous coagulase-positive bacterium and usually causes infection in humans. It is one of the most important causes of hospital-acquired (nosocomial) infections that are resistant to antibiotics, although more than 30% of healthy individuals are colonised asymptotically by this bacterium (Graffunder and Venezia, 2002). *S. epidermidis*, the well-known CoNS bacterium, like other CoNS, is one of the abundant commensal bacteria that colonise human skin. *S. epidermidis* forms small (1 – 2 mm) white colonies, and it is sensitive to deferoxamine (an iron chelating agent) (Lindsay and Riley, 1991). Although *S. epidermidis* can use glucose to grow anaerobically, it cannot ferment mannitol (Namvar *et al.*, 2014).

Despite having few virulence factors and being less pathogenic than *S. aureus*, *S. epidermidis* is also considered a frequent cause of nosocomial infections. The bacteria primarily infect compromised patients, including drug abusers, those on immunosuppressive therapy, acquired immune deficiency syndrome (AIDS) patients, and premature new-borns (Eiff *et al.*, 1998; Darouiche, 2004). In immune-competent patients, *S. epidermidis* infections are associated with indwelling medical devices such as catheters (Darouiche, 2004; Dong and Speer, 2014). The systemic infections of *S. epidermidis* can cause sepsis.

The virulence of *S. epidermidis* has been attributed to its biofilm formation through specific attachment and accumulation elements. Autolysin proteins (AtlE), teichoic acid (TA), lipoteichoic acid (LTA), and staphylococcal surface proteins (SSP) in *S. epidermidis* are some of the important factors in attachment to hydrophobic abiotic surfaces, which are often used in catheters and indwelling devices (Heilmann *et al.*, 2003; Banner *et al.*, 2007). Polysaccharide intercellular adhesin (PIA) is an essential component of the extracellular polymeric substances (EPS) of staphylococcal biofilm. PIA is a poly- $\beta$  (1-6)-N-acetylglucosamine (PNAG) responsible for the cell-to-cell adhesion in the accumulation stage of biofilm formation (Vuong *et al.*, 2004; Rohde *et al.*, 2010; Sabate Bresco *et al.*, 2017). PIA is encoded in *ica* locus, and the majority of the *S. epidermidis* strains that contain this gene are isolated from catheter infections, not from healthy skin, and are biofilm-forming strains (Zhang *et al.*, 2003).

Although most of the studies in the past investigated *S. epidermidis* as a pathogen, the mutualistic effect of *S. epidermidis* on the skin has recently been gaining attention (Chen *et al.*, 2018; Severn and Horswill, 2022). *S. epidermidis* produces five different lantibiotics: Pep5, epidermin, epicidin 280, epilancin K7, and epidermicin NI01 (Bierbaum *et al.*, 1996; Gotz *et al.*, 2013). Lantibiotics (lanthionine-containing-antibiotic), also known as bacteriocins, are antimicrobial peptides synthesised in ribosomes of some strains of certain species and are active against other strains of the same or related species (McAuliffe *et al.*, 2001).

Several studies have shown the beneficial effect of commensal bacteria on the homeostasis of the skin. For example, *S. epidermidis* induces the expression of antimicrobial peptides like HBD-3 and RNase7 through TLR-2 and activation of NF- $\kappa$ B signalling pathways in human keratinocytes, which results in the amplification of innate immune response. Interestingly this activation is distinct from *S. aureus*. (Wanke *et al.*, 2011).

Also, *S. epidermidis* produces its own antimicrobial peptides that have antimicrobial activity against *S. aureus* and group A streptococci. These peptides, known as phenol soluble modulins (PSMs), are small toxin peptides produced by staphylococcal species. PSM  $\delta$  and PSM  $\gamma$  (also known as  $\delta$ -toxin) produced by *S. epidermidis* work together with the skin antimicrobial peptide (cathelicidin LL-37) to protect the skin against pathogens. PSMs and mammalian antimicrobial peptides have similar characteristics and modes of action; they both interact with the lipid membrane (Cogen *et al.*, 2010). These antimicrobial peptides produced by *S. epidermidis* (and *S. hominis*) are strain specific. They are deficient in atopic dermatitis patients, causing the overgrowth of *S. aureus* (Nakatsuji *et al.*, 2017). In addition, autoinducing peptides produced by CoNS isolated from healthy skin can suppress the production of toxins (PSM $\alpha$  and protease) in *S. aureus*. PSM $\alpha$  and protease cause inflammation and epithelial damage in atopic dermatitis patients. Both production of autoinducing peptides and PSM $\alpha$  are controlled by the quorum sensing system (Williams *et al.*, 2019).

PSMs are amphipathic and  $\alpha$ -helical peptides, which their production in staphylococci is under the restrict control of *agr* (accessory gene regulator) quorum sensing system. The surfactant character of PSMs simplifies the growth of bacteria on the epithelial surface and might further facilitate biofilm formation. In highly virulent *S. aureus*, PSMs contribute to biofilm formation and aggressive virulence activities; however, in less pathogenic staphylococci, they have other roles in bacterial physiology. PSMs produced by *S. epidermidis* have moderate antimicrobial activity and can amplify the innate immune response in the skin. On the other hand, methicillin-resistant *S. aureus* has an extraordinary capacity to lyse human neutrophils and escape the innate immune system by the production of PSMs, which is only limited to methicillin-resistant *S. aureus* (Otto, 2014).

Skin microbiota can also regulate the skin's immune response to commensals and pathogens in the skin. Naik *et al.* showed that colonisation of the mice's skin with *S. epidermidis* could induce the production of IL-17A; this cytokine contributes to the pathology of various skin inflammatory disorders such as psoriasis. IL-17, along with IL-22, induce the expression of the antimicrobial peptides in keratinocytes, which are effective against *Candida albicans* infection. However, in psoriasis, the immune response to IL-17 stimulates the proliferation of keratinocytes, and this can cause the marked thickening of the epidermis. Skin's dendritic cells sense and respond to any changes in the microbial community living on the skin. This activates the specific T- cells' response to the commensal bacteria and regulates the immunity barrier against pathogens; this immunity is called heterologous protection. Also, this immune response to the skin commensals occurs in the absence of inflammation. This is in contrast to the response that is given in the presence of invading pathogens with inflammation (Naik *et al.*, 2015).

As well as modulating immune cells, *S. epidermidis* and other commensals promote epithelial integrity, especially during tissue repair. LTA, the major component of the *S. epidermidis* cell wall, can modulate inflammation triggered by injury. LTA, through a TLR-2 mechanism, inhibits the inflammatory cytokine release from keratinocytes and promotes healing after injury. Inflammation is a fundamental immune response, but in the absence of infections after the injury, dysregulated inflammation can delay the healing process, consequently causing extensive tissue damage (Lai *et al.*, 2009).

*S. epidermidis* metabolites even have a role in suppressing tumours' growth. Researchers have demonstrated that 6-N-hydroxyaminopurine (6-HAP), a nucleobase analogue produced by *S. epidermidis*, inhibits DNA polymerase activity, and subsequently inhibits tumour proliferation but not primary keratinocytes. When the live bacteria or the 6-HAP were administered to the ultraviolet-induced tumour on a mouse's skin, the tumour shrank (Nakatsuji *et al.*, 2018).

In addition to the beneficial roles of *S. epidermidis* on the overall homeostasis of the skin, several further studies have demonstrated the contribution of other members of skin microbiota to the skin barrier's wellbeing (Meisel *et al.*, 2018; Williams *et al.*, 2019; Patra

*et al.*, 2019; Zheng *et al.*, 2022). The interaction of commensal microbes and host cells appears to be critical for establishing homeostasis in the skin but is still not fully understood.

## 1.4 Wound healing

Skin protects the body against the invasion of pathogens and any environmental risks, but sometimes this structure is disrupted, and a wound is formed. In healthy skin, wound healing starts within a few minutes after the injury, and a set of biochemical events occurs to help the process of healing and restore the barrier function. Wound healing is a complex physiological function, which involves various cells and signalling molecules interacting with each other to regulate healing events. It consists of four overlapping repair stages (Figure 1.3): coagulation and haemostasis, inflammation, proliferation, and remodelling phase (Gosain and DiPietro, 2004; Velnar *et al.*, 2009).

### 1.4.1 Stages of wound healing

**Coagulation and haemostasis.** As blood spills to the site of injury, platelets in the blood are exposed to the collagen and extracellular matrix components of injured cells. This exposure activates platelets to attach to each other and to the matrix to form a blood clot. Blood clots, composed of platelets and extracellular matrix proteins such as fibronectins, fibrin, and vitronectin, provide a provisional network for the migration of immune cells to the site of injury. Platelets' cytoplasm contains growth factors and cytokines such as platelet-derived growth factor (PDGF), transforming growth factor- $\beta$  (TGF- $\beta$ ), epidermal growth factor (EGF), and insulin growth factor (IGF), which are released after activation of platelets. These growth factors direct the growth of new capillaries, regulate the production of extracellular matrix proteins, mediate other signalling cascades, and attract neutrophils, macrophages, endothelial cells, and fibroblasts to the injury site. Platelets also contain vasoactive amines that increase vascular permeability, leading to the leakage of fluid into the tissue, which is an important stage of inflammation (Barrientos *et al.*, 2008; Gonzalez *et al.*, 2016).

**Inflammation.** This phase establishes an immune barrier against the invasion of pathogens. After the injury, skin cells are exposed to alarm signals such as DAMP and PAMP; TLRs recognise these signals and initiate inflammation. Also, by an increase in blood vessel permeability, immune cells infiltrate the wound area. Neutrophils are the first cells to arrive at the site; they are attracted by chemokines produced from injured tissues and bacterial components. They phagocytise bacteria, remove damaged tissue (debridement), and produce antibacterial substances such as ROS. ROS are chemically reactive molecules (such as hydrogen peroxide  $H_2O_2$ ) and free radicals (such as hydroxyl radical  $\cdot OH$ ) derived from oxygen in cellular metabolism. They cause damage to biomolecules at high concentrations. Neutrophils remain at the site of injury till the infection and tissue debris are cleared. In addition, neutrophils secrete many pro-inflammatory cytokines and thereby amplify the inflammatory response (Wilgus *et al.*, 2013. Leoni *et al.*, 2015).

Later in the inflammation phase (48 – 72 hours), macrophages enter the wound area and replace neutrophils. Monocytes in the bloodstream infiltrate the injured tissue and mature into macrophages. Tissue-resident macrophages phagocytise dead neutrophils and ingest the fibrin clot and other cellular debris (Yanez *et al.*, 2017). There are two different phenotypes of macrophages in the wound area: M1: pro-inflammatory macrophages that are activated through “classical activation” and improve host defence against pathogens. They also promote the secretion of pro-inflammatory mediators such as  $TNF-\alpha$ , IL-6, nitric oxide (a type of ROS) and IL- $1\beta$  that contribute to the activation of different kinds of antimicrobial mechanisms. M1 macrophages identify and engulf pathogens into their organelles which are full of ROS and rapidly kill pathogens (Murray and Wynn, 2011; Yanez *et al.*, 2017). Most of the macrophages that migrate to the wound show the M1 phenotype. M2: M2 macrophages are tissue-resident with anti-inflammatory functions. When the inflammation persists (presence of a large number of inflammatory cytokines and impaired clearance of neutrophils), macrophages transit to the anti-inflammatory phenotype through “alternative activation.” They secrete anti-inflammatory cytokines such as IL-10 to promote the resolution of inflammation. M2 macrophages increase new vessel formation, which contributes to the migration of more macrophages and nutrients to the site of inflammation. They also release growth factors, which stimulate keratinocytes and



fibroblasts proliferation and epithelial barrier repair (Murray and Wynn, 2011; Rodrigues *et al.*, 2019).

**Proliferation.** When the ongoing injury has ceased, haemostasis has been achieved, and an immune response successfully set in place, the acute wound shifts toward tissue repair. In this phase, wound healing continues with neoangiogenesis (formation of new blood vessels from pre-existing ones), extracellular matrix formation, collagen synthesis, and re-epithelisation (Gurtner *et al.*, 2008). Macrophages produce several growth factors and cytokines that stimulate fibroblasts and keratinocytes to promote tissue regeneration. Macrophages play an important role in the transition from inflammation to proliferation (Murray and Wynn, 2011).

Fibroblasts that are attracted to the site of injury proliferate and produce matrix proteins such as hyaluronan, fibronectin, and, most importantly, collagen III. These extracellular proteins accumulate and form a new scaffold that replaces the provisional network; this scaffold supports cell migration and provides tissue integrity. Myofibroblasts – a differentiated type of fibroblasts – are responsible for wound contraction due to the presence of actin bundles in their cytoplasm. Wound contraction helps to reduce the size of the wound. Myofibroblasts are eliminated by apoptosis when tissue integrity is restored (Tomasek *et al.*, 2002; Darby *et al.*, 2014).

The skin's regenerative capacity relies on the local epidermal stem cells, which are located in separate sites: the epidermal hair follicles, the base of sebaceous glands, and the interfollicular epidermis. In response to injury, epidermal stem cells participate in re-epithelisation by proliferation and migration to the wound site (Fuchs, 2008. Sorg *et al.*, 2017). Proliferation and migration of epidermal stem cells and keratinocytes are initiated when several growth factors are released. Examples of common growth factors are: platelet-derived growth factor (PDGF), fibroblast growth factor (FGF), epidermal growth factor (EGF), and transforming growth factor (TGF- $\alpha$  or  $\beta$ ). Keratinocytes are responsible for barrier defence against pathogens and restoring the epidermis after injury. They produce various antimicrobial peptides, cytokines, and growth factors to establish homeostasis during wound healing (Barrientos *et al.*, 2008; Pastar *et al.*, 2014).

New blood vessel formation (angiogenesis) is required to deliver nutrients and maintain oxygen equilibrium in the wound area to enhance cellular proliferation and tissue regeneration. Hypoxia in the wound area and growth factors such as vascular endothelial growth factor (VEGF) and PDGF activate resident endothelial cells – which cover the surface of blood vessels – and promote their proliferation and growth.

Endothelial cells produce proteases to remove extracellular matrix to ease their movement. They proliferate, differentiate, and form a microvascular network composed of many new capillaries within a few days (Werner and Grose, 2003). At this stage of wound healing, granulation tissue is formed by developing new capillaries by endothelial cells, forming an extracellular matrix by fibroblasts, and migrating keratinocytes, myofibroblasts, and immune cells (Rodrigues *et al.*, 2019).

**Remodelling phase.** Tissue can undergo remodelling for several months or even several years to reconstitute scar tissue from granulation tissue. For remodelling, collagen III in granulation tissue is replaced by collagen I, which is stronger collagen. Matrix metalloproteinase (MMPs), synthesised by neutrophils, macrophages, and myofibroblasts, are responsible for the degradation of extracellular material such as collagen. This degradation induces cell migration. Macrophages also engulf extracellular matrix debris and apoptotic cells. Remodelling of the wound is tightly controlled by regulatory mechanisms with a delicate balance between degradation and synthesis, leading to regular healing (Gurtner *et al.*, 2008; Kawasumi *et al.*, 2012; Rodrigues *et al.*, 2019).

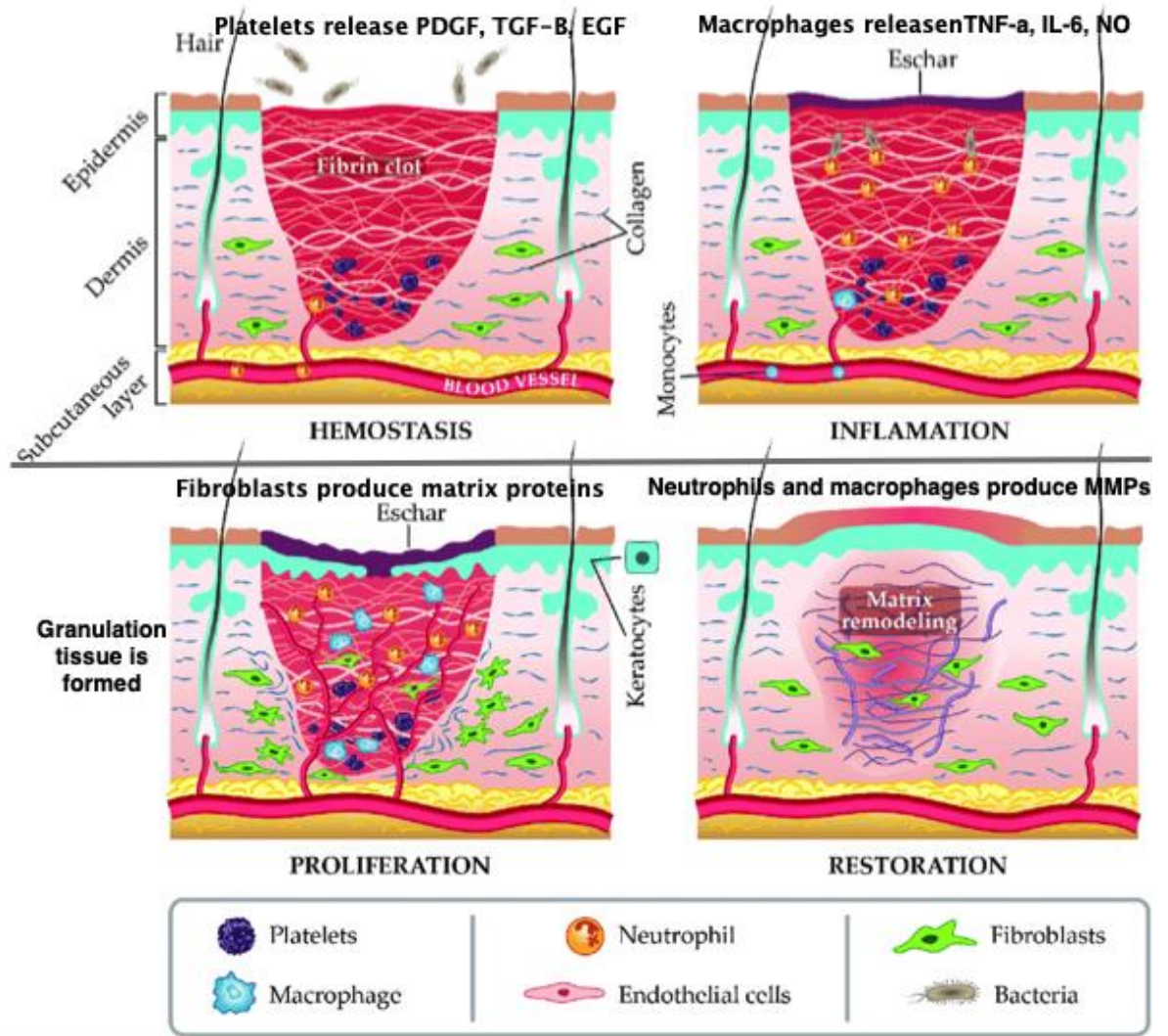


**Figure 1.3** Wound healing phases in normal skin.

Wound healing is a complex and overlapping process of haemostasis, inflammation, proliferation, and remodelling. In haemostasis, blood clots form, which consist of platelets, red blood cells, and extracellular matrix proteins. Inflammation starts immediately after injury and last for few days. Signalling molecules attract macrophages and neutrophils to the site of injury and triggering inflammatory responses. Macrophages produce several growth factors and cytokines that stimulate fibroblasts and keratinocytes migration and proliferation. Extracellular matrix proteins formed by fibroblast, new capillaries, and keratinocytes forms granulation tissue. In the restoration or remodelling phase, granulation tissue remodel to a collagen rich scar tissue. Platelet-derived growth factor (PDGF), transforming growth factor- $\beta$  (TGF- $\beta$ ), epidermal growth factor (EGF), nitric oxide (NO), and matrix metalloproteinase (MMPs). (Taken and adapted from Negut *et al.*, 2018).

## 1.4.2 Types of wounds

### 1.4.2.1 Acute wound

In acute wounds, there is a reasonable timespan and development from injury to wound healing. In normal conditions and in people with healthy immune function, wound healing starts with coagulation and inflammation and continues with proliferation and tissue regeneration. The whole process of healing might take up to one month without any complications (Velnar *et al.*, 2009). In acute wounds, the microbial composition of the skin changes, and there is an opportunity for pathogens to colonise the wound bed; however, a functional immune response in the area is able to overcome bacterial colonisation and establish homeostasis in the skin. In a study, researchers examined in 52 subjects, the microbial communities of traumatic open fracture wounds with culture-independent methods (such as sequencing). They showed that the mechanism of injury could determine the microbial community of the wound. They also demonstrated that the bacterial composition was significantly different in the wound centre from the adjacent tissue at the beginning of the injury, but the wound microbiota became similar to the skin microbiota over time (Bartow-McKenny *et al.*, 2018).

### 1.4.2.2 Chronic wound

Chronic wounds do not heal in a specific time span and do not progress to the late stages of tissue remodelling (Velnar *et al.*, 2009). They are usually caught in the inflammation stage, in which there is an imbalanced inflammatory response in the wound area. Several factors can contribute to chronic wounds: age, inadequate immune response, diabetes, and an excessive amount of ROS. This situation creates an opportunity for microbes to colonise the wound, which persists even with antibiotic treatment and wound dressing. The colonisation of the wound with microbes increases the inflammation and makes the situation perpetuated (Guo and DiPietro, 2010).

Chronic wounds usually are seen in people with underlying health issues, for example: diabetic foot ulcers in diabetic patients, venous leg ulcers in patients with artery disease and lack of exercise, pressure ulcers in patients with physical disabilities and malnutrition,

and post-surgical wounds in patients with immune deficiency (Rodrigues *et al.*, 2019). Many of these conditions affect blood flow to the tissues resulting in an imbalanced pH and oxygen and decreased activity of immune cells.

Several factors are involved in prolonged inflammation in chronic wounds: 1) the persistent presence of neutrophils and macrophages that cause increased secretion of inflammatory cytokines: microbial colonisation in the site of injury probably attracts neutrophils and macrophages; however, they are not effective against the biofilm of bacteria (Diegelmann, 2003), 2) imbalanced presence of matrix metalloproteinases and their inhibitors: matrix metalloproteinases are necessary for the degradation of collagen in tissue remodelling and activation of growth factors; however, excessive amounts of these enzymes increase tissue degradation and reduce proliferation and migration of keratinocytes and fibroblasts, 3) oxidative stress in wound area: amplified levels of oxygen and nitrogen free radicals cause tissue damage, 4) antibiotic-resistant bacterial biofilm that protects bacteria in the wound from immune cells and antibiotic treatment: the open and necrotic wound is a great environment for colonisation and biofilm formation of bacteria. Bacterial biofilm impairs the wound healing process significantly, and it is believed to be a reason for chronic inflammation (elevated number of immune cells, inflammatory cytokines, MMPs, and oxidative stress) in the wound area (Guo and DiPietro, 2010; Eming *et al.*, 2014; Leoni *et al.*, 2015).

### 1.4.3 The role of growth factors, cytokines, and chemokines in wound healing

The wound healing process starts immediately after injury when growth factors, cytokines, and chemokines from different types of cells in the wound area are released (Werner and Grose, 2003; Behm *et al.*, 2012). The growth factors release to the site of injury, such as PDGF, FGF, VEGF, EGF, and TGF, induce re-epithelisation through stimulation of cell proliferation and migration (Barrientos *et al.*, 2008).

Pro-inflammatory cytokines such as TNF, IL-1, IL-6, and IL-17 participate in the inflammation phase of wound healing and induce migration and proliferation of keratinocytes and fibroblasts, and regulate the immune response (Grellner and Wilske, 2000; Werner and Grose, 2003). The balance in the release of pro-inflammatory cytokines in the wound area is the key to time-efficient wound healing. A moderate level of pro-inflammatory cytokines accelerates keratinocytes' proliferation and re-epithelisation; however, excessive release of pro-inflammatory cytokines can cause prolonged inflammation and has a detrimental effect on the healing process (Xiao *et al.*, 2020). For example, wound healing in an IL-6 knock-out mice model took up to three times longer than in a wild animal. However, the administration of IL-6 completely resolved the wound, suggesting the crucial effect of IL-6 in re-epithelisation. On the other hand, the excessive expression of IL-6 has been associated with formation of cutaneous scar (Galluchi *et al.*, 2000). Anti-inflammatory cytokines such as IL-4, IL-13, and IL-10 regulate inflammation and regulate the production of pro-inflammatory cytokines, promote fibroblast proliferation, and induce extracellular matrix synthesis (Barrientos *et al.*, 2008; Mestrallet *et al.*, 2021).

Chemokines are also produced during wound healing. Chemokines are small chemoattractant cytokines released by several cells in the wound area and stimulate the migration of multiple cell types to the wound. Chemokines are divided into four groups of motifs C-C, C-X-C, C-X3-C, and C based on their amino acid composition and the location of cysteine residues on the N-terminal. They all mediate their action by coupling their ligand with transmembrane G-protein receptors on the surface of their target cells. Some of the chemokines present in the wound are CXCL1 (also known as GRO- $\alpha$ ), CXCL4, CXCL8 (also known as IL-8), and CXCL10 (Gillitzer and Goebeler, 2001; Ridiandries *et al.*, 2018). It has been shown that in chronic wounds. This suggests that specific chemokines are essential for wound healing (Gillitzer and Goebeler, 2001).

CXCL1, which is a neutrophil attractant, and its receptor CXCR1 are expressed in keratinocytes and are induced during the wound healing process, especially during re-epithelisation and angiogenesis. In fact, high level of CXCL1 and CXCL-8 has been associated with early wound neoangiogenesis in the wound (Devalaraja *et al.*, 2000). In an *in vitro* study, the strong mitogenic activity of CXCL1 on keratinocytes was observed, which

suggests this chemokine affects keratinocytes' re-epithelisation (Rennekampff *et al.*, 1997; Werner and Grose, 2003).

## 1.5 Wound microbiota

Infection is one of the factors that can make a wound chronic and delay its healing. So, it is important to study the microbiota of the wound and its impact on the healing process. To establish the role of bacteria in the chronicity of the wounds, it is wise to distinguish pathogens from normal colonisers or even beneficial bacteria present in the area.

Culture-dependent techniques have been proven limited and imperfect in analysing microbial samples compared to molecular gene sequencing techniques that recognise hard-to-culture and fastidious species. In the past decade, several studies investigated the microbiota of the different types of wounds using genomic techniques. Genomic tools such as DNA amplification, genome sequencing and pyrosequencing, and ribosomal RNA sequencing provide the opportunity to thoroughly investigate wound flora and acknowledge the composition, diversity, and prevalence of microbes in the wounds.

In a study in 2017, researchers investigated diabetic foot ulcer microbial composition by 16S rRNA sequencing and compared the result with samples from healthy people's feet. They showed diabetic foot ulcers are significantly less diverse in their microbial composition than healthy skin microbiota (reduced alpha diversity). They also showed that the most abundant bacteria on the healthy skin (such as *Staphylococcus* and *Corynebacterium*) were also present in the wounds of patients; however, the diversity of low-abundance bacteria between patients and control groups is significantly different (Gardiner *et al.*, 2017).

One of the limitations of amplicon sequencing (like 16S rRNA) is that it cannot distinguish different species within genera. So, Kalan and colleagues used shotgun metagenomic sequencing and 16S rRNA sequencing to investigate the strain and species-level microbial diversity of diabetic foot ulcers. They showed that the most abundant genera in their samples are *Staphylococcus*, *Corynebacterium*, and *Pseudomonas*, and the most abundant

species are *S. aureus*, *C. striatum*, and *P. aeruginosa*. They showed *S. aureus* strains that are associated with chronic wounds contain several antibiotic resistance genes and encode staphylococcal endotoxins genes. When they compared their data with the Bartow-McKenny study (Bartow-McKenny *et al.*, 2018), which investigated the microbiota of acute wounds, they found the same pattern of abundant genera in both studies (acute and chronic wounds) (Kalan *et al.*, 2019).

In a large clinical study to evaluate the bacterial composition of different wound types, scientists inspected 2936 patients' wound samples – the samples consisted of diabetic foot ulcers, venous leg ulcers, non-healing surgical wounds, and decubitus leg ulcers. They analysed the microbial composition with 16S rRNA pyrosequencing. The results revealed that chronic wounds are immensely polymicrobial and showed *Staphylococcus* species, such as *S. epidermidis* and *S. aureus*, and *Pseudomonas* species, such as *P. aeruginosa* were the most common bacteria in the analysed chronic wounds. Although the abundance of these species was different in various wounds, *P. aeruginosa* was the most common microbe seen in biofilms. They also detected vast numbers of anaerobic bacteria in the wound samples (Wolcott *et al.*, 2016).

In a recent study in 2020, scientists showed that facultative anaerobes (like *Enterobacter* genus) were associated with non-healing wounds and were not present in the normal skin of the patients in this study. Wounds that did not heal within six months were mainly colonised with facultative anaerobes compared to healed wounds; this might be because these bacteria can tolerate better the different metabolic environments and oxygen tensions; therefore, they can persist in biofilm in chronic wounds (Verbanic *et al.*, 2020).

In 2012 Han and colleagues analysed the bacterial flora of 45 chronic wound samples using 16S rRNA pyrosequencing, and they compared their results with studies on healthy skin microbiota. They found an increased proportion of anaerobic bacteria present in the wound, which are not detectable with standard culture-dependent techniques. Also, they showed the number of *Actinobacteria* (*Propionibacterium*) decreased, and *Proteobacteria* (*Pseudomonas* and *Klebsiella*) and *Firmicutes* (*Staphylococcus*) increased compared to the healthy flora. They were able to detect quorum sensing molecules – acyl homoserine



lactone (AHL) and autoinducer 2 (AI-2) – using bioluminescent assays from samples. They discovered AI-2 in 80% of their samples, although in different concentrations and detected AHL in 20% of samples. They assume the low concentration of AHL in the samples is because of the low abundance of Gram-negative bacteria colonising the wound and the quorum quenching effect of molecules produced by human cells and *P. aeruginosa*, which can degrade AHL. This data suggests that bacteria in chronic wounds communicate through interspecies signalling (Han *et al.*, 2011).

Several other studies confirmed the polymicrobial characteristic of different types of chronic wounds and the presence of *Staphylococcus*, *Pseudomonas*, *Enterobacter* (*Enterococcus faecalis*), and *Corynebacterium* species in the wound site. Furthermore, culture-independent studies recognised a higher incidence of anaerobe bacteria in different wound types, which were impossible to detect with standard culture-dependent techniques. These studies used different molecular techniques with varying numbers of samples, but all of them confirmed the presence of pathogens and biofilm-forming species in different wound types; however, the prevalence and abundance of different species are different in these studies. Several factors such as age, antibiotic treatment, underlying health issues, sample collection techniques, and different methods of analysis can impact the result of microbiome studies in wounds; therefore, better models are required to study wound microbiome to consider all these factors (Misic *et al.*, 2014; Price *et al.*, 2011; Dowd *et al.*, 2008; Jneid *et al.*, 2018).

### 1.5.1 *Pseudomonas aeruginosa*

*P. aeruginosa* is a rod-shaped, motile, and Gram-negative bacterium commonly present in the general environment, such as soil, water, and even on human skin. It is an opportunistic bacterium that can cause severe infections in the respiratory tract of cystic fibrosis patients, in soft tissue like chronic wounds, and in the urinary tract of immunocompromised patients (Moradali *et al.*, 2017). It is also responsible for nosocomial infections caused by multidrug resistant strains of *P. aeruginosa*. Several factors are responsible for antibiotic resistance in *P. aeruginosa*: a) a large and adaptable genome provides an arsenal of virulence factors to defeat the host immune response; b) biofilm protects bacterial cells in a stressful

environment and enables them to colonise in competitive niches; c) numerous efflux pumps present in the cell wall eject drugs and protect bacteria from antibiotics (Pang *et al.*, 2019). Besides antibiotic resistance that makes it difficult to eradicate *P. aeruginosa* infections, *P. aeruginosa* sp. has several virulence factors that cause harmful infection in their host.

### 1.5.1.1 Biofilm formation of *P. aeruginosa*

The chronic wound bed is a suitable environment for biofilm formation due to the presence of necrotic tissues and impaired immune response. Because of exposed extracellular polymers, necrotic tissue provides nutrition and a suitable surface for bacterial attachment. The presence of bacterial biofilm in the wound induces the host immune response and inflammation, but biofilm infection often persists and neutralises the effect of immune cells. Macrophages and neutrophils are abundantly present at the site of chronic wounds; however, it seems they are not sufficiently effective in eradicating bacterial infection. One study using biofilm infection in a mouse model showed that *S. aureus* attracts macrophages to the wound, but they changed from pro-inflammatory M1 phenotype to anti-inflammatory M2 macrophages upon contact with biofilm. M2 macrophages have less antimicrobial activity; therefore, the infection and inflammation will stay in the area (Thurlow *et al.*, 2011). Biofilm present in *in vitro* and animal models is quite different from chronic wounds in clinical cases. However, scientists have proved the presence of microbial aggregates in patients' chronic wounds using light and scanning electron microscopy by using fluorescence in situ hybridisation (FISH) probes (Davis *et al.*, 2008; James *et al.*, 2008). For further confirmation of biofilm in the wound bed, scientists have also illuminated alginate, an essential extracellular polymeric substance in *P. aeruginosa* biofilm (Bjarnsholt *et al.*, 2008). It has been shown that 60% of chronic wounds and 6% of acute wounds contain biofilms (James *et al.*, 2008).

Biofilm is a bacterial community structure composed of bacterial cells and extracellular polymeric substances (EPS) – comprised of polysaccharides, extracellular DNA (eDNA), and proteins. The EPS provides a suitable scaffold for the biofilm structure and the cell placement inside the structure, which is important in cell-to-cell communications (Mulcahy

*et al.*, 2014). Biofilm enables bacteria to colonise in stressful environments when there are insufficient nutrients and oxygen. It supports bacterial attachment to different surfaces and protects the bacterial cells against antimicrobial agents and predators (Flemming *et al.*, 2016).

*P. aeruginosa* produces several extracellular polysaccharides, which form the EPS scaffold. When *P. aeruginosa* initially colonise the site of infection, it produces Pel and Psl polysaccharides. Psl is a polysaccharide containing glucose, mannose, and rhamnose (Ma *et al.*, 2007). The structure of Pel is still unclear; however, in a recent study, Le Mauff and colleagues determined that Pel is composed of galactosamine and N-acetylgalactosamine (Le Mauff *et al.*, 2022). Non-mucoid clinical isolates of *P. aeruginosa* produce both Pel and Psl (Jennings *et al.*, 2021). In persistent infections, over the accumulation of mutations, non-mucoid strains convert to mucoid phenotype and produce extracellular polysaccharide alginate. Alginate is an anionic polymer rich in mannuronic acid and glucuronic acid. Extracellular polysaccharides play an important role in preventing the penetration of antibiotics into the biofilm of *P. aeruginosa* (Ryder *et al.*, 2007; Franklin *et al.*, 2011; Stoner *et al.*, 2022).

Extracellular proteins in the biofilm matrix of *P. aeruginosa* mostly contribute to the structural integrity of the biofilm and its attachment to a variety of surfaces. CdrA is an extracellular adhesin protein that promotes aggregate formation via binding with Psl and maintains biofilm integrity (Reichhardt *et al.*, 2020). *P. aeruginosa* also produces two small soluble lectins, LecA and LecB. Both LecA and LecB interact with sugars in the biofilm matrix (LecA binds to galactose, and LecB binds mainly to mannose), therefore helping the structure of the biofilm. The other primary function of lectins is mediating the attachment of bacterial cells to the host during infection and facilitating invading the host cells, and causing cytotoxicity (Tielker *et al.*, 2005; Diggle *et al.*, 2006; Grishin *et al.*, 2015; Passos da Silva *et al.*, 2019).

The eDNA in the biofilm matrix is another key factor in *P. aeruginosa* biofilm structure and integrity. There is evidence that eDNA is essential in the early stages of biofilm formation. DNase treatment of *P. aeruginosa* biofilm at early stages results in biofilm dissolution.

However, the mature biofilm stays intact after DNase treatment (Whitchurch *et al.*, 2002). In another study by Alleson-Holm and colleagues in 2006, it was confirmed that eDNA was concentrated towards the surface of a newly forming biofilm. In contrast, a mature biofilm showed a high concentration of eDNA towards the stalk of the biofilm structure (Alleson-Holm *et al.*, 2006).

The first step to forming a biofilm is the attachment of bacterial cells to the surface and each other. Due to the electrostatic and hydrophobic interaction between cells, the initial attachment is reversible and repulsive. Irreversible attachment is facilitated via flagella, pili, and adhesins, which overcome electrostatic forces and cease bacterial movement. Upon successful attachment, a complex intracellular signalling cascade changes the gene expression in planktonic cells and shifts them to the biofilm state phenotype. In a biofilm state, sessile bacterial cells start to divide and produce EPS to form microcolonies and establish biofilm structure. EPS enclose the bacterial community and provide structural support and stable attachment to the surface; it also traps nutrient and water via interspersed channels and pores to help the survival of bacteria in a stressful environment. Various types of biopolymers with different functions make EPS a heterogenous structure with vital properties (Flemming *et al.*, 2016; Omar *et al.*, 2017).

To form a mature biofilm, the microcolonies need to communicate with each other by signalling molecules. The intracellular signalling is coordinated through quorum sensing molecules secreted from bacterial cells and can be sensed by other cells at threshold concentrations. Quorum sensing molecules control the expression of specific genes, such as the expression of virulence factors at critical concentrations. Bacterial cells in the biofilm can shift to a planktonic state and leave the biofilm – a process known as detachment – and start new colonies (Mendoza *et al.*, 2019). The transition of cells from a biofilm state to a planktonic state is under the control of various molecular pathways, such as quorum sensing and small non-coding RNA (Wu *et al.*, 2019).

Biofilms are resistant to antimicrobial agents such as the host immune system and antibiotics because of: the slow rate of growth and metabolisms in biofilm cells; which affect the antibiotic mechanism of action, the presence of persister cells; which are

resistant to the treatment, overexpression of efflux pump; which restrict the penetration of xenobiotics, degradation of antimicrobial agents by exopolymers, and presence of antibiotic resistance gene in the community which is transferable to other cells (Flemming *et al.*, 2016; Wu *et al.*, 2019).

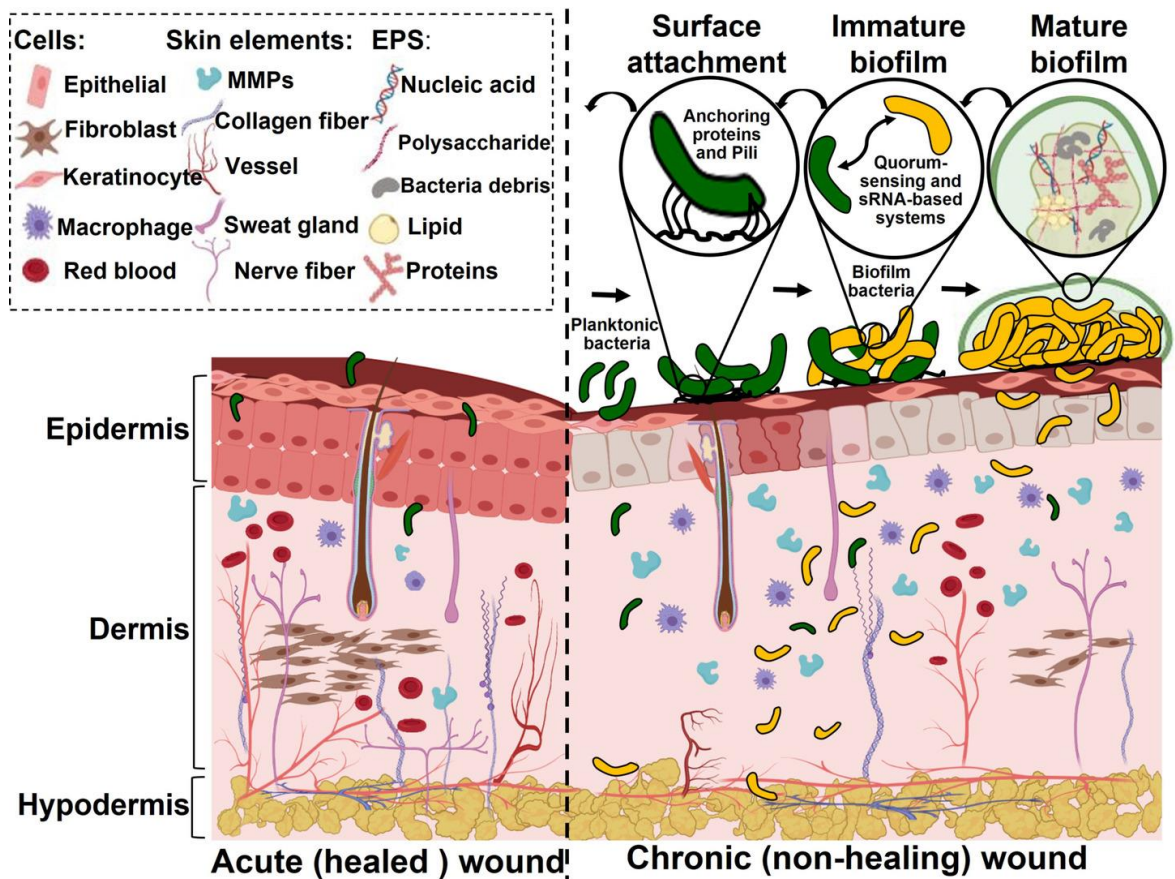


**Figure 1.4** Biofilm formation in the chronic wound.

Biofilm formation starts with the attachment of planktonic bacterial cells to the wound surface via flagella, pili, and anchoring (adhesin) proteins. A complex signalling cascade transforms planktonic cells to sessile cells. Sessile cells produce extracellular polymeric substances and gradually microcolonies (immature biofilm) transform to a mature biofilm. Small RNA (sRNA) (Taken from Darvishi *et al.*, 2022).

### 1.1.5.2 Virulence factors in *P. aeruginosa*

**Motility.** Motility is an important opportunity for bacterial cells to colonise and explore new niches. *P. aeruginosa* exhibits three types of motilities in the environment: swimming, swarming, and twitching (Khan *et al.*, 2020). A single polar flagellum is responsible for the swimming motility of *P. aeruginosa* in a liquid environment. Swimming motility is also important in biofilm dispersion. Twitching, bacterial movement through a solid environment, is facilitated by polar type IV pili. Swarming aids motility in semisolid environments like mucosal sites and is present in many organisms. Flagellum and pili also assist in the surface attachment of bacterial cells; therefore, they enable biofilm formation (Murray and Kazmierczak, 2008; Patriquin *et al.*, 2008).

**Siderophores.** Siderophores are bacterial extracellular compounds that bind to iron and transport it to the cells. Iron is an essential molecule for the growth and proliferation of most organisms. *P. aeruginosa* produces two compounds to uptake iron from the environment: pyoverdine and pyochelin (Cornelis and Dingemans, 2013). Pyoverdine is a green fluorescence compound with a high affinity to iron. Pyoverdine scavenges iron from the environment; it also uptake it from transferrin and lactoferrin – host proteins that bind to iron and transfer it in the blood – then transports iron to the cell. Pyoverdine can also acquire iron from mitochondria, which causes damage to the host cells. Furthermore, it plays a vital role in biofilm formation in poor nutrition niches (Kang and Kirienko, 2018; Kang *et al.*, 2018). Pyochelin has a lower affinity to iron compared to pyoverdine, and it has been shown to be associated with inflammation and oxidative damage in the host cells (Cornelis and Dingemans, 2013).

**Pyocyanin.** Pyocyanin is a blue redox-active toxin produced by *P. aeruginosa*. It is a nitrogen-containing aromatic compound with a low molecular weight that can infuse into the cell membrane easily (Lau *et al.*, 2004). Pyocyanin increases the intracellular levels of ROS, especially superoxide ( $O_2^-$ ) and hydrogen peroxide ( $H_2O_2$ ), so it can cause oxidative damage to the cells. Several studies have shown the toxic effect of pyocyanin through the generation of ROS on different cell lines and cellular components like DNA and mitochondria (Hall *et al.*, 2016).

**Rhamnolipid.** Rhamnolipids are rhamnose-containing glycolipid biosurfactants produced by *P. aeruginosa*. Biosurfactants are surface-active molecules that can minimise surface tension between two phases, which can have several biotechnological applications (Soberon-Chavez *et al.*, 2021). In *P. aeruginosa*, rhamnolipids promote the invasion of bacterial cells into respiratory epithelium, facilitate swarming motility, and help maintain the biofilm architecture (Zulianello *et al.*, 2006). In 2007, Pamp and Tolker-Nielsen showed that *P. aeruginosa* surfactants attributed to bacterial migration, therefore, are essential for migration-mediated structure formation in the later stages of biofilm development. They were also crucial in biofilm development in the early stages.

**Elastase B.** Secreted proteases such as elastase A (LasA), elastase B (LasB), alkaline protease (AP), protease IV (P IV), and *P. aeruginosa* aminopeptidase (PAAP) play a crucial role in the pathogenesis of *P. aeruginosa*. Elastase B, which is an elastolytic zinc metalloprotease (also known as pseudolysin), is the most abundant protease in *P. aeruginosa* (Cigana *et al.*, 2020). Elastase B damages host tissue by hydrolysis of elastin, collagen, and fibronectin in the extracellular matrix of epithelial cells and by degrading intercellular tight junctions in endothelial and epithelial layers (Azghani, 1996; De Bentzmann *et al.*, 2000). It also degrades several critical proteins in the human immune system, such as cytokines, chemokines, antibacterial peptides, immunoglobulin A, and immunoglobulin G (Parmely *et al.*, 1990; Kuang *et al.*, 2011; Saint-Criq *et al.*, 2018).

**Exotoxin A.** Exotoxin A is a soluble exoprotein and one of the most toxic virulence factors in *P. aeruginosa*. Exotoxin A inactivates eukaryotic elongation factor-2 (eEF-2) in host cells by targeting diphthamide, a post-translationally modified histidine on eEF-2. This mechanism is similar to the mechanism of action of diphtheria toxin from *Corynebacterium diphtheria*. eEF-2 is an essential factor in protein biosynthesis on the ribosome. Therefore, its inactivation terminates protein synthesis, eventually leading to cell apoptosis (Michalska and Wolf, 2015; Santajit *et al.*, 2019).

**Secretion system.** One of the essential mechanisms for Gram-negative bacteria to release enzymes, toxins, and virulence factors to the environment and host cells is protein secretion system. Secretion systems are made of a large number of proteins crossing

through the membrane. They can remain bound to the bacterial membrane, released to the environment, and be injected to the host cells. There are nine different types of secretion system (usually referred to as T1SS to T9SS) described in Gram-negative bacteria. T3SS is one of the most studied and most relevant secretion system in human infections in *P. aeruginosa*, which transport type three proteins from the bacterial cytosol to the extracellular environment. T3SS is a complex needle-like machine, which is composed of needle complex, the translocation apparatus, effector proteins, chaperon, and regulation proteins. During bacterial colonization on host cell, T3SS injects effector proteins to the host cells (Hauser, 2009; Horna and Ruiz, 2021; Liao *et al.*, 2022).

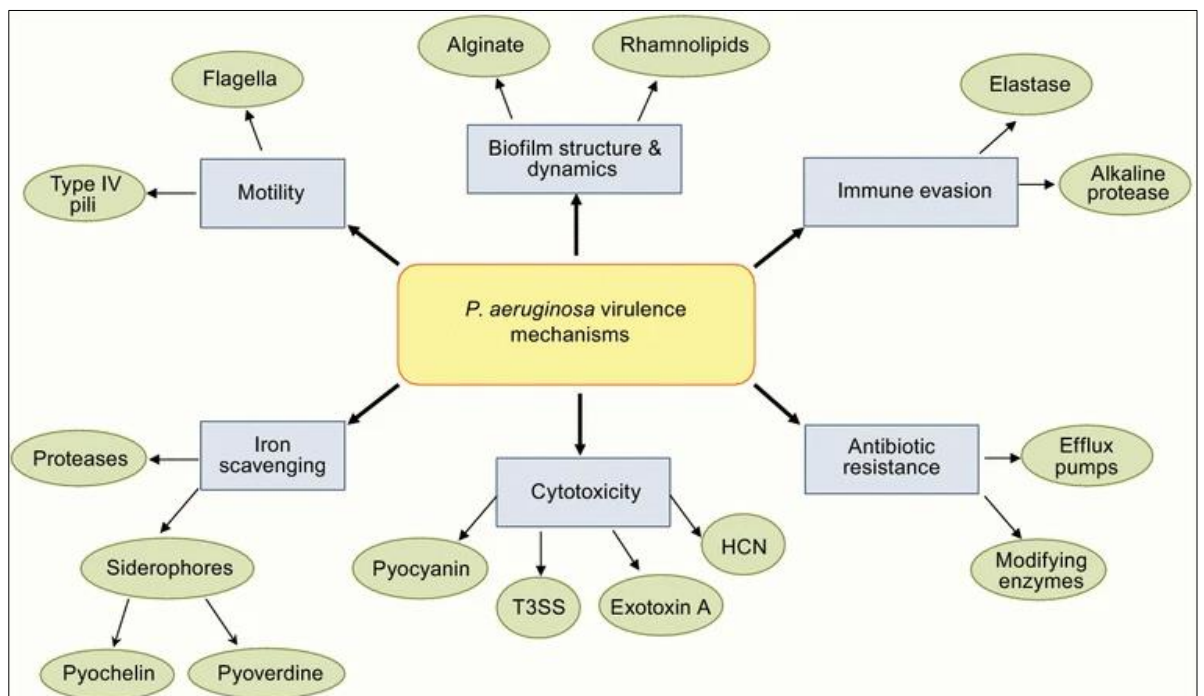


**Figure 1.5** Virulence mechanisms in *P. aeruginosa* (Taken from Lee and Zang, 2015).

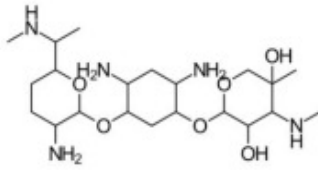
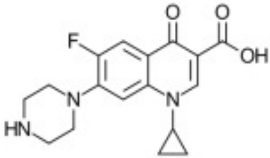
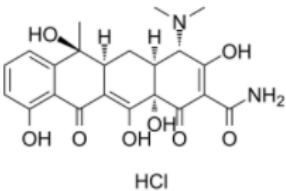
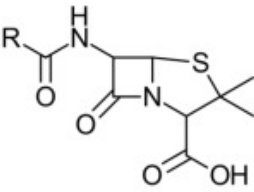
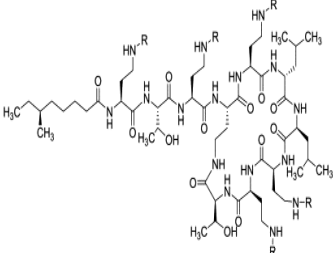


### 1.5.1.3 Antibiotics and resistance in *P. aeruginosa*

How *P. aeruginosa* acquires its antibiotics resistance mechanisms can be divided into three categories: intrinsic, acquired, and adaptive (Tenover, 2006). Intrinsic mechanisms are those whose genes are encoded in the core genome of bacterial cells. Bacterial cells can reduce the efficacy of specific antibiotics by inbuilt characteristics, which they inherit. Some of these characteristics are the low outer membrane permeability, efflux pumps, and enzymes to degrade antibiotics such as  $\beta$ -lactam (Langendonk *et al.*, 2021).

*P. aeruginosa* has 12- to 100- fold lower outer membrane permeability compared to *E. coli* (Bellido *et al.*, 1992). Acquired resistance comes from horizontal gene transfer and de novo mutational events. Bacterial cells can receive antibiotic modifying genes and  $\beta$ -lactamase genes via genetic information transfer by plasmids and transposons from the same or different bacterial species (Blair *et al.*, 2015). Also, de novo mutations such as point mutations, insertions, and gene deletions may cause antibiotic resistance gene overexpression (Dettman *et al.*, 2016). In adaptive mechanisms, antibiotic resistance is induced through environmental stimulations and stress factors, and they can be undone when the stimuli are removed. It gives the bacterial cells the ability to survive in an environment rich in antibiotics and host immune antimicrobials (Sandoval-Motta and Aldana, 2016; Coleman *et al.*, 2020). In this situation, they form biofilm and produce persister cells to survive in a stressed environment (Moradali *et al.*, 2017).

**Table 1.2** Antibiotics that have been used to treat *P. aeruginosa* infections.

Antibiotic Group	Antibiotic example	Structure	Mode of Action
Aminoglycoside	Gentamicin		Inhibits bacterial protein synthesis by irreversibly binding to ribosomal 30S subunits
Quinolone	Ciprofloxacin		Interfere with DNA replication by inhibiting DNA gyrase and topoisomerase IV
Tetracycline	Tetracycline hydrochloride	 HCl	Inhibits bacterial protein synthesis by reversibly binding to ribosomal 30S subunits
$\beta$ -lactam	Penicillin		Inhibits the synthesis of peptidoglycan that forms the cell walls by binding to penicillin-binding proteins in the cytoplasmic membrane
Polymyxin	Polymyxin E (Colistin)		Disrupts the lipopolysaccharides in the outer cell membrane

#### 1.5.1.4 Antibiotic resistance mechanisms in *P. aeruginosa*

**Outer membrane permeability.** Antibiotics must penetrate the microbial membrane in order to reach internal targets. The outer membrane of *P. aeruginosa*, composed of a symmetric bilayer of phospholipids and LPS implanted with porin channels, performs as a barrier to stop antibiotic diffusion. Porins are water-filled protein channels within the membrane, transporting nutrients and other molecules across the cellular membrane (Achouak *et al.*, 2001; Chevalier *et al.*, 2017). Quinolones such as ciprofloxacin and  $\beta$ -lactam antibiotics such as penicillin diffuse through the cell membrane via porins. *P. aeruginosa* has 26 different types of porin (Sugawara *et al.*, 2006; Langendonk *et al.*, 2021). To enter the bacterial cells, aminoglycoside, such as gentamicin and polymyxin, such as colistin interact with LPS and the outer membrane of bacterial cells (Pang *et al.*, 2019).

Efflux pumps are the other part of the membrane that determines the permeability of the bacterial cell membrane. They are comprised of cytoplasmic membrane transporter, periplasmic linker protein, and outer membrane porin channel (Munita and Arias, 2016). They transport toxic compounds such as antimicrobials and reactive oxygen species out of the bacterial cells into the environment, and their expression is modulated in response to external stimuli. Ribosome-blocking antibiotics like tetracycline induce efflux pump (MexXY-OprM) expression (Langendonk *et al.*, 2021). In the prokaryotic kingdom, there are five major families of efflux transporter: major facilitator (MF), multidrug and toxic efflux (MATE), resistance-nodulation-division (RND), small multidrug resistance (SMR) and ATP binding cassette (ABC) (Webber and Piddock, 2003; Marquez, 2005). All these systems generate energy for transport by transferring protons or electrons across the membrane, except the ABC family, which uses ATP hydrolysis to move substrates. Proteins belonging to the RND efflux pump are the leading player in multidrug resistance in *P. aeruginosa*. The cytoplasmic and periplasmic proteins in the RND family are called Mex, and the porin is called Opr. OprF is the most abundant porin in *P. aeruginosa*, and it is involved in a variety of functions (Sugawara *et al.*, 2006). The multidrug-resistant *P. aeruginosa* has been associated with the overexpression of multiple efflux pumps (Hancock and Brinkman, 2002; Langendonk *et al.*, 2021).

**Inactivating enzymes.** One of the significant intrinsic mechanisms that inactivate antibiotics is releasing bacterial enzymes.  $\beta$ -lactam antibiotics bind penicillin-binding proteins responsible for synthesizing peptidoglycan that forms bacterial cell walls. Therefore, they cause cell lysis. *P. aeruginosa* produces an enzyme,  $\beta$ -lactamase, that can hydrolyze the lactam ring in  $\beta$ -lactam antibiotics and inactivate them (Wright, 2005; Pang *et al.*, 2019).  $\beta$ -lactamases are classified based on different systems; a) the Ambler classification groups enzymes according to amino acid sequence, and b) the Bush-Jacoby-Medeiros system classifies enzymes according to function and phenotype (Bush *et al.*, 2010). *P. aeruginosa* is also able to modify antibiotics like aminoglycosides and therefore inactivate them. One of the mechanisms is the modifying amino and glycoside group in these antibiotics which cause a decrease in the binding affinity of antibiotics to their binding target (Pang *et al.*, 2019; Qin *et al.*, 2022).

**Biofilm formation.** By forming biofilm, bacterial cells increase their chance of survival in harsh environments. Biofilm, with the scaffold of EPS, decreases antibiotics' permeability to the core community of microbes. Even bacterial cells with low intrinsic resistance show less susceptibility to antibiotics when they form biofilm. Eradication of *P. aeruginosa* in biofilm form of growth in cystic fibrosis and chronic wound patients is one of the obstacles in clinical settings due to their increased resistance to antibiotics.

**Bacterial motility.** Swimming and swarming motility in *P. aeruginosa* are known to cause an increase in antibiotic resistance. They are the type of adaptive resistance mechanisms whose gene expression depends on the environment. Swarming cells are significantly more resistant to aminoglycosides,  $\beta$ -lactams, chloramphenicol, ciprofloxacin, tetracycline, ethoprim, erythromycin and azithromycin (Coleman *et al.*, 2020). Swimming cells, however, showed significantly higher resistance to polymyxins, aminoglycosides, fluoroquinolones, tetracycline, chloramphenicol, trimethoprim, and several  $\beta$ -lactams, but not to macrolides (Sun *et al.*, 2018)

### 1.5.1.5 Quorum sensing network in *P. aeruginosa*

Biofilm formation and expression of most virulence genes are under the control of the quorum sensing system. Quorum sensing is a cell-cell communication system that regulates the expression and production of metabolites in a cell-density-dependent manner. Bacterial cells produce signal molecules known as autoinducers. When the number of cells increases in the environment surrounding the cells, the concentration of autoinducer molecules increases as well (Figure 1.6). Autoinducer molecules can activate the transcription of genes that are important for the survival of bacterial cells only when they reach the threshold concentrations (Miller and Bassler, 2001; Rutherford and Bassler, 2012).

There are four major interconnected quorum sensing systems available in *P. aeruginosa*: LasI/LasR, RhlI/RhIR, quinolone-based quorum sensing, and integrated quorum sensing (IQS) (Lee and Zang, 2015; Moradali *et al.*, 2017).

Signal molecules in Las and Rhl systems are acyl-homoserine lactones (AHLs), a homoserine lactone ring with a fatty acyl side chain with 4 to 20 carbons. LasI and RhlI are signal synthases that produce N-3-oxo-dodecanoyl-homoserine lactone (3-oxo-C12-HSL) and N-butanoyl-homoserine lactone (C4-HSL), respectively. When the number of cells in the environment increases and the signal concentration reaches the threshold, 3-oxo-C12-HSL activates LasR and C4-HSL activates RhIR. LasR and RhIR are transcription regulatory proteins that control the expression of several virulence factor genes (Lee and Zang, 2015; Kostylev *et al.*, 2019; Qin *et al.*, 2022).

The signal molecules in quinolone-based quorum sensing are alkyl quinolones. There are two signal molecules in this system: 4-hydroxy-2-heptylquinoline (HHQ) and 2-heptyl-3,4-dihydroxyquinoline, called *Pseudomonas* quinolone signal (PQS). HHQ and PQS activate PqsR, a transcriptional regulator, which regulates the expression of virulence genes. Signal synthase in this system is a cluster gene made up of *pqsABCDE*, *phnAB*, and *pqsH* (Lin *et al.*, 2018).

IQS is an intercellular communication signalling regulated by several quorum sensing molecules. IQS signalling pathway is less understood, and its role in gene expression is not clear yet (Lee *et al.*, 2013; Kostylev *et al.*, 2019). IQS is a new class of quorum sensing signal identified as 2-(2-hydroxyphenyl)-thiazole-4-carbaldehyde3 (Lee *et al.*, 2013; Lee and Zang, 2015). It has been shown that IQS could inhibit eukaryotic host cell growth and induce apoptosis (Wang *et al.*, 2019). Quorum sensing is an interconnected and complicated signalling network often activated depending on the environmental conditions (Figure 1.6). It has been shown that cathelicidin LL-37 produced by keratinocytes promotes virulence factor production such as pyocyanin, elastase, and rhamnolipid in *P. aeruginosa* through the quorum sensing system (Stempel *et al.*, 2013).

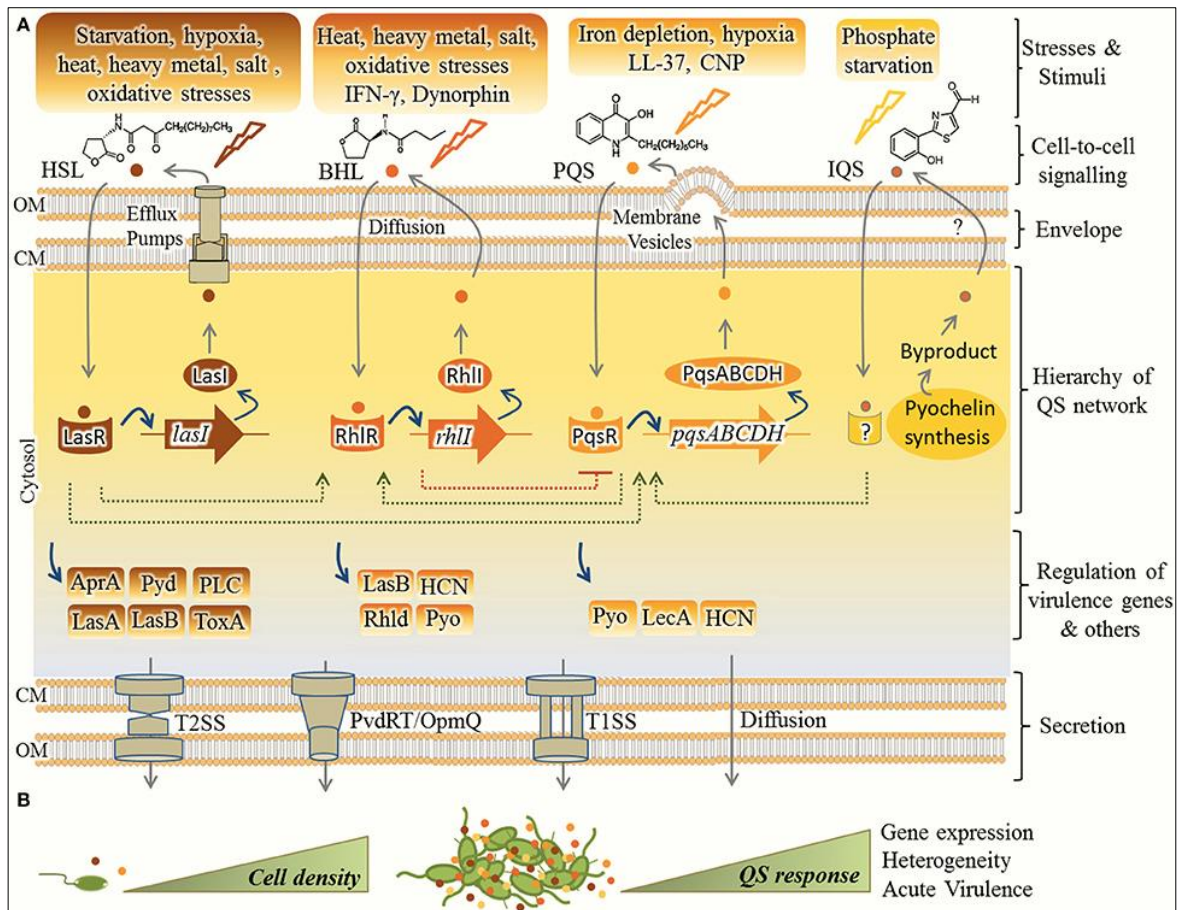


**Figure 1.6** Quorum sensing system in *P. aeruginosa* and regulation of virulence factors. (A) There are four interconnected quorum sensing systems: Las, Rhl, Pqs (or quinolone-based QS), and IQS, which in response to stress, produce signal molecules: HSL (N-3-oxododecanoyl-homoserine lactone), BHL (N-butanoyl-homoserine lactone or C4-HSL), PQS (*Pseudomonas* quinolone signal), and IQS signal, respectively. These signal molecules activate transcriptional regulators (LasR, RhIR, and PqsR), which consequently regulate the expression of virulence genes (AprA, alkaline protease; Pyd, pyoverdine; PLC, phospholipase C; ToxA, toxin A; LasA, LasA elastase; LasB, LasB elastase; HCN, hydrogen cyanide; Pyo, pyocyanin; RhId, rhamnolipids; Lec A, lectin A). Dashed lines represent the interaction of quorum sensing systems. Question marks represent unknown subjects. (B) Autoinducers (small colourful circles) concentrations in the environment increase when the number of cells increases (Taken from Moradali *et al.*, 2017).

## 1.6 Key factors involved in the study of wound healing

Chronic wounds affect millions of people annually, and the number of affected individuals is rising because of the increase in the ageing population, obesity, and the high prevalence of chronic wounds among the elderly, diabetic, and patients with cardiovascular diseases (Guest *et al.*, 2020; Sen, 2021). Also, the emergence of antibiotic-resistant pathogens makes the treatment of chronic wounds difficult. This puts a considerable burden on hospitalised patients and their quality of life. In some cases, amputation is the only way of treatment. Chronic wounds also impact the healthcare system with enormous financial consequences (Guest *et al.*, 2015; Guest *et al.*, 2020).

Infections in chronic wounds are critical factors that delay the wound healing process. Bacterial communities existing in chronic wounds are primarily present in biofilm form, which is highly resistant to the host immune system and antibiotic treatment, resulting in non-healing wounds (Ibberson and Whiteley, 2020; Johnson *et al.*, 2018; Frykberg and Banks, 2015; Siddiqui and Bernstein, 2010). Despite the importance of infection, the role of biofilm in the wound and its interaction with other components present in the wound has not been thoroughly investigated (Wolcott *et al.*, 2013; Kadam *et al.*, 2019). To develop novel and effective therapeutics to target biofilm infections, it is important to study the biofilm in the context of the wound bed and investigate the effect of all components involved in chronic wounds, such as microbial cells, human cells (skin and immune cells), extracellular matrix proteins, and chemicals on biofilm formation.

### 1.6.1 Microbial cells

Biofilms present in the wound bed are mostly polymicrobial, with two or more species of microbes involved in the community. The most abundant pathogenic bacteria present in the wounds are from *Staphylococcus* (*S. aureus*) and *Pseudomonas* (*P. aeruginosa*) genera, with a high number of facultative anaerobe microbes such as *Enterobacter* species. CONS that are mainly commensals on the skin (*S. epidermidis*) are also present in the wound (Wolcott *et al.*, 2016; Verbanic *et al.*, 2020). The role of commensals and facultative anaerobes in wound infection is still unclear (Verbanic *et al.*, 2020).



In addition to single-species biofilm research, several other studies have designed dual-species of *S. aureus* and *P. aeruginosa* biofilm models to investigate the complexity and dynamics of the biofilm in the development of chronic wounds (Dalton *et al.*, 2011; Sun *et al.*, 2013; Alves *et al.*, 2018; Cendra *et al.*, 2019; Tognon *et al.*, 2019). For example, there is evidence that *S. aureus* and *P. aeruginosa* colonise different spots in the wound bed; *S. aureus* tends to settle in the surface area, while *P. aeruginosa* forms biofilm deeper in the wound site. Hence, in this case, the co-infection and interaction of these two species seem unlikely (Fazli *et al.*, 2009). However, in 2018 Alves and colleagues conducted a co-culture biofilm model, which indicated in the early stage of biofilm formation, the interaction of these two bacteria is beneficial for their settlement and survival. They reported that *S. aureus* facilitated the attachment of *P. aeruginosa* in the early stages of biofilm formation, and *P. aeruginosa* promoted an invasive phenotype in *S. aureus*. This interaction can support a stable infection (Alves *et al.*, 2018). Despite a large number of studies on biofilm-forming pathogens such as *P. aeruginosa* and *S. aureus*, there are a few studies reporting the role of skin commensals in chronic wounds. In the light of microbiome studies, the beneficial functions of commensals such as *S. epidermidis* are being discovered; for example, a subset of *S. epidermidis* releases a serine protease that prevents biofilm formation of nasal *S. aureus* (Iwase *et al.*, 2010). So, it is essential to consider the effect of commensal microbes in a biofilm model.

## 1.6.2 Human cells

Human cells involved in chronic wounds are keratinocytes, fibroblasts, endothelial cells, and resident immune cells. The healing process is regulated by a complex signalling network among these cells through secretion and sensation of cytokines and growth factors. Bacterial colonisation can disturb the balanced microenvironment of the wound by over-attracting neutrophils and macrophages to the site of injury, which subsequently increases the production of pro-inflammatory cytokines such as IL-1 $\alpha$ , IL-1 $\beta$ , IL-6, and TNF- $\alpha$  and the release of ROS. An increase in pro-inflammatory cytokines escalates the secretion of metalloproteinases and elastases, which eventually degrade ECM and impair cell migration. Fragments of ECM and resistant biofilms stimulate the constant influx of

immune cells, therefore, amplifying the inflammation in the wound area (Frykberg and Banks, 2015). Keratinocytes produce cytokines and growth factors to control the wound healing process and re-epithelisation. They recognise pathogens in the wound area through TLRs and respond to them by secretion of antimicrobial peptides and inflammatory cytokines. For example, *S. aureus* can activate NF- $\kappa$ B in keratinocytes. NF- $\kappa$ B activates the transcription of the inflammation genes such as IL-8 and nitric oxide (Mempel *et al.*, 2003). There is evidence that *S. aureus* in the biofilm state increases inflammatory cytokine production, nitric oxide production, and reduced viability of human keratinocytes compared to *S. aureus* in the planktonic state. Excessive inflammations degrade ECM, impair keratinocytes migration and proliferation, and damage re-epithelisation, which is a significant step in wound healing (Tankersley *et al.*, 2014).

Host-microbe interactions at the wound site can determine the state of wound healing and direct it toward recovery or deterioration, so it is important to consider human cells in *in vitro* models to investigate wound physiology. Some studies reported the effect of biofilm on cytokine gene expression, proliferation, and cell apoptosis in co-cultured biofilm or biofilm-conditioned media with keratinocytes and fibroblast (Kirker *et al.*, 2009; Secor *et al.*, 2011; Kirker *et al.*, 2012; Tankersley *et al.*, 2014; 1Olender *et al.*, 2019).

One of the limitations of these studies is that they all use single-species biofilm, while for more realistic experiments, it would be helpful to consider dual or multi-species biofilm effects on human skin cells. Another way to improve the *in vitro* models to study host-microbe interactions is to use 3D human skin models, also known as Human Skin Equivalent. These models are made of keratinocytes and fibroblasts cultured on the protein matrix (composed of collagen and fibronectin). They can be a suitable model for studying chronic wounds as they are more relevant to human skin physiology (Haisma *et al.*, 2013).

### 1.6.3 Extracellular matrix proteins (ECM proteins)

ECM proteins comprised of organised macromolecules (such as collagen, fibrin, fibronectin, proteoglycan, glycosaminoglycan, and matricellular proteins) form a complex structure in wound bed with several roles in wound healing. They also provide a suitable surface for

bacterial attachment and colonisation in chronic wounds (Fitzpatrick *et al.*, 2012). So, it would be closer to reality in wound infection to investigate biofilm attachment to the protein matrix instead of the microplate's surface. Several *in vitro* models incorporated ECM proteins as a platform for biofilm development to stimulate the biofilm's structure in the wound (Werthen *et al.*, 2010; Chen *et al.*, 2014; Gounani *et al.*, 2020). In an *in vitro* study, researchers developed a collagen gel matrix model filled with serum proteins to provide a protein-rich platform for bacterial colonisation. The model enabled bacterial biofilm formation in a similar way to the structure of biofilm in chronic wound infection. This study indicated the presence of a wound-like microenvironment in the model that can be used for biofilm simulation (Werthen *et al.*, 2010).

### 1.6.4 Chemicals

In addition to the interaction between microbial cells and skin cells, the microenvironment of the wound is an important factor in the pathogenesis and healing process. The concentration/level of factors such as oxygen, ROS, pH, and signalling molecules in the wound affects the biochemical and cellular processes in wound healing.

**Oxygen.** A balanced oxygen level in the wound is vital for various steps in the healing process, such as collagen deposition, epithelisation, and angiogenesis. The formation of new blood capillaries (angiogenesis) is responsible for the oxygenation of the wound area; the concentration of oxygen in the area controls this process. However, there is inadequate oxygen in chronic wounds due to the increase in oxygen utilisation in chronic wounds and elevated ROS (Scalise *et al.*, 2015). Low oxygen level in the wound bed favours the growth of facultative bacteria, which in turn decreases the oxygen level further. Also, low or zero levels of oxygen (hypoxia and anoxia) in the wound can affect the efficacy of antibiotics and promote tolerance of biofilm to antibiotic therapy (Castilla *et al.*, 2012).

**pH.** The pH of the environment affects the oxygen released from blood to the tissue. Tissue oxygenation increases by a decline in pH level. The normal pH of the skin is acidic (4 – 6), which is one of the defence mechanisms of the skin against microbial colonisation. However, in chronic wounds, damaged cells and capillaries diffuse body fluid with a pH of

7.4 to the area; this can shift the pH of the skin from acidic to alkaline. Alkaline pH in the wound has some detrimental effects; for example, it can reduce the oxygenation to the tissue, it increases the risk of microbial colonisation as they favour neutral to an alkaline environment, and it increases the catalytic activity of proteases in the wound, which can cause degradation of ECM. Even subtle changes in a wound's pH can make a big difference in wound healing and antibiotic treatment (Scalise *et al.*, 2015).

**ROS.** Elevated ROS in the wound bed is one of the major factors that impairs wound healing. ROS are normal by-products of cellular respiration in mitochondria, and low levels of ROS mediate intracellular signalling; they are also required in defence against pathogens as neutrophils and macrophages secrete them. However, an excessive amount of ROS causes cellular damage due to their high reactivity, so the antioxidant system in the cells aims to neutralise excess ROS and ameliorate their toxic effect (Cano Sanchez *et al.*, 2018). When the antioxidant defence system fails to inactivate a high level of ROS, cells undergo "oxidative stress," which leads to the loss of function and even cell death. A chronic wound is one of the conditions in that oxidative stress is involved due to sustained inflammation, the constant presence of neutrophils and macrophages, and an increased level of ROS. An elevated level of ROS in chronic wounds is associated with delayed re-epithelisation, cellular damage, delayed angiogenesis, and a proteolytic environment. (Nouvong *et al.*, 2016).

## Aim and objectives

In this study, two strains of *P. aeruginosa* strains NCTC 10662 and PAO1, which are originally isolated from infected wounds, were selected. *S. epidermidis* NCTC 11047, a nose isolate, was also selected as a skin commensal. Immortalized human keratinocytes, HaCaT cell line, was used as a skin model system. The hypothesis that commensal bacteria can impact the pathogenicity of opportunistic bacteria and subsequently protect skin cells was explored.

The overall aim of this study was to investigate the interaction between *S. epidermidis* and its supernatant with planktonic growth and sessile cultures of *P. aeruginosa* to better understand how commensal bacteria affect skin cells during wound infection. To address the overall aim of this project, the following objectives were addressed:

- To investigate the effects of *S. epidermidis* supernatant on planktonic growth, biofilm formation, and virulence factors secretion of *P. aeruginosa*.
- To determine the role of the quorum sensing network in the interaction of *S. epidermidis* and *P. aeruginosa*.
- To study the co-culture of *S. epidermidis* and *P. aeruginosa* in planktonic and biofilm growth.
- To examine the effects of *S. epidermidis* and its supernatant on *P. aeruginosa*'s antibiotic susceptibility.
- To study the effects of *S. epidermidis* supernatant on an *in vitro* wound healing model of keratinocytes.
- To investigate the ability of *S. epidermidis* and its supernatant in protecting keratinocytes from the attachment of *P. aeruginosa*.

# Chapter 2 Material and Methods

## 2.1 Materials

All bacterial culture media ingredients were purchased from Oxoid (UK), Sigma-Aldrich (Dorset, UK), and Sigma Life Sciences (Dorset, UK).

Tissue culture media and reagents were purchased from ThermoFisher Scientific (Gibco and Invitrogen, Loughborough, UK) and Sigma Life Sciences (UK). Tissue culture vessels, including microwell plates, flasks, and falcon tubes, were obtained from Corning (UK).

All reagents for extraction and purification of RNA and reverse transcription reaction were obtained from ThermoFisher Scientific (Applied Biosystem and Invitrogen, Loughborough, UK). Eurofins Genomics (Ebensburg, Germany) provided the primers. The Proteome Profiler Human Cytokine Array kit was purchased from R&D Systems, Bio-Techne, (Minneapolis, USA). Unless otherwise stated, all other reagents were purchased from Sigma-Aldrich (Dorset, UK) or Fisher Scientific (Loughborough, UK).

The spectrophotometer used to measure the absorbance in a microplate was from SPECTROstar Nano, BMG Labtech, Germany, while the absorbance in cuvettes was measured using Jenway 6300 Spectrophotometer, UK.

### 2.1.1 Bacterial strains

*S. epidermidis* NCTC 11047, *P. aeruginosa* NCTC 10662 and *P. aeruginosa* PAO1 were obtained from the University of Westminster, London culture collection.

### 2.1.2 Mammalian cell line

Immortalized human keratinocytes cell line, HaCaT cells (ATCC CCL-185), was obtained from the University of Westminster cell culture collection, generally a donation from the Division of Surgery and Interventional Science, UCL, Royal Free Hospital, London, UK.

## 2.2 Bacterial cell culture methods

### 2.2.1 Media preparation

All media for bacterial cultures were prepared according to the manufacturer's instructions and sterilized by autoclaving at 121°C for 15 minutes. Briefly, to prepare the broth culture medium, the proper amount of medium powder was dissolved in distilled water for a final volume of 1 litre. If the medium required supplementation of agar, 15 g/L agar was added to the medium while being continuously stirred on a magnetic hot plate until the agar was completely dissolved. All culture media used in this study are listed in Table 2.1.

### 2.2.2 Bacterial culture conditions and inoculum preparation

All bacterial strains were maintained in 25% (v/v) glycerol stocks at -20°C for storage for up to 6 months and -80°C for long-term storage. To prepare working stocks, a loopful of bacteria from freezer stock was streaked on a tryptone soy agar (TSA) and incubated aerobically overnight (18 – 24 hours) at 37°C. A single colony of plated bacteria was inoculated in 10 ml tryptone soy broth (TSB) in a falcon tube and incubated overnight at 37°C at 180 rpm. A loopful of liquid culture was then streaked on TSA slants, incubated overnight at 37°C, and then stored at 4°C. The working stocks were refreshed every 4 months by culturing stocks from -80°C storage. As described by Cowan and Steel (2009), Gram stains were performed for the basic characterization of bacteria when they were received.

Bacterial cells were subcultured into TSB from a slant stock culture and incubated overnight at 37°C and 180 rpm. By adding fresh media, the overnight culture's optical density (OD) at 600 nm was adjusted to 0.08 – 0.12 using a spectrophotometer (Jenway 6300 Spectrophotometer, UK). The OD<sub>600</sub> of 0.08 – 0.12 is equivalent to 0.5 McFarland standard and contains approximately  $1.5 \times 10^8$  colony forming units (CFU)/ml. Subsequently, the culture was diluted 1:10 in fresh media for further experiments for consistency in the number of cells.

**Table 2.1** Media and their components used in this study.

Bacterial culture media	Composition
Tryptone Soy Broth (TSB)	pancreatic digest of casein 17.0 g/L, enzymatic digest of soya bean 3.0 g/L, sodium chloride 5.0 g/L, dipotassium hydrogen phosphate 2.5g/L, glucose 2.5 g/L
Tryptone Soy Agar (TSA)	agar 15 g/L, pancreatic digest of casein 17.0 g/L, enzymatic digest of soya bean 3.0 g/L, sodium chloride 5.0 g/L, dipotassium hydrogen phosphate 2.5g/L, glucose 2.5 g/L
Muller Hinton Broth (MHB)	beef infusion solids 2.0 g/L, starch 1.5 g/L, casein hydrolysate 17.5 g/L
Muller Hinton Agar (MHA)	agar 15.0 g/L, beef infusion solids 2 g/L, starch 1.5 g/L, casein hydrolysate 17.5 g/L
Luria Bertani Broth (LB)	sodium chloride 10.0 g/L, tryptone 10.0 g/L, yeast extract 5.0 g/L
Roswell Park Memorial Institute (RPMI)-1640 Nutrient Broth (NB)	glucose 2 g/L, phenol red 5 mg/L, salts without sodium bicarbonate, amino acids without L-glutamine, vitamins
Nutrient Agar (NA)	meat extract 1.0 g/L, yeast extract 2.0 g/L, peptone 5.0 g/L, sodium chloride 5.0 g/L
Staphylococcus Agar	agar 15.0 g/L, dipotassium hydrogen phosphate 5.0 g/L, gelatine 30.0 g/L, lactose 2.0 g/L, mannitol 10.0 g/L, sodium chloride 75.0 g/L, tryptone 10.0 g/L, yeast extract 2.5 g/L
Cetrimide Agar	agar 15 g/L, cetrimide, 0.3 g/L, gelatine peptone 20 g/L, magnesium chloride 1.4 g/L, potassium sulfate, 10 g/L, 1% (v/v) glycerol

### 2.2.3 Growth curve

The turbidity of the bacterial culture in TSB over 24 hours of growth was used to plot a growth curve against time. The OD<sub>600</sub> of overnight culture was adjusted to 0.08 – 0.12; next, it was diluted, 5 ml in 45 ml fresh media (1:10 ratio) in a shaking flask and incubated for 24 hours at 37°C and 180 rpm. The OD of the culture medium was measured at 600 nm every hour using a spectrophotometer. Every 2 hours, ten-fold serial dilution of the culture



was made using phosphate buffer saline (PBS) and drop plated on TSA, and subsequently, incubated overnight at 37°C to determine the CFU for each sample.

CFU per 1 ml of the original culture was calculated using the equation below (Equation 2.1):

$$\text{CFU/ml} = (\text{number of colonies} \times \text{dilution factor}) / \text{volume of culture per plate}$$

Generation time, also known as doubling time, can be measured by the equation below (Equation 2.2):

$$t_d = \text{Ln } 2 / \mu$$

Where:

$t_d$  = doubling time, and

$\mu$  = specific growth rate

The specific growth rate can be derived from the slope of the natural logarithm of the culture concentration (the exponential phase) against time. Measuring the growth rate can be based on the CFU/ml or OD against time (assuming that the OD is directly proportional to the number of live cells).

## 2.2.4 Preparation of *S. epidermidis* supernatant (SES)

The OD<sub>600</sub> of the overnight culture of *S. epidermidis* was adjusted to 0.08 – 0.12 and set as an inoculum. The inoculum was then diluted 1:10 in fresh TSB in shaking flasks and incubated at 37°C and 180 rpm for 24 hours. Samples were taken at different stages of bacterial growth: 3 hours after incubation for the early-exponential phase, 5 hours after incubation for the mid-exponential phase, 7 hours after incubation for the late-exponential phase, and 24 hours after incubation for full growth. After taking samples at different time points, bacterial cultures were centrifuged at 3000 rpm for 10 minutes to collect the SES. Afterwards, they were filtered using a 0.22 µm filter (Ministar Syringe Filter, Sartorius, Germany). The SES (30 µl) was transferred to agar plates to ensure no viable bacteria were present. The SES was stored at -20°C for further experiments. In all experiments, the concentration of SES in the culture medium was set at 10% (v/v) unless otherwise stated.

## 2.2.5 Protein assay on the SES

Protein concentrations in the SES were determined by Bradford Micro Assay (Quick Start Bradford, Bio-Rad, USA), a fast and accurate method to determine the total protein content of a sample. A microtiter-plate assay was adopted for this experiment. This assay is based on the reaction of Coomassie brilliant blue dye with protein in the given sample (Bradford, 1976). The colour change after the reaction was detected at 595 nm. Bovine serum albumin (BSA) (Sigma-Aldrich, UK) at 2 mg/ml was used as a stock to prepare standard protein solutions according to the manufacturer's instructions (Table 2.2). A series of dilutions of BSA was made from the stock in Eppendorf Tubes® at a final volume of 1 ml based on Table 2.2. Afterwards, 150 µl of the prepared standards and samples were added to each well of a 96-well plate, and then 150 µl of Bradford's dye reagent was added and mixed thoroughly with the samples. The plate was incubated at room temperature for 15 minutes. The absorbance was read at 595 nm using a spectrophotometer (SPECTROstar Nano, BMG Labtech, Germany). The standard curve was constructed based on the reading of serially diluted standard solutions. The protein concentration in each sample was calculated using the equation of the standard curve linear trendline (Figure 2.1).

**Table 2.2** Standard protein solution used to make a standard curve.

Tube	Protein Stock	Stock volume (µl)	Distilled water (µl)	Protein Conc. (µg/ml)
1	BSA (2 mg/ml)	10	790	25
2	BSA (2 mg/ml)	10	990	20
3	BSA (2 mg/ml)	6	794	15
4	Tube 2	500	500	10
5	Tube 4	500	500	5
6	Tube 5	500	500	2.5
7	Tube 6	500	500	1.25

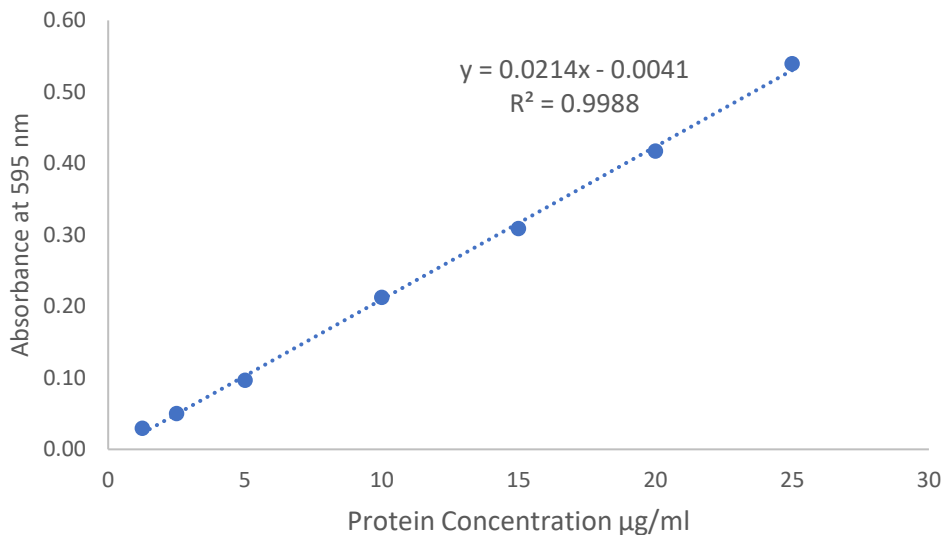


**Figure 2.1** Protein standard curve to measure protein concentration in SES sample. The protein concentrations were determined using the equation of linear trendline.

## 2.2.6 Crystal violet biofilm formation assay

*P. aeruginosa* biofilm formation in the presence and absence of SES was assessed using the microtiter plate crystal violet assay as described in several *in vitro* model studies (Merritt *et al.*, 2005; O Toole, 2011) with some modifications. *P. aeruginosa* biofilms were formed in a 96-well plate. The OD<sub>600</sub> of an overnight culture was adjusted to 0.08 – 0.12. Then 20 µl of the culture was added to 180 µl of fresh media (with and without SES) per well. The plates were then incubated at 37°C for 24 hours. After the incubation period, the contents of the wells were gently removed, and the wells were gently washed twice with distilled water to remove planktonic bacterial cells. Biofilm was stained with 220 µl of 1% (v/v) solution of crystal violet for 15 minutes at room temperature. Then the crystal violet solution was removed, and the plate was washed gently with distilled water till the water ran clear. The plate was then allowed to dry completely in a 37°C incubator before adding acetic acid. Acetic acid at 30% (v/v) (220 µl) was added to each well. The plate was incubated at room temperature for 15 minutes while shaking gently at 75 rpm on an orbital shaker. The absorbance at 570 nm was measured. Experiments were performed three times using three biological replicates each time.

## 2.2.7 Extraction of extracellular polymeric substances (EPS) from *P. aeruginosa* biofilm

To investigate the composition of *P. aeruginosa*'s EPS in the presence and absence of SES, the formaldehyde-sodium hydroxide (NaOH) method was used to extract the EPS (Liu and Fang, 2002). In this method, formaldehyde (Sigma Life Sciences, UK) is used to fix the cells to prevent them from lysis and release of their intracellular contents. NaOH increases the pH, which results in the increase of solubility of EPS in water, therefore, allowing a higher quantity of EPS to be extracted (Liu and Fang, 2002).

To extract the EPS, the biofilm was detached using a 100 µl pipette tip and resuspended in PBS. Formaldehyde at 6% (v/v) was added to the homogenized biofilm and incubated at 4°C for 1 hour. NaOH (1 M at 40% v/v) was added to the solution and incubated for another 3 hours at 4°C. The solution was then centrifuged at 8000 rpm at 4°C for 30 minutes. The resulting supernatant was filtered using a 0.22 µm membrane filter and stored at -20°C for further analysis.

### 2.2.7.1 Carbohydrate assay on EPS

The phenol-sulfuric acid method was used to determine the quantity of carbohydrates in *P. aeruginosa* biofilm. This method was adopted from Masuko and colleagues' study in 2005 with some modifications (Masuko *et al.*, 2005). Glucose solution at 1 mg/ml was used as a stock to prepare standard glucose solutions ranging from 1 -100 µg/ml (Figure 2.2). The carbohydrate assay was performed in a 96-well microtiter plate. Into 50 µl of the standard and the samples in each well, 150 µl of concentrated sulfuric acid was added, and the mixture was shaken on an orbital shaker for 5 minutes. Then 30 µl of 5% (v/v) phenol was added to the mixture, and the plate was carefully floated in a 90°C water bath for 5 minutes. The plate was cooled to room temperature for 5 minutes, and the absorbance was measured at 490 nm. The standard curve was created using the readings of the standard glucose solutions. The carbohydrate concentration in each sample was calculated using the equation of the standard curve linear trendline (Figure 2.2).

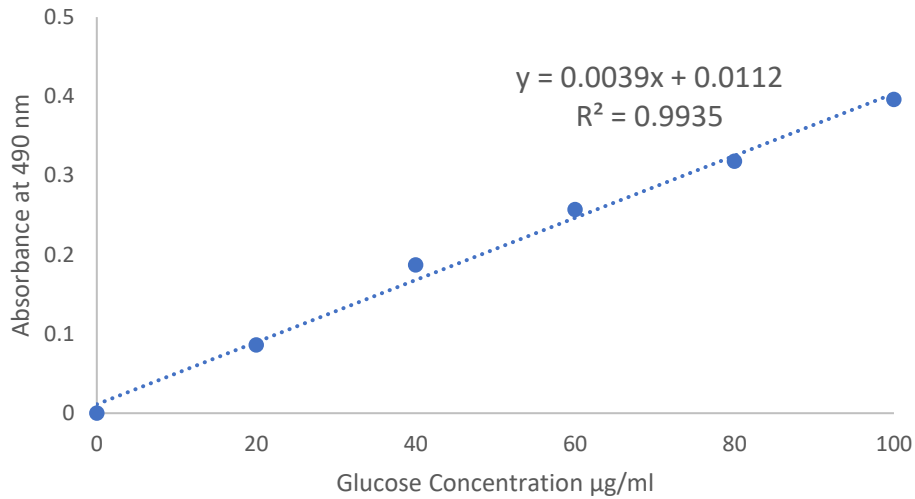


**Figure 2.2** Glucose standard curve to measure carbohydrate concentration in EPS sample. The carbohydrate concentration of the samples was determined using the equation of linear trendline.

### 2.2.7.2 Protein assay on EPS

The Bradford Micro Assay (Quick Start Bradford, BIO-RAD, USA), as described in Section 2.2.5, was used to determine the protein concentration in *P. aeruginosa* biofilm. Briefly, a series of dilutions were made from BSA stock (2 mg/ml) based on the instruction described in Table 2.2 (Section 2.2.5). Subsequently, 150 µl of the BSA standard solutions and the ESP samples were added to each well of a 96-well microtiter plate, and then 150 µl of Bradford's dye reagent was added and mixed properly with the standards and samples, incubated at room temperature for 15 minutes. The absorbance was measured at 595 nm, the standard curve was created using the reading of the standard solutions (Figure 2.3), and the protein concentration in each sample was calculated using the standard curve linear trendline equation. Each experiment was repeated three times with three biological replicates each time.

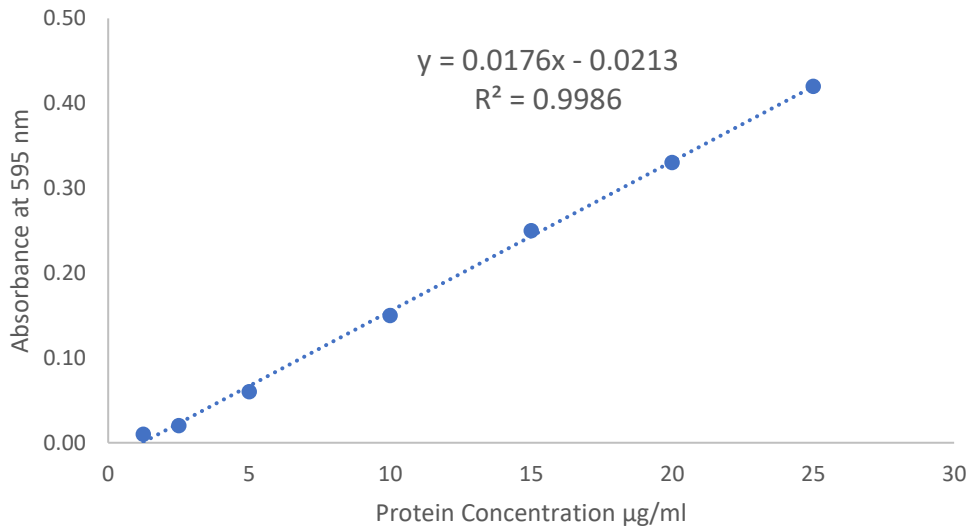


**Figure 2.3** Protein standard curve to measure protein concentration in EPS sample. The protein concentrations were determined using the equation of the linear trendline.

### 2.2.7.3 eDNA quantification in EPS

The eDNA content of the biofilm was measured using the NanoDrop™ spectrophotometer (Ambion, ThermoFisher Scientific, UK) based on the manufacturer's instructions. Briefly, the instrument was blanked using 1 µl of PBS in 40% (v/v) in 1 M NaOH solution. The concentration of dsDNA was calculated by the NanoDrop™ based on the absorbance at 260 nm and reported as ng/µl concentration.

## 2.2.8 Assessment of *P. aeruginosa* virulence factors

### 2.2.8.1 Pyocyanin quantification

To quantify pyocyanin production in the culture of *P. aeruginosa*, a method developed by Essar *et al.* 1999 with modification was adopted for this study.

*P. aeruginosa* was grown in 25 ml of LB medium in conical flasks in the presence and absence of SES at 37°C and 180 rpm. After 24 hours of incubation, the cultures were pelleted by 5000 rpm centrifugation for 20 minutes at 4°C, and the supernatants were filter-sterilized using 0.22 µm filters. Afterwards, a chloroform-hydrochloric acid extraction was performed; 7.5 ml of the supernatant was added to 4.5 ml of chloroform and vortexed

for 20 seconds to mix the supernatant with chloroform thoroughly. The tubes were then centrifuged at 5000 rpm at 4°C for 10 minutes, 3 ml of blue-green phase (chloroform phase) at the bottom was transferred to a new tube, and 1.5 ml of 0.2 M hydrochloric acid was added to it, vortexed for 20 seconds. Samples were centrifuged at 5000 rpm at 4°C for 5 minutes; 1 ml of pink solution at the top phase was used to measure the absorbance at 520 nm (0.2 M hydrochloric acid was used as blank). To calculate the pyocyanin concentration in 1 ml of *P. aeruginosa* culture supernatant, the absorbance was multiplied by the extinction coefficient of 17.072 and 1.5 (dilution factor) (Essar *et al.* 1999). This experiment was repeated three times and each time with three replicates reading.

### 2.2.8.2 Pyoverdine quantification

For pyoverdine quantification, *P. aeruginosa* was grown in RPMI 1640 medium as a defined medium with no traceable iron. *P. aeruginosa* was grown in 25 ml of in RPMI 1640 the presence and absence of SES in 100 ml conical flasks at 37°C and 180 rpm. After 24 hours of incubation, the absorbance of the cultures at 600 nm was measured to record the bacterial growth. The cultures were then centrifuged at 5000 rpm for 30 minutes and filtered through 0.22 µm filters. The absorbance of the supernatants was measured at 405 nm (Sass *et al.*, 2018). The pyoverdine production was normalized using the equation below (Equation 2.3):

$$\text{Relative Pyoverdine Expression} = \text{Absorbance at 405 nm} / \text{Absorbance at 600 nm}$$

### 2.2.8.3 Assessment of elastase activity

The elastase activity of *P. aeruginosa* was determined using elastin Congo red assay as described by Pesci and colleagues in 1997 with some modifications (Pesci *et al.*, 1997). Elastin Congo red (ECR) complex is insoluble in the ECR buffer (100 mM Tris, 1mM CaCl<sub>2</sub>, pH 7.5); however, in the presence of elastase activity, elastin is digested, and the Congo red is released from the dye-elastin complex, resulting in a colour change of the buffer from no colour to red. *P. aeruginosa* was grown in 25 ml of LB medium in the presence and absence of SES in 100 ml conical flasks at 37°C and 180 rpm. After 24 hours of incubation, the supernatant was separated by centrifugation at 5000 rpm for 20 minutes. ECR powder

at 20 mg/ml was added to the ECR buffer. Bacterial culture supernatant was mixed at a 1:1 ratio with ECR buffer mixture and incubated in shaking flasks at 37°C for 20 hours. The supernatant was then extracted by centrifugation, and the absorbance of released Congo red dye was measured at 495 nm. This experiment was performed three times with three replicates each time.

#### 2.2.8.4 Motility assay

The motility of *P. aeruginosa* was tested on agar plates containing different concentrations of agar powder, as described by Rashid and Kornberg in 2000, with some modifications. The nutrient broth was supplemented with 0.3% (w/v) agar to test swimming capability. For swarming motility assessment, the nutrient broth was supplemented with 0.5% (w/v) agar. For bacterial twitching evaluation, LB broth was supplemented with 1% (w/v) agar. To test the impact of SES on the motility of *P. aeruginosa*, the agar plates were supplemented with SES at 10% (v/v) before solidifying. All the agar plates were dried overnight in a safety cabinet to avoid any moisture on their surface.

The OD<sub>600</sub> of overnight cultures of *P. aeruginosa* was adjusted to 0.1. To test swimming and swarming motility, 3 µl of the cell suspension was added to the centre of 0.3% (w/v) nutrient agar and 0.5% (w/v) nutrient agar, respectively. For the twitching assay, 1% (w/v) LB agar was stab inoculated with a needle. The plates were incubated at 37°C for 24 hours prior to measuring the diameter of the migration zone.

#### 2.2.9 Evaluating antibiotics susceptibility in *P. aeruginosa*

The minimum inhibitory concentration (MIC) of antibiotics tetracycline hydrochloride (Sigma Aldrich, UK), gentamicin (ThermoFisher Scientific, UK), and ciprofloxacin (Sigma Aldrich, UK) were determined by the micro-dilution assay in 96-well microtiter plates according to the recommendation of the European Committee for Antimicrobial Susceptibility Testing (EUCAST) regulations (Leclercq *et al.*, 2013). Briefly, serial dilution of antibiotics in MHB and TSB ranging from 0.25 to 512 µg/ml was prepared in 96-well microtiter plates. The OD<sub>600</sub> of overnight bacterial culture was adjusted to 0.09 – 0.11, representing  $1.5 \times 10^8$  CFU/ml and equivalent to 0.5 McFarland. The suspension was



subsequently diluted 1:100 (v/v) in the antibiotic microplates to achieve  $1.5 \times 10^5$  CFU/ml cell suspension. The culture was incubated then at 37°C for 24 hours. The MIC was determined as the lowest concentration of antibiotic for which no visible growth could be observed after 24 hours of incubation. Also, the absorbance of the cultures was determined by spectrophotometry at 600 nm, and the absorbance below or equal to 0.05 was considered MIC. To determine the minimum bactericidal concentration (MBC) of antibiotics, 10 µl of culture with no visible growth was cultured on MHA, and TSA followed with 24 hours of incubation. The MBC was determined as the lowest concentration of the antibiotic when no visible growth was observed, and it ultimately killed all bacterial cells within the population during the incubation period of 24 hours, according to the EUCAST of the European Society of Clinical Microbiology and Infectious Diseases (ESCMID). To further evaluate the viability of bacterial cells in co-culture and after antibiotic treatment, a series of ten-fold dilutions of cultures were made and 10 µl of each sample was dropped on the selective agar plates. CFUs were counted from the sample, which contained 5 – 20 colonies.

## 2.2.10 Evaluating the combined activity of antibiotics and SES on preformed biofilm of *P. aeruginosa*

The established biofilm of *P. aeruginosa* was prepared by inoculating 20 µl of bacterial cell suspension ( $OD_{600}$  adjusted to 0.08 – 0.12) into a total volume of 200µl of fresh TSB in 96-well plates. The cultures were incubated at 37°C for 24 hours. After 24 hours, planktonic cells were gently removed, and the wells were washed gently with PBS to remove the remaining non-attached cells. Then serial dilutions of antibiotics solutions ranging from 0.25 – 512 µg/ml with and without SES were added to corresponding wells. Then the plates were incubated at 37°C for another 24 hours. After the incubation period, wells were washed twice with PBS, and the biofilm biomass and cell viability after treatment were determined by crystal violet and MTT (3-(4,5-dimethylthiazol-2-yl)-2,5-diphenyltetrazolium bromide) assay, respectively. This experiment was repeated three times and each time with at least three biological replicates.

### 2.2.10.1 Crystal violet assay on preformed biofilm

For the crystal violet assay, after two washing steps, 220  $\mu\text{l}$  of 0.1% (v/v) crystal violet was added into each well and incubated for 15 minutes at room temperature. The crystal violet solution was removed gently and washed off with distilled water three times, and the plate was air dried for a few hours. The dye was then solubilized using 220  $\mu\text{l}$  of 30% (v/v) acetic acid solution and incubated at room temperature for 15 minutes. The absorbance of each well was measured at 570 nm using a spectrophotometer.

### 2.2.10.2 MTT assay on preformed biofilm

MTT is a water-soluble yellow tetrazolium salt. Metabolically active cells reduce MTT to water-insoluble purple formazan crystals. Then the crystals will be dissolved in dimethyl sulfoxide (DMSO), and the formazan production is quantified by spectrophotometry. The total amount of formazan produced is directly proportional to the number of viable cells in the culture (Mosmann, 1983; Tom *et al.*, 1993). To determine the viability of the cells in the biofilm after treatment, the MTT assay was performed. After the incubation period of 48 hours, wells were washed twice with PBS and then were filled with 200  $\mu\text{l}$  of fresh TSB. Subsequently, 20  $\mu\text{l}$  of 5 mg/ml MTT reagent (Vybrant MTT cell viability assay, ThermoFisher Scientific, UK) in PBS was added to all wells. Plates were incubated at 37°C for 3 hours in the dark. The formazan crystal produced by metabolically active cells was solubilized using 220  $\mu\text{l}$  of DMSO and mixed by gentle pipetting. The absorbance of the solution was measured at 570 nm using a spectrophotometer. The percentage of viability of the cells was reported using the equation below (Equation 2.4):

$$\text{Viability of cells \%} = \frac{\text{Absorbance of treated wells}}{\text{Absorbance of non treated wells}} \times 100$$

## 2.2.11 Accumulation assay

To assess the activity of *P. aeruginosa*'s efflux pump in the presence and absence of SES, a fluorometric assay based on ethidium bromide's (EtBr) fluorescent signal was performed. Bacterial cells uptake ethidium bromide if present in their culture medium through the efflux system and cell wall permeability. The fluorescent signal of ethidium bromide in the

culture medium is weak; however, when it is accumulated inside the cells and bound to DNA, it radiates a strong signal (Paixao *et al.*, 2009). By tracking the fluorescent signal of ethidium bromide over an hour, the uptake of the ethidium bromide can be tracked and therefore identify efflux system activity (Blair and Piddock, 2016). Bacterial cells were grown till they reached the OD of 0.8 to 1 at 600 nm. The OD then was adjusted to 0.4 at 600 nm by centrifugation at 3000 rpm for 5 minutes and resuspending the pellet in PBS. SES was added to the bacterial suspension at the final concentration of 10% (v/v). Glucose was used as an energy source at the final concentration of 0.4% (w/v). Then bacterial suspension with the supernatant and glucose was transferred to a 96-well plate and the ethidium bromide at the final concentration of 2 µg/ml was added to each well. Bacterial suspension without SES and with glucose and ethidium bromide was set as control. The reaction was run using a Fluostar Optima plate reader (SPECTROstar Nano, BMG Labtech, Germany) at 37°C for an hour. Every minute the absorbance was taken at excitation 520 nm and emission at 590 nm.

To assess the activity of the efflux pump in *P. aeruginosa* in co-culture with *S. epidermidis*, *P. aeruginosa* and *S. epidermidis* were grown separately till they reached OD of 0.8 to 1 at 600 nm. The OD of each bacterial suspension was adjusted to 0.4 at 600 nm. Bacterial suspensions were then mixed at a 1:1 ratio and transferred to a 96-well plate. Glucose at the final concentration of 0.4% (w/v) and ethidium bromide at the final concentration of 2 µg/ml were added to each well. The mono-culture of *P. aeruginosa* with glucose and ethidium bromide was set as control. The reaction was run as described previously using a Fluostar Optima plate reader.

## 2.2.12 Planktonic co-culture growth curve

The overnight cultures of *P. aeruginosa* and *S. epidermidis* were centrifuged at 3000 rpm for 5 minutes. The pellets were resuspended in fresh TSB, and their OD<sub>600</sub> was adjusted to 0.08 – 0.12; then, they were mixed in a 1:1 (v/v) ratio to be used as inoculum for the co-culture growth. The mixed culture inoculum (5 ml) was added to 45 ml of TSB in a 250 ml shaking flask and incubated at 37°C and 180 rpm. The OD<sub>600</sub> of the cultures was measured hourly using a spectrophotometer. Also, every 2 hours, samples from the cultures were

ten-fold serially diluted in PBS and plated on selective agars: cetrimide agar (Sigma-Aldrich, UK) and staphylococcus agar (Sigma-Aldrich, UK) to measure *P. aeruginosa* and *S. epidermidis* CFU/ml, respectively. For control, mono-cultures of *P. aeruginosa* and *S. epidermidis* were also set up, and the OD<sub>600</sub> and the CFU/ml were measured as described above.

**Assess the competition between *S. epidermidis* and *P. aeruginosa* in a co-culture growth**

The competitive index (CI) in mixed infections or co-culture provides an accurate and sensitive comparison between each species' growth within the co-culture. The competitive index in dual-species growth indicates the competition between two species and any growth advantage of one species over the other.

To calculate CI at a specific time, the ratio of total viable cells (CFU) of each species at the desired time is divided by the ratio of the viable cell at time zero or inoculation. CFU data is obtained from the growth of the co-culture suspension on the selective agar. The CI was calculated using the equation below (Equation 2.5):

$$CI = \frac{(\log\text{CFU species A}/\log\text{CFU species B}) \text{ at } t = n \text{ in the coculture}}{(\log\text{CFU species A}/\log\text{CFU species B}) \text{ at } t = 0 \text{ in the coculture}}$$

If the CI value equals 0, it means equal competition between two species.

If the CI value > 0, it means a competitive advantage for the species on the numerator (species A).

If the CI value < 0, it means a competitive advantage for the species on the denominator (species B).

On the other hand, the relative increase ratio (RIR) compares the growth curves of both species in single-species culture. RIR is calculated based on the count of viable cells obtained from the single-species culture of each strain and is calculated in a similar way to CI using the equation below (Equation 2.6):

$$RIR = \frac{(\log\text{CFUml species A growth}/\log\text{CFU species B growth}) \text{ at } t = n}{(\log\text{CFU species A growth}/\log\text{CFU species B growth}) \text{ at } t = 0}$$

To determine which species has an advantage over the other or how they grow together, two values must be known: CI and RIR. These values can be depicted together in one figure

to compare the growth of each species on its own and in co-culture (Mach *et al.*, 2007; Milho *et al.*, 2019).

### 2.2.13 Biofilm co-culture model set up

To investigate the biofilm formation of *P. aeruginosa* in co-culture with *S. epidermidis*, a 48-hour biofilm model in a 96-well plate was set up. In this model, *P. aeruginosa* biofilm formation was investigated in three ways: 1) *P. aeruginosa* and *S. epidermidis* were co-cultivated at the same time for 48 hours, 2) *P. aeruginosa* was added to the 24-hour preformed biofilm of *S. epidermidis*, and 3) *S. epidermidis* was added to the 24-hour preformed biofilm of *P. aeruginosa*.

The overnight cultures of *P. aeruginosa* and *S. epidermidis* were centrifuged at 3000 rpm for 5 minutes. The pellets were resuspended in fresh TSB, and their OD<sub>600</sub> was adjusted to 0.08 – 0.12; the suspensions were diluted 10 times in TSB. The bacterial suspensions were mixed at a 1:1 (v/v) ratio, and 200 µl of the suspension was added to the individual wells of the 96-well plate for the co-culture model. The plates were incubated at 37°C for 24 hours.

To set up the mono-culture biofilm, the overnight cultures of *P. aeruginosa* and *S. epidermidis* were centrifuged at 3000 rpm for 5 minutes. The pellets were resuspended in fresh TSB, and their OD<sub>600</sub> was adjusted to 0.08 – 0.12; each bacterial suspension was diluted 10 times in TSB separately. From each bacterial suspension, 200 µl was added to the individual wells of the 96-well plate. The plates were incubated at 37°C for 24 hours.

After the 24 hours incubation period, the planktonic phase was discarded, and all the wells were washed gently once with PBS. As described above, a fresh 1:1 mixed suspension of *P. aeruginosa* and *S. epidermidis* was made, and 200 µl of the suspension was added to the co-culture wells. Fresh *S. epidermidis* suspension was prepared as described above, and 200 µl of the suspension was added to the preformed biofilm of *P. aeruginosa*. Freshly made suspension of *P. aeruginosa* (200 µl) was added to the *S. epidermidis* preformed biofilm. The plates were incubated for another 24 hours at 37°C (Figure 2.4).

The biofilm biomass after 48 hours of incubation was determined by the crystal violet assay, as described in Section 2.2.6.

To evaluate the viability of cells in the biofilm, after 48 hours of incubation, planktonic cells were removed gently, and all the biofilm containing wells were washed twice with 250  $\mu$ l of PBS to remove non-attached cells. The biofilm was then scraped off the surface of the wells using a pipette tip, and it was collected using 100  $\mu$ l of PBS. The bacterial aggregates were resuspended with vigorous pipetting and 10 seconds vortex to homogenize the suspension. A series of ten-fold dilutions were prepared using PBS and drop-plated on selective agar plates of cetrimide and staphylococcal selective agar to determine the CFU of *P. aeruginosa* and *S. epidermidis*, respectively. The agar plates were incubated at 37°C for 24 hours.

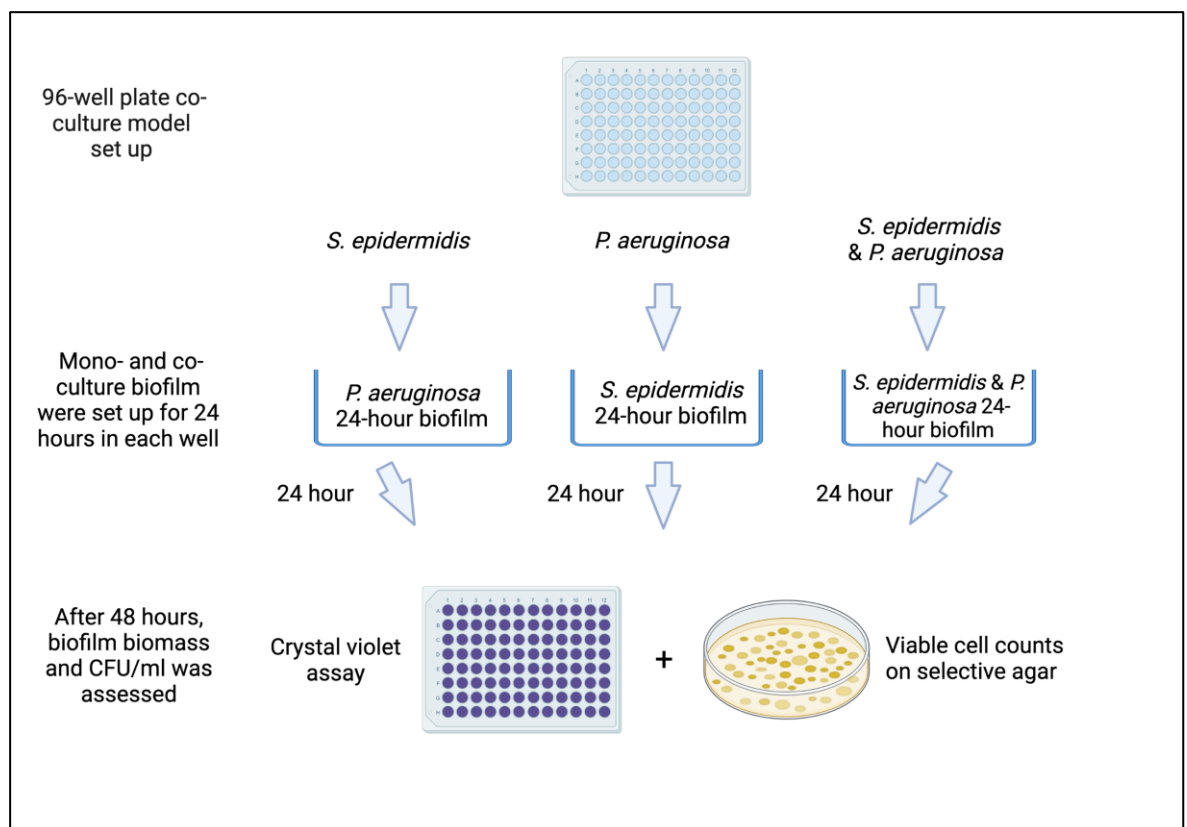


**Figure 2.4** Schematic illustration of biofilm co-culture set-up.

Mono-culture and co-culture of *S. epidermidis* and *P. aeruginosa* were set up for 24 hours at 37°C. After incubation, fresh bacterial suspension in mono-culture and co-culture was added to the respective wells and incubated for another 24 hours at 37°C. Crystal violet assay and viable cell count were performed to measure biofilm biomass and viable cell per ml, respectively.

## 2.2.14 Quantitative Reverse Transcription Polymerase Chain Reaction (RT-qPCR)

### 2.2.14.1 RNA extraction and purification

Based on the manufacturer's instruction, RNA from bacterial cells was extracted using the total RNA isolation (TRI) Reagent® (Invitrogen, ThermoFisher, UK). The OD<sub>600</sub> of the overnight culture of *P. aeruginosa* was adjusted to 0.08 – 0.12, and then the biofilm in the presence and absence of SES was set up in a 6-well plate at 37°C for 24 hours. After incubation, wells were washed once with PBS then 1 ml of TRI reagent per 10 cm<sup>2</sup> of culture dish was added. Lysing of the cells embedded in the biofilm was performed directly in the culture dish by pipetting them up and down several times until a homogenous mixture was attained. The mixture was then collected in 1.5 ml Eppendorf tubes, and 0.2 mL chloroform (Sigma Aldrich, UK) per 1 ml of TRI reagent was added, and RNA was separated from DNA and proteins in the sample by centrifugation at 2000 rpm for 15 minutes at 4°C. The aqueous phase at the top, which solely contained RNA, was collected. For RNA precipitation, 0.5 ml of isopropanol (Sigma Aldrich, UK) per 1 ml of TRI reagent was added; the mixture was vortexed for 10 seconds, then incubated for 10 minutes at room temperature, followed by centrifugation at 2000 rpm for 15 minutes at 4°C. RNA formed a white pellet at the bottom of the tube. RNA was washed with 75% ethanol (Sigma Aldrich, UK), and then the pellet was dissolved in 30 µl of nuclease-free water. The RNA was stored at 4°C for immediate analysis, and for long-term storage was stored at – 80°C.

RNA was purified using a DNA-free™ DNA Removal kit (Invitrogen, ThermoFisher, UK) according to the manufacturer's instructions. Briefly, 3 µl of 10X DNase I buffer with 1 µl of DNase I enzyme were added to 30 µl of RNA sample (1 µg/µl) and incubated at 37°C for 30 minutes. DNase I was inactivated by adding DNase Inactivation Reagent to the sample. RNA concentrations of the samples were determined using the NanoDrop™ instrument (Ambion, ThermoFisher Scientific, UK).

## 2.2.14.2 Reverse transcription

To synthesize complementary DNA (cDNA) from total RNA, a High Capacity cDNA Reverse Transcription Kit (Applied Biosystems, ThermoFisher) was used.

The reverse transcription master mix was prepared based on the manufacturer's instructions (Table 2.3), and it was kept on ice. For the cDNA reverse transcription reaction, 10  $\mu\text{l}$  of the master mix was mixed with 10  $\mu\text{l}$  of RNA (1  $\mu\text{g}/\mu\text{l}$ ) by pipetting up and down twice, followed by brief centrifugation (at 1000 rpm for 10 seconds) to spin down all the content. The reaction mixture was then incubated in a thermal cycler (T100™ Thermal Cycler, Bio-Rad, USA) at 25°C for 10 minutes, 37°C for 120 minutes, and 85°C for 5 minutes. cDNA was stored at -20°C.

**Table 2.3** Reverse transcription master mix composition.

Component	Reaction Volume ( $\mu\text{L}$ )
10 $\times$ RT Buffer	2.0
25 $\times$ dNTP Mix (100 mM)	0.8
10 $\times$ RT Random Primers	2.0
MultiScribe™ Reverse Transcriptase	1.0
RNase Inhibitor	1.0
Nuclease-free Water	3.2

## 2.2.14.3 Quantitative real-time PCR

The primers used in this study were purchased from Eurofins Genomics, Germany, and they are listed in Table 2.4. The stock of primers (100  $\mu\text{M}$ ) in nuclease-free water was made based on the manufacturer's instruction and stored at -20°C.

Quantitative real-time PCR was performed in Bio-Rad Hard-Shell® 96-Well microplates (Bio-Rad, USA), using the protocol from PowerTrack™ SYBR™ Green Master Mix (Applied Biosystems, ThermoFisher, UK). For 10  $\mu\text{l}$  of the reaction per well, 5  $\mu\text{l}$  of the SYBR™ Green Master Mix was mixed with 0.5  $\mu\text{l}$  of 8  $\mu\text{M}$  forward and reverse primers and 3.5  $\mu\text{l}$  of nuclease-free water. Then, 1  $\mu\text{l}$  of 5  $\text{ng}/\mu\text{l}$  cDNA was added to the mixture.



**Table 2.4** The primers that were used in this study (Kalgudi *et al.*, 2021).

Gene	Primer	Sequence
<i>lasI</i>	Forward	5' CGTGCTCAAGTGTTCAAGG 3'
	Reverse	5' TACAGTCGAAAAGCCCAG 3'
<i>lasR</i>	Forward	5'AAGTGGAAAATTGGAGTGGAG3'
	Reverse	5' GTAGTTGCCGACGACGATGAAG 3'
<i>rhII</i>	Forward	5' TTCATCCTCCTTAGTCTTCCC 3'
	Reverse	5' TTCCAGCGATTCAGAGAGC 3'
<i>rhIR</i>	Forward	5' TGCATTTTATCGATCAGGGC 3'
	Reverse	5' CACTTCCTTTCCAGGACG 3'
<i>toxA</i>	Forward	5' GGAGCGCAACTATCCCACT 3'
	Reverse	5' TGGTAGCCGACGAACACATA 3'
<i>rhIAB</i>	Forward	5' TCATGGAATTGTCACAACCGC 3'
	Reverse	5' ATACGGCAAATCATGGCAAC 3'
<i>rpsL</i>	Forward	5' CCTCGTACATCGGTGGTGAAG 3'
	Reverse	5' CCCTGCTTACGGTCTTTGACAC 3'

The reaction was set up in a centrifuge tube, then 10  $\mu$ l aliquots were added to the wells in triplicates. In control wells, nuclease-free water was used instead of cDNA. The housekeeping gene *rpsL* was used as endogenous control. The plate was sealed with an optical adhesive cover and centrifuged briefly to spin down the contents. The reaction was run in Bio-Rad CFX96™ Real-Time instrument (Bio-Rad, USA) with enzyme activation at 95°C for 2 minutes and 40 cycles of amplification, including denaturation at 95°C for 5 seconds and annealing/extension at 60°C for 30 seconds. Melting curve generation was followed in three steps of 1.99°C/second increase at 95°C for 15 seconds, 1.77°C/second at 60°C for 1 minute, and 0.1°C/second at 95°C for 15 seconds.

The cycle threshold was determined by the Bio-Rad CFX Maestro software, and relative gene expression was calculated using the  $\Delta\Delta$ Ct method (Livak and Schmittgen, 2001). The data obtained were normalized against the untreated control and represented a relative fold change in gene expression.

## 2.3 Mammalian cell culture methods

### 2.3.1 Mammalian cell culture conditions and maintenance

Keratinocytes were maintained in complete high glucose (4.5 g/l) Dulbecco's Modified Eagle Medium (DMEM) containing phenol red. DMEM was supplemented with 10% (v/v) foetal bovine serum (FBS) and 1% (v/v) penicillin-streptomycin solution, which contains 10,000 units/ml of penicillin, 10,000 µg/ml streptomycin, and 25 µg/ml Fungizone. The complete DMEM medium was used throughout the study unless otherwise stated. For long-term storage, cells were maintained in complete media containing 10% (v/v) DMSO, 10% (v/v) FBS, and 1% (v/v) penicillin-streptomycin at approximately  $1 \times 10^7$  cells/ml in cryovials. Cells were frozen slowly first at -80°C freezer before transferring into liquid nitrogen storage. A list of cell culture media and reagents to grow and maintain keratinocytes used in this study is shown in Table 2.5.

**Table 2.5** Cell culture media and reagents used in this study.

Cell Culture Media and Reagents	Supplier
High Glucose (4.5 g/l) Dulbecco's Modified Eagle Medium (DMEM)	Gibco, ThermoFisher Scientific, Loughborough, UK
Foetal Bovine Serum (FBS)	Sigma Life Sciences, UK
Penicillin-Streptomycin Solution	Gibco, ThermoFisher Scientific, Loughborough, UK
Dimethyl Sulfoxide (DMSO)	Sigma Life Sciences, UK
Dulbecco's Phosphate Buffered Saline (DPBS) (1X)	Gibco, ThermoFisher Scientific, Loughborough, UK
Trypan Blue Solution 0.4% (w/v)	Invitrogen, ThermoFisher Scientific, Loughborough, UK
0.25% (w/v) Trypsin- Ethylenediaminetetraacetic acid (EDTA) (1X)	Gibco, ThermoFisher Scientific, Loughborough, UK

Cells were grown in a 75 cm<sup>2</sup> cell culture flask (T-75) at 37°C in a humid atmosphere of 5% CO<sub>2</sub>. The medium was changed twice weekly till the cells reached 80% confluency. Once the cells were 80% confluent, they were washed with 10 ml of DPBS. Cells were then detached using 3 ml of 0.25% Trypsin-EDTA for 10 minutes in a 37°C incubator. Subsequently, the cells were collected by adding 7 ml of medium followed by centrifugation at 1000 rpm for 5 minutes. The supernatant was discarded, and the pellet was resuspended in 1 ml of fresh medium. Viable cell count was carried out on the cell suspension by performing the trypan blue exclusion assay (Section 2.3.2). Cells were re-seeded to 12-well and 24-well plates at approximately  $5 \times 10^5$  cells per well in 1 ml growth media, to 96-well plates at approximately  $1 \times 10^5$  cells per well in 0.2 ml growth medium, and to 6-well plates at approximately  $3 \times 10^6$  cells per well in 2 ml medium for further experiments.

### 2.3.2 Trypan blue exclusion assay

To test the viability of keratinocytes in the presence and absence of SES, *S. epidermidis*, and *P. aeruginosa*, a trypan blue exclusion assay was performed. The culture medium was removed from cells growing in multi-well plates. Cells were washed with 1 ml DPBS and then detached using 0.1 ml of 0.25% Trypsin-EDTA per 1 cm<sup>2</sup> of well surface area for 10 minutes in a 37°C incubator. Subsequently, the cells were collected by adding medium followed by centrifugation at 1000 rpm for 5 minutes. The cell pellet was resuspended in 1 ml fresh medium.

Viable cell count was carried out on the cell suspension by mixing 20 µl of cell suspension with 20 µl of 0.4% (w/v) trypan blue solution. This suspension (10 µl) was loaded to the Countess™ cell-counting chamber slides (Invitrogen, ThermoFisher, UK), and the viable cells were measured using an automated cell counter (Countess™ automated cell counter, Invitrogen, ThermoFisher, UK). Trypan blue dye is negatively charged and does not interact with cells unless the membrane is damaged. Therefore, non-viable cells stained blue while the viable cells remained unstained (Strober, 2001).

### 2.3.3 Microscopy

The keratinocytes' morphology in the presence and absence of SES was assessed using an EVOS FL Auto2 microscope (Invitrogen, ThermoFisher, UK). CellTracker™ Red CMTPX dye (ThermoFisher Scientific, UK) is a fluorescent dye for tracking cells through the cell membrane and can be retained in living cells for several generations. It is transferred to daughter cells and is not toxic to cells. Once the cells reached 80% confluency, the medium was removed, and the cells were washed once with DPBS. A stock solution of CMTPX dye was prepared based on the manufacturer's instructions. The dye was added to each well at the final concentration of 0.5  $\mu$ M in a serum-free medium (DMEM without FBS). The plates were incubated at 37°C for 30 minutes. After the incubation, the dye was removed, and the fresh medium with and without the SES was added to the cells; the plates were incubated at 37°C in a 5% CO<sub>2</sub> environment for 24 and 48 hours. Microscopy was then performed on the fixed cells with 4% formaldehyde (Sigma Life Sciences, UK).

### 2.3.4 Scratch wound healing assay

Scratch assay is a standard method used to investigate the effect of different treatments on wound healing. In this method, a scratch is created in a cell monolayer, and the closure of the scratch is observed over time. This assay facilitates the study of an essential component of wound healing; re-epithelialization, which is due to keratinocyte migration, proliferation, or a combination of both. Factors altering the migration or proliferation of the cells may increase or decrease the rate of healing (Guan *et al.*, 2007; Martinotti and Ranzato, 2019; Kauanova *et al.*, 2021).

Keratinocytes were seeded in a 24-well plate and grown to 90 % confluency. A scratch was made through the monolayer of cells using a sterile 100  $\mu$ l pipette tip. Cells were washed with DPBS; fresh medium was added to them, then incubated for 8, 16, 24, and 48 hours in the presence and absence of bacterial cultures spent medium. Images were taken at times zero and 8, 16, 24, and 48 hours of incubation to observe the scratch closure. The images were analysed using Image-J 64 software program (<https://imagej.nih.gov/>). Re-epithelialization of keratinocytes was measured using the equation (Equation 2.7):

$$\text{Re – epithelialisation\%} = \frac{(\text{area of the scratch at } t = 0) - (\text{area of the scratch at } t = n)}{\text{area of the scratch at } t = 0} \times 100$$

### 2.3.5 Keratinocytes proliferation assay

The MTT assay was performed in 96-well plates to assess the proliferation of keratinocytes after treatment with SES for 24 and 48 hours. Keratinocytes were seeded into 96-well plates and incubated at 37°C in 5% CO<sub>2</sub> environment till they reached 70% confluency. Cells were then washed, and SES at the final concentration of 10% v/v in DMEM was added to the wells. For control comparison, DMEM was added to the control wells. Cells were incubated for 24 and 48 hours at 37°C in 5% CO<sub>2</sub> environment with and without SES. After the incubation period, an MTT assay was performed on cells. For the MTT assay, first, 5 mg/ml stock of MTT reagent (Vybrant MTT cell viability assay, ThermoFisher scientific) in DPBS was prepared; the reagent was filtered by a 0.22 µm filter prior to use. Then, 20 µl of MTT reagent (10% of the volume of medium in the well) was added to each well; the plate was covered in foil to protect against light and incubated at 37°C in 5% CO<sub>2</sub> environment for 3 hours. After the incubation period, the medium was discarded, and the formazan crystals formed at the bottom of the wells were dissolved in 100 µl of DMSO. The plate was incubated at room temperature on a rocking shaker for 15 minutes prior to reading the absorbance at 570 nm using a spectrophotometer. The absorbance of formazan produced by keratinocytes at time zero at 70% confluency was considered as a normalized control. The absorbance of formazan produced at any other time point was compared to the normalized control. The percentage of the proliferation was measured using the equation (Equation 2.8):

$$\text{Proliferation\%} = \frac{\text{The absorbance of formazan at any time point}}{\text{The absorbance of formazan at time zero(normalized control)}} \times 100$$

### 2.3.6 Human cytokine array

To evaluate the cytokine production by keratinocytes when they were exposed to SES, Proteome Profiler™ Human Cytokine Array kit (R&D Systems, Bio-Techne, USA) was used in accordance with the manufacturer's instructions. Extracellular signalling molecules such

as cytokines and chemokines have critical roles in inflammation and cell migration. In the cell communication process, multiple cytokines operate in an extensive network, where the action of one cytokine is regulated by the presence or absence of other cytokines. The Human Cytokine Array kit, which is a membrane-based sandwich immunoassay, detects the relative expression of 36 human cytokines on two nitrocellulose membranes, which selected antibodies are spotted on them (Figure 2.5 and Table 2.6).

To the monolayer of confluent cells grown in a 6-well plate, a scratch was made. Subsequently, the cells were exposed to the SES for 24 hours. After the incubation, the cell culture supernatant was collected, and cell debris was removed by centrifugation at 1000 rpm for 5 minutes. The supernatants were used immediately or stored at -20°C for future assay. Human Cytokine Array membranes and cell culture supernatants were prepared based on the manufacturer's instructions. Then 15 µl of reconstituted Human Cytokine Array Antibody Cocktail was added to 1.5 ml of prepared cell culture supernatant; the mixture was incubated at room temperature for 1 hour. Then the mixture was added to the membrane in a 4-well multi-dish plate; the plate was incubated for 18 hours at 2 – 8°C on a rocking shaker. After the incubation period, the membranes were washed three times with a wash buffer provided by the manufacturer. The wash took 10 minutes each time using a rocking shaker. Afterwards, diluted Streptavidin-HRP (horseradish peroxidase) (1:5000) was added to the membranes; the membranes were incubated for 30 minutes at room temperature on a rocking shaker and washed three more times. The membranes were removed from the plate and placed on a cling film; 1 ml of Chemiluminescence Reagent Mix was evenly added to each membrane and incubated for 1 minute at room temperature. Membranes were visualized using an enhanced chemiluminescence technique by exposing the membrane to a chemiluminescent gel imager (UVP BioSpectrum® Imaging System, USA). The pixel intensity of the dots that appeared on the membrane's pictures after visualization was analysed using the Image-J 64 software program (<https://imagej.nih.gov/>) (Figure 2.5 and Table 2.6).

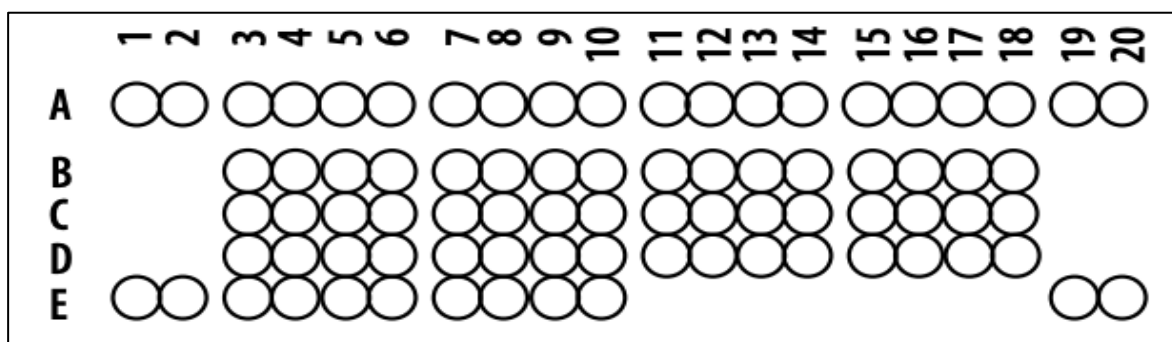


**Figure 2.5** Schematic picture for coordination of cytokines on the nitrocellulose membrane of Human Cytokine Array kit.

**Table 2.6** List of detectable cytokines using Human Cytokine Array kit and their coordination on the nitrocellulose membrane.

Coordinates	Cytokines	Coordinates	Cytokines
A1, A2	Reference Spots	C7, C8	IL-4
A3, A4	CCL1	C9, C10	IL-5
A5, A6	CCL2	C11, C12	IL-6
A7, A8	MIP-1 $\alpha$	C13, C14	IL-8
A9, A10	CCL5	C15, C16	IL-10
A11, A12	CD40 Ligand	C17, C18	IL-12 p70
A13, A14	Complement Component C5	D3, D4	IL-13
A15, A16	CXCL1	D5, D6	IL-16
A17, A18	CXCL10	D7, D8	IL-17A
A19, A20	Reference Spots	D9, D10	IL-17E
B3, B4	CXCL11	D11, D12	IL-18
B5, B6	CXCL12	D13, D14	IL-21
B7, B8	G-CSF	D15, D16	IL-27
B9, B10	GM-CSF	D17, D18	IL-32 $\alpha$
B11, B12	ICAM-1	E1, E2	Reference Spots
B13, B14	IFN- $\gamma$	E3, E4	MIF
B15, B16	IL-1 $\alpha$	E5, E6	Serpin E1
B17, B18	IL-1 $\beta$	E7, E8	TNF- $\alpha$
C3, C4	IL-1ra	E9, E10	TREM-1
C5, C6	IL-2	E19, E20	Negative Control

## 2.3.7 Co-culture of keratinocytes with bacterial cells

### 2.3.7.1 Preparation of bacterial cells for co-culture with keratinocytes

To prepare the bacterial suspensions for co-culture with keratinocytes, the overnight cultures of *S. epidermidis* and *P. aeruginosa* were centrifuged at 3000 rpm for 5 minutes; the pellets were washed twice in PBS, and then the OD<sub>600</sub> was adjusted to 0.09 – 0.11 in 10 ml PBS. The suspensions were centrifuged again, and this time the pellets were resuspended in 10 ml DMEM without the antibiotic solution. Next, 100 µl of this suspension was used to infect  $5 \times 10^5$  confluent cells in 1 ml DMEM in a 12-well plate at approximately 1:20 multiplicity of infection (MOI).

To prepare the supernatant of *P. aeruginosa*, the OD<sub>600</sub> of the overnight culture of *P. aeruginosa* was adjusted to 0.08 – 0.12 and set as an inoculum. The inoculum was then diluted 1:10 in fresh TSB in shaking flasks and incubated at 37°C and 180 rpm for 24 hours. Afterwards, the bacterial culture was centrifuged at 3000 rpm for 10 minutes to collect the supernatant. The supernatant was filtered using a 0.22 µm filter. Next, 30 µl of the supernatant was transferred to agar plates to ensure that there were no viable bacteria present.

### 2.3.7.2 Assessment of keratinocytes viability after infection with bacterial cells

To test if the SES or *S. epidermidis* can protect keratinocytes against *P. aeruginosa*, keratinocytes were grown to full confluency in a 12-well plate containing approximately  $5 \times 10^5$  cells per well in 1 ml of medium. Keratinocytes were pre-, co-, and post-treated with SES or *S. epidermidis* cells prior to infecting with *P. aeruginosa*. For pre-treatment, keratinocytes were exposed to SES or *S. epidermidis* for one hour at 37°C in 5% CO<sub>2</sub> environment, then infected with *P. aeruginosa* for two hours. For co-treatment, keratinocytes were exposed to SES or *S. epidermidis* at the same time as *P. aeruginosa* for two hours. For post-treatment, keratinocytes were infected with *P. aeruginosa* for one hour, and then SES or *S. epidermidis* were added to the cells plus *P. aeruginosa* for further 1 hour of incubation. After the incubation period, the trypan blue exclusion assay, as



described in Section 2.3.2, was performed on the cells to check their viability after infection.

### 2.3.7.3 Assessment of bacterial cells' adhesion to the keratinocytes

Confluent keratinocytes were exposed to the SES and bacterial cell suspension as described in Section 2.3.7.2. After the incubation period, cells were washed with DPBS three times to remove all non-adherent bacterial cells. The cells were detached using 0.25% trypsin-EDTA and collected in 1 ml of medium. The cell suspension was then serially diluted in DPBS, and spot plated on selective agar plates to assess the number of adherent cells as CFU per ml.

## 2.4 Statistical analysis

The data for each experiment were collected from three independent sets, which were performed in triplicate, unless otherwise stated. All data in this study were statistically analyzed using Prism GraphPad version 9. For experiments comparing one variable between several groups within the same experiment, one-way ANOVA with a post hoc Dunnett's was used. For experiments comparing two or more treatments in one experiment, a two-way ANOVA with a post hoc Tukey test was used to analyze the main effects and the interaction between multiple factors. For comparing two variables in one experiment unpaired Student's *t test* was performed. Error bars are reported as mean  $\pm$  standard error of the mean (SEM), and *P* values  $< 0.05$  were considered statistically significant.

# Chapter 3 The effect of *S. epidermidis* supernatant on the biofilm formation and virulence factors of *P. aeruginosa*

## 3.1 Introduction

*P. aeruginosa* is one of the most widespread opportunistic pathogens causing several nosocomial infections in immunocompromised patients. *P. aeruginosa* is mainly responsible for pneumonia in cystic fibrosis patients and severe infection in non-healing wounds (Nathwani *et al.*, 2014). The main virulence characteristic in *P. aeruginosa* is biofilm formation, which provides several opportunities for the organism to escape the host immune system and antibiotic treatment (Mulcahy *et al.*, 2014). *P. aeruginosa* is well-known for producing numerous toxins, enzymes, and proteins that help the colonisation of bacteria during infection (Qin *et al.*, 2022). The orchestrated quorum sensing signalling system in *P. aeruginosa* regulates the biofilm formation and release of several virulence factors. *P. aeruginosa* has a remarkable capacity to resist antibiotics through its intrinsic, adaptive, and acquired resistance mechanisms (Tenover, 2006). Given the increasing prevalence of antibiotic resistance, especially after the coronavirus disease 2019 (COVID-19) pandemic, it is crucial to investigate antibiotic alternatives (Nieuwlaat *et al.*, 2021; Tanne, 2022).

The human microbiota is considered one of the crucial features influencing health and disease in the human body. Many studies are focusing on the gut microbiota and the way commensal microbes in the gut affect the human body. However, little is known about the skin microbiota (Byrd *et al.*, 2018). Coagulase-negative staphylococci, including *S. epidermidis*, are one of the most abundant members of the skin microbiota. Although in the past, *S. epidermidis* was only considered as a potential pathogen causing infection in patients receiving medical devices, recent studies highlight its potential roles in modulating skin immunity and promoting antimicrobial defence as a commensal microbe (Severn and Horswill, 2022).

The following chapter examined the effect of *S. epidermidis* liquid culture extract on the biofilm formation of *P. aeruginosa*. It also investigates possible effect of the extract on a range of virulence factors and antibiotic susceptibility in *P. aeruginosa*. Finally, this chapter studied the expression of quorum sensing genes in *P. aeruginosa* in the presence of *S. epidermidis* liquid culture extract.

## 3.2 Results

### 3.2.1 *S. epidermidis* growth curve

The growth of the bacterial cells in liquid media is normally presented by logarithmic progression curves. The time that takes a bacterial population to divide and double in numbers is called the generation time or doubling time. The cell numbers in an appropriate medium will increase exponentially until the nutrient is exhausted and the cells' toxins and waste are accumulated. In a simplified picture, the bacterial growth curve determines three different phases of lag, exponential and stationary, during the growth of bacteria in an appropriate medium.

The growth curve for *S. epidermidis* was generated following the inoculation of bacteria into TSB. The absorbance (as measured by OD) of the bacterial culture was measured every hour for 24 hours at 600 nm to determine the growth curve of the bacterium. Furthermore, the number of viable cells (CFU/ml) at each time point (every two hours) was determined by counting bacterial colonies on the TSA to correlate the OD<sub>600</sub> of the bacterial culture with the number of viable (CFU/ml) cells in the culture for further assays. The generation time was calculated based on the logarithmic growth of the culture (the exponential phase) against time (Section 2.2.3). Generation time was calculated using the equation below:

$$t_d = \ln 2 / \mu$$

Where:

$t_d$  = doubling time, and

$\mu$  = specific growth rate

*S. epidermidis* stationary phase began at approximately 10 hours post-incubation. The generation time during the exponential phase was calculated as 59.5 minutes (Figure 3.1).

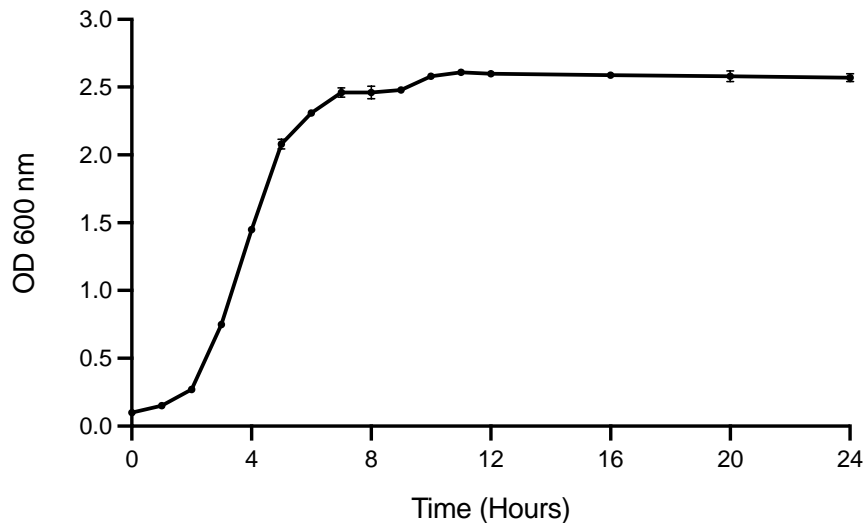


**Figure 3.1** Growth curve of *S. epidermidis* in TSB. *S. epidermidis* was grown in 50 ml TSB in a 250 ml shaking flask at 37°C and 180 rpm for 24 hours.

The OD of the bacterial culture was measured at 600 nm every hour to determine the bacterial growth profile. Error bars are reported as mean  $\pm$  SEM, n=9.

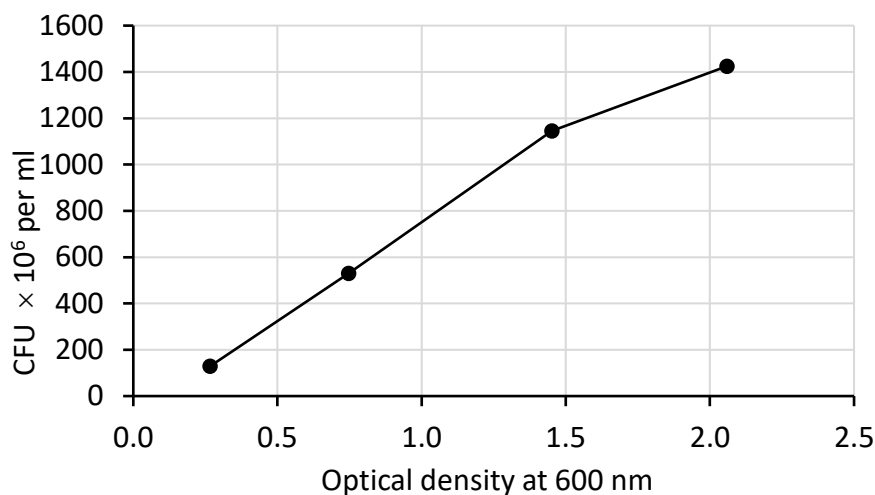


**Figure 3.2** Correlation between the number of viable bacterial cells (CFU/ml) in the culture of *S. epidermidis* and the OD of the culture measured at 600 nm.

*S. epidermidis* was grown in 50 ml TSB in a 250 ml shaking flask at 37°C and 180 rpm for 24 hours. The OD<sub>600</sub> of the culture was measured every hour during the exponential phase. The number of viable cells in the culture corresponding to the measured OD<sub>600</sub> was calculated by determining CFU/ml. The experiment was repeated three times, with three replicates in each experiment. The points marked on the graph are the mean of 9 replicated values of the OD<sub>600</sub> and CFU/ml.

### 3.2.2 Protein concentration in the *S. epidermidis* supernatant (SES)

The protein concentration in the SES was quantified as an indicator of metabolite production during bacterial growth (Table 3.1). *S. epidermidis* was grown in TSB in a shaken flask at 37°C. The supernatant of *S. epidermidis* was obtained from different stages of bacterial growth. These stages were determined based on the growth curve in the previous experiment (Figure 3.1): early exponential phase (3 hours post-incubation), mid-exponential phase (5 hours post-incubation), and late exponential phase (7 hours post-incubation). The supernatant was also collected at the end of the 24-hour growth. The protein concentration in each sample was measured using Bradford Micro Assay, Quick Start Bradford kit (Section 2.2.5).

**Table 3.1** Protein concentration in each SES sample at different stages of growth.

Hours Post-incubation	Absorbance at 595 nm	Protein Conc. µg/ml
3	0.21	59.7
5	0.25	72.5
7	0.27	78.0
24	0.37	106.1

### 3.2.3 Biofilm formation of *P. aeruginosa* in the presence of SES

*P. aeruginosa* was exposed to SES (obtained at different stages of growth) at two different concentrations of 10% and 20% (v/v) to investigate the activity of SES on the biofilm formation of *P. aeruginosa* as one of its main pathogenesis characteristics. Two strains of *P. aeruginosa* were grown in 96-well plates in a TSB medium supplemented with SES, which was obtained at different stages of growth and at final concentrations of 10% and 20% (v/v). For control comparison, *P. aeruginosa* was grown in TSB without SES. Crystal violet assay was performed on 96-well plates to measure the biofilm biomass at 570 nm (Section 2.2.6). Each experiment was performed three times with three repeats in each experiment.

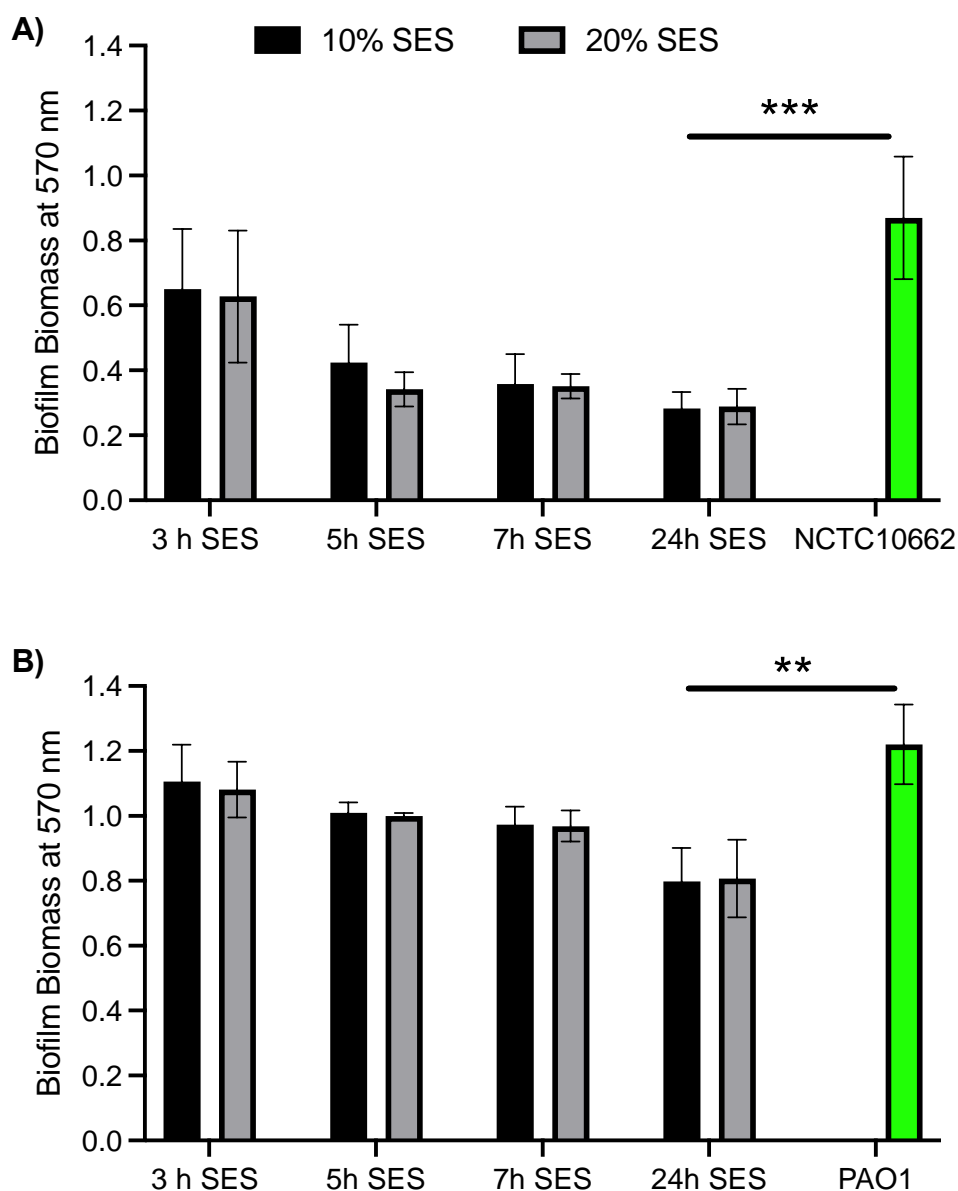


**Figure 3.3** Biofilm formation of *P. aeruginosa* NCTC 10662 (A), and *P. aeruginosa* PAO1 (B) in the presence and absence of SES.

The SES was obtained after 3, 5, 7, and 24 hours of *S. epidermidis* growth. The SES was added to the growth medium (TSB) of *P. aeruginosa* at time zero at two different concentrations (10% and 20% v/v). *P. aeruginosa* cultures with and without the SES in 96-well plates were incubated at 37°C for 24 hours. Biofilm biomass was measured by crystal violet assay at 570 nm. This experiment was repeated three times in triplicate reading (n=9). Error bars are reported as mean  $\pm$  SEM. \*  $P \leq 0.05$ , \*\*  $P \leq 0.01$ , \*\*\*  $P \leq 0.001$ .

Both strains of *P. aeruginosa* formed visible biofilm after 24 hours of incubation. Biofilm formation by *P. aeruginosa* PAO1 was ~28.7% higher than *P. aeruginosa* NCTC 10662 (Figure 3.3). The effect of 3-hour SES at both 10% and 20% (v/v) on biofilm formation of

both strains of PAO1 and NCTC 10662 was insignificant, as analysed by Tukey's multiple comparison test. However, 5-hour, 7-hour, and 24-hour SES at both 10% and 20% (v/v) significantly decreased biofilm formation in both strains (Figure 3.3). SES from 5-hour, 7-hour, and 24-hour growth decreased biofilm formation in NCTC 10662 with *P* values at 0.004, 0.0004, and 0.0001, respectively, and in PAO1 with *P* values at 0.02, 0.01, and 0.002, respectively (Figure 3.3). SES from 24-hour growth decreased biofilm formation by ~67.8% in *P. aeruginosa* NCTC 10662 and ~34.4% in *P. aeruginosa* PAO1, which was higher than the effect of other SESs. The difference between the effect of 10% and 20% (v/v) on biofilm formation was insignificant. However, keratinocytes showed a higher viability percentage when treated with SES at 10% (v/v) concentration than 20% (v/v), as shown in chapter 5. Therefore, 24-hour SES at 10% (v/v) was chosen for use in further experiments.

### 3.2.4 Growth curve of *P. aeruginosa* in the presence of SES

Following determining the effect of SES on the biofilm formation of *P. aeruginosa*, the activity of SES on the planktonic growth of *P. aeruginosa* was investigated. In order to examine if the impact on biofilm formation is due to the effect on bacterial growth, *P. aeruginosa* was grown in the presence and absence of SES in the planktonic state. Two strains of *P. aeruginosa* were grown in 250 ml shaking flasks; TSB medium was supplemented with 24-hour SES (10% v/v) and incubated at 37°C for 24 hours. For control comparison, two strains of *P. aeruginosa* were grown in TSB without SES. The growth was monitored by measuring the OD of growth media at 600 nm every hour using spectrophotometry. The impact of SES on *P. aeruginosa* planktonic growth was verified, and no significant effect was observed (Figure 3.4).

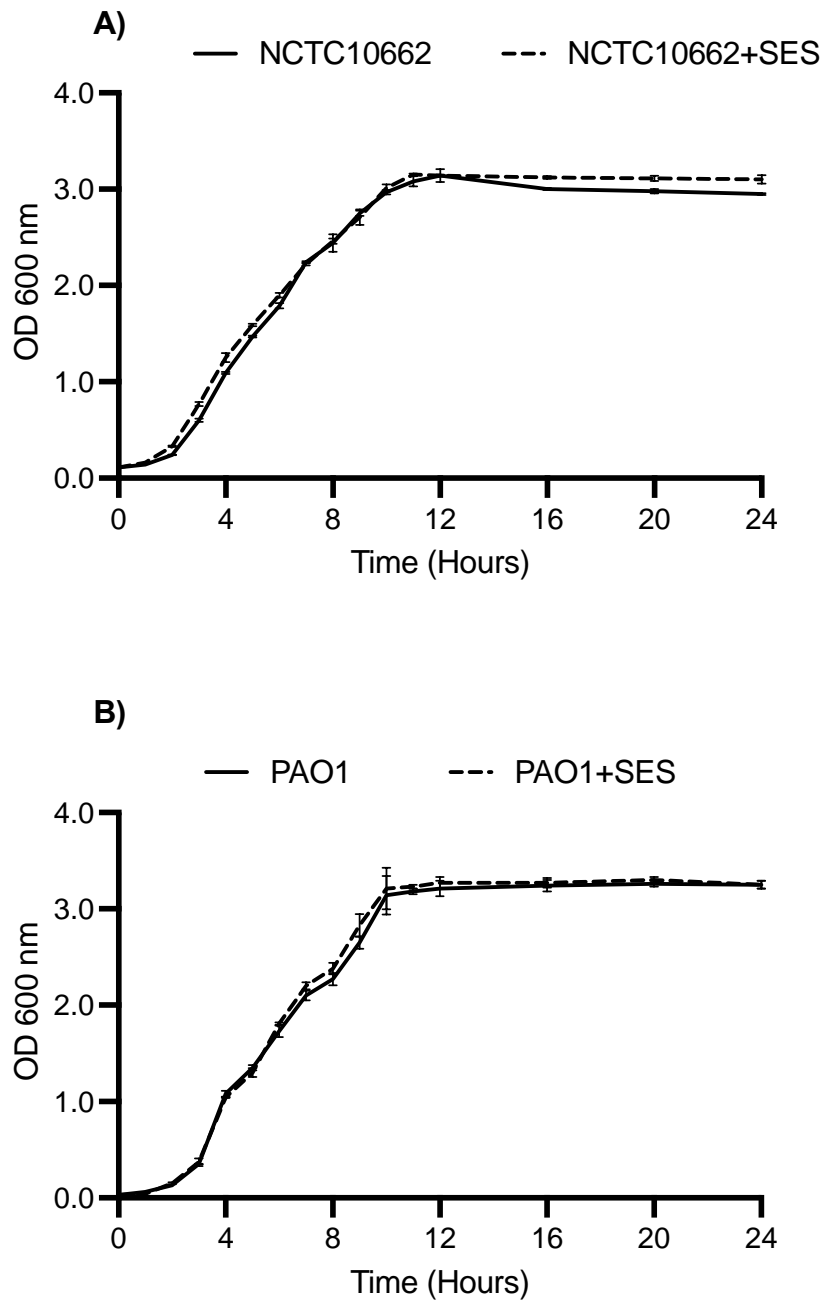


**Figure 3.4** Growth curve of *P. aeruginosa* NCTC 10662 (A), and *P. aeruginosa* PAO1 (B) in the presence and absence of SES.

*P. aeruginosa* strains were grown in 250 ml shaking flasks containing 50 ml of TSB at 37°C for 24 hours. To assess the effect of SES, the culture media of *P. aeruginosa* strains were supplemented with the SES (10% v/v) at time zero. The OD of the culture media at 600 nm was measured every hour for 24 hours. Error bars are reported as mean  $\pm$  SEM, n=9. No significant change was observed in the growth of *P. aeruginosa* strains in the presence of SES.



### 3.2.5 The effect of SES on extracellular polymeric substances (EPS) of *P. aeruginosa* biofilm

EPS, comprised of polysaccharides, eDNA, and proteins, provide a suitable scaffold for biofilm structure. In addition to their roles in preserving the structure and integrity of the biofilm, they each have specific functions. For example, extracellular polysaccharides prevent antibiotics penetration, proteins facilitate the attachment of bacterial cells to the host, and eDNA mediates early biofilm stages development.

The next step of the investigation focused on the impact of SES on each EPS component. *P. aeruginosa* biofilm was set up in the presence and absence of SES at 37°C for 24 hours. The EPS from the biofilm was extracted in a way to prevent the release of intracellular polymers, as mentioned in Section 2.2.7. The total carbohydrate content of the biofilms was quantified by the phenol-sulfuric acid method, proteins concentrations were quantified by Bradford Micro Assay, and eDNA concentration was measured by a NanoDrop™ (Section 2.2.7.1, 2.2.7.2, and 2.2.7.3, respectively).

Production of all components of EPS (eDNA, protein, and carbohydrate) decreased significantly in the presence of SES compared to the control with no SES (Figure 3.5). In *P. aeruginosa* NCTC 10662, eDNA, protein and carbohydrate concentration diminished evidently ( $P=0.0001$ ,  $P=0.0001$ , and  $P=0.002$ , respectively,  $n=3$ , Figure 3.5). A similar result was observed with *P. aeruginosa* PAO1, in which EPS components were reduced in the presence of SES. The concentration of eDNA ( $P=0.0007$ ), protein ( $P=0.0004$ ), and carbohydrate ( $P=0.004$ ) showed a significant reduction in the presence of SES (Figure 3.5).

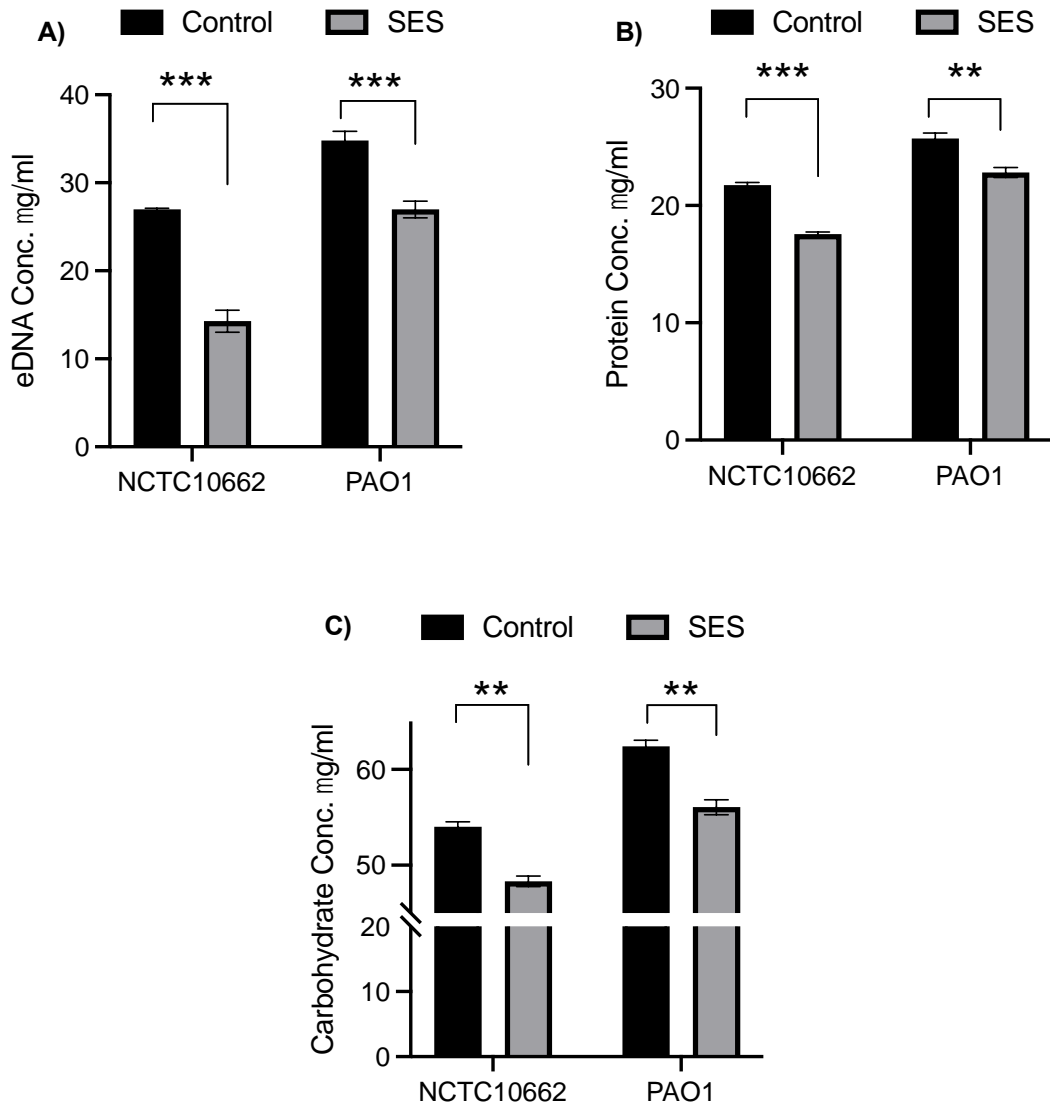


**Figure 3.5** Quantification of EPS components, eDNA (A), protein (B), and carbohydrate (C) in the presence and absence of SES in two strains of *P. aeruginosa* PAO1 and NCTC 10662. *P. aeruginosa* biofilm was set up in the presence and absence of SES at 37°C for 24 hours. The EPS from the biofilm was extracted in a way to prevent the release of intracellular polymers. The total carbohydrate content of the biofilms was quantified by the phenol-sulfuric acid method, protein concentration was quantified by Bradford Micro Assay, and eDNA concentration was measured using a NanoDrop™. Error bars are reported as mean ± SEM, n = 3. \* P ≤ 0.05, \*\* P ≤ 0.01, \*\*\* P ≤ 0.001.

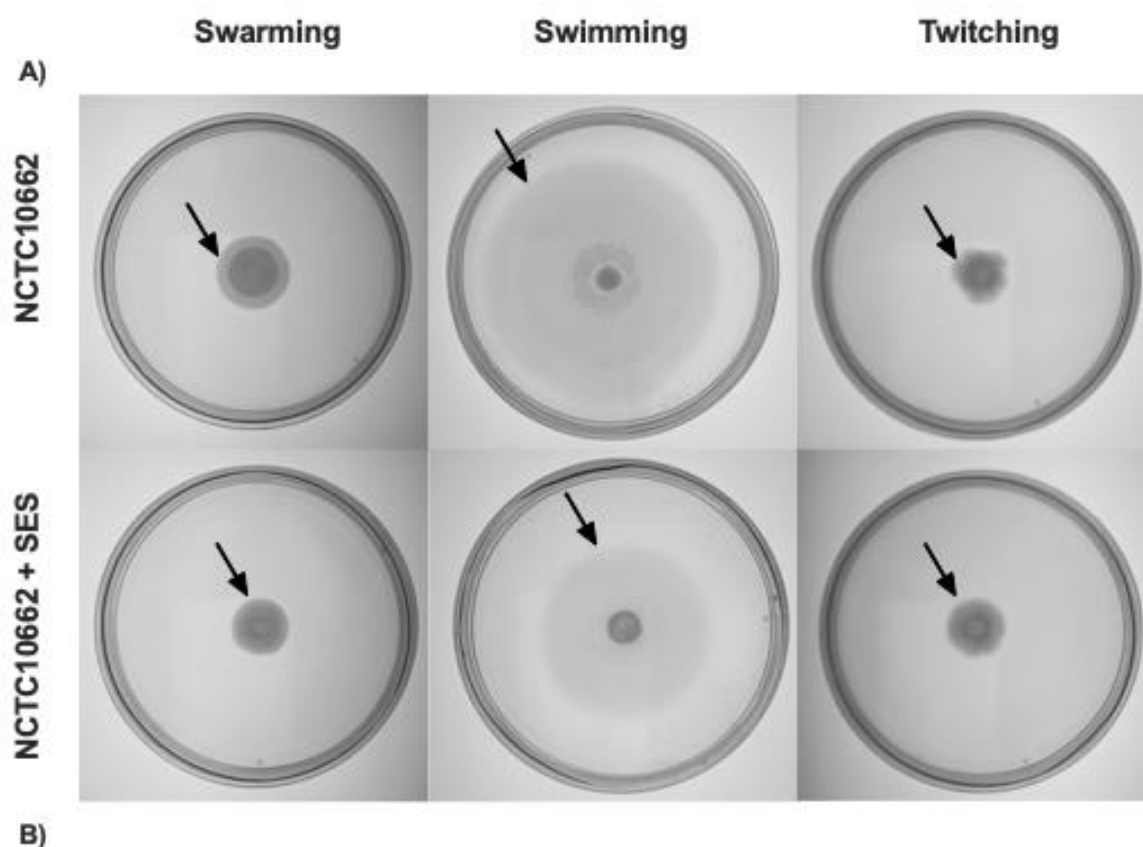
## 3.2.6 The effect of SES on the virulence factors production of *P. aeruginosa*

### 3.2.6.1 The impact on motility of *P. aeruginosa*

*P. aeruginosa* produces several virulence factors during infection. Some of them are the structural components of bacterial cells, and others are released to the host cells through secretion systems. Flagellum and pili are structural components of *P. aeruginosa* responsible for bacterial motility and attachment to the host cells.

*P. aeruginosa* harbours three types of motion; swimming facilitated by flagellum, twitching by a polar type IV pili, and swarming through secretion of surfactants like rhamnolipids. Swimming and twitching motility occurs in individual cells moving in a semi-liquid environment, unlike swarming motion, which is established by rapid multicellular movements. Flagellum and type IV pili also initiate the attachment of bacterial cells to the surface and facilitate biofilm formation in the early stages of colonization. (Murray and Kazmierczak, 2008; Patriquin *et al.*, 2008; Khan *et al.*, 2020). Motility studies are based on the capacity of the bacterium to migrate from the point of inoculation.

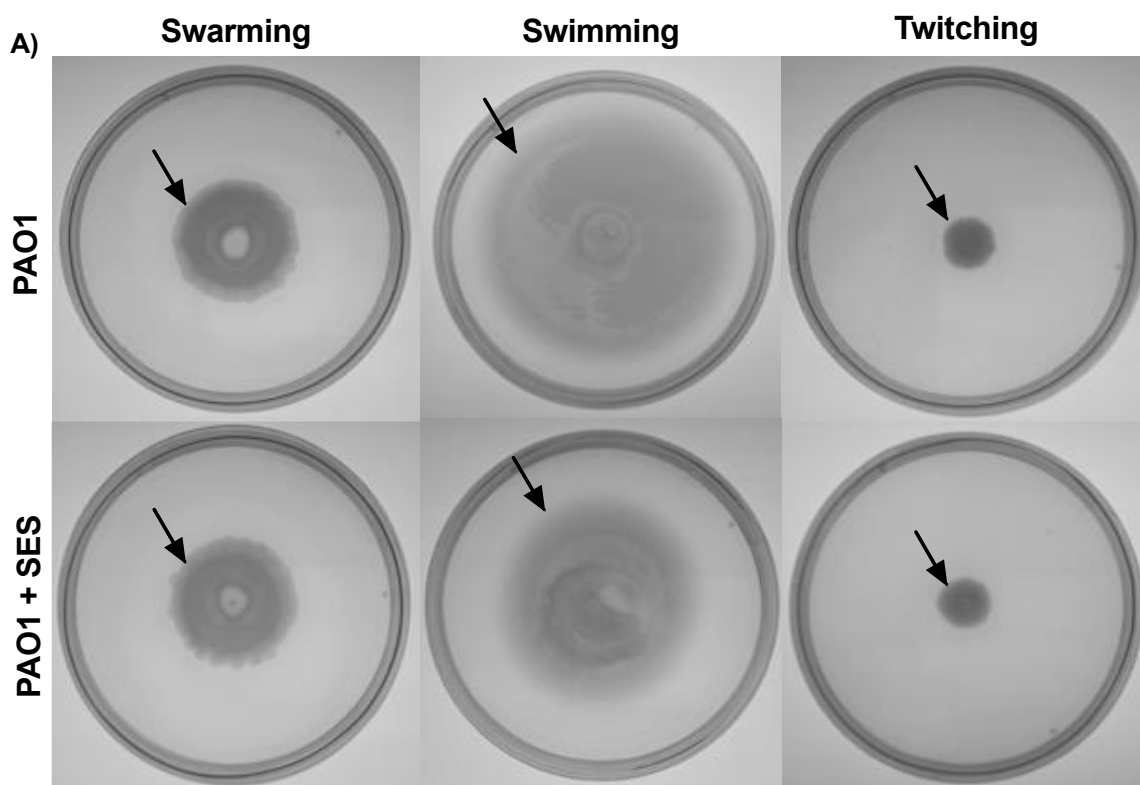
Motility assay was performed on agar plates with different agar concentrations (0.3% w/v for swimming, 0.5% w/v for swarming, and 1% w/v for twitching) to facilitate bacterial motions. The plates supplemented with and without SES before solidifying were used to investigate the effect of SES on the motility of *P. aeruginosa*. The agar plates were then inoculated with the bacterial suspension and incubated at 37°C for 24 hours (Section 2.2.8.4). The diameter of the growth zone formed by bacterial migration was then measured in millimeters (mm) (Figure 3.6 and Figure 3.7).



	Swarming Colony Diameter (mm)	Swimming Colony Diameter (mm)	Twitching Colony Diameter (mm)
Control	23 ± 0.2	71 ± 2.9	17.7 ± 0.5
10% SES	18.7 ± 1.2	51.3 ± 4.7	17.3 ± 0.9

**Figure 3.6** The impact of SES on swarming, swimming, and twitching motility of *P. aeruginosa* NCTC 10662.

Representative images of bacterial motion on agar plates in the presence and absence of SES (A) along with the colony diameter (mm) of *P. aeruginosa* on an agar plate with and without SES (B). A motility assay was performed based on the capacity of the bacterium to migrate from the point of inoculation. Agar plates with different agar concentrations (0.5% w/v for swarming, 0.3% w/v for swimming, and 1% w/v for twitching) were prepared to assess bacterial motility. The agar plates were then inoculated with the bacterial suspension and incubated at 37°C for 24 hours. The diameter of the growth zone formed by the bacterial migration was then measured in mm.



B)

	Swarming Colony Diameter (mm)	Swimming Colony Diameter (mm)	Twitching Colony Diameter (mm)
Control	28.7 ± 2.5	75 ± 0.8	13 ± 0.2
10% SES	31.3 ± 2.5	57.3 ± 1.7	12.7 ± 0.5

**Figure 3.7** The impact of SES on swarming, swimming, and twitching motility of *P. aeruginosa* PAO1.

Representative images of bacterial motion on agar plates in the presence and absence of SES (A) along with the colony diameter (mm) of *P. aeruginosa* on agar plates with and without SES (B). A motility assay was performed based on the capacity of the bacterium to migrate from the point of inoculation. Agar plates with different agar concentrations (0.5% w/v for swarming, 0.3% w/v for swimming, and 1% w/v for twitching) were prepared to assess bacterial motility. The agar plates were then inoculated with the bacterial suspension and incubated at 37°C for 24 hours. The diameter of the growth zone formed by the bacterial migration was then measured in mm.

As it is shown in figure 3.8, both strains of *P. aeruginosa* NCTC 10662 and PAO1 harbour swimming, swarming, and twitching motility. Both NCTC 10662 and PAO1 strains showed quite similar swimming capacities (Figure 3.8 B). The experiment result shown in figure 3.8 (B) demonstrated that in the presence of SES, the migration zone formed by swimming motility reduced significantly in both NCTC 10662 and PAO1 ( $P=0.0075$  and  $P=0.0002$  respectively,  $n=3$ ). However, this reduction in individual cell movement seems not to affect the collective swarming movement of PAO1 strain ( $P= 0.345$ ,  $n=3$ , Figure 3.8 A). On the other hand, SES significantly reduced both individual and collective movement of NCTC 10662 strain as the migration zone in the swarming and swimming experiment decreased ( $P=0.008$  and  $P=0.0075$ , respectively,  $n=3$ , Figure 3.8 A). Twitching motility, a form of surface-associated movement, is mediated through type IV pili in *P. aeruginosa*. Twitching motility is known as a vital factor in biofilm formation on abiotic surfaces, and it is also involved in the cytotoxic capacity of *P. aeruginosa* in infections. The SES was found to have no significant effect on the twitching motility of NCTC 10662 and PAO1 ( $P=0.67$  and  $P=0.37$ , respectively, Figure 3.8 C).

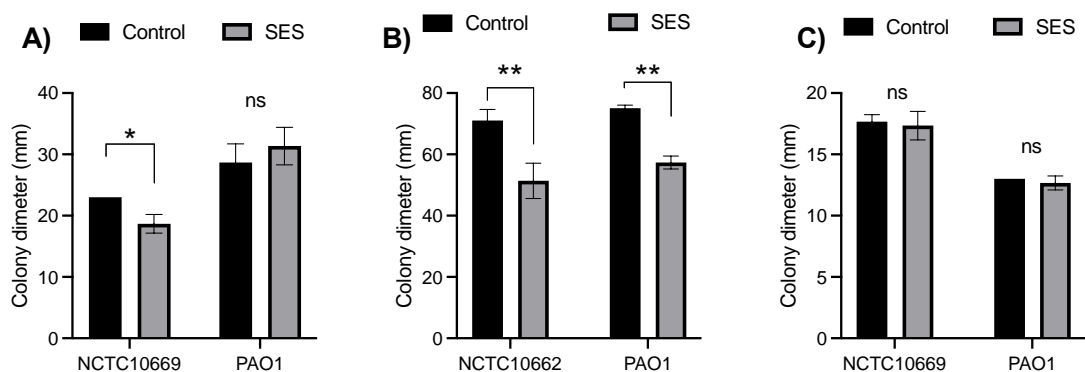


**Figure 3.8** Motility of *P. aeruginosa* PAO1 and NCTC 10662 in the absence and presence of SES.

The diameter of the migration zone formed by two strains of *P. aeruginosa* cultured on agar plates with and without SES was measured to test three types of motilities, swarming (A), swimming (B), and twitching (C). Error bars are reported as mean  $\pm$  SD. ns = not significant, \*  $P \leq 0.05$ , \*\*  $P \leq 0.01$ .

### 3.2.6.2 The impact on the enzyme, toxin, and pigment production of *P. aeruginosa*

Elastase and pyocyanin are released through type II and type III secretion systems (T2SS and T3SS) in *P. aeruginosa*, and both have a deleterious effect on epithelial cells during infections (Galle *et al.*, 2013; Ruffin and Brochiero, 2019). Elastase degrades type I and type IV collagen proteins in the extracellular matrix of epithelial cells, therefore triggering tissue damage (De Bentzmann *et al.*, 2000). Pyocyanin, a blue pigment with redox activity, causes cell growth inhibition, apoptosis, and tissue damage, probably through the induction of reactive oxygen species (Caldwell *et al.*, 2009; Lau *et al.*, 2004). Pyoverdine is an iron scavenging molecule whose synthesis is strongly related to iron starvation. Pyoverdine's high affinity to iron can hijack iron from host sources such as transferrin, lactoferrin, and mitochondria which can cause damage to host cells. Iron-bound pyoverdine acts as a signalling molecule which activates the release of other virulence factors. It is also essential in biofilm formation (Meyer, 2000).

An elastin Congo red assay was used to assess the activity of elastase in the presence and absence (control) of SES (Section 2.2.8.3). Pyocyanin was extracted from the LB culture medium of *P. aeruginosa* in the presence and absence (control) of SES using a chloroform-hydrochloric acid extraction method (Section 2.2.8.1). To investigate the effect of SES on the release of pyoverdine, *P. aeruginosa* was grown in a low-in-iron medium to induce pyoverdine production. The release of pyoverdine was measured at 405 nm (Section 2.2.8.2).

Elastase activity was decreased in both strains of *P. aeruginosa* in the presence of SES. ( $P=0.02$ ,  $n=6$ , Figure 3.9 A). It is noticeable that PAO1 produced seven times more elastase compared to NCTC 10662. A similar result was observed in pyocyanin production; PAO1 produced a significant concentration of pyocyanin compared with the trace amount produced by NCTC 10662. The SES reduced the production of pyocyanin in *P. aeruginosa* PAO1 ( $P=0.007$ ,  $n=6$ , Figure 3.9 B), whereas there was no effect on NCTC 10662 pyocyanin production. The SES induced a significant decrease ( $P=0.0001$ ,  $n=6$ , Figure 3.9 C) in relative pyoverdine production in PAO1. There was no difference in pyoverdine production when NCTC 10662 was treated with SES ( $P=0.06$ ).

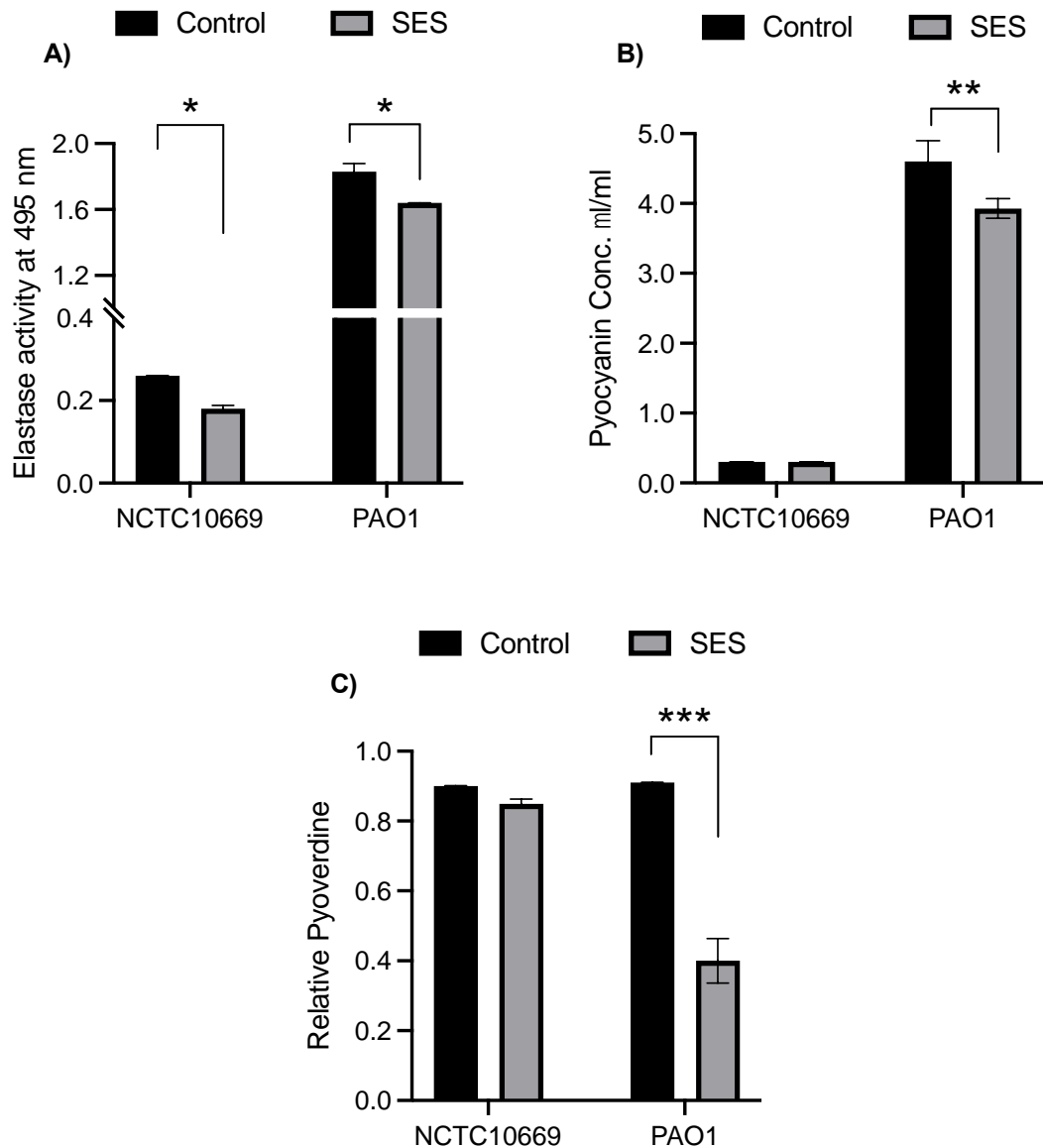


**Figure 3.9** Quantification of virulence factors released from *P. aeruginosa* NCTC 10662 and PAO1 in the presence and absence (control) of SES.

A) shows the elastase activity in two strains of *P. aeruginosa* in the presence and absence (control) of SES. Elastase activity is measured by reading the absorbance of released Congo red dye from the ECR complex at 495 nm. B) demonstrates the concentration of pyocyanin extracted from the LB culture of two strains of *P. aeruginosa* in the presence and absence (control) of SES. C) shows relative pyoverdine production normalised against the number of bacterial cells in the RPMI culture of two strains of *P. aeruginosa* in the presence and absence (control) of SES. Error bars are reported as Mean  $\pm$  SEM, n=9. \*  $P \leq 0.05$ , \*\*  $P \leq 0.01$ , \*\*\*  $P \leq 0.001$ .



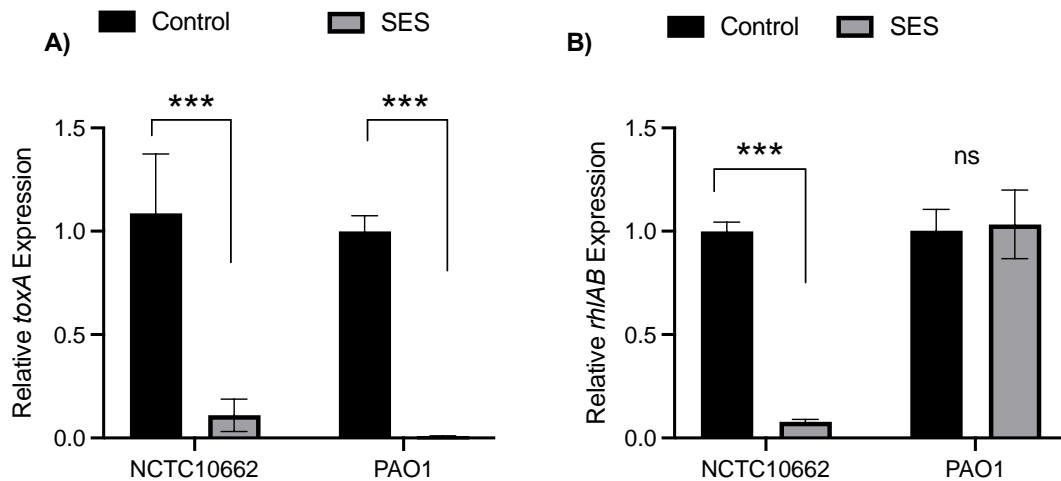


**Figure 3.10** Virulence factors gene expression of *P. aeruginosa* in the presence and absence of SES.

A) demonstrates the relative expression of *toxA* in *P. aeruginosa* NCTC 10662 and PAO1 in the presence and absence of SES. B) demonstrates the relative expression of *rhlAB* in *P. aeruginosa* NCTC 10662 and PAO1 in the presence and absence of SES. The expression of virulence genes in the biofilm of *P. aeruginosa* was assessed by RT-qPCR analysis. Results are expressed as the mean  $\pm$  SEM, n=3. ns=not significant, \*  $P \leq 0.05$ , \*\*  $P \leq 0.01$ , \*\*\*  $P \leq 0.001$ .

To further investigate the influence of SES on other virulence factors of *P. aeruginosa*, the expression of virulence genes in the biofilm of *P. aeruginosa* treated with SES was assessed by RT-qPCR analysis. Rhamnolipids are actively involved in the invasion of *P. aeruginosa* to the host epithelial cells and facilitate motility in *P. aeruginosa*. The *rhlAB* operon encodes rhamnosyltransferase 1, which is an enzyme involved in the synthesis of surfactant rhamnolipid (Medina *et al.*, 2003). Exotoxin A inhibits protein biosynthesis in host cells leading to great tissue and even organ damage; the *toxA* gene regulates the expression of exotoxin A (Hirakata *et al.*, 1993; Jenkins *et al.*, 2004). The expression of both genes is under the control of quorum sensing genes in *P. aeruginosa* (Duplantier *et al.*, 2021). The expression of *toxA* in the presence of SES decreased significantly in both NCTC 10662 and PAO1 compared with the control ( $P=0.0001$  and  $P<0.0001$ , respectively, n=3). There was a statistically significant reduction in the expression of *rhlAB* in NCTC 10662 ( $P<0.0001$ ), however, no significant change was observed in the expression of *rhlAB* in the PAO1 strain ( $P=0.07$ ).

### 3.2.7 Antibiotic susceptibility of *P. aeruginosa* in the presence of SES

Biofilm formation is one of the antibiotic resistance mechanisms in *P. aeruginosa*. Since the SES caused a decrease in biofilm formation in *P. aeruginosa*, the effect of SES on antibiotic susceptibility was tested. Antibiotic susceptibility was investigated on NCTC 10662 and PAO1 strains in two different culture media MHB, the standard medium for antibiotic susceptibility test, and TSB, as it is the main medium used in this study. The MIC of tetracycline hydrochloride, gentamicin, and ciprofloxacin alone and in combination with the SES were evaluated by the micro-dilution assay in 96-well microtiter plates according to the EUCAST regulations (Leclercq *et al.*, 2013). MBC was determined by plating the cultures treated with antibiotics and a combination of antibiotics and SES on MHA and TSA. The MBC was reported as the lowest concentration of the antibiotic when no visible growth was observed (Section 2.2.9). Three types of antibiotics were selected for this experiment. Tetracycline hydrochloride was selected as an inefficient antimicrobial against *P. aeruginosa*. Ciprofloxacin (from a quinolone family of antibiotics) and gentamicin (from aminoglycosides) were chosen as broad-spectrum antimicrobials, which are active against *P. aeruginosa*. These experiments were repeated three times, with three replicates each time.

The efficiency of tetracycline in combination with SES did not change at MIC and MBC in NCTC 10662 compared with tetracycline alone. However, in combination with SES, tetracycline resulted in a two-fold decrease in the MIC in the PAO1 treatment compared with the treatment with tetracycline alone. This effect was not observed in MBC in PAO1 (Table 3.2). In combination with SES, gentamicin showed the best outcome among all other antibiotics tested in this experiment. There was a two-fold reduction in MIC and MBC of gentamicin when it was combined with SES. The same result was observed in the treatment of PAO1 with gentamicin in combination with SES. A two-fold reduction in MIC and MBC of gentamicin was observed when gentamicin was mixed with SES (Table 3.2).

The combination of SES with ciprofloxacin did not improve the efficacy of the antibiotic at MIC against NCTC 10662 and PAO1. However, the MBC of ciprofloxacin in combination with SES was reduced by two folds in both NCTC 10662 and PAO1. When ciprofloxacin alone was used, a concentration of 1 µg/ml was required to eradicate bacterial cells in NCTC 10662. When ciprofloxacin was mixed with SES, a concentration of 0.5 µg/ml was enough to eradicate NCTC 10662. In PAO1, 1 µg/ml of ciprofloxacin with SES was required to eradicate bacteria compared with 2 µg/ml of ciprofloxacin alone.

**Table 3.2** Susceptibility of *P. aeruginosa* to antibiotics tetracycline, gentamicin, and ciprofloxacin alone and in combination with SES.

	TSB		MHB	
	MIC (µg/ml)	MBC (µg/ml)	MIC (µg/ml)	MBC (µg/ml)
<b>Tetracycline</b>				
NCTC 10662	32	512	8	nd*
NCTC 10662 plus SES	32	512	8	nd*
PAO1	32	512	16	nd*
PAO1 plus SES	16	512	8	nd*
<b>Gentamicin</b>				
NCTC 10662	4	8	1	4
NCTC 10662 plus SES	2	4	0.5	2
PAO1	4	8	1	4
PAO1 plus SES	2	4	0.5	2
<b>Ciprofloxacin</b>				
NCTC 10662	0.25	1	0.12	1
NCTC 10662 plus SES	0.25	0.5	0.12	0.5
PAO1	0.25	2	0.25	2
PAO1 plus SES	0.25	1	0.25	1

\*not defined

### 3.2.7.1 Evaluating the combined activity of antibiotics and SES on preformed biofilm of *P. aeruginosa*

Next, the effect of combination therapy was investigated on the eradication of the preformed biofilm of *P. aeruginosa*. The biofilms of the two strains of *P. aeruginosa* were established over 24 hours. After 24 hours, planktonic cells were discarded, and the wells were washed with PBS to remove the remaining non-attached cells. Then the established biofilm was treated with different concentrations (including  $\frac{1}{2}$  MIC, MIC, and 2MIC as determined in Section 3.7) of the three antibiotics (tetracycline, gentamicin, and ciprofloxacin) alone and in combination with SES. The biofilm was incubated for another 24 hours. Crystal violet assay (Section 2.2.6) was used to measure biofilm formation after the treatment, and MTT assay (Section 2.2.10.2) was used to evaluate the viability of cells in the biofilm. Biofilm biomass after 48 hours without any treatment was considered as control. The viability of cells after 48 hours of incubation without any treatment in culture media was considered 100% cell viability (control), and the viability of cells after the other treatments were compared to the control (as mentioned in Section 2.2.10.2).

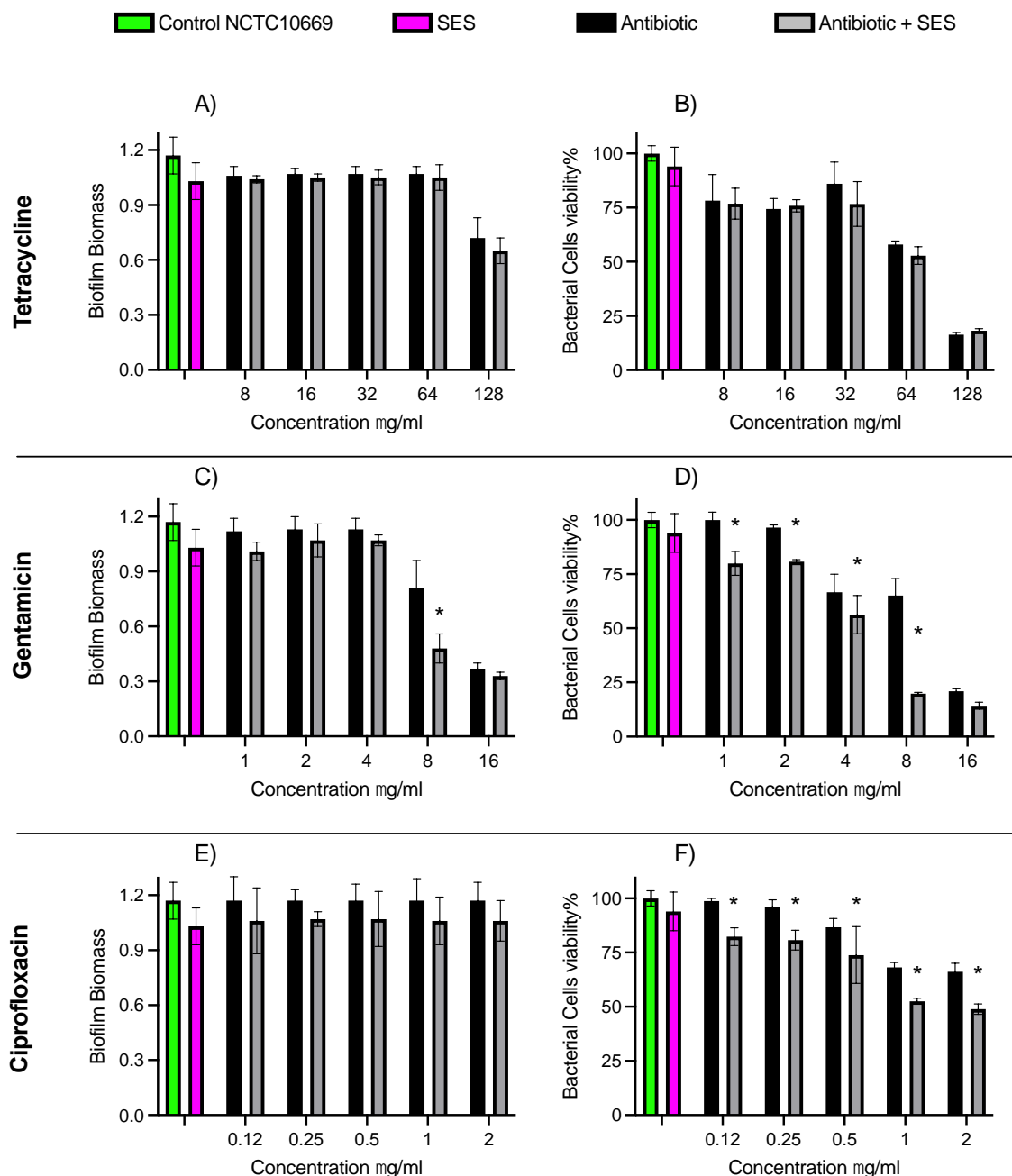


**Figure 3.11** The effect of SES on antibiotic susceptibility of the established biofilm of *P. aeruginosa* NCTC 10662.

Biofilm of NCTC 10662 was set up in 96-well plates for 24 hours at 37°C. Then 24-hour established biofilm of *P. aeruginosa* was treated with SES, three types of antibiotics, and a combination of SES and antibiotics for 24 hours. The three antibiotics tetracycline (A and B), gentamicin (C and D), and ciprofloxacin (E and F) at different concentrations, including ½ MIC, MIC, 2MIC alone and in combination with SES at 10% v/v were used to treat the preestablished biofilm of *P. aeruginosa*. Biofilm biomass after 48 hours was quantified by crystal violet assay (A, C, and E). The viability of the cells in the biofilm after 48 hours was determined by MTT assay. The number of viable cells present in the biofilm of *P. aeruginosa* NCTC 10662 without any treatment in the control media after 48 hours was considered to have 100% viability (control), and the number of cells after treatments were compared to it (B, D, and F). Results are expressed as the mean ± SEM, n=9, \* P ≤ 0.05.

Figure 3.11 shows that SES alone has no significant effect on the eradication of the established biofilm and the viability of cells embedded in the biofilm. However, the combination of SES with antibiotics in some concentrations showed an additional effect. Tetracycline at 128 µg/ml concentration depicted the highest efficacy in biofilm eradication and reduction in bacterial cell viability compared to control with no treatment (P=0.01 and P=0.003, respectively, n=9). This is four times higher than tetracycline MIC in *P. aeruginosa* NCTC 10662. The combination therapy of tetracycline and SES didn't demonstrate any significant alteration in biofilm eradication and bacterial cell viability compared to the antibiotic treatment alone.

Gentamicin at 16 µg/ml concentration showed the highest efficacy in biofilm eradication and elimination of the bacterial cells compared to other antibiotics tested on the established biofilm of NCTC 10662 (P=0.001 and P=0.002 respectively, n=9, Figure 3.11). Combination of gentamicin at 8 µg/ml with SES significantly reduced biofilm formation and viability of cells compared to gentamicin at 8 µg/ml alone (P=0.02 and P=0.005, respectively, n=9, Figure 3.11). In combination therapy, only 8 µg/ml of gentamicin was enough to achieve the level of biofilm disruption and elimination of the cells at 16 µg/ml of gentamicin, suggesting an additive effect between gentamicin and SES.

Although ciprofloxacin showed no significant effect on biofilm disruption at any concentrations, high concentrations of 1 and 2 µg/ml of ciprofloxacin displayed lower viable cells compared to the control (P=0.02, n=9). Combination of SES with ciprofloxacin at all concentrations of the antibiotic (2, 1, 0.5, 0.25, and 0.12 µg/ml) improved ciprofloxacin effect on eradication of the viable cells in the established biofilm (P=0.002, P=0.002, P=0.04, P= 0.03, P=0.03 respectively, n=9, Figure 3.11).

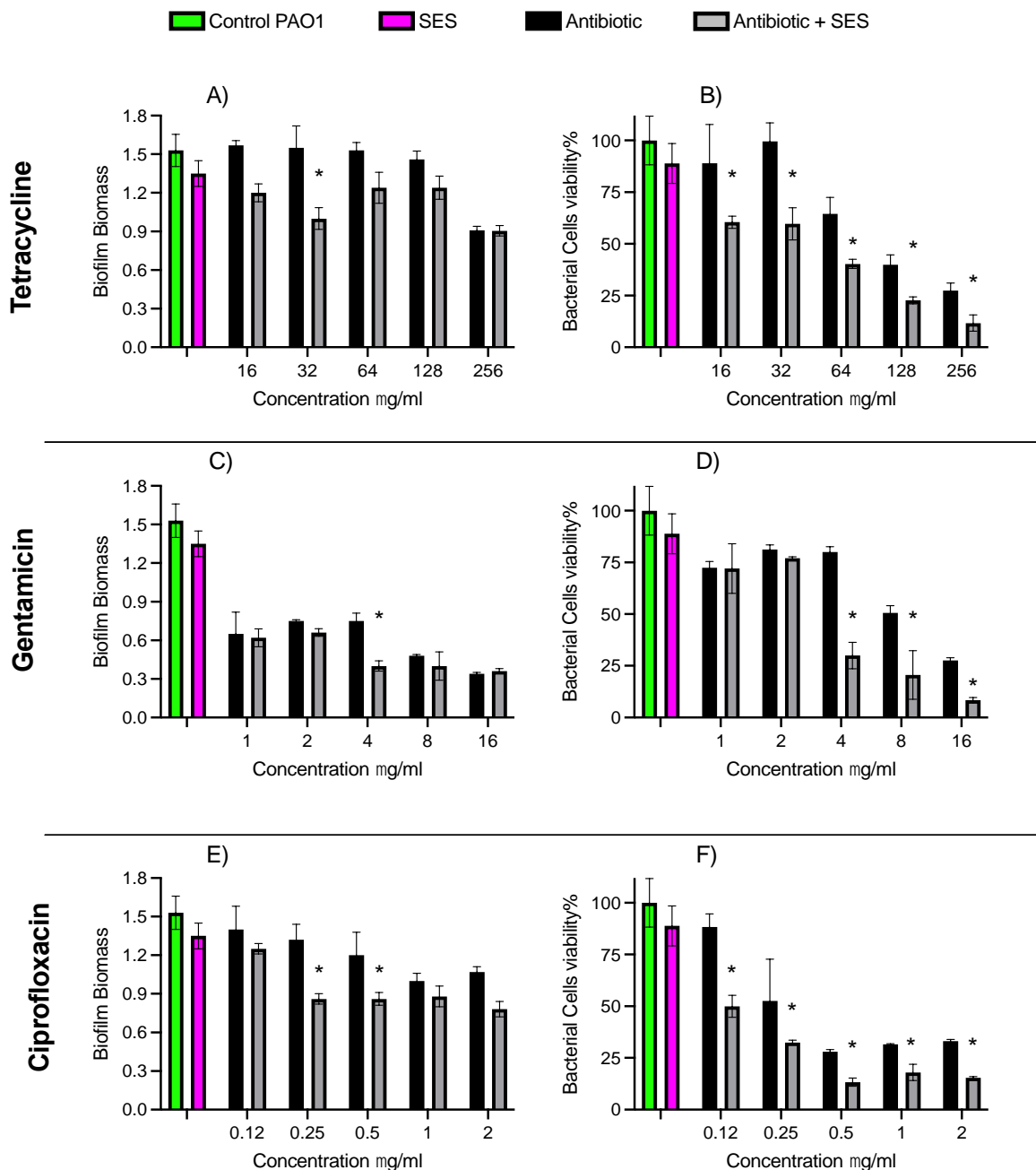


**Figure 3.12** The effect of SES on antibiotic susceptibility of established biofilm of *P. aeruginosa* PAO1.

Biofilm of PAO1 was set up in 96-well plates for 24 hours at 37°C. Then 24-hour established biofilm of *P. aeruginosa* was treated with SES, three types of antibiotics, and a combination of SES and antibiotics for another 24 hours. The three antibiotics tetracycline (A and B), gentamicin (C and D), and ciprofloxacin (E and F) at different concentrations, including ½ MIC, MIC, 2MIC alone and in combination with SES at 10% v/v were used to treat the preestablished biofilm of *P. aeruginosa*. Biofilm biomass after 48 hours was quantified by crystal violet assay (A, C, and E). The viability of the cells in the biofilm after 48 hours was determined by MTT assay. The number of viable cells present in the biofilm of *P. aeruginosa* PAO1 without any treatment in the control media after 48 hours was considered to have 100% viability (control), and the number of cells after treatments were compared to it (B, D, and F). Results are expressed as the mean ± SEM, n=9, \* P ≤ 0.05.

As shown in figure 3.12, SES alone showed no significant effect on biofilm disruption and reduction of the bacterial cells from the preformed biofilm of *P. aeruginosa* PAO1. Tetracycline only at 256 µg/ml was effective in eradicating the established biofilm of PAO1 (P=0.005, n=9), even though other concentrations of 128 and 64 µg/ml were also effective in eliminating viable cells from the established biofilm (P=0.0007, P=0.004 respectively, n=9, Figure 3.12). The addition of tetracycline at 32 µg/ml alone did not affect the biofilm disruption in PAO1. However, when tetracycline at 32 µg/ml was used in combination with SES, biofilm disruption was significantly reduced compared to tetracycline alone (P=0.005, n=9). This effect was similar to the effect of 256 µg/ml tetracycline alone on biofilm eradication. It was noticeable that the combination of SES with tetracycline at all concentrations (256, 128, 64, 32, and 16 µg/ml) had an additive effect on reducing viable cells in the biofilm (P=0.01, P=0.01, P=0.008, P=0.001, and P=0.03 respectively, n=9, Figure 3.12).

Gentamicin displayed the highest biofilm eradication compared to the other two antibiotics, tetracycline and ciprofloxacin. Gentamicin at all concentrations (16, 8, 4, 2, and 1 µg/ml) significantly disrupted the biofilm compared to the control (P=0.0005, P=0.0005, P=0.001, P=0.001, and P=0.001 respectively, n=9, Figure 3.12). However, only gentamicin at concentrations of 16 and 8 µg/ml was able to reduce viable cells in the biofilm (P=0.0002 and P=0.003, respectively, n=9, Figure 3.12). Combination of SES with gentamicin at 4 µg/ml displayed a greater biofilm eradication compared to gentamicin at 4 µg/ml alone (P=0.01, n=9). This effect was similar to the effect of 8 µg/ml gentamicin alone on biofilm eradication. Combination of gentamicin at 16, 8, and 4 µg/ml with SES displayed greater efficiency in diminishing bacterial cells in the biofilm (P=0.02, P=0.008, P=0.002 respectively, n=9, Figure 3.12).

Ciprofloxacin alone at concentrations 2 and 1 µg/ml demonstrated significant biofilm eradication compared to the control, although the efficacy of the combination therapy was not significant in comparison to ciprofloxacin alone, it was effective compared to the control. Ciprofloxacin could not diminish the biofilm at 0.5 and 0.25 µg/ml; however, mixed with SES, it was able to disrupt the biofilm significantly compared to the control (P=0.03



and  $P=0.01$ , respectively, Figure 3.12). The combination of ciprofloxacin with SES (under all concentrations 2, 1, 0.5, 0.25, and 0.12  $\mu\text{g/ml}$ ) with SES significantly reduced the percentage of viable cells in the biofilm compared to ciprofloxacin alone ( $P=0.02$ ,  $P=0.04$ ,  $P=0.02$ ,  $P=0.008$ , and  $P=0.006$ , respectively,  $n=9$ ).

### 3.2.7.2 Evaluating the effect of SES on the efflux pumps activity of *P. aeruginosa*

Efflux pumps allow bacterial cells to control the absorption of chemical substances and monitor the intake of toxic molecules in *P. aeruginosa*. They also extrude antimicrobial agents from within cells to the extracellular environment. The mechanism of antibiotic resistance is multifactorial and complicated, but the capacity of bacterial cells to repel antimicrobial agents through efflux pumps is one of the main factors (Du *et al.*, 2018). As SES in combination with antibiotics showed some promising results, the effect of SES on efflux pump activity was evaluated to further investigate the mechanism of SES action.

The uptake of ethidium bromide from the culture medium in the presence and absence (control) of SES and its accumulation inside bacterial cells through efflux pumps were monitored to test the activity of efflux pumps. Efflux pump inhibitors can interfere with the transfer of chemicals into bacterial cells, leading to the accumulation of antimicrobial agents inside cells. An accumulation assay (Section 2.2.11) was performed on both strains of NCTC 10662 and PAO1 in the presence of ethidium bromide with and without (control) SES. The accumulation of ethidium bromide inside the bacterial cells was assessed over an hour by measuring the excitation at 520 nm and emission at 590 nm every minute. SES showed no significant effect on the efflux pump activity of *P. aeruginosa* NCTC 10662 and PAO1 (Figure 3.13).

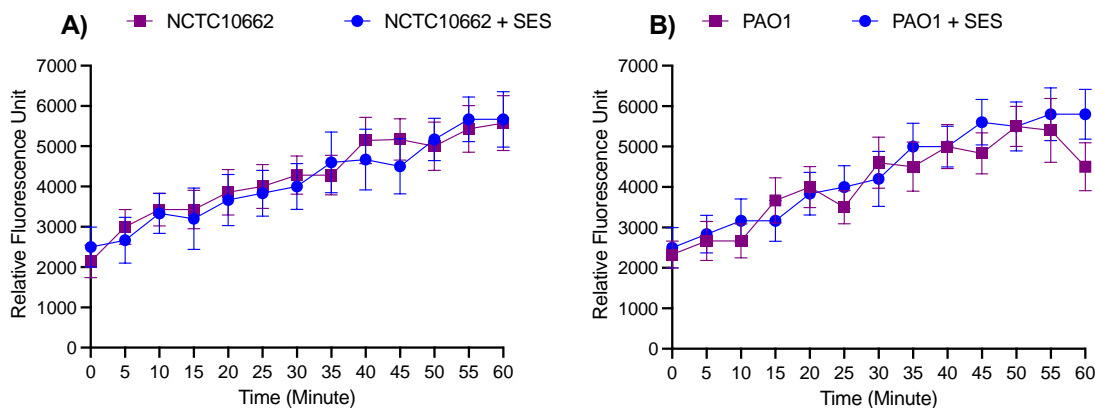


**Figure 3.13** Fluorometric accumulation assay of *P. aeruginosa* NCTC 10662 (A) and PAO1 (B) in the presence of SES, compared to the untreated control.

The OD of *P. aeruginosa* suspension was adjusted to 0.4 at 600 nm. The bacterial suspension was then added to each well of a 96-well plate. SES at the final concentration of 10% (v/v), glucose at the final concentration of 0.4% (w/v), and ethidium bromide at the final concentration of 2 µg/ml were added to each well. The reaction was run using a Fluostar Optima plate reader at 37°C for an hour. Every minute the absorbance was taken at excitation 520 nm and emission at 590 nm. Results are expressed as the mean ± SEM, n=6.

### 3.2.8 Evaluating the effect of SES on the expression of quorum sensing genes in *P. aeruginosa*

The quorum sensing system controls biofilm formation and production of most virulence factors in *P. aeruginosa*. As it was shown that biofilm formation and release of at least some virulence factors were affected by the presence of SES, the impact of SES on quorum sensing genes in *P. aeruginosa* was assessed. Two major interconnected quorum sensing systems of *lasI/lasR* and *rhlI/rhlR* were analysed in this experiment. Acyl-homoserine lactones (AHLs) are the signal molecules in these systems.

RT-qPCR analysis of quorum sensing genes in NCTC 10662 presented in figure 3.14 showed that SES effected the down-regulation of the expression of *lasI* and *rhlI* compared with the control ( $P < 0.0001$  and  $P = 0.004$  respectively,  $n = 3$ ). However, no significant change in the expression of *lasR* and *rhlR* was observed when NCTC 10662 was treated with SES ( $P = 0.53$ ,  $n = 3$ , Figure 3.14).

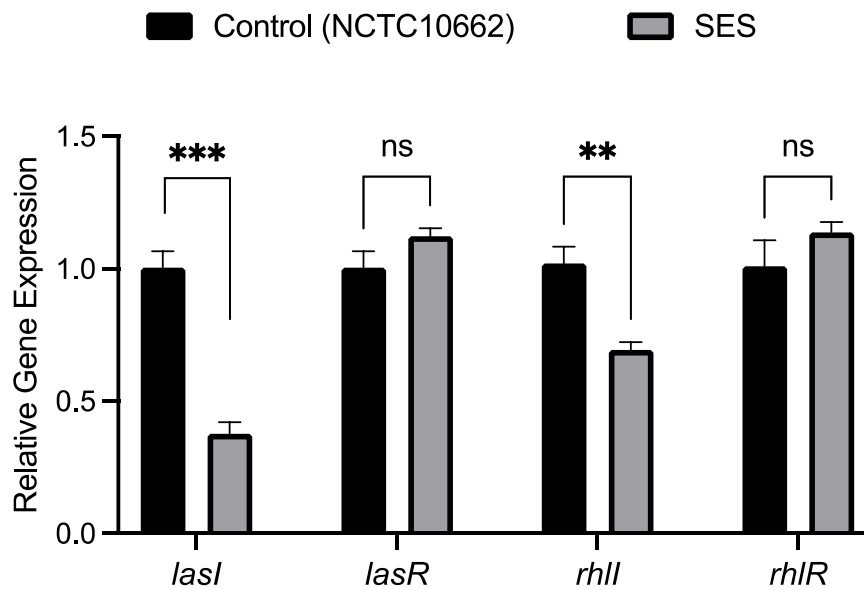


**Figure 3.14** Quorum sensing gene expression in *P. aeruginosa* NCTC 10662 in the absence and presence of SES.

NCTC 10662 was cultured in the absence (control) and presence of SES in biofilm. RNAs were extracted, and gene expression was monitored by RT-qPCR. The relative fold change of gene expression was determined by normalizing data against the untreated control. Results are expressed as the mean  $\pm$  SEM, n=3. ns = not significant, \*  $P \leq 0.05$ , \*\*  $P \leq 0.01$ , \*\*\*  $P \leq 0.001$ .

As it is demonstrated in figure 3.15, SES effected the down-regulation of the expression of *lasI* and *rhII* significantly ( $P < 0.0001$ , n=3). The expression of *lasR* in the presence of SES was up-regulated compared with control ( $P < 0.0001$ , n=3), and no significant change was observed in the expression of *rhIR* in PAO1 when it was treated with SES compared with control ( $P = 0.1$ , n=3).

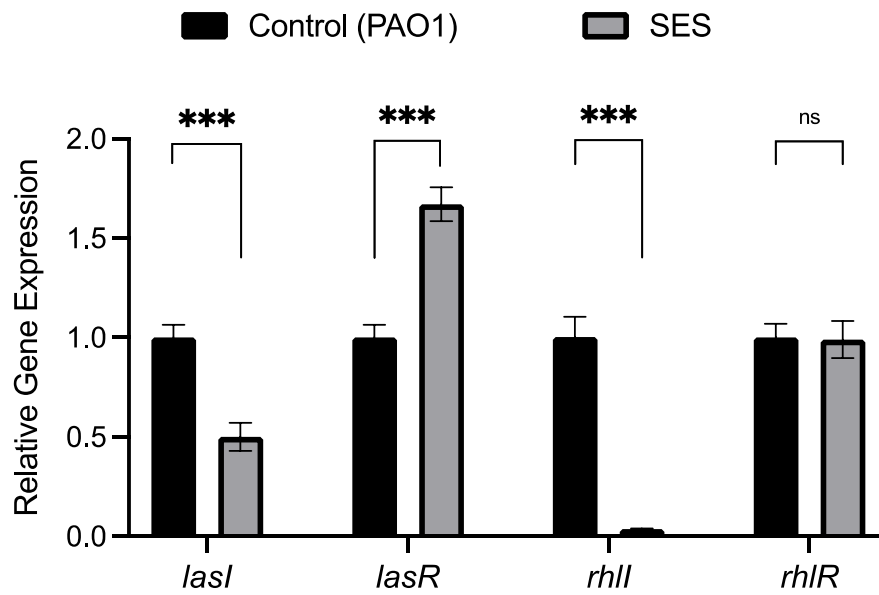


**Figure 3.15** Quorum sensing gene expression in *P. aeruginosa* PAO1 in the absence and presence of SES.

PAO1 was cultivated in the absence and presence of SES in a biofilm state. RNAs were extracted, and gene expression was monitored by RT-qPCR. The relative fold change of gene expression was determined by normalizing data against the untreated control. Results are expressed as the mean  $\pm$  SEM, n=3. ns = not significant, \*  $P \leq 0.05$ , \*\*  $P \leq 0.01$ , \*\*\*  $P \leq 0.001$ .

### 3.3 Discussion

This chapter investigated the biofilm formation and virulence factors production of *P. aeruginosa* in the presence of SES. Two phenotypically different strains of *P. aeruginosa* were chosen for this study, *P. aeruginosa* NCTC 10662 and PAO1. PAO1 forms a mucoid biofilm due to the production of alginate, while NCTC 10662 is a non-mucoid biofilm-forming human isolate (Kalgudi *et al.*, 2021). Although *P. aeruginosa* PAO1 was originally obtained as a wound clinical isolate, it is a laboratory strain that has been passaged numerous times in laboratories since its initial isolation. However, it has been used in the laboratory as a reference clinical isolate. *S. epidermidis* strains have noticeably diverse characteristics with differences in their genome content, metabolite production, and relationship to the host (Gallo and Nakatsuji, 2011; Naik *et al.*, 2015; Severn and Horswill, 2022). In this study, the supernatant of *S. epidermidis* NCTC 11047, which is a human nose isolate, was used.

*P. aeruginosa* is one of the leading pathogens associated with human infections due to its ability for biofilm formation, resistance to antimicrobial agents, and possession of numerous virulence factors. Therefore, initial experiments in this study aimed to determine the effect of SES on biofilm formation and the composition of EPS of biofilms formed by *P. aeruginosa*. Biofilm formation was significantly decreased in the presence of SES in both strains of *P. aeruginosa* without affecting bacterial growth. The transition between planktonic to biofilm state is accompanied by EPS production (Thi *et al.*, 2020). Additional analysis of the components of EPS revealed that SES also diminished the carbohydrate, protein, and eDNA content of *P. aeruginosa* biofilm. All components of EPS primarily operate for the structural integrity of the biofilm. They all form an integrated network of structures to protect bacterial cells against foreign threats (Ma *et al.*, 2009; Ciofu and Tolker-Nielsen, 2019). Carbohydrates in the biofilm, such as Pel and Psl polysaccharides, form the scaffold (Franklin *et al.*, 2011). In persistent infections, polysaccharides' production extends to alginate production to convert the bacterial biofilm to a mucoid phenotype (Kalgudi *et al.*, 2021). Proteins in biofilm matrix have a structural role by cross-linking to polysaccharides. CdrA is an extracellular adhesin protein that promotes

aggregate formation via binding with Psl and maintains biofilm architecture (Reichhardt *et al.*, 2020). Structural proteins such as flagella and pili are also important in the establishment and integrity of the biofilm (Valentin *et al.*, 2022). The primary role of eDNA within the biofilm is to facilitate attachment and stabilisation of the biofilm. DNase treatment of *P. aeruginosa* biofilm at early stages results in biofilm dissolution; however, the mature biofilm stays intact after DNase treatment (Whitchurch *et al.*, 2002), showing the important role of eDNA in aggregation. A decrease in the concentration of all components of EPS after treatment with SES is consistent with a decrease in total biofilm biomass in the presence of SES in both strains of *P. aeruginosa*, as shown in this study. However, a better understanding of the effect of SES on the composition of EPS needs the identification and broad characterisation of active molecule(s) in SES.

Motility in *P. aeruginosa* is considered a structural virulence factor, which also plays a vital role in biofilm formation. The formation of a biofilm begins with the interaction of planktonic cells with a surface. Extensive studies have characterised the role of the flagellum and type IV pili in the initiation and development of biofilm (O'Toole and Kolter, 1998; Klausen *et al.*, 2003; Barken *et al.*, 2008; Valentin *et al.*, 2022). The main types of motilities in *P. aeruginosa* are flagellum-mediated swimming and pili-mediated twitching. Moreover, flagella-mediate swarming motility is aided by the release of rhamnolipids and involves multicellular group movement on a surface. Attachment and the initial formation of microcolonies in a biofilm are associated with type IV pili, while flagellum-mediated motility is essential in the development of mature biofilm. Social swarming motility later aids the dispersal of biofilm (Barken *et al.*, 2008). The presence of SES in the growing culture of *P. aeruginosa* reduced flagellum-mediated swimming in both strains of NCTC 10662 and PAO1. The multicellular social swarming motility also was decreased in NCTC 10662. However, type IV pili-mediated twitching did not change in the presence of SES. This result indicates that SES could inhibit the maturation of biofilm through the inhibition of swimming rather than the initiation and attachment of bacteria through type IV pili. Also, SES might be able to inhibit biofilm dispersal through inhibition of flagella-mediated swarming in NCTC 10662; however, more studies are needed to confirm this result.

*S. epidermidis* produces several metabolites that have been shown to impact other microorganisms' growth and biofilm formation. However, the impact of *S. epidermidis* exoproducts on *P. aeruginosa* is rarely described. It has been shown that a serine protease secreted by *S. epidermidis* degrades *S. aureus* adhesin proteins (Iwase *et al.*, 2010; Sugimoto *et al.*, 2013). Adhesin proteins, such as extracellular adherence proteins, are essential in the biofilm formation of *S. aureus* on biotic and abiotic surfaces. *S. epidermidis*' serine protease also degrades several *S. aureus* binding proteins, such as fibronectin-binding protein A, which is involved in attachment to human cells (Sugimoto *et al.*, 2013). Flagella and pili are the major components in *P. aeruginosa*'s adhesion to surfaces. Several other adhesin proteins, such as *cdrA*, also promote the attachment and colonisation of *P. aeruginosa* (Reichhardt *et al.*, 2020; Valentin *et al.*, 2022). Furthermore, proteins have structural roles in *P. aeruginosa* biofilm, as discussed earlier. Therefore, it can be considered that *S. epidermidis*, by degrading adhesin proteins and structural proteins, might have an impact on biofilm formation and maturation in *P. aeruginosa*.

It is well known that *P. aeruginosa* produces several other virulence factors that help bacterial colonisation during infection. This study showed that the production of elastase and exotoxin A in both strains of NCTC 10662 and PAO1 decreased in the presence of SES. Elastase and exotoxin A are directly responsible for tissue damage during the infection by degrading proteins and inhibiting protein synthesis in the host cells (Casilag *et al.*, 2016). SES also reduced the production of pyocyanin in *P. aeruginosa* PAO1. Pyocyanin, a blue pigment with redox activity, is another vital virulence factor in *P. aeruginosa*. Pyocyanin is often detected in large quantities in the sputum of cystic fibrosis patients (Caldwell *et al.*, 2009). It is noteworthy that PAO1 produced a significantly higher amount of elastase and pyocyanin compared with NCTC 10662. Rhamnolipid surfactant release, which facilitates the multicellular swarming motility, also was decreased in NCTC 10662 in the presence of SES. This result was in accordance with the reduction in swarming motility in NCTC 10662, as discussed earlier. The SES did not affect rhamnolipid release in PAO1.

Quorum sensing gene expression analysis in this study showed that SES effected the down-regulation of the expression of autoinducer synthases *LasI* and *RhlI* in both PAO1 and NCTC 10662 strains. In the *las* and *rhl* quorum sensing systems, autoinducer synthases *LasI*

and RhII produce the 3-oxo-C12-HSL and C4-HSL signals, respectively (Kievit *et al.*, 2003; Wilder *et al.*, 2011). These signals interact with their cognate receptors, LasR and RhIR, respectively, to activate the regulation of several virulence genes in *P. aeruginosa*. The expression of *lasR* and *rhIR* did not change in the presence of SES in NCTC 10662. The expression of *lasR* was up-regulated with no change in the expression of *rhIR* in PAO1 in the presence of SES. This result indicated that SES reduced the release of 3-oxo-C12-HSL and C4-HSL signals in both strains of *P. aeruginosa*. Acyl homoserine lactone-mediated quorum sensing systems are associated with the regulation of virulence genes expression and biofilm formation in *P. aeruginosa*. Research has revealed that *las* and *rhl* quorum sensing systems regulate the expression of 315 genes in *P. aeruginosa* (Schuster *et al.*, 2003). The expression of virulence factors investigated in this study are also under the control of *las* and *rhl* quorum sensing systems. The decline in the release of virulence factors such as elastase, pyocyanin, rhamnolipids, and exotoxin A could be the result of the effect of SES on the production of quorum sensing signals. Some genes, such as *lasA*, which is responsible for the expression of elastase protein, respond well to the 3-oxo-C12-HSL signal, while some genes, like *rhIAB*, respond well to the C4-HSL signal, and some genes would be activated only in response to both signals (Schuster *et al.*, 2003; Schuster and Greenberg, 2006). Both signal synthases LasI/RhII and their receptor proteins LasR/RhIR are necessary to form a complex of signal-receptor and activate the promoter of target genes for gene expression (Lee and Zhang, 2015).

Unlike the effect of SES on the biofilm formation of *P. aeruginosa*, the SES had no significant impact on the preformed biofilm of *P. aeruginosa*. However, the combination of SES with antibiotics showed promising results in reducing biofilm biomass and viable cells residing in the preformed biofilm. In order to assess the impact of SES on the activity of effective and ineffective antibiotics against *P. aeruginosa*, three antibiotics of tetracycline, gentamicin, and ciprofloxacin were chosen. Tetracycline, typically ineffective against *P. aeruginosa*, inhibits bacterial protein synthesis by reversibly binding to ribosomal 30S subunit. Tetracycline passively diffuses through bacterial cells and has short-term action. The combination of SES with tetracycline did not change the efficacy of tetracycline against *P. aeruginosa* NCTC 10662. However, the combination of tetracycline with SES led to a drop in PAO1 cell viability at all concentrations tested on the preformed biofilm.



The combination of SES with gentamicin also improved the efficacy of gentamicin in diminishing bacterial cells in the preformed biofilm of PAO1, especially in higher concentrations of the antibiotic. Interestingly, the efficacy of combination therapy of gentamicin and SES on NCTC 10662 biofilm only improved at 8 µg/ml of gentamicin and was not observed at other concentrations. Gentamicin also inhibits bacterial protein synthesis by irreversibly binding to the ribosomal 30S subunit. Gentamicin has a prolonged action against *P. aeruginosa*; however, *P. aeruginosa* produces several aminoglycoside-modifying enzymes as part of its resistance mechanisms (Poole, 2005). SES might have inactivated these modifying enzymes and improved the efficacy of gentamicin in reducing viable cells.

Ciprofloxacin, on the other hand inhibits DNA replication and is the most active quinolone against *P. aeruginosa*. A combination of ciprofloxacin and SES improved the efficacy of ciprofloxacin in diminishing biofilm and bacterial cells embedded in the biofilm of PAO1. However, the SES did not change the effect of ciprofloxacin on the reduction of the preformed biofilm of NCTC 10662. The combination therapy of ciprofloxacin and SES reduced the number of viable cells in NCTC 10662 biofilm compared with ciprofloxacin alone. This study suggests that the impact of SES on the antibiotic susceptibility of *P. aeruginosa* could be strain specific and remains to be investigated on other clinical isolates. However, the data indicate that presumably certain metabolites of *S. epidermidis* are responsible for improving the efficacy of antibiotics, while the exact molecule(s) remain to be identified. In a recent study, researchers showed that the cell-free culture medium of *S. aureus* could also sensitise *P. aeruginosa* to antibiotics (Trizna *et al.*, 2020). In their study, the certain metabolites in the culture of *S. aureus* responsible for the impact on *P. aeruginosa* susceptibility were not identified either. This data and data from current study suggest the potential impact of staphylococci species on *P. aeruginosa* antibiotic susceptibility, which needs further investigation.

The results of this study in determining the impact of SES on efflux pump activity in *P. aeruginosa* showed no significant change in the efflux pump activity in both strains of NCTC 10662 and PAO1. The efflux pump activity determines the permeability of the bacterial cell membrane. As the effect of SES on the improvement of the antibiotic's

efficacy was not the same for all antibiotics tested, and the efflux pump activity did not change in the presence of SES, we can rule out the impact of SES on the permeability of *P. aeruginosa* to antibiotics. The reason for the effect of SES on the susceptibility of *P. aeruginosa* remains to be discussed.

# Chapter 4 Investigation of *P. aeruginosa* and *S. epidermidis* co-culture in planktonic and biofilm state

## 4.1 Introduction

Most microorganisms are frequently present in poly-microbial communities where there are different microbial interactions between individual species. In infections such as cystic fibrosis and chronic wounds, the interaction between species can influence pathogenic behaviour, such as biofilm formation and antibiotic resistance of the bacterial communities (Korgaonkar *et al.*, 2013; Omar *et al.*, 2017; Brown *et al.*, 2022).

In the case of skin wounds, the bacterial infection is an important factor that strongly affects wound healing in both acute and chronic wounds. Current clinical data suggest that bacterial infection present in the wound is in the form of poly-microbial biofilm; bacterial pathogenicity in polymicrobial infections could be enhanced in comparison to mono-culture infections (Wolcott *et al.*, 2016; Buch *et al.*, 2019; Loesche *et al.*, 2017; Sachdeva *et al.*, 2022). Furthermore, managing multidrug-resistant bacterial infections is a significant challenge for clinicians and researchers (Guest *et al.*, 2020). Already a complex challenge, now due to the COVID-19 pandemic and a surge in patients' hospitalization and an increase in prescribed antibiotics, antimicrobial resistance needs further attention (Taylor, 2021). Unravelling the interaction of microbiota in the wound can lead to the development of new therapeutics.

So, in recent years extensive research has been carried out to uncover the interaction mechanisms of bacterial cells present in the wound. Advances in genomic sequencing have helped to understand the wound microbiome better (Wolcott *et al.*, 2016). A recent study revealed when coagulase-negative staphylococci are present in the wound, there is a better chance of wound healing (Verbanic *et al.*, 2020). Current knowledge is limited about commensal skin microbiota's impact on the development or improvement of the wound. Further research is needed to discover how the interaction of commensal microbes with

opportunistic pathogens during infection could affect the wound-healing process (Ruff *et al.*, 2020; Sachdeva *et al.*, 2022).

This study aimed at investigating the interaction of *S. epidermidis*, a major skin commensal, and *P. aeruginosa*, an opportunistic pathogen residing on the skin, in both planktonic and biofilm states to assess the relative competition between *S. epidermidis* and *P. aeruginosa*.

## 4.2 Results

### 4.2.1 Co-culture of *P. aeruginosa* and *S. epidermidis* in the planktonic state

To better understand the interaction of *P. aeruginosa* and *S. epidermidis*, the competition of these bacteria was tested first in the planktonic growth state. Although there is no investigation of the interaction of *P. aeruginosa* and *S. epidermidis* in the literature, the interaction between *P. aeruginosa* with *S. aureus* has been investigated extensively (Biswas *et al.*, 2009; Briaud *et al.*, 2019; Gounani *et al.*, 2020). *P. aeruginosa* and *S. aureus* are recognised as the most important pathogens in causing nosocomial infections, and they usually are isolated from wound and lung infections in cystic fibrosis patients (Fazli *et al.*, 2009; Pallett *et al.*, 2019). Both competitive and co-existing phenotypes have been reported for *S. aureus* in the co-culture of *P. aeruginosa* and *S. aureus* (Tognon *et al.*, 2019; Trizna *et al.*, 2020). These phenotypes have been determined by analysing the growth curve, number of colonies, and size of colonies after the co-colonisation of the two bacteria. Therefore, this study aimed to investigate the interaction between *P. aeruginosa* and *S. epidermidis* first by analysing the growth curve.

The growth of *S. epidermidis* and *P. aeruginosa* alone and in co-culture with each other was analysed by monitoring the absorbance of the culture at 600 nm every hour for 12 hours. Bacterial cells were inoculated at a 1:1 ratio in 250 ml flasks containing 50 ml of TSB and incubated at 37°C at 180 rpm in shaking flasks. Mono-cultures of both strains were also incubated under the same conditions for control comparison. Every two hours, samples from each culture (mono-cultures and co-cultures) were plated on cefrimide and staphylococcal selective agars to determine the number of CFU per ml of the culture of

*P. aeruginosa* and *S. epidermidis*, respectively. The size and shape of colonies were also examined from mono-cultures and co-cultures (Section 2.2.12).

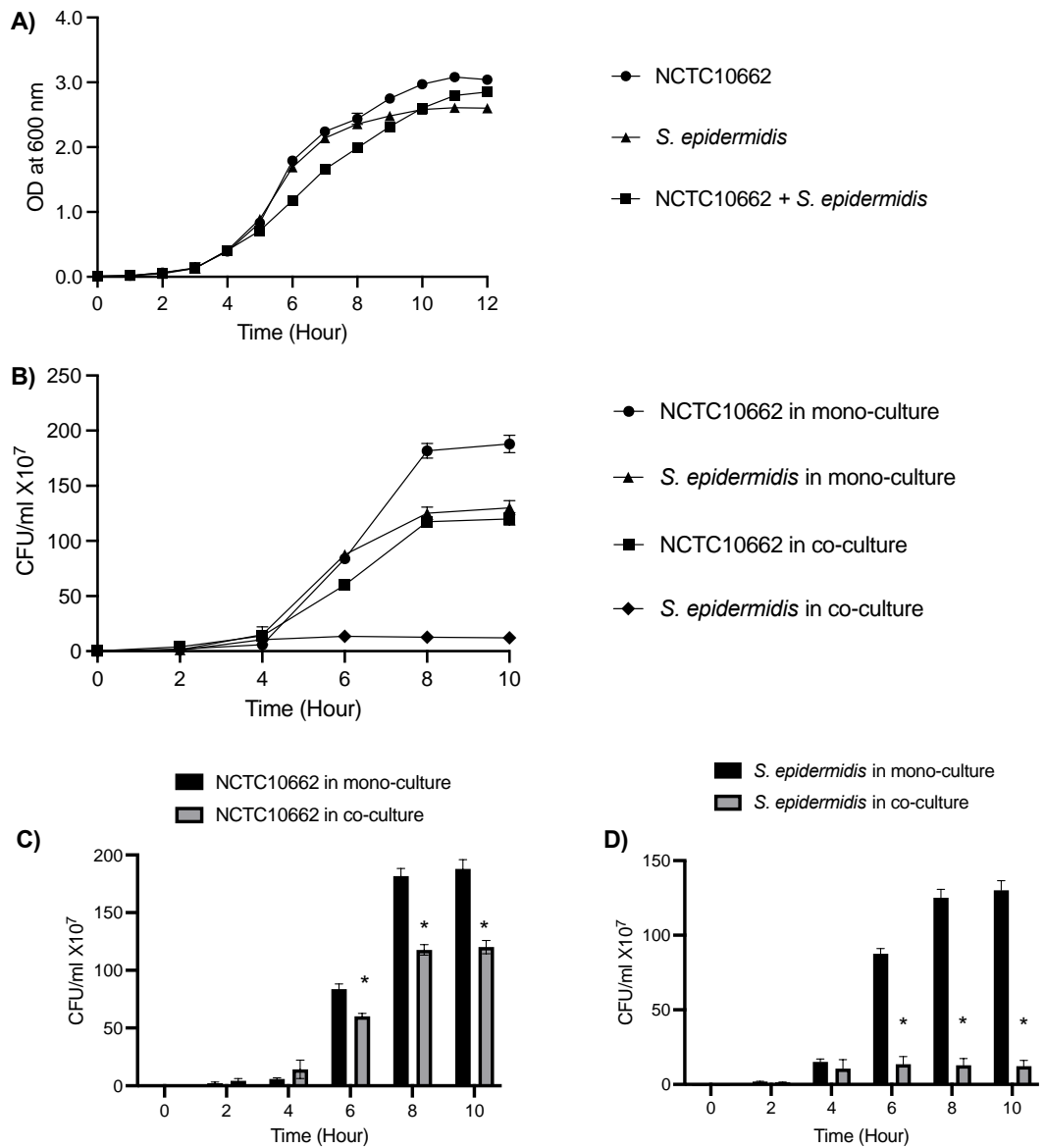


**Figure 4.1** Planktonic growth of *P. aeruginosa* NCTC 10662 and *S. epidermidis* in mono- and co-culture.

A) *P. aeruginosa* NCTC 10662 and *S. epidermidis* were mono- and co-cultured in 250 ml flasks containing 50 ml of TSB for 12 hours at 37° C and 180 rpm. The OD of the cultures was measured at 600 nm every hour. B) Every two hours, bacterial culture samples from mono- and co-culture growth were plated on cetrimide and staphylococcal selective agar to determine CFU/ml of *P. aeruginosa* NCTC 10662 and *S. epidermidis*, respectively. C) Comparison of CFU/ml of *P. aeruginosa* NCTC 10662 in mono- and co-culture. D) Comparison of CFU/ml of *S. epidermidis* in mono- and co-culture. This experiment was repeated three times in triplicate reading. Error bars are reported as mean ± SEM, \* P ≤ 0.05.

As shown in figure 4.1 (A), the growth curve of the co-culture of *P. aeruginosa* NCTC 10662 and *S. epidermidis* showed the same trend as the mono-culture of each bacterium growth curve during the 12 hours of growth. Analysing the number of bacterial cells in the cultures reported as CFU/ml revealed a better insight into determining the interaction of NCTC 10662 and *S. epidermidis* (Figure 4.1 B, C, and D). Although the number of *S. epidermidis* cells in the co-culture was lower than the number of cells at the same time in the mono-culture, this number did not decline to zero, suggesting *S. epidermidis*' survival in the co-culture with NCTC 10662 (Figure 4.1 B and D). The stationary phase of *S. epidermidis* in mono-culture started at 8 hours after the inoculation. However, in the co-culture, the stationary phase of *S. epidermidis* started after 4 hours of growth, and the number of CFU/ml did not increase after 4 hours (Figure 4.1 D). Analysing colonies from mono-culture and co-culture of *S. epidermidis* showed no discernible differences in shape and size.

*P. aeruginosa* NCTC 10662 in mono-culture and co-culture showed a similar trend of growth (Figure 4.1 B). However, the number of cells in co-culture was lower than the number of cells in mono-culture at the same time-points after 6 hours of incubation ( $P=0.01$ ,  $P=0.002$ , and  $P=0.002$ , respectively, Figure 4.1 C). Colonies from mono-culture and co-culture of *P. aeruginosa* NCTC 10662 were analysed, and no differences were observed in the colonies' shape, size, and colour.

The interaction of *P. aeruginosa* NCTC 10662 and *S. epidermidis* was further investigated using a mathematical method by calculating the CI and RIR of NCTC 10662 over *S. epidermidis* (Section 2.2.12, Figure 4.2). RIR index compares the growth of both species when they are in their mono-culture, and CI compares each species' growth when they are in co-culture. A positive CI was detected for all time-points of growth; however, there were no significant differences between CI and RIR at any time-point, indicating no competitive advantage of NCTC 10662 over *S. epidermidis* through 10 hours of planktonic growth (Figure 4.2 B). This data indicates that *P. aeruginosa* NCTC 10662 grows better in mono- and co-culture compared to *S. epidermidis*.

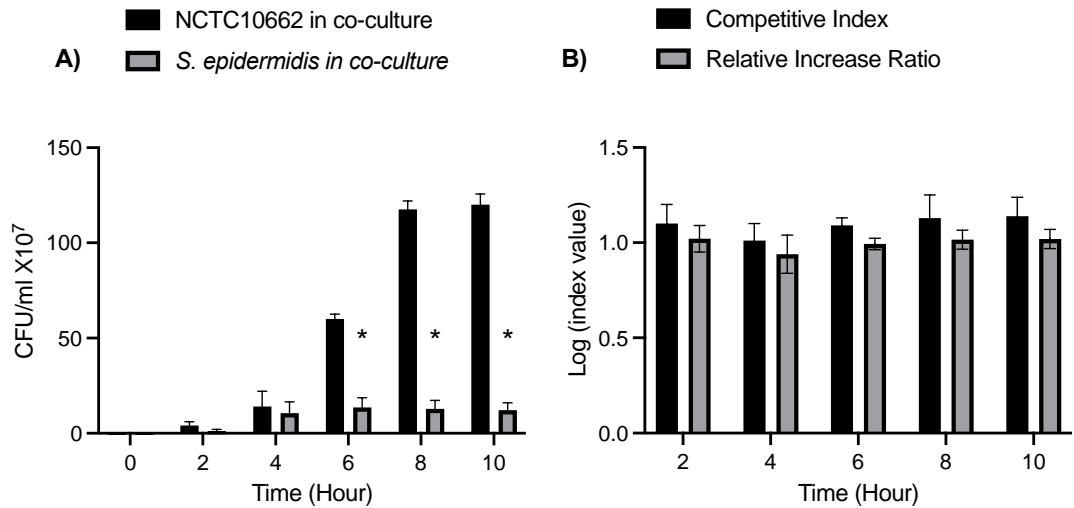


**Figure 4.2** Competition growth profile between *P. aeruginosa* NCTC 10662 and *S. epidermidis* in co-culture.

A) Number of bacterial cells reported as CFU/ml in planktonic co-culture of *P. aeruginosa* NCTC 10662 and *S. epidermidis*. Samples from every two hours of planktonic growth were plated on ceftrimide and staphylococcal selective agar to determine the number of cells of NCTC 10662 and *S. epidermidis*, respectively, in the co-culture growth media. B) The RIR was calculated for NCTC 10662 and *S. epidermidis* by comparing the growth curve (based on the CFU/ml) of both species in their mono-culture. The CI was calculated for NCTC 10662 and *S. epidermidis* by comparing the number of bacterial cells of the two species when they were cultivated together. CI and RIR were calculated by comparing NCTC 10662 advantages over *S. epidermidis*. This experiment was repeated three times in triplicate reading. Error bars are reported as mean  $\pm$  SEM, \*  $P \leq 0.05$ .

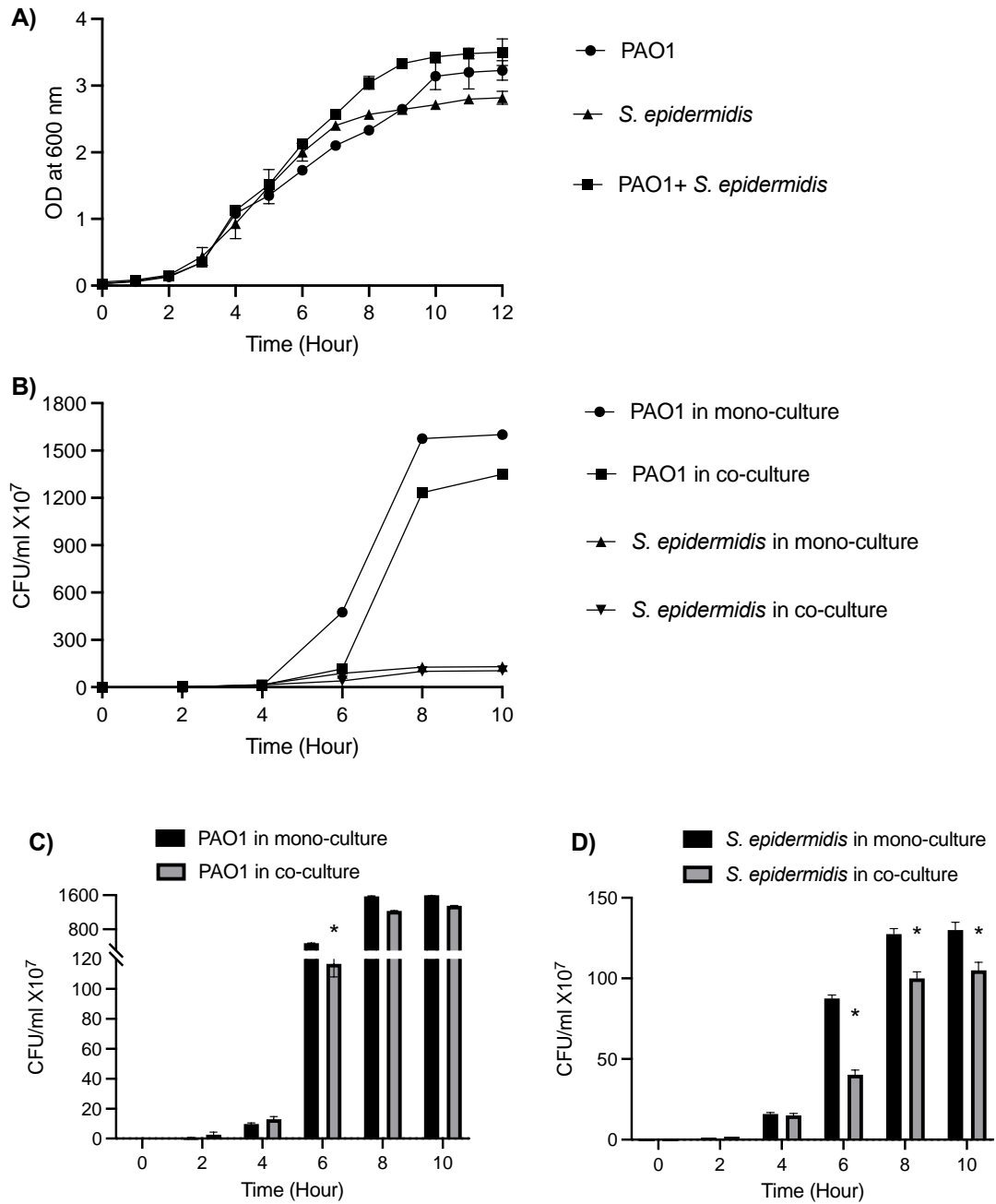


**Figure 4.3** Planktonic growth of *P. aeruginosa* PAO1 and *S. epidermidis* in mono- and co-culture.

A) *P. aeruginosa* PAO1 and *S. epidermidis* were mono- and co-cultivated in 250 ml shaking flasks containing 50 ml of TSB for 12 hours at 37° C and 180 rpm. The OD of the cultures was measured every hour at 600 nm. B) Every two hours, bacterial culture samples from mono- and co-culture growth were plated on cetrimide and staphylococcal selective agar to determine CFU/ml of *P. aeruginosa* PAO1 and *S. epidermidis* respectively. C) Comparison of CFU/ml of *P. aeruginosa* PAO1 in mono- and co-culture. D) Comparison of CFU/ml of *S. epidermidis* in mono- and co-culture. This experiment was repeated three times in triplicate reading. Error bars are reported as mean ± SEM, \* P ≤ 0.05.



Measuring the OD<sub>600</sub> of mono-culture and co-culture of *P. aeruginosa* PAO1 and *S. epidermidis*, as it is presented in figure 4.3 A, showed the same trend on all growth curves profiles during 12 hours of growth. Further analysing the number of bacterial cells at each time-point and in mono-cultures and co-cultures revealed a significantly higher number of PAO1 cells reported as CFU/ml compared to *S. epidermidis* CFU/ml from the 6-hour time-point onward (P=0.01, P=0.001, P=0.002, respectively, Figure 4.3 B and Figure 4.4 A). There was no significant difference between the number of bacterial cells in the mono-culture of *P. aeruginosa* PAO1 and its co-culture, except at 6 hours after incubation which the CFU/ml of PAO1 in co-culture was significantly lower than the CFU/ml at the same time in mono-culture (P=0.001, Figure 4.3 B and C). The analysis of colonies from mono-culture and co-culture of PAO1 at any time-point showed no significant change in size, shape, and colour.

*S. epidermidis* in mono-culture and co-culture showed a similar growth trend; however, the number of bacterial cells in co-culture was significantly lower than in mono-culture from 6 hours post incubation onward. The stationary phase in both mono-culture and co-culture of *S. epidermidis* was started 8 hours after the incubation (Figure 4.3 B and D). Analysing the colonies of *S. epidermidis* in mono-culture and co-culture showed no significant changes in size and shape.

To better understand the differences between *P. aeruginosa* PAO1 and *S. epidermidis* in the planktonic growth co-culture, the CI and RIR indexes were calculated as described in Section 2.2.12 (Figure 4.4). RIR index compares the growth of both species when they are in their mono-culture, and CI compares each species' growth when they are in co-culture. There is a negative CI at the 2-hour post-incubation time-point, suggesting the advantage of *S. epidermidis* in co-culture over PAO1 at this time-point. However, there is no statistically significant difference between CI and RIR. A positive CI was detected in all other time-points; however, only at 4-hour and 6-hour post incubation a significant difference between CI and RIR was observed (P=0.0003 and P=0.002, respectively, Figure 4.4 B), suggesting a competitive advantage of *P. aeruginosa* PAO1 over *S. epidermidis* during the exponential phase of planktonic growth of co-culture (Figure 4.4).

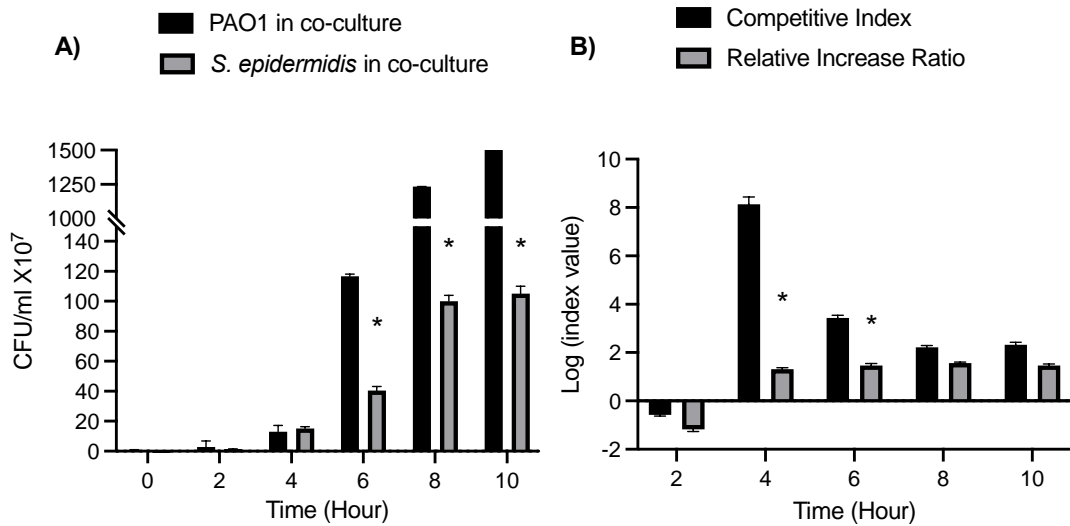


**Figure 4.4** Competition growth profile between *P. aeruginosa* PAO1 and *S. epidermidis* in co-culture.

A) Number of bacterial cells reported as CFU/ml in planktonic co-culture of *P. aeruginosa* PAO1 and *S. epidermidis*. Samples from every two hours of planktonic growth were plated on cetrimide and staphylococcal selective agar to determine the number of PAO1 and *S. epidermidis*, respectively, in the co-culture growth media. B) The RIR was calculated for PAO1 and *S. epidermidis* by comparing the growth curve of both species in their mono-culture. The CI was calculated for PAO1 and *S. epidermidis* by comparing the number of bacterial cells of the two species when they were cultivated together. CI and RIR were calculated by comparing PAO1 growth advantages over *S. epidermidis*. This experiment was repeated three times in triplicate reading. Error bars are reported as mean  $\pm$  SEM, \*  $P \leq 0.05$ .

## 4.2.2 Co-culture of *P. aeruginosa* and *S. epidermidis* in biofilm state

In order to further study the interaction of *P. aeruginosa* and *S. epidermidis*, they were grown in a biofilm state, and their biofilm growth was assessed. Biofilms are present in most chronic infections, especially in lung infections in cystic fibrosis patients and in wounds. Little is known about the impact of bacterial interactions in polymicrobial biofilms on the evolution of infections, specifically about the interaction of *P. aeruginosa* and *S. epidermidis*.

The first step in biofilm formation is the attachment of bacterial cells to the surface. Therefore, successful attachment and placement of bacterial cells on a surface can determine their survival in polymicrobial infections. One mechanism by which *S. epidermidis* may affect biofilm formation of *P. aeruginosa* is through the inhibition of adhesion to the surface. To test this hypothesis, three different *in vitro* scenarios were simulated to assess the effect of *S. epidermidis* on the biofilm formation of *P. aeruginosa* (Section 2.2.13).

In the first scenario, *S. epidermidis* mono-culture biofilm was formed in a 96-well plate at 37°C for 24 hours. After the incubation time, the established biofilm was washed with PBS to discard unattached cells. Then, 200 µl of the fresh culture of *P. aeruginosa* was added to the *S. epidermidis* preformed biofilm and incubated for another 24 hours at 37°C (Figure 4.5 and Figure 4.8).

In the second scenario, 24-hour preformed biofilm of *P. aeruginosa* in a 96-well plate was washed with PBS; then, 200 µl of the fresh culture of *S. epidermidis* was added to the biofilm and incubated for another 24 hours at 37°C (Figure 4.6 and Figure 4.9).

The third scenario was the co-exposure of *S. epidermidis* and *P. aeruginosa* (200 µl of mixed culture at 1:1 ratio). Both *P. aeruginosa* and *S. epidermidis* were inoculated at the same time at 1:1 ratio in a 96-well plate and grown at 37°C for 24 hours. After the incubation time, the biofilm was washed, and a fresh suspension of bacterial cells at a 1:1 ratio was added for another 24 hours of incubation (Figure 4.7 and Figure 4.10).

Alongside these simulated scenarios, as control, separate mono-culture biofilms of *P. aeruginosa* and *S. epidermidis* were also set up. The control experiments were incubated for 24 hours followed by biofilm wash and the addition of fresh bacterial suspension of the same culture and incubated for another 24 hours at 37°C. After 48 hours of incubation, biofilm biomass from all experiments was measured by crystal violet assay, and the number of bacterial cells in mono-culture and co-culture was measured by plating bacterial suspension from the biofilm cultures on cefrimide and staphylococcal selective agar to determine *P. aeruginosa* and *S. epidermidis*, respectively (Section 2.2.13).

From the first scenario, an investigation was done to determine whether *S. epidermidis* could inhibit *P. aeruginosa* NCTC 10662 adhesion through exclusion. The data shown in figure 4.5 demonstrates that if NCTC 10662 suspension was added to the preformed biofilm of *S. epidermidis*, the NCTC 10662 biofilm forming abilities would decrease ( $P=0.03$ ,  $n=9$ , Figure 4.5 A). Also, the number of adherent NCTC 10662 cells reduced when NCTC 10662 was added to *S. epidermidis* ( $P=0.01$ ,  $n=9$ , Figure 4.5 B), suggesting *S. epidermidis* is able to mitigate NCTC 10662 adhesion through exclusion.

Next, the ability of *S. epidermidis* to inhibit NCTC 10662 adhesion through the displacement of the biofilm was investigated by executing the second scenario experiments. The data presented in figure 4.6 demonstrates that when 200  $\mu\text{l}$  of *S. epidermidis* suspension was added to 24-hour biofilm of NCTC 10662, no change in NCTC 10662 biofilm formation occurred ( $P=0.06$ ,  $n=9$ , Figure 4.6 A), and the number of NCTC 10662 adherent cells did not change ( $P=0.06$ ,  $n=9$ , Figure 4.6 B). Indicating *S. epidermidis* would not be able to reduce NCTC 10662 adhesion through displacement.

To investigate if *S. epidermidis* and NCTC 10662 would compete to adhere to the surface of tissue culture, both strains were co-cultured at the same time for 48 hours (as explained in the third scenario). Figure 4.7 shows that although the biofilm biomass did not change at the co-exposure of the two strains to the surface, the number of adherent cells in both strains decreased significantly ( $P=0.02$ ,  $n=9$ , Figure 4.7 A and B).

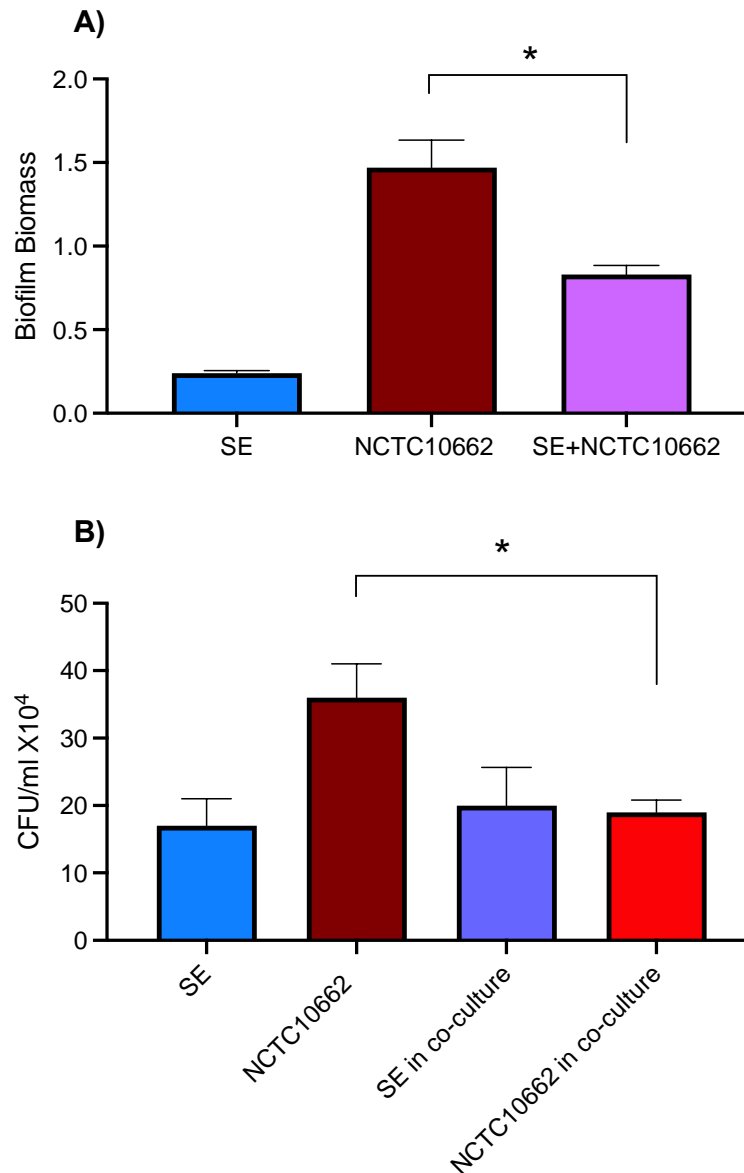


**Figure 4.5** Biofilm growth of *P. aeruginosa* NCTC 10662 in co-culture with *S. epidermidis* (SE) when NCTC 10662 was added to the 24-hour preformed biofilm of *S. epidermidis*. A) Biofilm biomass of *S. epidermidis* and NCTC 10662 in mono-culture and co-culture for 48 hours. In the co-culture, *S. epidermidis* biofilm was formed in a 96-well plate for 24 hours, then 200  $\mu$ l of NCTC 10662 fresh culture was added to the 24-hour preformed biofilm of *S. epidermidis* and incubated for another 24 hours (SE+NCTC 10662). Biofilm biomass was measured using the crystal violet assay. B) Number of bacterial cells reported as CFU/ml in mono-culture and co-culture biofilm of *S. epidermidis* and NCTC 10662 when NCTC 10662 is added to the 24-hour preformed biofilm of *S. epidermidis*. Samples from the biofilms were plated on cetrimide and staphylococcal selective agar to determine CFU/ml of NCTC 10662 and *S. epidermidis*, respectively. This experiment was repeated three times, and in each case, triplicate readings were made. Error bars are reported as mean  $\pm$  SEM, \*  $P \leq 0.05$ .

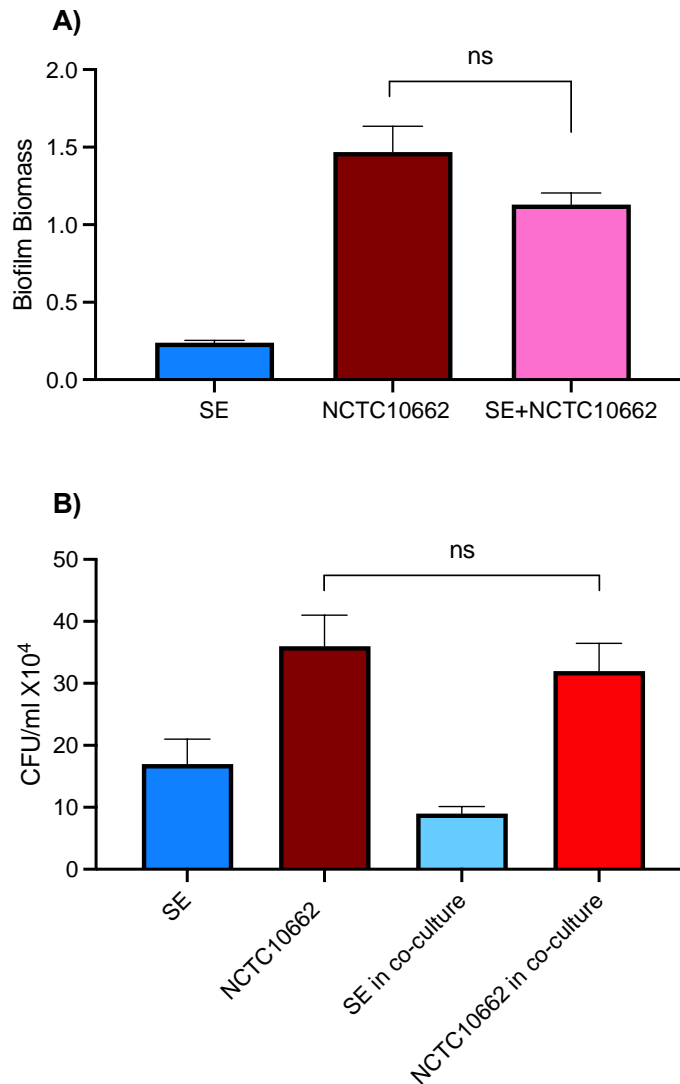


**Figure 4.6** Biofilm growth of *P. aeruginosa* NCTC 10662 in co-culture with *S. epidermidis* (SE) when *S. epidermidis* was added to the 24-hour preformed biofilm of NCTC 10662.

A) Biofilm biomass of *S. epidermidis* and NCTC 10662 in mono-culture and co-culture for 48 hours. In the co-culture, NCTC 10662 biofilm was formed a 96-well plate up for 24 hours, then 200  $\mu$ l of *S. epidermidis* fresh culture was added to the preformed biofilm of NCTC 10662 and incubated for another 24 hours (SE+NCTC 10662). Biofilm biomass was measured using crystal violet assay at 570 nm. B) Number of bacterial cells reported as CFU/ml in mono-culture and co-culture biofilm of *S. epidermidis* and NCTC 10662 when *S. epidermidis* was exposed to the 24-hour preformed biofilm of NCTC 10662. Samples from the biofilms were plated on cetrimide and staphylococcal selective agar to determine CFU/ml of NCTC 10662 and *S. epidermidis*, respectively. This experiment was repeated three times, and in each case, triplicate readings were made. Error bars are reported as mean  $\pm$  SEM, and ns = not significant.

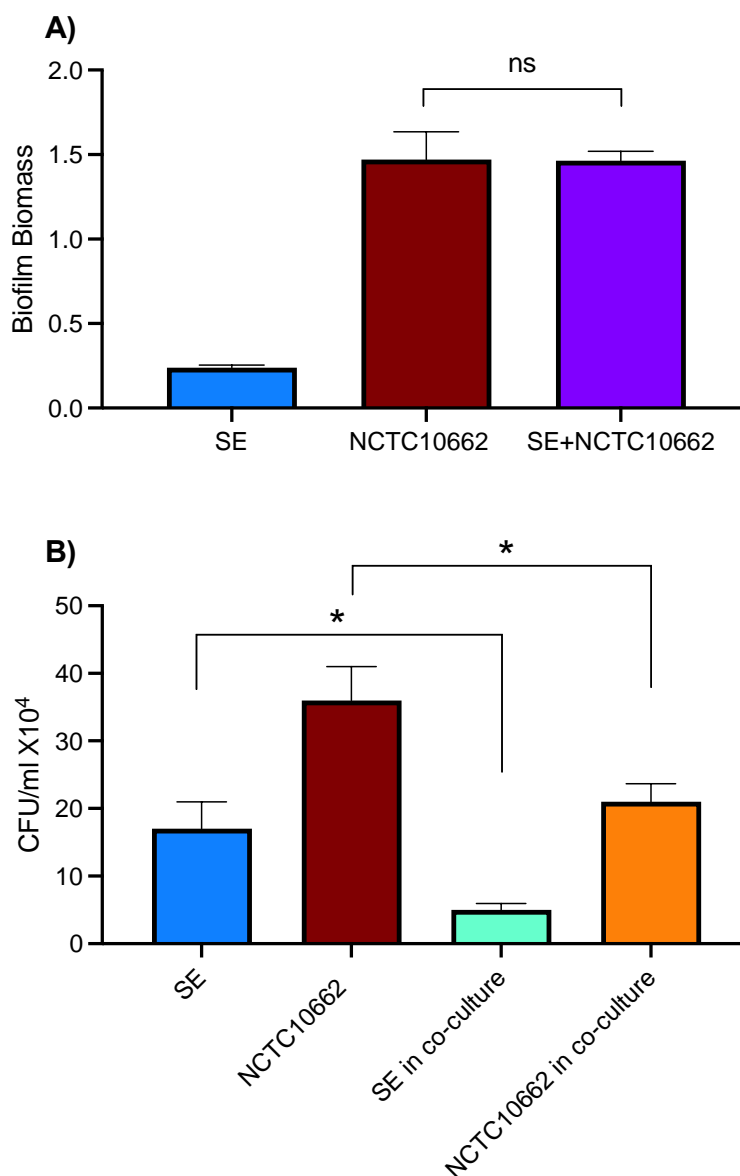


**Figure 4.7** Biofilm growth of *P. aeruginosa* NCTC 10662 in co-culture with *S. epidermidis* (SE) when NCTC 10662 and *S. epidermidis* were co-cultivated at the same time.

A) Biofilm biomass of *S. epidermidis* and NCTC 10662 in mono-culture and co-culture for 48 hours. In the co-culture, NCTC 10662 and *S. epidermidis* co-culture biofilm was formed over 24 hours. Then fresh mixed suspension of the *S. epidermidis* and NCTC 10662 was added to the preformed biofilm and incubated for another 24 hours (SE+NCTC 10662). Biofilm biomass was measured using crystal violet assay at 570 nm. B) Number of bacterial cells reported as CFU/ml in mono-culture and co-culture biofilm of *S. epidermidis* and NCTC 10662 when *S. epidermidis* and NCTC 10662 were co-cultivated at the same time. Samples from the biofilms were plated on cetrimide and staphylococcal selective agar to determine CFU/ml of NCTC 10662 and *S. epidermidis*, respectively. This experiment was repeated three times, and in each case, triplicate readings were made. Error bars are reported as mean  $\pm$  SEM, ns = not significant, and \*  $P \leq 0.05$ .

A similar set of experiments as described previously was carried out to investigate the interaction of *S. epidermidis* and *P. aeruginosa* PAO1 in biofilm state.

The data shown in figures 4.8, 4.9, and 4.10 highlight the interaction of *P. aeruginosa* PAO1 and *S. epidermidis*. To investigate if *S. epidermidis* can inhibit the adhesion of PAO1 by exclusion, PAO1 was added to the preformed biofilm of *S. epidermidis*. The data in Figure 4.8 demonstrates that the biofilm biomass in the co-culture of PAO1 and *S. epidermidis*, when PAO1 was added to *S. epidermidis*, did not change compared to the mono-culture of PAO1 (Figure 4.8 A). However, the number of adherent cells in *S. epidermidis* and PAO1 biofilm diminished significantly ( $P=0.004$  and  $P=0.01$ , respectively,  $n=9$ , Figure 4.8 B). This data suggests that *S. epidermidis* cannot impact the biofilm-forming ability of PAO1 through exclusion, but it decreases its adhesion ability.

To further explore the potential of *S. epidermidis* to inhibit biofilm formation and adhesion of PAO1, the 24-hour preformed biofilm of PAO1 was post-exposed to *S. epidermidis*. Interestingly, as shown in figure 4.9, not only was *S. epidermidis* unable to diminish the biofilm biomass and cell adhesion, but also the *S. epidermidis*' attachment was inhibited by PAO1 ( $P=0.002$ ,  $n=9$ , Figure 4.9 B). This data indicates that *S. epidermidis* is not able to inhibit the PAO1 attachment through displacement. However, PAO1 can inhibit the adhesion of *S. epidermidis* by exclusion.

Next, the ability of *S. epidermidis* and PAO1 to compete in adhesion to the tissue culture surface was investigated when both strains were co-cultivated at the same time (Figure 4.10). *S. epidermidis* and PAO1 in a 1:1 ratio was cultivated in a biofilm set-up; after 24 hours of incubation, the biofilm was rinsed carefully, and the fresh mixed suspension was added to the preformed biofilm of PAO1 and *S. epidermidis*. The data in figure 4.10 shows that biofilm biomass decreased in the co-culture of *S. epidermidis* and PAO1 ( $P=0.04$ ,  $n=9$ , Figure 4.10 A). Also, the number of attached *S. epidermidis* and PAO1 decreased in the co-culture ( $P=0.003$  and  $P=0.02$ , respectively,  $n=9$ , Figure 4.10 B).



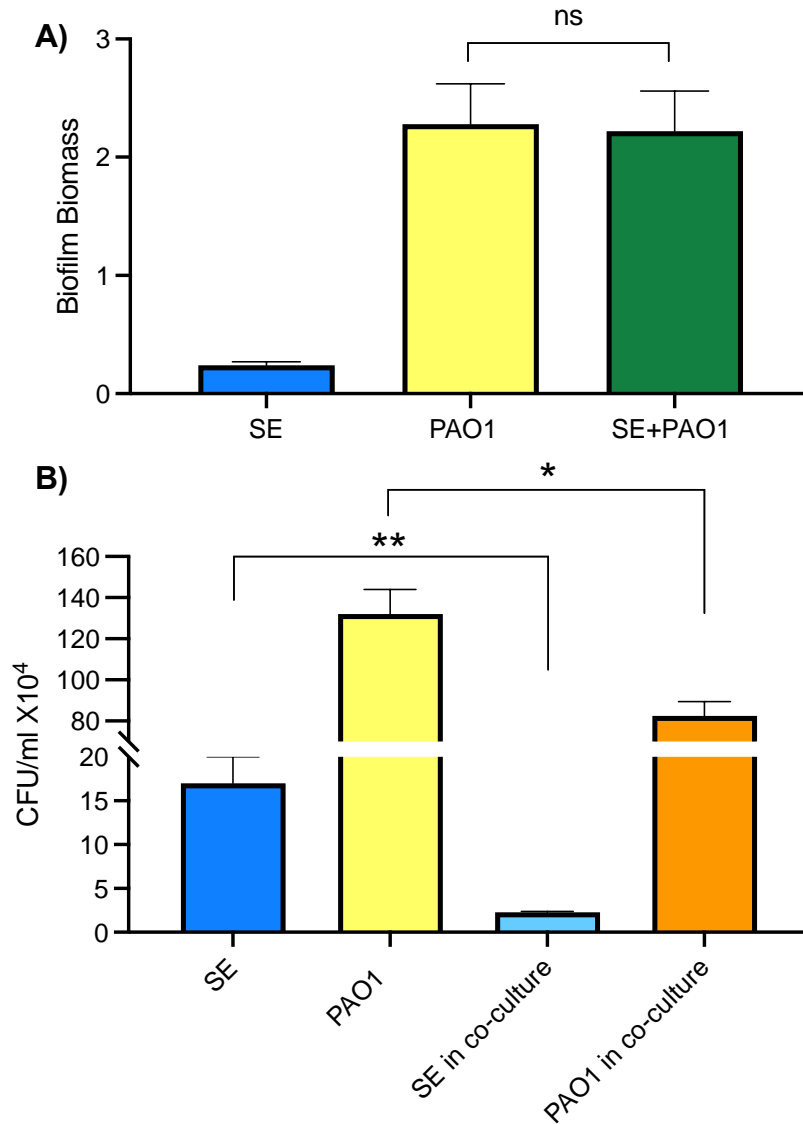


**Figure 4.8** Biofilm growth of *P. aeruginosa* PAO1 in co-culture with *S. epidermidis* (SE) when PAO1 was added to the 24-hour preformed biofilm of *S. epidermidis*.

A) Biofilm biomass of *S. epidermidis* and PAO1 in mono-culture and co-culture for 48 hours. In the co-culture, *S. epidermidis* biofilm was formed in a 96-well plate for 24 hours, then 200  $\mu$ l of PAO1 fresh culture was added to the 24-hour preformed biofilm of *S. epidermidis* and incubated for another 24 hours (SE+PAO1). Biofilm biomass was measured using the crystal violet assay at 570 nm. B) Number of bacterial cells reported as CFU/ml in mono-culture and co-culture biofilm of *S. epidermidis* and PAO1 when PAO1 is added to the 24-hour preformed biofilm of *S. epidermidis*. Samples from the biofilms were plated on cetrimide and staphylococcal selective agar to determine CFU/ml of PAO1 and *S. epidermidis*, respectively. This experiment was repeated three times, and, in each case, triplicate readings were made. Error bars are reported as mean  $\pm$  SEM. ns = not significant, \*  $P \leq 0.05$ , and \*\*  $P \leq 0.01$ .

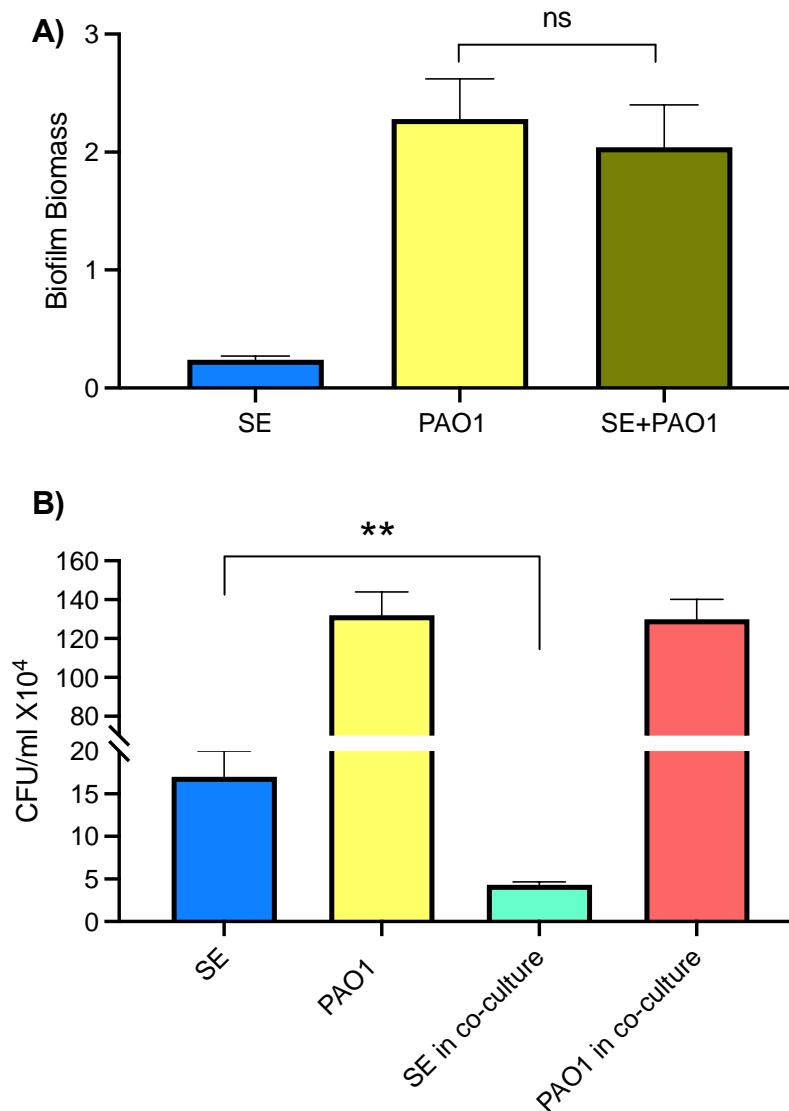


**Figure 4.9** Biofilm growth of *P. aeruginosa* PAO1 in co-culture with *S. epidermidis* (SE) when *S. epidermidis* was added to the 24-hour preformed biofilm of PAO1.

A) Biofilm biomass of *S. epidermidis* and PAO1 in mono-culture and co-culture for 48 hours. In the co-culture, the PAO1 biofilm was formed in a 96-well plate for 24 hours, and then 200  $\mu$ l of *S. epidermidis* fresh culture was added to the preformed biofilm of PAO1 and incubated for another 24 hours (SE+PAO1). Biofilm biomass was measured using crystal violet assay at 570 nm. B) Number of bacterial cells reported as CFU/ml in mono-culture and co-culture biofilm of *S. epidermidis* and PAO1 when *S. epidermidis* is added to the 24-hour preformed biofilm of PAO1. Samples from the biofilms were plated on cetrimide and staphylococcal selective agar to determine CFU/ml of PAO1 and *S. epidermidis*, respectively. This experiment was repeated three times, and in each case, triplicate readings were made. Error bars are reported as mean  $\pm$  SEM. ns = not significant and \*\*  $P \leq 0.01$ .

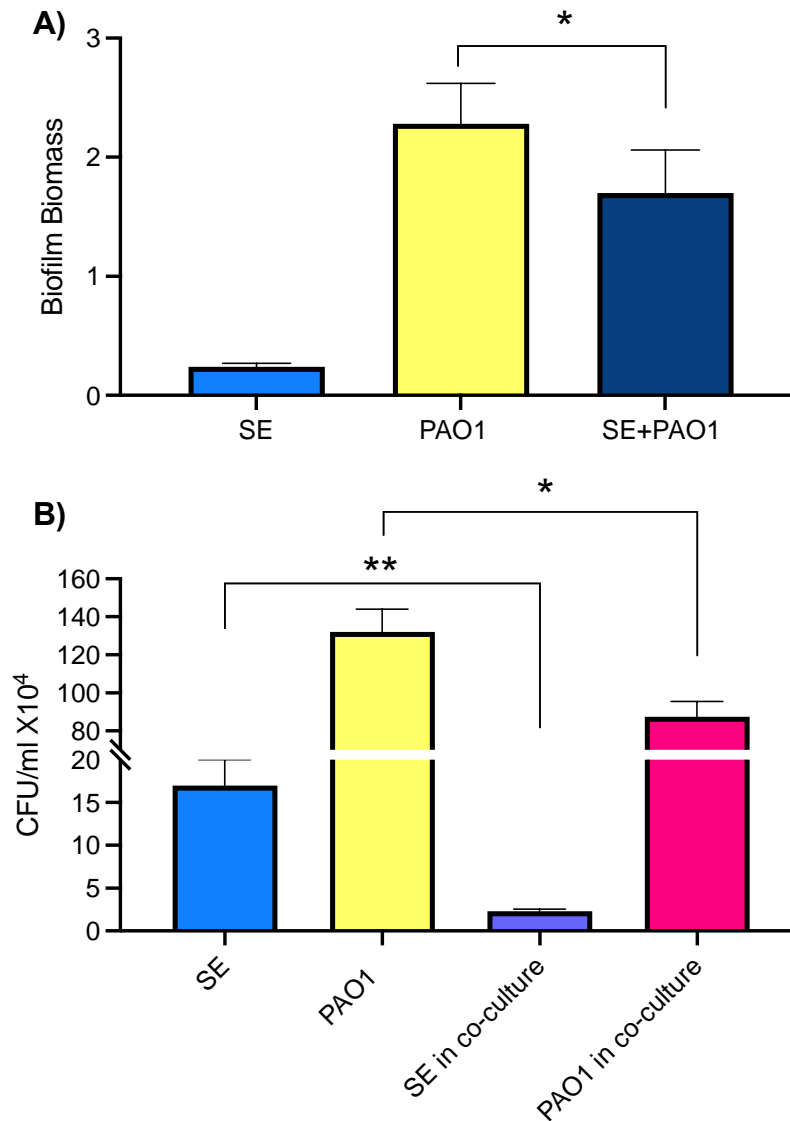


**Figure 4.10** Biofilm growth of *P. aeruginosa* PAO1 in co-culture with *S. epidermidis* (SE) when PAO1 and *S. epidermidis* were co-cultivated at the same time.

A) Biofilm biomass of *S. epidermidis* and PAO1 in mono-culture and co-culture for 48 hours. In the co-culture, PAO1 and *S. epidermidis* co-culture biofilm was formed over 24 hours. Then fresh mixed suspension of *S. epidermidis* and PAO1 was added to the preformed biofilm and incubated for another 24 hours (SE+PAO1). Biofilm biomass was measured using the crystal violet assay at 570 nm. B) Number of bacterial cells reported as CFU/ml in mono-culture and co-culture biofilm of *S. epidermidis* and PAO1 when *S. epidermidis* and PAO1 were co-cultivated at the same time. Samples from the biofilms were plated on cetrimide and staphylococcal selective agar to determine CFU/ml of PAO1 and *S. epidermidis*, respectively. This experiment was repeated three times, and in each case, triplicate readings were made. Error bars are reported as mean  $\pm$  SEM. ns = not significant, \*  $P \leq 0.05$ , and \*\*  $P \leq 0.01$ .

### 4.2.3 Antibiotic susceptibility of *P. aeruginosa* when is co-cultivated with *S. epidermidis*

Infections often are known to be composed of multiple combinations of bacteria, involving complex interactions that can influence the fitness and antibiotic tolerance of the involved bacteria (Murray *et al.*, 2014; Algburi *et al.*, 2017). Therefore, the antibiotic susceptibility of *P. aeruginosa* in co-culture with *S. epidermidis* was investigated.

Antibiotic susceptibility of *P. aeruginosa* NCTC 10662 and PAO1 in co-culture with *S. epidermidis* was investigated on TSB medium, the main medium in the study of co-culture. Three types of antibiotics were selected for this experiment. Tetracycline hydrochloride was chosen as an ineffective antimicrobial against *P. aeruginosa*. Ciprofloxacin (from a quinolone family of antibiotics) and gentamicin (from aminoglycosides) were selected as broad-spectrum antimicrobials, which are active against *P. aeruginosa* (Trizna *et al.*, 2020).

A range of the antibiotic's concentrations (tetracycline hydrochloride, gentamicin, and ciprofloxacin) was added to the mono-cultures and co-cultures of *P. aeruginosa* and *S. epidermidis* based on the micro-dilution assay in 96-well microtiter plates according to the EUCAST regulations (Section 2.2.9). MIC was determined as the lowest concentration of antibiotic for which no visible growth (no turbidity in the culture) could be observed after 24 hours of incubation. MBC was determined by plating the cultures treated with the antibiotics on cefrimide and staphylococcal selective agar to measure the CFU/ml of *P. aeruginosa* and *S. epidermidis*, respectively. The MBC was reported as the lowest concentration of the antibiotic when no visible growth on the selective agars was observed (Table 4.1 and Table 4.2).

**Table 4.1** Antibiotic susceptibility of *P. aeruginosa* NCTC 10662 and *S. epidermidis* in a co-culture.

	MIC ( $\mu\text{g/ml}$ )	MBC ( $\mu\text{g/ml}$ )
<b>Tetracycline</b>		
NCTC 10662 mono-culture	32	512
NCTC 10662 co-culture	32	512
<i>S. epidermidis</i> mono-culture	32	32
<i>S. epidermidis</i> co-culture	32	64
<b>Gentamicin</b>		
NCTC 10662 mono-culture	4	8
NCTC 10662 co-culture	2	4
<i>S. epidermidis</i> mono-culture	0.25	0.25
<i>S. epidermidis</i> co-culture	2	2
<b>Ciprofloxacin</b>		
NCTC 10662 mono-culture	0.25	1
NCTC 10662 co-culture	0.25	0.5
<i>S. epidermidis</i> mono-culture	0.25	0.5
<i>S. epidermidis</i> co-culture	0.25	0.5

The susceptibility of *P. aeruginosa* NCTC 10662 to tetracycline did not change when *P. aeruginosa* was in co-culture with *S. epidermidis*. There was no change in MIC and MBC of tetracycline in the co- and mono-culture of NCTC 10662. However, two times higher concentration of tetracycline was needed to completely eradicate *S. epidermidis* in the co-culture with NCTC 10662 compared with its mono-culture (Table 4.1). In the mixed culture of PAO1 and *S. epidermidis*, the presence of *S. epidermidis* did not affect the susceptibility of PAO1 to tetracycline. However, as the tolerance of *S. epidermidis* increased in co-culture with NCTC 10662, a similar result was repeated in co-culture with PAO1. Importantly, a four times higher concentration of tetracycline was needed to eradicate *S. epidermidis* in co-culture with PAO1 (Table 4.2).

Tolerance of NCTC 10662 to gentamicin was lower when co-cultured with *S. epidermidis*. The MIC and MBC for NCTC 10662 decreased twice in co-culture with *S. epidermidis* compared with its mono-culture. In the presence of *S. epidermidis*, just 0.5 MIC and 0.5 MBC of gentamicin were enough to inhibit the growth of NCTC 10662 and ultimately eradicate it. Conversely, the MBC to eradicate *S. epidermidis* in co-culture with NCTC 10662 increased eight times from 0.25 µg/ml to 2 µg/ml (Table 4.1). This increase was observed with the formation of small colony variants (SCVs). The susceptibility of PAO1 decreased to gentamicin in co-culture with *S. epidermidis*. In the presence of *S. epidermidis*, only 0.5 MIC of gentamicin was sufficient to inhibit the growth of PAO1; however, no reduction in MBC of PAO1 was observed in the mixed culture. The MBC to eradicate *S. epidermidis* in co-culture with PAO1 increased sixteen times from 0.25 µg/ml to 4 µg/ml (Table 4.2). This increase was also observed with the formation of SCVs on *S. epidermidis* selective agar.

The MBC of ciprofloxacin for NCTC 10662 decreased twofold from 1 µg/ml to 0.5 µg/ml in the co-culture with *S. epidermidis*. When the mixed culture was treated with ciprofloxacin, twofold lower concentration of the antibiotic was sufficient to obtain a similar eradication of NCTC 10662 in the mono-culture. *S. epidermidis* susceptibility to ciprofloxacin in co-culture with NCTC 10662 did not change compared with its mono-culture (Table 4.1). Interestingly, when the co-culture of PAO1 and *S. epidermidis* was treated with ciprofloxacin, 0.25 MBC (a four-fold lower concentration of the antibiotic) was enough to eradicate PAO1. However, the MIC needed to inhibit the growth of PAO1 was not affected in the presence of *S. epidermidis*. The susceptibility of *S. epidermidis* to ciprofloxacin did not change in the co-culture with PAO1 (Table 4.2).

**Table 4.2** Antibiotic susceptibility of *P. aeruginosa* PAO1 and *S. epidermidis* in a co-culture.

	MIC ( $\mu\text{g/ml}$ )	MBC ( $\mu\text{g/ml}$ )
<b>Tetracycline</b>		
PAO1 mono-culture	32	512
PAO1 co-culture	32	512
<i>S. epidermidis</i> mono-culture	32	32
<i>S. epidermidis</i> co-culture	32	128
<b>Gentamicin</b>		
PAO1 mono-culture	4	8
PAO1 co-culture	2	8
<i>S. epidermidis</i> mono-culture	0.25	0.25
<i>S. epidermidis</i> co-culture	2	4
<b>Ciprofloxacin</b>		
PAO1 mono-culture	0.25	2
PAO1 co-culture	0.25	0.5
<i>S. epidermidis</i> mono-culture	0.25	0.5
<i>S. epidermidis</i> co-culture	0.25	0.5

#### 4.2.3.1 Evaluating *P. aeruginosa* efflux pumps activity in the co-culture of *P. aeruginosa* and *S. epidermidis*

To further investigate if *S. epidermidis* can influence the efflux pump activity of *P. aeruginosa*, the uptake of ethidium bromide in the mono-culture of *P. aeruginosa* and co-culture of *P. aeruginosa* with *S. epidermidis* was assessed. When present in their culture medium, bacterial cells uptake ethidium bromide through the efflux system and cell wall permeability. Ethidium bromide is fluorescent when bound to DNA; therefore, the intracellular fluorescent intensity is higher than extracellular (Blair and Piddock, 2016). An accumulation assay was performed on both strains of NCTC 10662 and PAO1 in mono-culture and in co-culture with *S. epidermidis* (Section 2.2.11). The accumulation of ethidium bromide inside the bacterial cells was assessed over an hour by measuring the excitation at 520 nm and emission at 590 nm every minute (Figure 4.11).

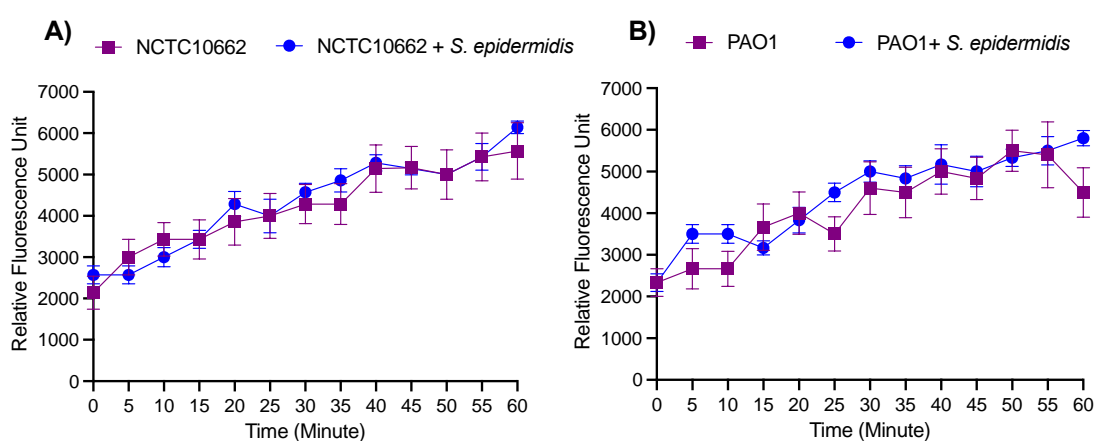


**Figure 4.11** Fluorometric accumulation assay of *P. aeruginosa* NCTC 10662 (A) and PAO1 (B) in their mono-culture and co-culture with *S. epidermidis*.

The OD of *S. epidermidis* and *P. aeruginosa* suspension was adjusted to 0.4 at 600 nm. Bacterial suspensions were then mixed at a 1:1 ratio and transferred to a 96-well plate. Glucose at the final concentration of 0.4% (w/v) and ethidium bromide at the final concentration of 2  $\mu\text{g}/\text{ml}$  were added to each well. The mono-culture of *P. aeruginosa* with glucose and ethidium bromide was set as control. The reaction was run using a Fluostar Optima plate reader at 37°C for an hour. Every minute the absorbance was taken at excitation 520 nm and emission at 590 nm. Results are expressed as the mean  $\pm$  SEM, n=6.



## 4.3 Discussion

This chapter investigated the interaction of *P. aeruginosa* and *S. epidermidis* in co-culture during planktonic and biofilm growth conditions. Also, it evaluated the antibiotic susceptibility of *P. aeruginosa* during the co-culture. These experiments were performed on two phenotypically different human isolates of *P. aeruginosa*: PAO1, a mucoid strain and NCTC 10662, a non-mucoid strain (Kalgudi *et al.*, 2021). *S. epidermidis* NCTC 11047 is a commensal nasal isolate and is a non-biofilm forming strain, and it was used as a skin commensal in this study (Banner *et al.*, 2007).

Both *P. aeruginosa* and *S. epidermidis* colonise the skin and have been isolated from infected wounds; therefore, it would be reasonable to assume they can co-exist within the wounds (Wolcott *et al.*, 2016; Kalan *et al.*, 2019). The presence of *S. epidermidis* and other coagulase-negative staphylococci in the wound has been associated with a faster healing process (Verbanic *et al.*, 2020). So far, there is no published study on the interaction of *P. aeruginosa* and *S. epidermidis*. However, there are extensive research on the interaction of *S. aureus* and *P. aeruginosa* (Mashburn *et al.*, 2005; Briaud *et al.*, 2019; Trizna *et al.*, 2020), and also on the interaction between *S. epidermidis* and *S. aureus* (Iwase *et al.*, 2010; Fredheim *et al.*, 2015; Nakatsuji *et al.*, 2017).

The initial experiments investigated the growth profile of *P. aeruginosa* and *S. epidermidis* in mono- and co-culture. The data was further analysed by determining CI and RIR indexes to better understand the state of co-existence between the two bacteria. Although *P. aeruginosa* NCTC 10662 showed better growth in mono- and co-culture compared to *S. epidermidis*, NCTC 10662 indicated no competitive advantage over *S. epidermidis* in the co-culture (Figure 4.2). On the other hand, PAO1 showed a competitive advantage over *S. epidermidis* during the exponential phase of planktonic growth (Figure 4.4). It is reasonable to assume that PAO1, through producing a higher amount of virulence factors such as pyocyanin and elastase compared to NCTC 10662 (Chapter 3, Figure 3.9), was able to suppress *S. epidermidis* during co-culture. Several studies have indicated that *P. aeruginosa* suppresses *S. aureus*'s growth during *in vitro* planktonic and biofilm co-

culture. *P. aeruginosa* is known as a common dominator in polymicrobial infections due to harbouring several virulence factors and adaptation mechanisms such as biofilm formation (Mashburn *et al.*, 2005; Briaud *et al.*, 2019; Trizna *et al.*, 2020). It has been suggested that *P. aeruginosa*, through the production of siderophores such as pyoverdine and pyocyanin, inhibits the electron transport chain in *S. aureus* and, therefore, shifts *S. aureus* to a fermentative growth mode. This eventually leads to reduced viability in *S. aureus*, but it does not instigate complete eradication of *S. aureus* (Voggu *et al.*, 2006). *S. epidermidis*, similar to *S. aureus*, is a facultative anaerobe and can switch to alternative electron acceptors in the electron transport chain (Uribe-Alvarez *et al.*, 2016). These data suggest that *P. aeruginosa*, through the release of pyocyanin, might have a similar effect on *S. epidermidis*. It was noticeable that the number of *S. epidermidis* cells in the co-culture with PAO1 decreased at all times; however, it did not decline to zero. Hence, a continuous culture study would be beneficial to better understand the suppression effect of *P. aeruginosa* on *S. epidermidis*.

The interaction of *P. aeruginosa* and *S. epidermidis* was further investigated when they were grown as biofilms. The aim of the study was to investigate the impact of *S. epidermidis* on the biofilm formation of *P. aeruginosa* on a 96-well tissue culture plate surface (abiotic surface). Since attachment is an essential step in biofilm formation, the study was designed in a way to evaluate the impact of *S. epidermidis* on the attachment of *P. aeruginosa* to the surface, therefore, evaluate its biofilm formation. *S. epidermidis* diminished biofilm formation in *P. aeruginosa* NCTC 10662 when it was added before NCTC 10662 biofilm formation (Figure 4.5 A). However, the biofilm formation in NCTC 10662 did not change when *S. epidermidis* was added to the culture simultaneously with NCTC 10662 or after NCTC 10662 biofilm was formed for 24 hours (Figure 4.7 A, Figure 4.6 A). In addition, the number of NCTC 10662 cells in the biofilm in the presence of *S. epidermidis* decreased when *S. epidermidis* was added before or at the same time as NCTC 10662 (Figure 4.5 B and Figure 4.7 B). On the other hand, the biofilm formation in PAO1 diminished only when PAO1 was co-cultured with *S. epidermidis* at the same time (Figure 4.10 A). The number of PAO1 cells in the biofilm also decreased when PAO1 was co-cultured with *S. epidermidis* simultaneously (Figure 4.10 B). Pre-exposure of PAO1 to

*S. epidermidis* culture reduced the number of PAO1 cells in the biofilm, although it was ineffective in diminishing biofilm formation (Figure 4.8).

*S. epidermidis* NCTC 11047 is a non-biofilm forming strain due to the lack of polysaccharide intercellular adhesin, which is an essential protein for the development of biofilm in biofilm-forming strains of staphylococci (Banner *et al.*, 2007). However, *S. epidermidis* possesses several other factors, such as autolysin and staphylococcal surface proteins, which are highly effective in attachment to hydrophobic abiotic surfaces (Heilmann *et al.*, 2003; Otto, 2009; Foster, 2020). This suggests that *S. epidermidis* might be able to compete with *P. aeruginosa* (PAO1 and NCTC 10662) to attach to abiotic surfaces and limit *P. aeruginosa's* access to the establishment. Furthermore, it has been demonstrated that *S. epidermidis* strains isolated from the nasal cavity produce serine proteases which inhibit biofilm formation and colonisation of *S. aureus* (Iwase *et al.*, 2010; Fredheim *et al.*, 2015). Although the mechanism of action of serine proteases in *in vitro* and *in vivo* has not been confirmed yet, serine proteases can be the reason for the decrease in the attachment through the degradation of adhesin proteins such as cdr A in *P. aeruginosa*.

Presence of exopolysaccharides, namely alginate, Psl, and Pel in mucoid PAO1 and Pel and Psl in non-mucoid NCTC 10662 exhibit structural and protective functions in a mature biofilm (Franklin *et al.*, 2011); so accordingly, *S. epidermidis* might be unable to penetrate to the preformed biofilm of *P. aeruginosa*.

As discussed earlier, *P. aeruginosa*, through pyoverdine production, can reduce the viability of *S. epidermidis* by inhibiting the electron transport chain. This might be the reason for the reduction in the number of *S. epidermidis* in co-culture with *P. aeruginosa*, especially the co-culture with PAO1 strain, which is a stronger producer of pyocyanin than NCTC 10662.

Biofilm formation is an important virulence factor for many bacteria, as EPS decreases antimicrobial susceptibility. Furthermore, polymicrobial communities with numerous interspecies interactions could alter bacterial susceptibility to antimicrobials (Qin *et al.*, 2022). Several studies have indicated that the mixed culture of pathogens such as *P. aeruginosa* and *S. aureus* have different tolerance to antibiotics compared to their mono-cultures (Alves *et al.*, 2018; Briaud *et al.*, 2019; Trizna *et al.*, 2020).

The data from this study indicate that the susceptibility of PAO1 and NCTC 10662 to tetracycline in their mono-culture is similar to when they are co-cultured with *S. epidermidis*. However, the susceptibility of *S. epidermidis* to tetracycline increased in co-culture with both strains of *P. aeruginosa* (Table 4.1 and 4.2). Tetracycline is generally ineffective against *P. aeruginosa*, while it is effective against a range of staphylococci species. The increased susceptibility of *S. epidermidis* to tetracycline in co-culture with *P. aeruginosa* might be because of the protective effect of *P. aeruginosa*'s EPS for *S. epidermidis* cells. Tetracycline is not effective against *P. aeruginosa* even when *P. aeruginosa* is in the co-culture with *S. epidermidis*. Thus, the presence of *P. aeruginosa* biofilm and its EPS might provide a shield for *S. epidermidis* cells and reduce the moderate circumstances for penetration of the antibiotic to cells. Further investigation is necessary to confirm this hypothesis.

On the other hand, in the co-culture with *S. epidermidis*, both strains of *P. aeruginosa* became more susceptible to gentamicin and ciprofloxacin (Table 4.1 and 4.2). Gentamicin and ciprofloxacin are typically active against *P. aeruginosa*. A similar result was observed in a study wherein a mixed culture of *S. aureus* and *P. aeruginosa* was treated with broad-spectrum antibiotics, and the susceptibility of *P. aeruginosa* decreased significantly in the co-culture (Trizna *et al.*, 2020). *S. epidermidis* supernatant also showed a similar effect and sensitised *P. aeruginosa* to gentamicin and ciprofloxacin (Chapter 3, Table 3.2). One of the active molecules among exoproducts of *S. epidermidis* is phenol soluble modulins (PSMs) that have been shown to have antimicrobial activity against *S. aureus* and Group A *Streptococcus* (Cogen *et al.*, 2010). PSMs might have an additional effect on gentamicin and ciprofloxacin effect; however, this needs further research for confirmation.

Both strains of *P. aeruginosa* in the mixed culture decreased the efficacy of gentamicin against *S. epidermidis* (Table 4.1 and 4.2). *S. epidermidis* formed SCVs on the selective agar when they were treated with gentamicin in co-culture with *P. aeruginosa*. SCVs are smaller than wild-type colonies and grow significantly slower, with weaker metabolic function than wild-type bacteria. *S. aureus* and various coagulase-negative staphylococci shift toward SCV phenotype during unfavorable conditions. The data from this study is in accordance with the data indicating the formation of SCVs in *S. aureus* when growing with

*P. aeruginosa* and treated with aminoglycosides (Mitchell *et al.*, 2010). Resistance to aminoglycosides such as gentamicin in *S. aureus* in co-culture with *P. aeruginosa* has been attributed to the formation of SCV and reduction of active transport, which directly affects the efficacy of aminoglycosides (Hoffman *et al.*, 2006; Orazi and O'Toole, 2017). As it was discussed earlier, pyoverdine, pyocyanin, 2-heptyl-4-quinolone N-oxide (HQNO), and even hydrogen cyanide (HCN) produced by *P. aeruginosa* suppress the electron transport chain in *S. aureus*; therefore, decreasing the active transport of aminoglycosides to the bacterial cells (Voggu *et al.*, 2006; Biswas *et al.*, 2009; Biswas and Gotz, 2021).

Several factors can contribute to the efficacy of antibiotics in the co-culture of bacterial cells, such as the effect of metabolites of one species on the growth or biofilm formation of the other. One of the crucial factors that can determine the interaction of bacteria in a mixed culture and their impact on each other's growth is the localisation of bacteria in a biofilm. As it is important to investigate the impact of the mechanism of action of metabolites on the interaction of bacterial cells, it is essential to monitor the placement of bacterial cells in a community of microbes.

Lastly, the efflux pump's activity in *P. aeruginosa* in co-culture with *S. epidermidis* was investigated. Efflux pumps are one the crucial mechanisms in resistance to antibiotics in *P. aeruginosa*. Efflux pumps alongside porins determine the permeability of the cell membrane to environmental molecules. The accumulation assay in this study indicated that the efflux pump activity in PAO1 and NCTC 10662 did not change in the presence of *S. epidermidis*. Tetracycline induces the expression of efflux pumps in *P. aeruginosa*; this is why tetracycline is ineffective against *P. aeruginosa*, as it cannot penetrate the cell. *S. epidermidis* could not impact the efflux pump system in *P. aeruginosa* and subsequently could not affect tetracycline efficiency.

# Chapter 5 Investigation of the effect of *S. epidermidis* and its supernatant on protecting keratinocytes against *P. aeruginosa* infection

## 5.1 Introduction

Keratinocytes are one of the important components of chronic wound microenvironment; they actively interact with immune cells and bacterial cells to maintain the homeostasis of the skin. They are also essential in re-epithelisation and wound healing. By releasing cytokines, chemokines, and AMPs, Keratinocytes fight bacterial infections (Kadam *et al.*, 2019). In recent years skin microbiota has gain attention because of its influence on the skin homeostasis. The beneficial role of *S. epidermidis* colonisation on keratinocytes has been attributed to the stimulation of the immune response, such as antimicrobial peptides expression in keratinocytes (Lai *et al.*, 2010). A number of studies also suggested that probiotic bacteria can reduce the *S. aureus* infection by inhibiting the adhesion and internalisation of the pathogens to the keratinocytes (Prince *et al.*, 2012; Mohammedsaeed *et al.*, 2014). Reducing the pathogenicity and enhancing the immune response can be promising options in controlling infections on the skin. *P. aeruginosa* is an opportunistic pathogen residing on the skin. *P. aeruginosa* is one of the leading pathogens in nosocomial infections and has been isolated from chronic wound. It is also one of the most prevalent pathogens in polymicrobial biofilm-associated infections. Since both *P. aeruginosa* and *S. epidermidis* residing on the skin, it is likely that they interact with each other. In a recent study in 2020, both *P. aeruginosa* and *S. epidermidis* have been isolated from wound (Verbanic *et al.*, 2020). The interaction of *S. epidermidis* and *P. aeruginosa* on the skin has not been explored yet.

In this chapter a monolayer of immortalised human keratinocytes cell line (HaCaT) was used as a model system to monitor the possible protective effect of *S. epidermidis* on the keratinocytes. In this study, first, the effect of SES on keratinocytes was tested through several assays. Then the interaction of *P. aeruginosa* and *S. epidermidis* on a monolayer of keratinocyte was investigated.

## 5.2 Results

### 5.2.1 Investigation of the effect of SES on keratinocytes

#### 5.2.1.1 Viability of keratinocytes

First, the effect of SES on the viability of keratinocytes (HaCaT cell line) was investigated at different time-points using trypan blue exclusion assay (Section 2.3.3).

Keratinocytes were grown in the presence and absence of SES at 10% v/v and 20% v/v for 8, 16, 24, and 48 hours at 37°C in a humid atmosphere of 5% CO<sub>2</sub>. After the incubation period, cells were detached, and a viable cell count was performed on the cells mixed with trypan blue solution.

Figure 5.1 shows the viability of keratinocytes in the presence of 10% v/v and 20% v/v SES at different time-points during 48 hours of incubation. Viability of keratinocytes decreased after 48 hours of incubation with 20% SES ( $P=0.02$ ,  $n=3$ ) but there was no significant change in viability with 10% v/v SES. Therefore the 10% v/v SES was chosen for further experiments.

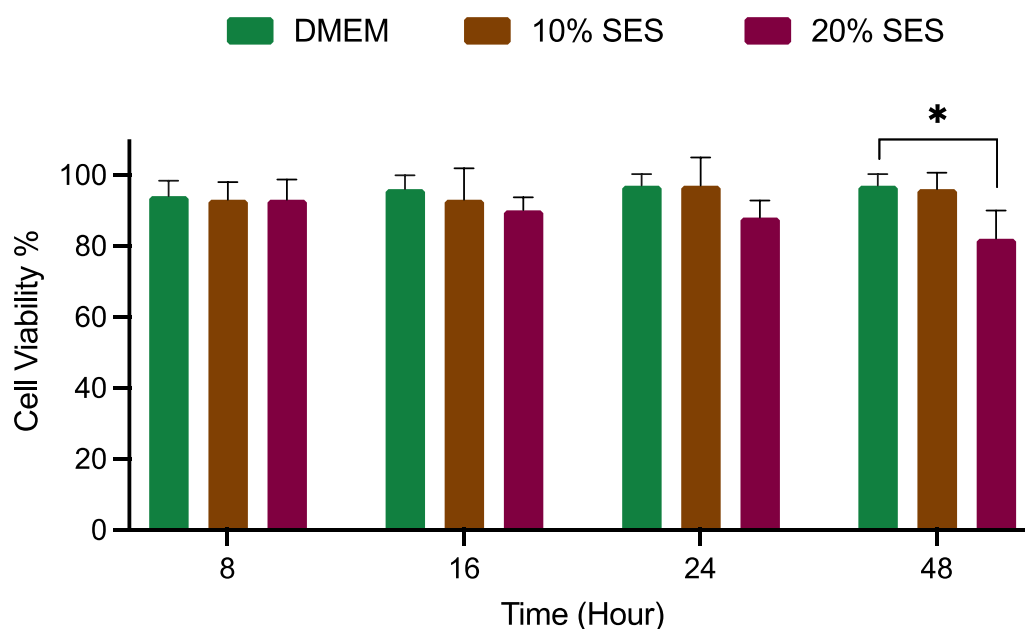


**Figure 5.1** The viability of keratinocytes in the absence and presence of SES.

Cells grown in DMEM (keratinocytes complete medium) were used as control. Error bars are reported as mean  $\pm$  SEM,  $n=3$ , and \*  $P \leq 0.05$ .

### 5.2.1.2 Morphology assessment by microscopy

To confirm cells' viability after treatment with the SES, the cells were tracked by cell tracker red fluorescence dye (CMTPX) and observed using the EVOS microscope for 24 hours (Section 2.3.3). The morphology of keratinocytes was also assessed using crystal violet dye and without any dye on the bright field of the EVOS microscope. The morphology of cells did not change when they were treated with 10% SES for 24 hours (Figure 5.2).

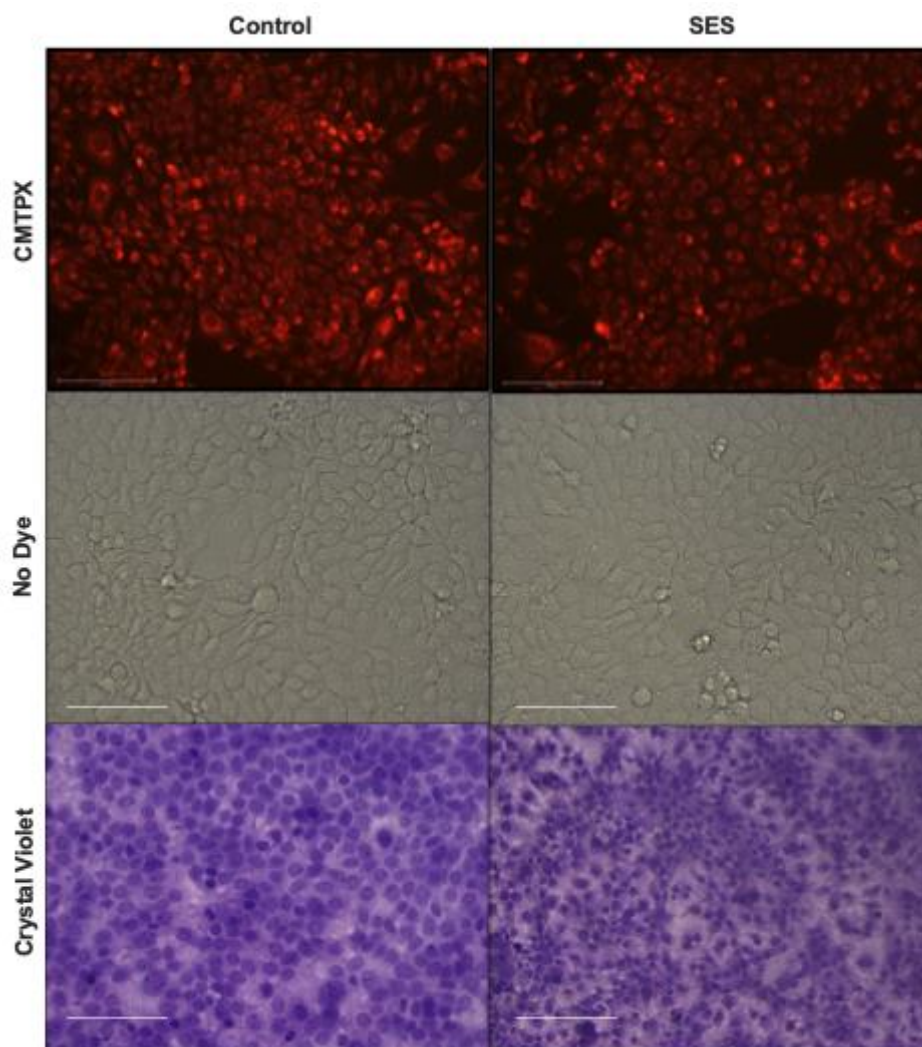


**Figure 5.2** The morphology of the keratinocytes was assessed using an EVOS microscope. Keratinocytes in the presence and absence of 10% v/v SES were tracked with CMTPX dye for 24 hours under 5% CO<sub>2</sub> environment at 37°C. Keratinocytes were also dyed using crystal violet after 24 hours of growth with and without 10% v/v SES. The morphology was also assessed on the bright field of the EVOS microscope. The scale bar is 200 μm.



### 5.2.1.3 The effect of SES on keratinocyte wound healing

The scratch assay is a low-cost and standard method to study the effect of different treatments on the re-epithelisation of keratinocytes. By making a scratch on a monolayer of confluent keratinocytes, an artificial wound can be created. Observing the closure of the scratch over time under the microscope facilitates studying the wound healing and re-epithelisation of keratinocytes (Guan *et al.*, 2007). Proliferation and cell migration are two of the most important factors involved in wound healing.

Keratinocytes were grown to full confluency, and using a 100 µl pipette tip, a scratch was made on a monolayer of cells. Scratched cells were then treated with SES at 10% v/v or without SES in DMEM for control comparison. For comparison between different bacterial culture supernatants, the supernatants of *P. aeruginosa* NCTC 10662 and PAO1 were also extracted and added to the scratched cells at 10% v/v. The cells were then incubated under 5% CO<sub>2</sub> environment at 37°C. The closure of the scratches was assessed at 8, 16, 24, and 48 hours after the incubation by taking microscope images (Section 2.3.4).

The effect of SES on keratinocytes' wound healing was determined by the scratch assay, as it is shown in figure 5.3. Re-epithelisation in keratinocytes was accelerated by SES compared to control at 16 and 24 hours after incubation (Figure 5.3). By 16 hours after the incubation, the scratch on keratinocytes that were treated with SES was healed up to 50% compared with 26% re-epithelisation in the control scratch (P=0.01, n=3, Figure 5.3 B). After 24 hours of incubation, the 86% of the scratch area treated with SES was healed compared with 68% of the gap closure in the control (P=0.01, n=3, Figure 5.3 B). Scratches on the monolayer of keratinocytes were also treated with the supernatants of NCTC 10662 and PAO1, which showed a considerable difference compared to SES. Supernatant from the culture of NCTC 10662 did not have any effect on wound healing during 24 hours of incubation, and only 7% re-epithelisation was occurred. There was an increase in the scratch area after 48 hours post-treatment with NCTC 10662 supernatant compared with the control (P=0.0001, n=3, Figure 5.3). What can be clearly seen in the figure 5.3 is that no healing was occurred in the case of PAO1 supernatant, and the scratch area increased by two-fold after 8 hours of incubation (P=0.002, n=3, Figure 5.3).

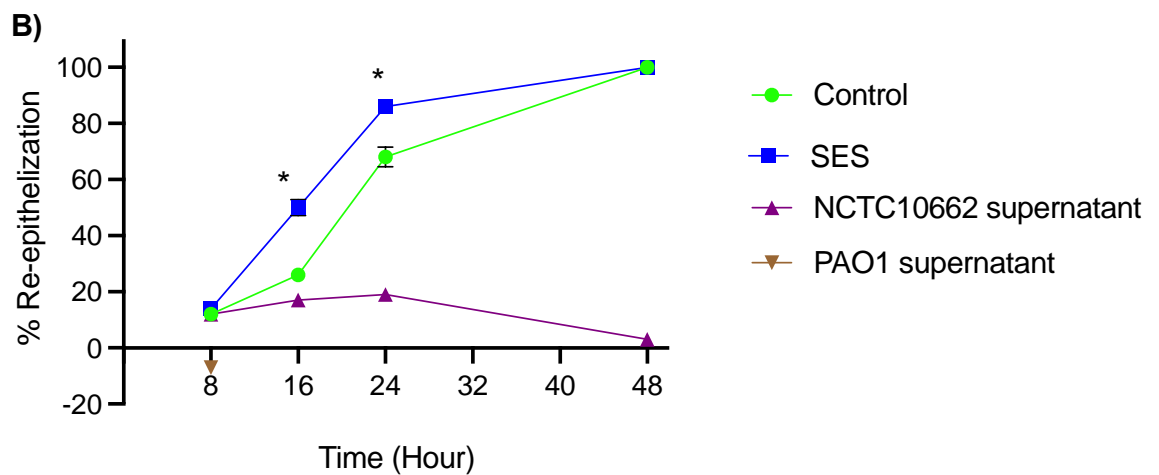
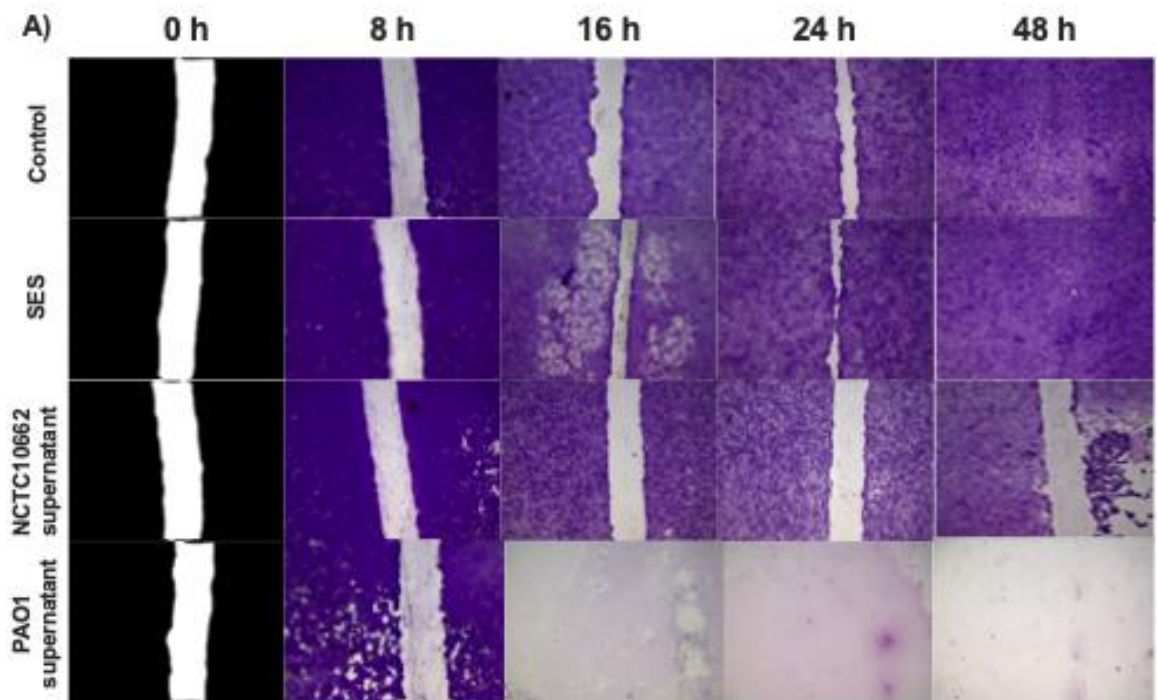


**Figure 5.3** Keratinocytes' re-epithelisation during wound healing in the presence and absence of bacterial cultures supernatants.

A) Microscopy images of scratches on the monolayers of keratinocytes at different time-points with and without SES, NCTC 10662 supernatant, and PAO1 supernatant. B) Percentage of keratinocytes scratch re-epithelisation in the presence and absence of SES, NCTC 10662 supernatant, and PAO1 supernatant. Error bars are reported as mean  $\pm$  SEM, n=3, and \*  $P \leq 0.05$ .

### 5.2.1.4 The effect of SES on keratinocytes proliferation

Keratinocytes' proliferation is one of the important attributors in wound healing. The proliferation of keratinocytes was studied using the MTT assay. Metabolically active cells reduce MTT to water-insoluble purple formazan crystals. The total amount of formazan produced is directly proportional to the number of viable cells in the culture (Mosmann, 1983; Tom *et al.*, 1993). The amount of formazan produced by keratinocytes at the beginning of the experiment (at time zero) at 70% confluency was considered as a normalised control. The amount of formazan was then measured at 24 and 48 hours of incubation in the presence and absence of SES. The amount of formazan produced by cells at any time-point was compared to the normalised control (Section 2.3.5).

Incubation of keratinocytes with SES resulted in increased formazan production, which could be the indication of increased proliferation of cells compared with non-treated cells (DMEM) after 24 and 48 hours of incubation ( $P=0.001$  and  $P=0.01$ , respectively,  $n=6$ , Figure 5.4).

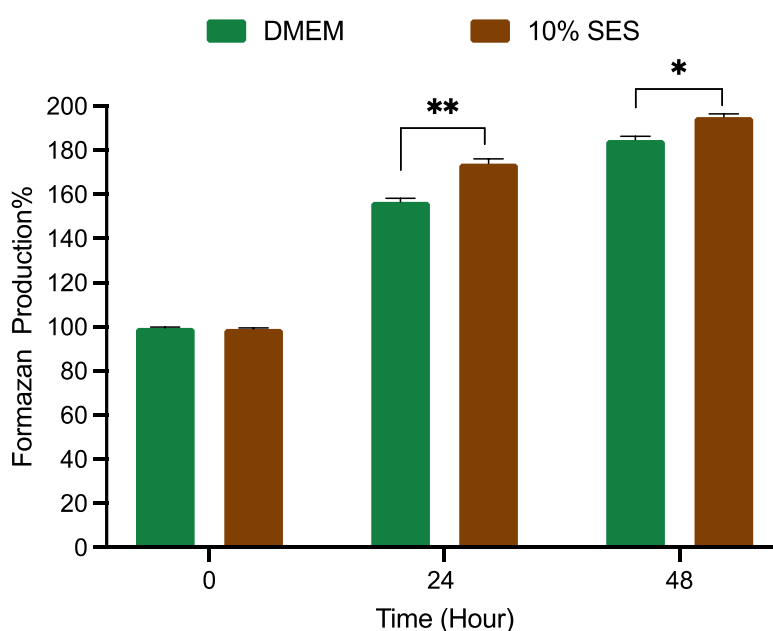


**Figure 5.4** Proliferation of keratinocytes in the presence and absence of SES.

The absorbance of formazan produced by metabolically active keratinocytes in the presence and absence of SES after 24 and 48 hours of incubation was measured at 570 nm. The absorbance of formazan at time zero at 70% confluency was measured and considered as a control. Error bars are reported as mean  $\pm$  SEM,  $n=6$ . \*  $P \leq 0.05$ , \*\*  $P \leq 0.01$ .

### 5.2.1.5 The effect of SES on the cytokine production of keratinocytes

So far, the data presented suggest that SES has the potential to increase keratinocytes re-epithelization through stimulating proliferation. Cytokines and chemokines released from the cells in the wound area are among the essential factors during wound healing process. Therefore, to better understand the underlying pathways of the stimulated proliferation by SES, the production of cytokines by keratinocytes in the presence of SES was investigated.

The Proteome Profiler™ Human Cytokine Array kit allows to measure the relative expression of 36 human cytokines in a sample (Section 2.3.6). Keratinocytes were grown to full confluency, and using a 100 µl pipette tip, a scratch was made on a monolayer of the cells. The scratched cells were incubated either in DMEM or DMEM plus SES (10% v/v) for 24 hours. After the incubation period, the supernatants were collected and mixed with a cocktail of biotinylated detection antibodies. The mixtures were incubated with the array membranes for 18 hours. The array membrane is spotted in duplicate with capture antibodies to specific target cytokines and chemokines. Captured cytokines were visualised using chemiluminescence detection reagents and subsequently exposing the membranes to a chemiluminescent gel imager for 13 minutes (Figure 5.5). The pixel intensity of the signals that appeared on the spots on the membrane's images were analysed using Image-J 64 software program (<https://imagej.nih.gov/>) (Section 2.3.6) (Figure 5.6). The signal produced is proportional to the amount of analyte bound. This experiment was repeated twice with two repeats each time.

This technique revealed seven proteins in the supernatants of keratinocytes grown in the presence or absence of SES. Macrophage migration inhibitory factor (MIF), serpin E1 also known as plasminogen activator inhibitor-1 (PAI-1), and CXCL8 (also known as IL-8) were detected in a moderate level. The CXCL1 and IL-6 were detected in a low level. The CCL5 and intercellular adhesion molecule 1 (ICAM-1) were detected in a very low level (Figure 5.5).

1	MIF
2	Serpin E1
3	CCL5
4	CXCL1
5	ICAM-1
6	IL-6
7	CXCL8

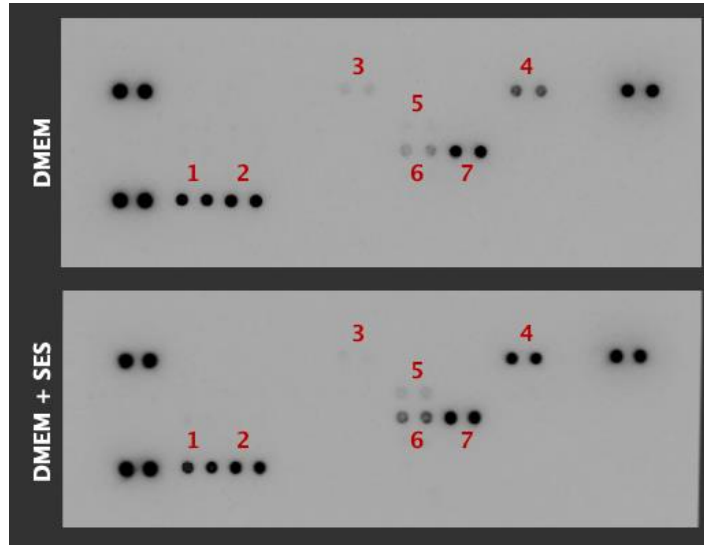


**Figure 5.5** Representative image of nitrocellulose membranes of Human Cytokine Array and the detected cytokines and chemokines present in the keratinocyte's supernatant. The scratched keratinocytes were grown in DMEM or DMEM plus SES (10% v/v) for 24 hours. The cell culture supernatants were collected after 24 hours of incubation. The supernatant mixed with a cocktail of biotinylated detection antibodies was added onto each membrane array and incubated for 18 hours. The captured cytokines and chemokines on the membranes were visualized using a chemiluminescent imager.

The presence of SES in the growth medium of scratched keratinocytes increased the release of CXCL1, ICAM-1, IL-6, and CXCL8 from keratinocytes ( $P=0.0001$ ,  $P=0.015$ ,  $P=0.0001$ , and  $P=0.0001$ , respectively,  $n=4$ , Figure 5.6).

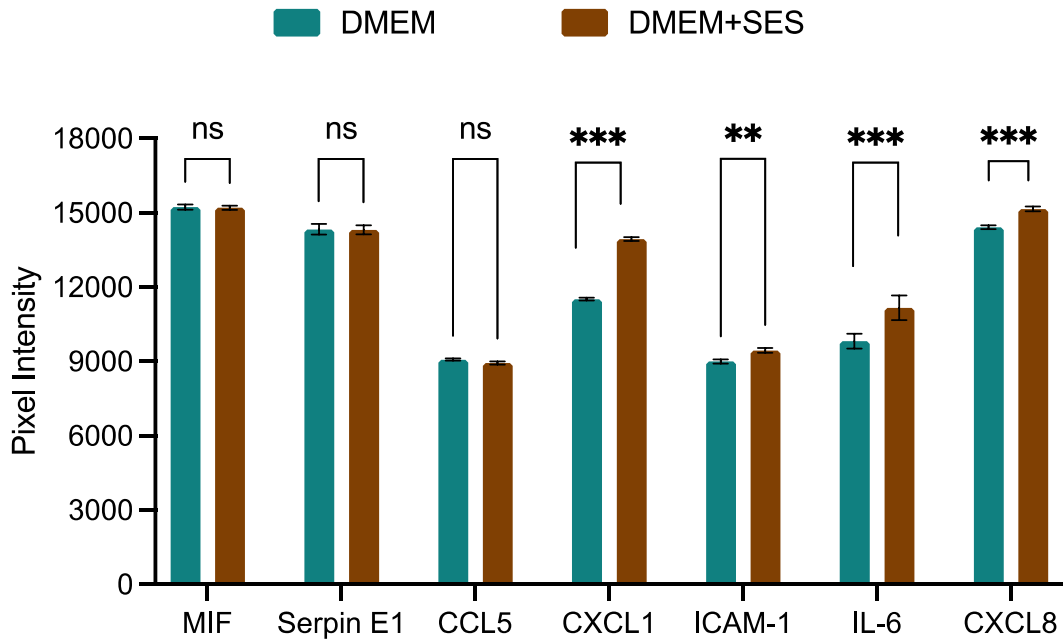


**Figure 5.6** Cytokines and chemokines detected in the supernatant of keratinocytes treated or untreated with SES, spotted by Proteome Profiler™ Human Cytokine Array. The scratched keratinocytes were grown in DMEM or DMEM plus SES (10% v/v) for 24 hours. The cell culture supernatants were collected after 24 hours of incubation. The supernatant mixed with a cocktail of biotinylated detection antibodies was added onto each membrane array and incubated for 18 hours. The detected cytokines and chemokines on the membranes were visualized using a chemiluminescent imager. The pixel intensity of the signals appeared on the spots on the membrane's image were analysed using Image-J 64 software program. Error bars are reported as mean  $\pm$  SEM, n=4. ns = not significant, \*  $P \leq 0.05$ , \*\*  $P \leq 0.01$ , \*\*\*  $P \leq 0.001$ .

## 5.2.2 Investigation of the protective effect of *S. epidermidis* and its supernatant on keratinocytes against *P. aeruginosa* infections

One of the mechanisms by which *S. epidermidis* and its supernatant may protect keratinocytes is through the inhibition of *P. aeruginosa* adhesion to the keratinocytes (biotic surface). Adhesion of bacterial pathogens is a critical step in biofilm formation and pathogenicity of the microorganisms.

This experiment was performed to determine whether *S. epidermidis* or its supernatant inhibit the adhesion of *P. aeruginosa* to keratinocytes through competition, exclusion, or displacement. Keratinocytes were infected with *P. aeruginosa* at 1:20 MOI before, after, or simultaneously treated with *S. epidermidis* or its supernatant. Keratinocytes were incubated with bacterial cells for maximum three hours to avoid overgrowth of bacterial cells on keratinocytes. Therefore, keratinocytes were pre-treated with *S. epidermidis* for only one hour to reduce the exposure time to bacterial cells and remain in the three-hour incubation window. After being exposed to the bacterial cells, the viability of keratinocytes was determined using trypan blue exclusion assay (Section 2.3.7.2). To determine the number of bacterial cells attached to the keratinocytes, first the keratinocytes were washed and then detached. The suspension of keratinocytes and bacterial cells was then spot plated on the selective agar (cetrimide) to count the number of adherent *P. aeruginosa* (Section 2.3.3.7).

To investigate the potential of *S. epidermidis* to protect keratinocytes from toxic effect of *P. aeruginosa*, viability of the infected keratinocytes monolayer was estimated after exposure to *S. epidermidis* and its supernatant. *P. aeruginosa* NCTC 10662 caused significant reduction in the viability of keratinocytes ( $P=0.0001$ ,  $n=3$ , Figure 5.7). Uninfected keratinocytes had a mean viability of 96%, while keratinocytes infected with NCTC 10662 indicated ~36% viability. The keratinocytes showed the viability of ~68.3% when exposed to *S. epidermidis*. The viability of keratinocytes infected with NCTC 10662 increased to ~49.3% in the presence of *S. epidermidis* and to ~54.6% in the presence of SES ( $P=0.003$

and 0.0002 respectively, n=3 Figure 5.7 A). Furthermore, the number of attached NCTC 10662 to keratinocytes was reduced in the presence of *S. epidermidis* and SES (P=0.02 and P=0.004 respectively, n=3, Figure 5.7 B).

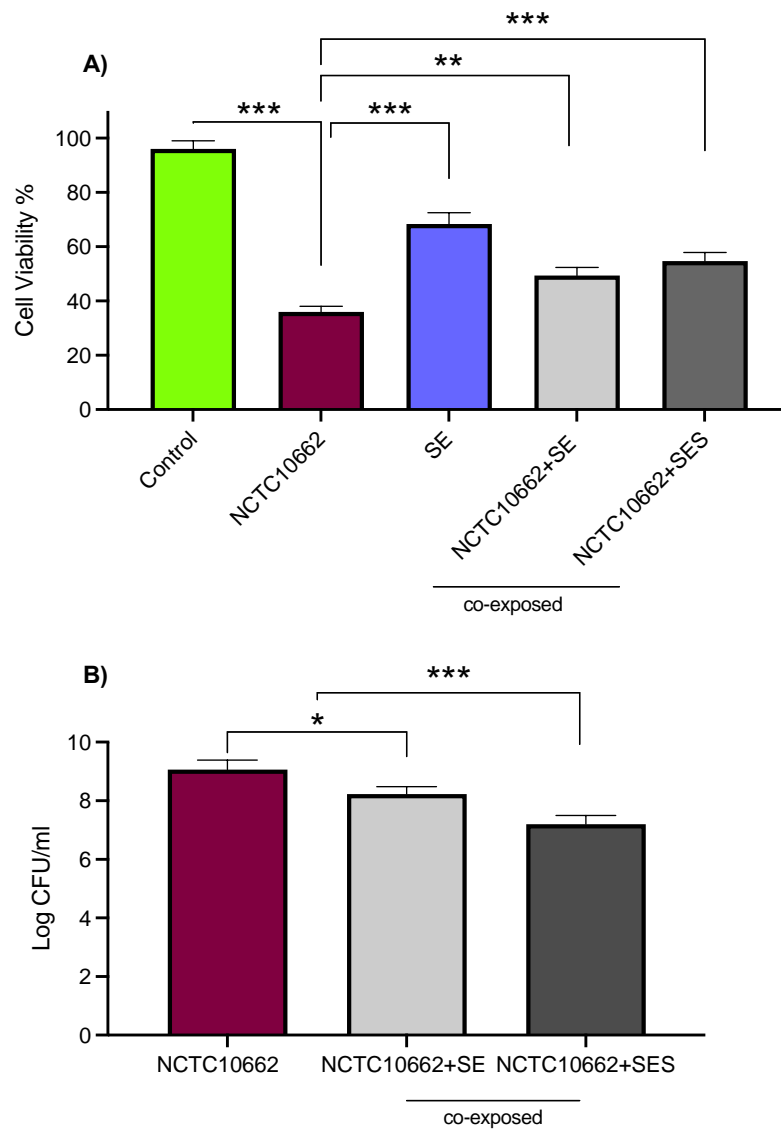


**Figure 5.7** Infection of keratinocytes with *P. aeruginosa* NCTC 10662.

A) Keratinocytes were co-exposed to *P. aeruginosa* NCTC 10662 plus *S. epidermidis* (NCTC 10662+SE) or its supernatant (NCTC 10662+SES) at the same time. The viability of cells was measured after two hours of incubation using the trypan blue exclusion assay. B) The number of adherent *P. aeruginosa* NCTC 10662 to the keratinocytes in the co-culture was measured by spot plating the suspension on selective agar (cetrimide). Error bars are reported as mean  $\pm$  SEM, n=3. \* P  $\leq$  0.05, \*\* P  $\leq$  0.01, \*\*\* P  $\leq$  0.001.



Next, an investigation was performed to determine whether *S. epidermidis* and its supernatant could inhibit the adhesion of NCTC 10662 through exclusion. Therefore, keratinocytes were pre-exposed to *S. epidermidis* or SES for one hour before being infected with NCTC 10662. Data presented in figure 5.8 shows that the addition of *S. epidermidis* to keratinocytes before infecting them with NCTC 10662 increased keratinocytes' viability to ~50% (P=0.01, n=3, Figure 5.8 A). However, pre-treatment of keratinocytes with SES did not protect keratinocytes against NCTC 10662 infection (P=0.06, Figure 5.8 A). The number of attached NCTC 10662 to keratinocytes also decreased when keratinocytes were pre-exposed to *S. epidermidis* (P=0.04, n=3, Figure 5.8 B). Pre-exposure to SES had no effect on the attachment of NCTC 10662 to keratinocytes (P=0.06, Figure 5.8 B).

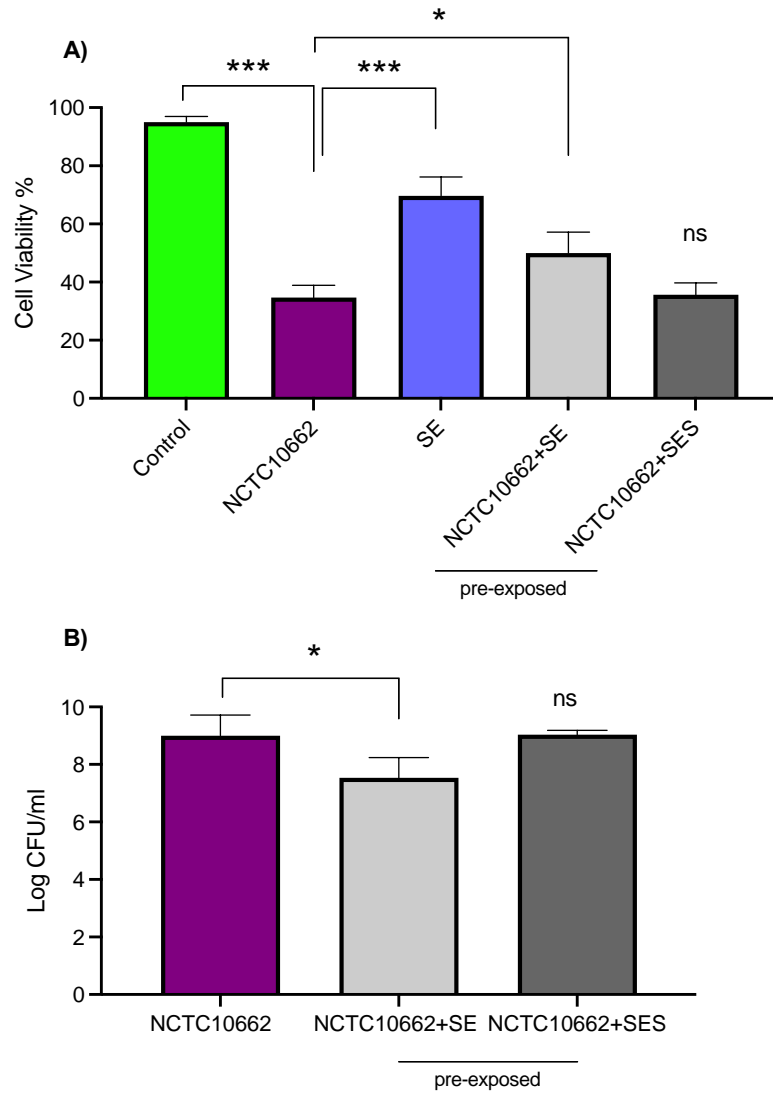


**Figure 5.8** Infection of keratinocytes with *P. aeruginosa* NCTC 10662.

A) Keratinocytes were pre-exposed to *S. epidermidis* (SE) or SES for one hour before being infected with *P. aeruginosa* NCTC 10662 for two hours. The viability of cells was measured using the trypan blue exclusion assay. B) The number of adherent *P. aeruginosa* NCTC 10662 to the keratinocytes in the co-culture was measured by spot plating the suspension on selective agar (cetrimide). Error bars are reported as mean  $\pm$  SEM, n=3. ns = not significant, \*  $P \leq 0.05$ , \*\*  $P \leq 0.01$ , \*\*\*  $P \leq 0.001$ .

Subsequently, the ability of *S. epidermidis* and SES to inhibit *P. aeruginosa* NCTC 10662 to keratinocytes by displacement was investigated. Keratinocytes were infected with NCTC 10662 for an hour; afterwards, *S. epidermidis* or SES were added to the infected keratinocytes and incubated for another hour. The addition of SES to the infected keratinocytes increased the viability of Keratinocytes to ~48.3% compared with ~36%

viability of infected cells alone ( $P=0.04$ ,  $n=3$ , Figure 5.9 A). However, the number of attached NCTC 10662 to keratinocytes did not change after the addition of SES ( $P=0.06$ , Figure 5.9 B). *S. epidermidis* was not able to inhibit the adhesion of NCTC 10662 to keratinocytes through displacement ( $P=0.07$ , Figure 5.9 B).

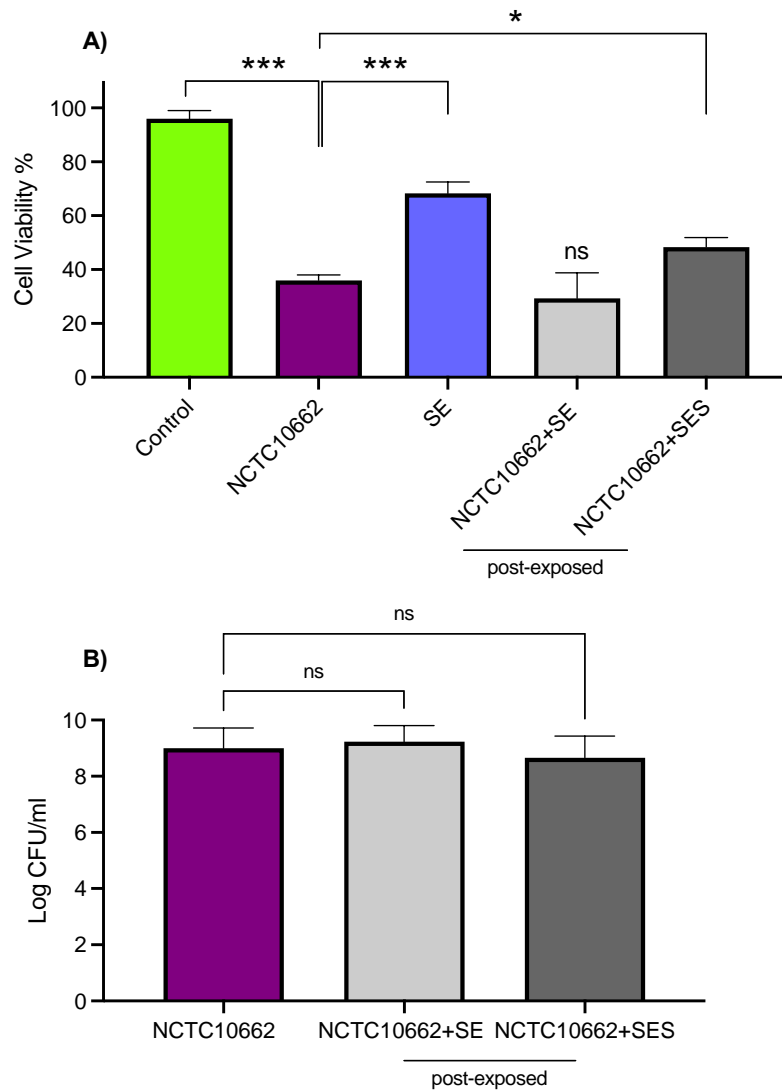


**Figure 5.9** Infection of keratinocytes with *P. aeruginosa* NCTC 10662.

A) Keratinocytes were infected with NCTC 10662 for two hours. After one hour of infection, keratinocytes were post-exposed to SES or *S. epidermidis* (SE) for another hour. The viability of cells was measured after two hours of incubation using the trypan blue exclusion assay. B) The number of adherent *P. aeruginosa* NCTC 10662 to the keratinocytes in the co-culture was measured by spot plating the suspension on selective agar (cetrimide). Error bars are reported as mean  $\pm$  SEM,  $n=3$ . ns = not significant, \*  $P \leq 0.05$ , \*\*  $P \leq 0.01$ , \*\*\*  $P \leq 0.001$ .

This experiment was also performed to investigate the impact of *S. epidermidis* and SES on the infection of keratinocytes with *P. aeruginosa* PAO1. Keratinocytes infected with PAO1 showed the viability of ~28%, while the viability of keratinocytes infected with PAO1 in the presence of SES was as high as ~43.3% ( $P=0.005$ ,  $n=3$ , Figure 5.10 A). The number of attached PAO1 to keratinocytes was also reduced in the presence of SES compared with the adhering PAO1 with cells alone ( $P=0.02$ ,  $n=3$ , Figure 5.10 B). *S. epidermidis* was unable to inhibit the adhesion of PAO1 to keratinocytes through competition; therefore, it was unable to protect keratinocytes ( $P=0.08$ , Figure 5.10).

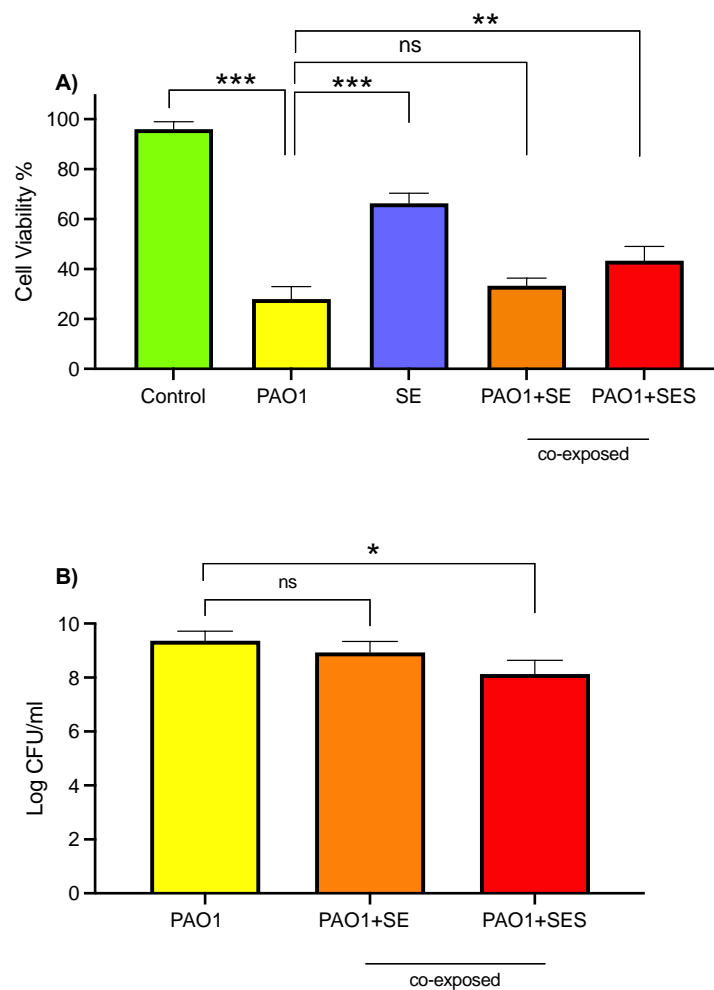


**Figure 5.10** Infection of keratinocytes with *P. aeruginosa* PAO1.

A) Keratinocytes were co-exposed to *P. aeruginosa* PAO1 plus *S. epidermidis* (PAO1+SE) or its supernatant (PAO1+SES) at the same time. The viability of cells was measured after two hours of incubation using the trypan blue exclusion assay. B) The number of adherent *P. aeruginosa* PAO1 to the keratinocytes in the co-culture was measured by spot plating the suspension on selective agar (cetrimide). Error bars are reported as mean  $\pm$  SEM,  $n=3$ . ns = not significant, \*  $P \leq 0.05$ , \*\*  $P \leq 0.01$ , \*\*\*  $P \leq 0.001$ .

Next, the ability of *S. epidermidis* and its extract to exclude PAO1 from binding to the keratinocytes was investigated. Keratinocytes were treated with *S. epidermidis* or SES for one hour before being infected with PAO1. Pre-exposure of keratinocytes with *S. epidermidis* or SES did not protect the PAO1 infected cells; the viability of keratinocytes did not change ( $P=0.1$ , Figure 5.11 A). However, pre-exposure of keratinocytes to *S. epidermidis* reduced the attachment of PAO1 to keratinocytes through exclusion ( $P=0.005$ ,  $n=3$ , Figure 5.11 B).

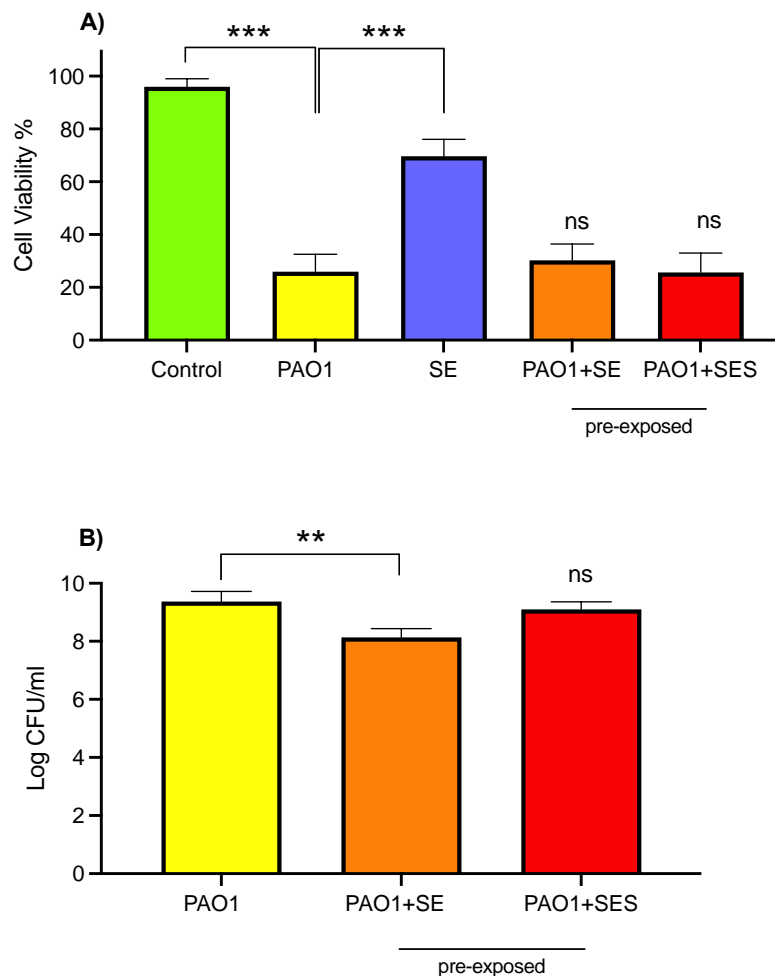


**Figure 5.11** Infection of keratinocytes with *P. aeruginosa* PAO1.

A) Keratinocytes were pre-exposed to *S. epidermidis* (SE) and SES for one hour before being infected with *P. aeruginosa* PAO1 for two hours. The viability of cells was measured using the trypan blue exclusion assay. B) The number of adherent *P. aeruginosa* PAO1 to the keratinocytes in the co-culture was measured by spot plating the suspension on selective agar (cetrimide). Error bars are reported as mean  $\pm$  SEM,  $n=3$ . ns = not significant, \*  $P \leq 0.05$ , \*\*  $P \leq 0.01$ , \*\*\*  $P \leq 0.001$ .

Post-exposure of keratinocytes to *S. epidermidis* and SES had no significant effect on the viability of the cells and the attachment of PAO1 to the keratinocytes ( $P>0.05$ , Figure 5.12).

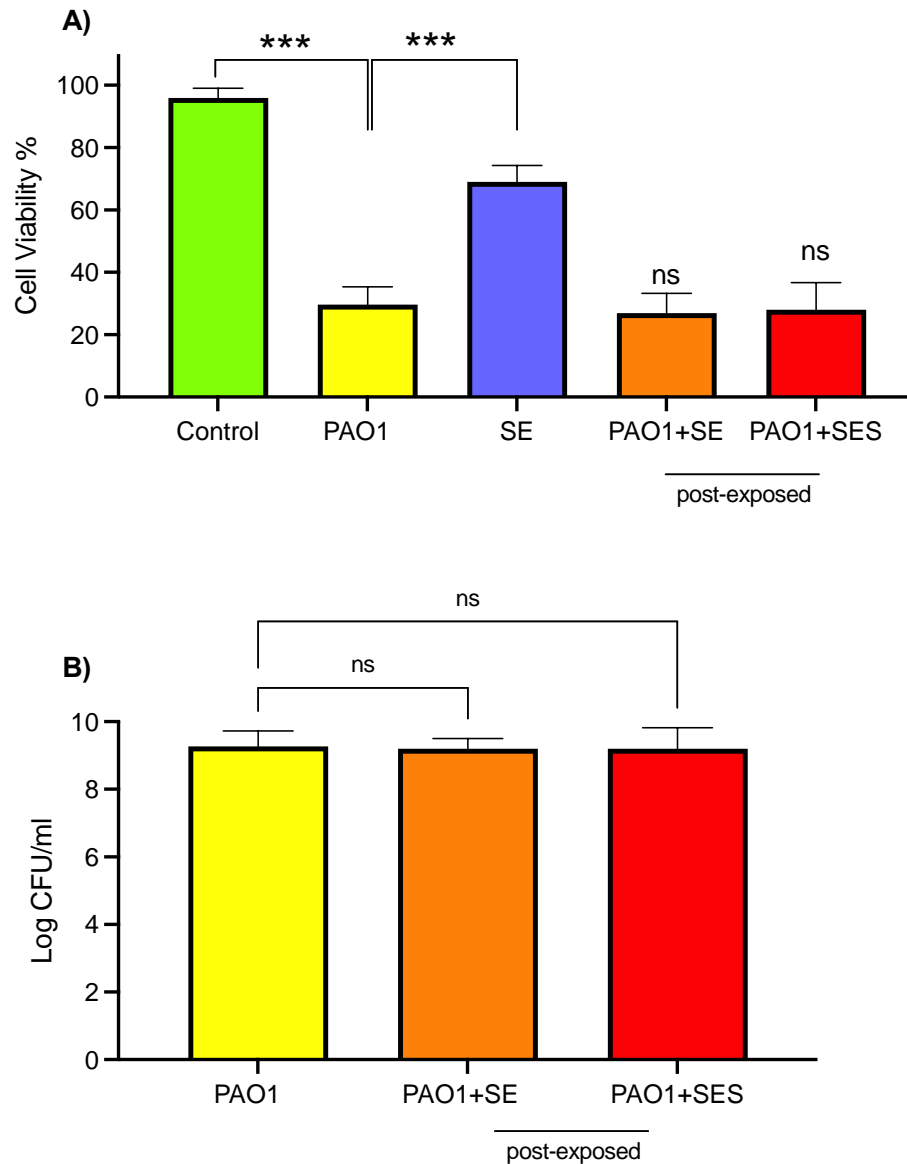


**Figure 5.12** Infection of keratinocytes with *P. aeruginosa* PAO1.

A) Keratinocytes were infected with PAO1 for two hours. After one hour of infection, keratinocytes were post-exposed to SES or *S. epidermidis* (SE) for another hour. The viability of cells was measured after two hours of incubation using the trypan blue exclusion assay. B) The number of adherent *P. aeruginosa* PAO1 to the keratinocytes in the co-culture was measured by spot plating the suspension on selective agar (cetrimide). Error bars are reported as mean  $\pm$  SEM,  $n=3$ . ns = not significant, \*  $P \leq 0.05$ , \*\*  $P \leq 0.01$ , \*\*\*  $P \leq 0.001$ .

The data presented in table 5.1 further summarizes the data collected from the experiments stated above. What stands out in this table is that the co-exposure of SES to the *P. aeruginosa* (both strains) infection on keratinocytes, it is able to improve the viability of keratinocytes and decrease the adhesion of *P. aeruginosa* to the cells.

**Table 5.1** The summary of the protective impact of *S. epidermidis* and its supernatant on *P. aeruginosa* infected keratinocytes.

		<i>S. epidermidis</i>		<i>S. epidermidis</i> Supernatant	
		Improved keratinocytes viability	Decreased bacterial attachment to keratinocytes	Improved keratinocytes viability	Decreased bacterial attachment to keratinocytes
NCTC 10662	Pre-exposure	✓	✓	✗	✗
	<b>Co-exposure</b>	✓	✓	✓	✓
	Post-exposure	✗	✗	✓	✗
PAO1	Pre-exposure	✗	✓	✗	✗
	<b>Co-exposure</b>	✗	✗	✓	✓
	Post-exposure	✗	✗	✗	✗

## 5.3 Discussion

This chapter investigated the impact of SES on keratinocytes and wound healing. Also, it evaluated the protective effect of *S. epidermidis* and its supernatant on keratinocytes against *P. aeruginosa*. *P. aeruginosa* is one of the leading pathogens in chronic wound infections. Biofilm formation of *P. aeruginosa* in the wound area following its attachment to the cells has a deleterious impact on wound healing (Qin *et al.*, 2022). On the other hand, *S. epidermidis*, as a skin commensal, has been shown to protect the skin against pathogens (Sugimoto *et al.*, 2013). In this study, a monolayer of keratinocytes was used as a model to study wound healing and the interaction between *S. epidermidis* and *P. aeruginosa* on the biotic surface.

The SES at 10% v/v preserved the viability and morphology of keratinocytes (Figure 5.1 and Figure 5.2). It was also able to increase the re-epithelization of keratinocytes during scratch wound healing at a faster rate than the control from 16 hours of incubation onward (Figure 5.3). Proliferation and migration of keratinocytes are two of the most important attributers in wound healing (Pastar *et al.*, 2014). Thus, cytokines and chemokines released from keratinocytes in the presence of SES were investigated to understand the underlying pathways of SES impact on keratinocyte re-epithelization.

SES increased the release of two chemokines, CXCL1 and CXCL8, from keratinocytes after 24 hours of incubation (Figure 5.6). This time-point was selected to collect the cell culture supernatant because SES showed increased re-epithelization from 16 hours of incubation. Also, keratinocytes begin migration and proliferation during normal wound-healing process within 12 to 24 hours after injury (Nagaoka *et al.*, 2000).

CXCL8 and CXCL1 are potent neutrophil attractants to the site of inflammation, therefore, are important in early antimicrobial response at the site of injury (Fujiwara *et al.*, 2002; Ridiandries *et al.*, 2018). Furthermore, CXCL1 and CXCL8 both belong to the glutamate-leucine-arginine (ELR) positive motif group of chemokines, which means they can bind with CXCR1 and CXCR2 receptors, especially CXCR2 (Kroeze *et al.*, 2012). Keratinocytes express CXCR2 receptors (Michel *et al.*, 1992). Activation of CXCR2 through binding with CXCL1 and



CXCL8 induces various signalling cascades, which lead to the proliferation and migration of keratinocytes and neoangiogenesis in the wound area (Cheng *et al.*, 2019). Moreover, according to Devalaraja *et al.*, (2000) CXCR2-knockout mice exhibited reduced neutrophil recruitment, keratinocyte migration and proliferation during re-epithelialization (Devalaraja *et al.*, 2000). It seems that SES, by influencing chemokine release in keratinocytes through CXCL1 and CXCL8/CXCR2 activation pathways, may mediate the accelerated re-epithelization of keratinocytes during scratch wound healing. However, this does not exclude other activation pathways, which need more studies to confirm.

SES also increased the release of IL-6 and ICAM-1 from keratinocytes (Figure 5.6). IL-6 is a pro-inflammatory cytokine playing a crucial role in the inflammation and resolution of the wound repair in a timely manner. As it has been reported in numerous studies, IL-6 promote keratinocytes proliferation and migration (Grossman *et al.*, 1989; Gallucci *et al.*, 2004; Johnson *et al.*, 2020). ICAM-1 is a cell surface glycoprotein and an adhesion receptor that is best known for regulating leukocyte attraction to sites of inflammation (Hubbard and Rothlein, 2000). ICAM-1 is also expressed in epithelial cells, and its expression is upregulated in response to inflammation (Bui *et al.*, 2020). According to an *in vivo* study wound healing in mice lacking ICAM-1 was inhibited; the keratinocytes migration from the edges of the wound toward the centre was also repressed (Nagaoka *et al.*, 2000).

The data from this study suggest that not only SES can help attracting immune cells to the site of injury, but it also promotes keratinocytes proliferation and migration. Wound healing is a dynamic and complex process that requires the controlled release of diverse cytokines and chemokines. Overproduction of pro-inflammatory cytokines such as IL-6 can cause prolonged inflammation and delayed healing. Nevertheless, it has been revealed that pro-inflammatory cytokines, released during the early phase of wound healing are effective stimulators of the expression of various growth factors and chemokines from different types of cells (Hernandez-Quintero *et al.*, 2006; Ghazizadeh, 2007; Piipponen *et al.*, 2020).

In the context of tissue damage, other studies confirm that LTA from the *S. epidermidis* cell wall could dampen excess inflammation and promote wound healing (Lai *et al.*, 2009; Xia *et al.*, 2016). This anti-inflammatory communication occurs through discrete mechanisms.

TLR2 activation by *S. epidermidis*' LTA inhibits pro-inflammatory TLR3 signalling in response to double-stranded RNA from damaged host cells (Lai *et al.*, 2009). This has been confirmed in *C. acnes* induced inflammation, wherein *S. epidermidis*' LTA via induction of microRNA, reduce the inflammation (Xia *et al.*, 2016). *S. epidermidis* is also associated with healing wound, and it has been suggested to act as an early bioindicator of non-chronic wounds. A recent study discovered a specific lipopeptide (lipopeptide 78) in *S. epidermidis*, which inhibits TLR-3 mediated inflammation, therefore promoting wound healing (Li *et al.*, 2019).

In a set of studies, researchers have shown that the application of *S. epidermidis* on mice's skin induced the IL-1 signalling pathways through the activation of skin resident immune cells, which promotes innate barrier immunity (Naik *et al.*, 2012; Naik *et al.*, 2015). Secretion of IL-1 from the keratinocytes was not observed in the current study. Although Human Cytokine Array test is a suitable start for qualitatively screening cytokine production, it cannot be the only test to rely on. Further, enzyme-linked immunosorbent assay (ELISA) and gene expression analysis would be beneficial to confirm the data obtained.

The present study also investigated the potential of *S. epidermidis* and SES to protect keratinocytes against the toxic effect of *P. aeruginosa* infection. It also aimed to examine the effect of *S. epidermidis* and its supernatant on the attachment of *P. aeruginosa* to the monolayer of keratinocytes as a biotic surface. The viability of infected keratinocytes with *P. aeruginosa* (at 1:20 MOI) was examined when treated with *S. epidermidis* (at 1:20 MOI) or SES. It was observed that the viability of keratinocytes was significantly reduced when exposed to *P. aeruginosa* NCTC 10662 and PAO1, while exposure to live *S. epidermidis* caused a slight reduction in cell viability (Figure 5.7 and Figure 5.10). SES, as shown before in this chapter, even preserved the viability of cells with no decrease in viability being observed after 24 hours (Figure 5.1). SES was able to provide protection to keratinocytes when it was co-exposed with both strains of *P. aeruginosa*. In contrast, live *S. epidermidis* cells were unable to improve the viability of cells when co-exposed with *P. aeruginosa* (Figure 5.7 A and Figure 5.10 A). SES also reduced the attachment of NCTC 10662 and PAO1 to keratinocytes (Figure 5.7 B and Figure 5.10 B). The decreased attachment of *P. aeruginosa* to keratinocytes might be the reason for the improved viability of cells. The

attachment of bacteria to the host cells is the first step in biofilm formation and pathogenicity. It has been reported previously that a reduction in *P. aeruginosa* adhesion could decrease its pathogenicity (Sadikot *et al.*, 2005; Kuchma *et al.*, 2014). This confirms the data presented in chapter 3 that SES was able to reduce the biofilm formation and virulence factor release of *P. aeruginosa* through modulating quorum sensing network. This result also concurs with previous studies showing the impact of *S. epidermidis* extract on protecting keratinocytes against pathogens (Iwase *et al.*, 2010; Fredheim *et al.*; 2015).

Live *S. epidermidis* cells were the most effective in protecting keratinocytes once it was added to the cells before *P. aeruginosa* infection. *S. epidermidis* reduced the attachment of NCTC 10662 to keratinocytes and also increased the viability of cells during infection with NCTC 10662 (Figure 5.8). Although *S. epidermidis* was able to reduce the attachment of PAO1 to keratinocytes, it was unable to protect cells during infection, and the viability of keratinocytes did not change (Figure 5.11). This can be due to the production of more virulence factors in higher concentration by PAO1 (shown in chapter 3), which are deleterious to the cells. Similar results have been demonstrated in chapter 4, when *S. epidermidis* was pre-exposed to *P. aeruginosa*, the attachment of *P. aeruginosa* to the abiotic surface reduced. These data suggest that *S. epidermidis* diminished *P. aeruginosa* attachment to biotic and abiotic surfaces through competitive exclusion.

SES had no protective effect on keratinocytes when it was added before the infection. In pre-treatment of cells with SES, the SES was removed from the cell layer after one hour and the *P. aeruginosa* was added to the cells thereafter. Removing SES from the cells might remove the active molecule(s), presumably quorum quenching molecule(s), responsible for attenuating PAO1 and NCTC 10662. Therefore, pre-treatment with SES was unable to protect keratinocytes. Further studies are required to characterize the active molecule(s) in SES.

The addition of *S. epidermidis* to the post-infection of *P. aeruginosa* (both strains) on keratinocytes did not change the attachment of *P. aeruginosa* to the cells or the viability of keratinocytes (Figure 5.9 and Figure 5.12). SES was also ineffective in protecting the cells in post-infection of PAO1 and adhesion reduction of PAO1 to the cells (Figure 5.12). However,

the addition of SES to the NCTC 10662 infected keratinocytes improved the viability of cells with no effect on the attachment of bacterial cells to the keratinocytes (Figure 5.9). It appears that the infection of *P. aeruginosa* inserts its toxic impact on the keratinocytes even during the short incubation period therefore, addition of *S. epidermidis* or its supernatant could not protect keratinocytes after the infection.

In summary, the data presented in this chapter suggests that SES can improve proliferation and migration of keratinocytes through induction of chemokines and cytokines release from keratinocytes during scratch wound healing. Also, when the SES is added simultaneously with *P. aeruginosa*, it is capable to reduce *P. aeruginosa* adhesion to keratinocytes therefore increase the cell viability. Furthermore, *S. epidermidis* could inhibit *P. aeruginosa* adhesion to keratinocytes through exclusion.

## Chapter 6 Overall discussion

The general aim of this study was to investigate the interaction between *S. epidermidis*, a major human skin commensal, and *P. aeruginosa*, an opportunistic pathogen, in the context of wound infections.

The data obtained from chapter 3 of this study demonstrate that *S. epidermidis* secreted molecules diminished biofilm formation of mucoid and non-mucoid biofilm-forming strains of *P. aeruginosa* without any impact on their growth. This result was supported by the data showing a decrease in the flagellum-mediated motility in NCTC 10662 and PAO1 in the presence of SES. In *P. aeruginosa*, swimming motility is directly related to the ability of biofilm formation (Khan *et al.*, 2020). The results presented in this thesis is in agreement with a work published in 2020, where researchers also showed that small molecules produced by *S. epidermidis* could disrupt the biofilm formation of *S. aureus* (Glatthardt *et al.*, 2020). The impact of active molecules in SES was not limited to biofilm disruption of *P. aeruginosa*. SES also effected several key virulence factors. SES inhibited elastase activity and *toxA* expression in both strains of *P. aeruginosa*. PAO1 is a strong pyocyanin producer compared to NCTC 10662; pyocyanin production by *P. aeruginosa* PAO1 also decreased in the presence of SES. Biofilm formation, pyocyanin production, and *toxA* expression are under the control of quorum sensing genes involving the *las* and *rhl* quorum sensing system (Lee and Zang, 2015; Jenkins *et al.*, 2004). The analysis of the impact of SES on the quorum sensing gene expression of *P. aeruginosa* revealed the down-regulation of autoinducer synthases *lasI* and *rhlI* expression. There are several reports that bacterial cells use quorum sensing signalling system to reduce the fitness of their competitors and to gain the advantage of resources in the environment; there is also evidence of quorum sensing molecules in chronic wounds clinical samples (Han *et al.*, 2012; Paharik *et al.*, 2017). Hence, the inhibition of quorum sensing signal production might be a solid weapon to suppress infection in wound areas.

One of the reasons that biofilm is an important virulence factor is that the EPS of biofilm drastically reduce the susceptibility of bacteria to antimicrobials. Therefore, disruption of

biofilm might increase the susceptibility of *P. aeruginosa* to antibiotics. Treatment of established biofilm of *P. aeruginosa* using the combination of gentamicin with SES increased this antibiotic's efficacy in reducing biofilm-embedded cells. The same result was observed in combination therapy using ciprofloxacin and SES. However, the combination of SES with tetracycline could not improve the efficacy of tetracycline against *P. aeruginosa*. *P. aeruginosa* is generally resistant to tetracycline due to the efflux pump activity on the outer membrane, which is one of the primary intrinsic drug resistance mechanisms in bacteria. There is evidence that tetracycline could increase the activity of the efflux pump in *P. aeruginosa*, thus reducing its own efficacy (Morita *et al.*, 2014). The experiment in this study on the efflux pump activity in *P. aeruginosa* confirmed that SES has no impact on efflux pump activity, thus ineffective in improving the efficacy of tetracycline. The mechanism of action of SES to improve the effectiveness of gentamicin and ciprofloxacin remains to be investigated. However, in a study in 2020, researchers showed that the cell-free culture liquid of *S. aureus* could also enhance the susceptibility of *P. aeruginosa* to aminoglycosides (Trizna *et al.*, 2020). The active molecule in the culture of staphylococcal species responsible for the increase might be similar and remains to be identified. Yet, it seems that SES might be able to improve the efficacy of gentamicin and ciprofloxacin through disruption of biofilm in *P. aeruginosa*.

An *in vivo* study on a wound-bearing mouse model showed that bacterial species associated with chronic wounds differ from the microbial community in non-chronic wounds. Researchers identified several specific species that can be used as bioindicators of chronic and non-chronic wounds. This suggests that bacterial species found in healing wounds might be beneficial in controlling infectious wounds. *S. epidermidis* has been found to be associated with healing wounds, and it is an early bioindicator of non-chronic wounds (Kim *et al.*, 2020). Additionally, it seems likely that *S. epidermidis* and *P. aeruginosa* interact within the cutaneous wound (Jneid *et al.*, 2018; Kalan *et al.*, 2019). Commensal bacteria compete for resources with pathogens and produce compounds to limit pathogens' growth and biofilm formation (Iwase *et al.*, 2010; Paharik *et al.*, 2017). Therefore, in chapter 4 of this study, the interaction of *S. epidermidis* and *P. aeruginosa* in planktonic and biofilm states was explored.

The initial data from chapter 4 showed that in planktonic co-culture, the number of *S. epidermidis* cells was significantly lower than *P. aeruginosa*. Although NCTC 10662 had no competitive gain over *S. epidermidis* in planktonic co-culture, PAO1 showed a competitive advantage. PAO1, through high production of pyocyanin and pyoverdine, could inhibit the electron transport chain in *S. epidermidis* and shift it to fermentative mode, which can eventually reduce the number of bacterial cells. Interestingly in biofilm co-culture, *S. epidermidis* diminished the number of the attached *P. aeruginosa* to the abiotic surface. The preformed biofilm of *S. epidermidis* likewise decreased the number of the attached *P. aeruginosa*. While *S. epidermidis* is not a biofilm-forming strain, it still has the potential to attach to abiotic surfaces through surface proteins. This might be the reason for the exclusion of *P. aeruginosa* by *S. epidermidis* from attachment to the surface. Moreover, several studies confirm that serine proteases secreted from *S. epidermidis* could degrade *S. aureus* adhesion proteins, subsequently inhibiting the colonization through obstructing adhesion to the surface (Iwase *et al.*, 2010; Sugimoto *et al.*, 2013; Fredheim *et al.*, 2015). Pre-exposure to *S. epidermidis* in NCTC 10662 co-culture and co-exposure to *S. epidermidis* in PAO1 co-culture also reduced the biofilm biomass.

*S. epidermidis* showed higher tolerance to tetracycline in co-culture with *P. aeruginosa*, while the susceptibility of *P. aeruginosa* did not change. However, the susceptibility of *P. aeruginosa* to gentamicin and ciprofloxacin was reduced in co-culture with *S. epidermidis*. This suggests that the interaction of *S. epidermidis* and *P. aeruginosa* would induce phenotypical changes, which can alter some of the important pathogenesis characteristics of microbes. This has been supported by several studies on the interaction of bacterial cells in co-culture conditions (Alves *et al.*, 2018; Cendra *et al.*, 2019; Briaud *et al.*, 2019). A thorough transcriptomic profile of co-existing *S. epidermidis* and *P. aeruginosa* would be beneficial to shed light on the complex interaction of *S. epidermidis* and *P. aeruginosa*.

Chapter 5 of this study explored the impact of SES on keratinocytes and the interaction of *S. epidermidis* and *P. aeruginosa* on keratinocytes. The current results revealed the protective effect of SES on keratinocytes, especially during the wound healing process. Scratched keratinocytes showed better healing outcomes when treated with SES than

untreated wounds. SES induced keratinocytes' proliferation and migration through stimulation of chemokines and cytokines release from keratinocytes. CXCL1 and CXCL8 release from keratinocytes increased in the presence of SES; these chemokines could induce proliferation and migration in keratinocytes, thus improving wound healing. Although activation of CXCR2 in the presence of SES needs to be confirmed with further experiments, CXCL1 and CXCL8 generally activate CXCR2 to induce proliferation and migration. SES also increased the release of IL-6 and ICAM-1, which are important factors in the proliferation of keratinocytes after injury. The SES may provide a novel approach to protect keratinocytes during the wound healing process that has not been studied before. The role of *S. epidermidis* in enhancing the cutaneous immune system has been established in several studies (Stacy and Belkaid, 2019; Yang *et al.*, 2022).

In 2020, researchers made a discovery by demonstrating that innate immune responses during wound healing are not solely reliant on host-derived signals, but also on the presence of skin microbiota (Di Domizio *et al.*, 2020). Commensal bacteria, including *S. epidermidis*, play a crucial role in activating neutrophils to express CXCL10, which, in turn, stimulates fibroblasts and macrophages to produce essential growth factors that facilitate wound healing (Di Domizio *et al.*, 2020). The current study provided evidence that the supernatant of *S. epidermidis* triggers the release of chemokines such as CXCL1 and CXCL8 in keratinocytes, thereby potentially enhancing wound closure. Furthermore, certain strains of *S. epidermidis* have been found to produce trace amines as by-products of aromatic amino acid metabolism, which have been shown to contribute to improved wound healing (Luqman *et al.*, 2020). The beneficial effects of skin microbiota in wound healing extend beyond the production of metabolites. In 2009, researchers discovered that LTA derived from the cell wall of *S. epidermidis* can inhibit skin inflammation induced by UVB radiation through the activation of TLR3. They also demonstrated that LTA could reduce TNF- $\alpha$  production following injury (Lai *et al.*, 2009). These findings highlight the potential of skin microbiota in promoting the wound healing process and emphasize the need for caution in the prolonged use of antibiotics for acute and even chronic skin wounds.



The current study also showed that SES could decrease the adhesion of *P. aeruginosa* to the keratinocytes when it is added simultaneously with *P. aeruginosa* to the keratinocytes. It also increased the viability of keratinocytes during *P. aeruginosa* infection. Taken together, the result suggests that SES might possess potential molecule(s) that reduce the pathogenicity of *P. aeruginosa* as well as protect the keratinocytes during the infection with *P. aeruginosa*. These data provide a preliminary platform to further investigate the complicated interaction of microbe-microbe and microbe-host.

# Chapter 7 Conclusion and future work

## 7.1 Conclusion

Biofilm-associated infections are one of the most challenging infections to deal with in the healthcare system due to their ability to resist host antimicrobial agents and external antibiotic treatment (Sen *et al.*, 2021; Benjamin *et al.*, 2022). *P. aeruginosa* is one of the well-recognized biofilm-forming pathogens in nosocomial infections, and new therapeutics are urgently needed for its control (Moradali *et al.*, 2017; Qin *et al.*, 2022). On the other hand, human microbiome studies are revealing the fundamental role of the human microbiome on human health and disease (Byrd *et al.*, 2018; Hou *et al.*, 2022). Although evidence supports that the commensal microbial community on the skin could modulate the immune system and deter the invasion of opportunistic pathogens (Lai *et al.*, 2009; Nakatsuji *et al.*, 2017; Williams *et al.*, 2019), only a few studies have investigated the interactions between commensals with pathogens in skin infections such as a wound (Hou *et al.*, 2022). Several clinical studies have shown that loss of microbial diversity in the skin can cause disorders such as atopic dermatitis and psoriasis, in which patients suffer from prolonged inflammation due to the microbial imbalance (Williams *et al.*, 2019; Benhadou *et al.*, 2018; Byrd *et al.*, 2018). Also, in chronic wounds, the diversity and abundance of microbes change and provide a situation for the growth of biofilm-forming pathogens. Biofilm in the wound worsens the inflammation and delays wound healing (Johnson *et al.*, 2018; Benjamin *et al.*, 2022).

Most research has investigated the interaction of co-infecting pathogens in the wound (Fazli *et al.*, 2009; Alves *et al.*, 2018; Trizna *et al.*, 2020); however, commensals' role in communication with pathogens and the wound healing process is still unclear. The current study highlighted the potential of skin commensal in combating *P. aeruginosa* infections during wound healing.

The anti-biofilm effect of active molecule(s) present in the supernatant of *S. epidermidis* has a strong potential for the development of innovative therapeutics for biofilm-

associated infections, which can reduce biofilm formation and increase antimicrobial treatment efficiency. This can be used as an alternative to the currently available antibiotics.

The active molecule(s) present in the supernatant, which can counteract virulence factors of *P. aeruginosa* without any effect on the growth of bacterial cells, might provide many benefits compared to the use of traditional antibiotics. It can preserve the host's beneficial microbiome and create less selective pressure on the bacteria, which potentially could reduce resistance.

On the other hand, maybe the introduction of commensal species to the wound as probiotics or adding compounds that support the growth of commensals as prebiotics could save the microbial diversity in the wound, therefore, restore the skin homeostasis. *S. epidermidis* extract can boost local proliferation, therefore, promote wound healing while also preserving tissue homeostasis and cell viability. Application of *S. epidermidis'* active molecule(s) to the wound area could be a potential treatment to conventional therapies to reduce the infection and improve wound healing. Clearly, more investigation is needed to develop novel treatment using the *S. epidermidis* extract before applying it to human skin. Based on The Human Microbiome Project (Turnbaugh *et al.*, 2007; Byrd *et al.*, 2018), new probiotics and prebiotics can be developed for skin conditions. However, in situations such as open wounds on the skin, the use of live probiotics might have a risk of bacterial cells invading the bloodstream. In this case, using the extract is safer, with the potential to reduce the infection and improve wound healing.

## 7.2 Future work

For a deeper understanding of the impact of commensal bacteria on the pathogens and human host, thorough identification of all active molecule(s) present in the supernatant of *S. epidermidis* would be beneficial using a range of analytical equipment/techniques. The skin microbiota plays an important role in skin homeostasis and skin disease development. Therefore, modulation of skin microbiota and harnessing its potential metabolites could be a prospective strategy in skin disease treatment.

There are several *S. epidermidis* strains living on human skin with different genome contents, characteristics, and levels of pathogenicity (Turnbaugh *et al.*, 2007; Byrd *et al.*, 2018; Boxberger *et al.*, 2021; Severn and Horswill, 2022). Identifying and characterising these strains and evaluating their potential for skin health and diseases will expand the current understanding of skin microbiome behaviour. While metagenomic analysis has focused on identifying the microbes on the skin, it is essential to continue to unravel the mechanisms that regulate commensal colonization and pathogenicity on the skin. In addition, further analysis of the mechanistic interactions between the commensals, skin cells, and opportunistic pathogens remains to be discovered.

Although *in vitro* cell culture, using a cell line such as HaCaT, is an ideal primary method in skin cell studies, the development of an optimized 3D skin model could offer a better understanding of the skin microenvironment and physiology. An optimized 3D skin model that includes immune, nervous, and endothelial cells could be an advantageous option to investigate host-microbe interaction.

It is not fully understood how microbial cells interact with each other in an infection site. The omics analysis of the impact of commensals, such as *S. epidermidis*, on opportunistic bacteria, such as *P. aeruginosa*, help to better understand the microbe-microbe interactions. Furthermore, in situ monitoring of skin microbiota's spatial distribution in the infection site and identifying pathogens and commensals' locations will provide essential preliminary information on how microbes interact and manage infections. Identification of signalling molecules in the co-culture supernatant of *S. epidermidis* with other

opportunistic pathogens is another appealing approach to further investigate the communication network between microbial cells present on different skin sites.

## References

- ACHOUAK, W., HEULIN, T. and PAGÈS, J., 2001. *Multiple facets of bacterial porins*. Oxford: Elsevier B.V.
- ALGBURI, A., COMITO, N., KASHTANOV, D., DICKS, L.M.T. and CHIKINDAS, M.L., 2017. Control of Biofilm Formation: Antibiotics and Beyond. *Applied and environmental microbiology*, **83**(3), pp. E02508.
- ALLESEN-HOLM, M., BARKEN, K.B., YANG, L., KLAUSEN, M., WEBB, J.S., KJELLEBERG, S., MOLIN, S., GIVSKOV, M. and TOLKER-NIELSEN, T., 2006. A characterization of DNA release in *Pseudomonas aeruginosa* cultures and biofilms. *Molecular microbiology*, **59**(4), pp. 1114-1128.
- ALVES, P.M., AL-BADI, E., WITHYCOMBE, C., JONES, P.M., PURDY, K.J. and MADDOCKS, S.E., 2018. Interaction between *Staphylococcus aureus* and *Pseudomonas aeruginosa* is beneficial for colonisation and pathogenicity in a mixed biofilm. *Pathogens and Disease*, **76**(1).
- AZGHANI, A.O., 1996. *Pseudomonas aeruginosa* and epithelial permeability: role of virulence factors elastase and exotoxin A. *American journal of respiratory cell and molecular biology*, **15**(1), pp. 132-140.
- BANNER, M.A., CUNNIFFE, J.G., MACINTOSH, R.L., FOSTER, T.J., ROHDE, H., MACK, D., HOYES, E., DERRICK, J., UPTON, M. and HANDLEY, P.S., 2007. Localized Tufts of Fibrils on *Staphylococcus epidermidis* NCTC 11047 Are Comprised of the Accumulation-Associated Protein. *Journal of Bacteriology*, **189**(7), pp. 2793-2804.
- BARKEN, K.B., PAMP, S.J., YANG, L., GJERMANSEN, M., BERTRAND, J.J., KLAUSEN, M., GIVSKOV, M., WHITCHURCH, C.B., ENGEL, J.N. and TOLKER-NIELSEN, T., 2008. Roles of type IV pili, flagellum-mediated motility and extracellular DNA in the formation of mature multicellular structures in *Pseudomonas aeruginosa* biofilms. *Environmental microbiology*, **10**(9), pp. 2331-2343.
- BARRIENTOS, S., STOJADINOVIC, O., GOLINKO, M.S., BREM, H. and TOMIC-CANIC, M., 2008. PERSPECTIVE ARTICLE: Growth factors and cytokines in wound healing. *Wound repair and regeneration*, **16**(5), pp. 585-601.
- BARTOW-MCKENNEY, C., HANNIGAN, G.D., HORWINSKI, J., HESKETH, P., HORAN, A.D., MEHTA, S. and GRICE, E.A., 2018. The microbiota of traumatic, open fracture wounds is associated with mechanism of injury. *Wound repair and regeneration: official publication of the Wound Healing Society [and] the European Tissue Repair Society*, **26**(2), pp. 127-135.

- BEHM, B., BABILAS, P., LANDTHALER, M. and SCHREML, S., 2012. Cytokines, chemokines and growth factors in wound healing. *Journal of the European Academy of Dermatology and Venereology*, **26**(7), pp. 812-820.
- BELLIDO, F., MARTIN, N.L., SIEHNEL, R.J. and HANCOCK, R.E.W., 1992. Reevaluation, using intact cells, of the exclusion limit and role of porin OprF in *Pseudomonas aeruginosa* outer membrane permeability. *Journal of Bacteriology*, **174**(16), pp. 5196-5203.
- BENHADOU, F., MINTOFF, D., SCHNEBERT, B. and THIO, H., 2018. Psoriasis and Microbiota: A Systematic Review. *Diseases*, **6**(2), pp. 47.
- BENJAMIN A R N DURAND, POUGET, C., MAGNAN, C., MOLLE, V., LAVIGNE, J. and DUNYACH-REMY, C., 2022. Bacterial Interactions in the Context of Chronic Wound Biofilm: A Review. *Microorganisms (Basel)*, **10**(8), pp. 1500.
- BIERBAUM, G., GÖTZ, F., PESCHEL, A., KUPKE, T., VAN DE KAMP, M. and SAHL, H.-., 1996. The biosynthesis of the lantibiotics epidermin, gallidermin, Pep5 and epilancin K7, 1996, Springer, pp. 119-127.
- BISWAS, L., BISWAS, R., SCHLAG, M., BERTRAM, R. and GÖTZ, F., 2009. Small-Colony Variant Selection as a Survival Strategy for *Staphylococcus aureus* in the Presence of *Pseudomonas aeruginosa*. *Applied and Environmental Microbiology*, **75**(21), pp. 6910-6912.
- BISWAS, L. and GÖTZ, F., 2021. Molecular Mechanisms of *Staphylococcus* and *Pseudomonas* Interactions in Cystic Fibrosis. *Frontiers in cellular and infection microbiology*, **11**, pp. 824042.
- BJARNSHOLT, T., 2013. The role of bacterial biofilms in chronic infections. *APMIS*, **121**(s136), pp. 1-58.
- BJARNSHOLT, T., KIRKETERP-MØLLER, K., JENSEN, P.Ø, MADSEN, K.G., PHIPPS, R., KROGFELT, K., HØIBY, N. and GIVSKOV, M., 2008. Why chronic wounds will not heal: a novel hypothesis. *Wound Repair and Regeneration*, **16**(1), pp. 2-10.
- BLAIR, J.M.A. and PIDDOCK, L.J.V., 2016. How to Measure Export via Bacterial Multidrug Resistance Efflux Pumps. *mBio*, **7**(4).
- BLAIR, J.M.A., WEBBER, M.A., BAYLAY, A.J., OGBOLU, D.O. and PIDDOCK, L.J.V., 2015. Molecular mechanisms of antibiotic resistance. *Nature reviews. Microbiology*, **13**(1), pp. 42-51.
- BOXBERGER, M., CENIZO, V., CASSIR, N. and LA SCOLA, B., 2021. Challenges in exploring and manipulating the human skin microbiome. *Microbiome*, **9**(1), pp. 1-125.

BRADFORD, M.M., 1976. A rapid and sensitive method for the quantitation of microgram quantities of protein utilizing the principle of protein-dye binding. *Analytical biochemistry*, **72**(1), pp. 248-254.

BRIAUD, P., CAMUS, L., BASTIEN, S., DOLÉANS-JORDHEIM, A., VANDENESCH, F. and MOREAU, K., 2019. Coexistence with *Pseudomonas aeruginosa* alters *Staphylococcus aureus* transcriptome, antibiotic resistance and internalization into epithelial cells. *Scientific Reports*, **9**(1), pp. 16564-14.

BROWN, J.L., TOWNSEND, E., SHORT, R.D., WILLIAMS, C., WOODALL, C., NILE, C.J. and RAMAGE, G., 2022. Assessing the inflammatory response to in vitro polymicrobial wound biofilms in a skin epidermis model. *NPJ biofilms and microbiomes*, **8**(1), pp. 19.

BUCH, P.J., CHAI, Y. and GOLUCH, E.D., 2019. Treating Polymicrobial Infections in Chronic Diabetic Wounds. *Clinical microbiology reviews*, **32**(2),.

BUI, T.M., WIESOLEK, H.L. and SUMAGIN, R., 2020. ICAM-1: A master regulator of cellular responses in inflammation, injury resolution, and tumorigenesis. *Journal of leukocyte biology*, **108**(3), pp. 787-799.

BUSH, K. and JACOBY, G.A., 2010. Updated Functional Classification of  $\beta$ -Lactamases. *Antimicrobial Agents and Chemotherapy*, **54**(3), pp. 969-976.

BYRD, A.L., BELKAID, Y. and SEGRE, J.A., 2018. The human skin microbiome. *Nature Reviews Microbiology*, **16**(3), pp. 143-155.

CALDWELL, C.C., CHEN, Y., GOETZMANN, H.S., HAO, Y., BORCHERS, M.T., HASSETT, D.J., YOUNG, L.R., MAVRODI, D., THOMASHOW, L. and LAU, G.W., 2009. *Pseudomonas aeruginosa* Exotoxin Pyocyanin Causes Cystic Fibrosis Airway Pathogenesis. *The American journal of pathology*, **175**(6), pp. 2473-2488.

CANO SANCHEZ, M., LANCEL, S., BOULANGER, E. and NEVIERE, R., 2018. Targeting Oxidative Stress and Mitochondrial Dysfunction in the Treatment of Impaired Wound Healing: A Systematic Review. *Antioxidants*, **7**(8).

CARMONA-CRUZ, S., OROZCO-COVARRUBIAS, L. and SÁEZ-DE-OCARIZ, M., 2022. The Human Skin Microbiome in Selected Cutaneous Diseases. *Frontiers in cellular and infection microbiology*, **12**, pp. 834135.

CASILAG, F., LORENZ, A., KRUEGER, J., KLAWONN, F., WEISS, S. and HÄUSSLER, S., 2016. The LasB Elastase of *Pseudomonas aeruginosa* Acts in Concert with Alkaline Protease AprA To Prevent Flagellin-Mediated Immune Recognition. *Infection and immunity*, **84**(1), pp. 162-171.



CASTILLA, D.M., LIU, Z. and VELAZQUEZ, O.C., 2012. Oxygen: Implications for Wound Healing. *Advances in Wound Care*, **1**(6), pp. 225-230.

CENDRA, M.D.M., BLANCO-CABRA, N., PEDRAZ, L. and TORRENTS, E., 2019. Optimal environmental and culture conditions allow the in vitro coexistence of *Pseudomonas aeruginosa* and *Staphylococcus aureus* in stable biofilms. *Scientific Reports*, **9**(1), pp. 1-17.

CHEHOUD, C., RAFAIL, S., TYLDSLEY, A.S., SEYKORA, J.T., LAMBRIS, J.D. and GRICE, E.A., 2013. Complement modulates the cutaneous microbiome and inflammatory milieu. *Proceedings of the National Academy of Sciences - PNAS*, **110**(37), pp. 15061-15066.

CHEN, Y.E., FISCHBACH, M.A. and BELKAID, Y., 2018. Skin microbiota-host interactions. *Nature (London)*, **553**(7689), pp. 427-436.

CHEN, Z., YANG, J., WU, B. and TAWIL, B., 2014. A Novel Three-Dimensional Wound Healing Model. *Journal of developmental biology*, **2**(4), pp. 198-209.

CHENG, Y., MA, X., WEI, Y. and WEI, X., 2019. Potential roles and targeted therapy of the CXCLs/CXCR2 axis in cancer and inflammatory diseases. *Biochimica et biophysica acta. Reviews on cancer*, **1871**(2), pp. 289-312.

CHEUNG, G.Y.C., JOO, H., CHATTERJEE, S.S. and OTTO, M., 2014. Phenol-soluble modulins – critical determinants of staphylococcal virulence. *FEMS microbiology reviews*, **38**(4), pp. 698-719.

CHEVALIER, S., BOUFFARTIGUES, E., BODILIS, J., MAILLOT, O., LESOUHAITIER, O., FEUILLOLEY, M.G.J., ORANGE, N., DUFOUR, A. and CORNELIS, P., 2017. Structure, function and regulation of *Pseudomonas aeruginosa* porins. *FEMS microbiology reviews*, **41**(5), pp. 698-722.

CIGANA, C., CASTANDET, J., SPRYNSKI, N., MELESSIKE, M., BEYRIA, L., RANUCCI, S., ALCALÁ-FRANCO, B., ROSSI, A., BRAGONZI, A., ZALACAIN, M. and EVERETT, M., 2020. *Pseudomonas aeruginosa* Elastase Contributes to the Establishment of Chronic Lung Colonization and Modulates the Immune Response in a Murine Model. *Frontiers in microbiology*, **11**, pp. 620819.

CIOFU, O. and TOLKER-NIELSEN, T., 2019. Tolerance and Resistance of *Pseudomonas aeruginosa* Biofilms to Antimicrobial Agents-How *P. aeruginosa* Can Escape Antibiotics. *Frontiers in Microbiology*, **10**, pp. 913.

COGEN, A.L., YAMASAKI, K., SANCHEZ, K.M., DORSCHNER, R.A., LAI, Y., MACLEOD, D.T., TORPEY, J.W., OTTO, M., NIZET, V., KIM, J.E. and GALLO, R.L., 2010. Selective Antimicrobial Action Is Provided by Phenol-Soluble Modulins Derived from *Staphylococcus epidermidis*, a Normal Resident of the Skin. *Journal of Investigative Dermatology*, **130**(1), pp. 192-200.

COLEMAN, S.R., BLIMKIE, T., FALSAFI, R. and HANCOCK, R.E.W., 2020. Multidrug Adaptive Resistance of *Pseudomonas aeruginosa* Swarming Cells. *Antimicrobial agents and chemotherapy*, **64**(3).

CORNELIS, P. and DINGEMANS, J., 2013. *Pseudomonas aeruginosa* adapts its iron uptake strategies in function of the type of infections. *Frontiers in Cellular and Infection Microbiology*, **3**.

COSTELLO, E.K., LAUBER, C.L., HAMADY, M., FIERER, N., GORDON, J.I. and KNIGHT, R., 2009. Bacterial community variation in human body habitats across space and time. *Science (New York, N.Y.)*, **326**(5960), pp. 1694-1697.

COWAN, S.T. and STEEL, K.J., 2009. *Cowan and Steel's Manual for the Identification of Medical Bacteria*. Cambridge University Press.

DALTON, T., DOWD, S.E., WOLCOTT, R.D., SUN, Y., WATTERS, C., GRISWOLD, J.A. and RUMBAUGH, K.P., 2011. An In Vivo Polymicrobial Biofilm Wound Infection Model to Study Interspecies Interactions. *PLOS ONE*, **6**(11), pp. e27317.

DARBY, I.A., LAVERDET, B., BONTÉ, F. and DESMOULIÈRE, A., 2014. Fibroblasts and myofibroblasts in wound healing. *Clinical, Cosmetic and Investigational Dermatology*, **7**, pp. 301-311.

DAROUICHE, R.O., 2004. Treatment of Infections Associated with Surgical Implants. *The New England Journal of Medicine*, **350**(14), pp. 1422-1429.

DAVIS, S.C., RICOTTI, C., CAZZANIGA, A., WELSH, E., EAGLSTEIN, W.H. and MERTZ, P.M., 2008. Microscopic and physiologic evidence for biofilm-associated wound colonization in vivo. *Wound Repair and Regeneration*, **16**(1), pp. 23-29.

DARVISHI, S., TAVAKOLI, S., KHARAZIHA, M., GIRAULT, H.H., KAMINSKI, C.F. and MELA, I., 2022. Advances in the Sensing and Treatment of Wound Biofilms. *Angewandte Chemie (International ed.)*, **61**(13), pp. e202112218-n/a.

DE BENTZMANN, S., POLETTE, M., ZAHM, J.-., HINNRASKY, J., KILEZTKY, C., BAJOLET, O., KLOSSEK, J.-., FILLOUX, A., LAZDUNSKI, A. and PUCHELLE, E., 2000. *Pseudomonas aeruginosa* Virulence Factors Delay Airway Epithelial Wound Repair by Altering the Actin Cytoskeleton and Inducing Overactivation of Epithelial Matrix Metalloproteinase-2. *Laboratory investigation*, **80**(2), pp. 209-219.

DE KIEVIT, T.R., KAKAI, Y., REGISTER, J.K., PESCI, E.C. and IGLEWSKI, B.H., 2002. Role of the *Pseudomonas aeruginosa* las and rhl quorum-sensing systems in rhlI regulation. *FEMS microbiology letters*, **212**(1), pp. 101-106.

DE VUYST, E., SALMON, M., EVRARD, C., LAMBERT DE ROUVROIT, C. and POUMAY, Y., 2017. Atopic Dermatitis Studies through In Vitro Models. *Frontiers in medicine*, **4**, pp. 119.

DETTMAN, J.R., SZTEPANACZ, J.L. and KASSEN, R., 2016. The properties of spontaneous mutations in the opportunistic pathogen *Pseudomonas aeruginosa*. *BMC genomics*, **17**(12), pp. 27.

DEVALARAJA, R.M., NANNEY, L.B., QIAN, Q., DU, J., YU, Y., DEVALARAJA, M.N. and RICHMOND, A., 2000. Delayed Wound Healing in CXCR2 Knockout Mice. *Journal of Investigative Dermatology*, **115**(2), pp. 234-244.

DI DOMIZIO, J., BELKHODJA, C., CHENUET, P., FRIES, A., MURRAY, T., MONDÉJAR, P.M., DEMARIA, O., CONRAD, C., HOMEY, B., WERNER, S., SPEISER, D.E., RYFFEL, B. and GILLIET, M., 2020. The commensal skin microbiota triggers type I IFN–dependent innate repair responses in injured skin. *Nature immunology*, **21**(9), pp. 1034-1045.

DIEGELMANN, R.F., 2003. Excessive neutrophils characterize chronic pressure ulcers. *Wound Repair and Regeneration*, **11**(6), pp. 490-495.

DIGGLE, S.P., STACEY, R.E., DODD, C., CÁMARA, M., WILLIAMS, P. and WINZER, K., 2006. The galactophilic lectin, LecA, contributes to biofilm development in *Pseudomonas aeruginosa*. *Environmental microbiology*, **8**(6), pp. 1095-1104.

DONG, Y. and SPEER, C.P., 2014. The role of *Staphylococcus epidermidis* in neonatal sepsis: Guarding angel or pathogenic devil? *International journal of medical microbiology*, **304**(5), pp. 513-520.

DOWD, S.E., SUN, Y., SECOR, P.R., RHOADS, D.D., WOLCOTT, B.M., JAMES, G.A. and WOLCOTT, R.D., 2008. Survey of bacterial diversity in chronic wounds using Pyrosequencing, DGGE, and full ribosome shotgun sequencing. *BMC Microbiology*, **8**, pp. 43.

DU, D., WANG-KAN, X., NEUBERGER, A., VAN VEEN, H.W., POS, K.M., PIDDOCK, L.J.V. and LUISI, B.F., 2018. Multidrug efflux pumps: structure, function and regulation. *Nature reviews. Microbiology*, **16**(9), pp. 523-539.

DUPLANTIER, M., LOHOU, E. and SONNET, P., 2021. Quorum Sensing Inhibitors to Quench *P. aeruginosa* Pathogenicity. *Pharmaceuticals (Basel, Switzerland)*, **14**(12), pp. 1262.

EIFF, C.V., HEILMANN, C. and PETERS, G., 1998. *Staphylococcus epidermidis*: why is it so successful? *Clinical Microbiology and Infection*, **4**(6), pp. 297-300.

EMING, S.A., MARTIN, P. and TOMIC-CANIC, M., 2014. Wound repair and regeneration: mechanisms, signalling, and translation. *Science Translational Medicine*, **6**(265), pp. 265sr6.

ESSAR, D.W., EBERLY, L., HADERO, A. and CRAWFORD, I.P., 1990. Identification and characterization of genes for a second anthranilate synthase in *Pseudomonas aeruginosa*: interchangeability of the two anthranilate synthases and evolutionary implications. *Journal of bacteriology*, **172**(2), pp. 884-900.

FAHLÉN, A., ENGSTRAND, L., BAKER, B.S., POWLES, A. and FRY, L., 2011. Comparison of bacterial microbiota in skin biopsies from normal and psoriatic skin. *Archives of Dermatological Research*, **304**(1), pp. 15-22.

FAZLI, M., BJARNSHOLT, T., KIRKETERP-MØLLER, K., JØRGENSEN, B., ANDERSEN, A.S., KROGFELT, K.A., GIVSKOV, M. and TOLKER-NIELSEN, T., 2009. Nonrandom distribution of *Pseudomonas aeruginosa* and *Staphylococcus aureus* in chronic wounds. *Journal of Clinical Microbiology*, **47**(12), pp. 4084-4089.

FINDLEY, K., OH, J., YANG, J., CONLAN, S., DEMING, C., MEYER, J.A., SCHOENFELD, D., NOMICOS, E., PARK, M., KONG, H.H. and SEGRE, J.A., 2013. Topographic diversity of fungal and bacterial communities in human skin. *Nature*, **498**(7454), pp. 367-370.

FITZPATRICK, T.B., WOLFF, K. and GOLDSMITH, L.A., 2012. *Fitzpatrick's dermatology in general medicine*. 8. ed. edn. New York [u.a.]: McGraw-Hill.

FLEMMING, H., WINGENDER, J., SZEWZYK, U., STEINBERG, P., RICE, S.A. and KJELLEBERG, S., 2016. Biofilms: an emergent form of bacterial life. *Nature Reviews Microbiology*, **14**(9), pp. 563-575.

FOSTER, T.J., 2020. Surface Proteins of *Staphylococcus epidermidis*. *Frontiers in microbiology*, **11**, pp. 1829.

FRANKLIN, M.J., NIVENS, D.E., WEADGE, J.T. and HOWELL, P.L., 2011. Biosynthesis of the *Pseudomonas aeruginosa* extracellular polysaccharides, alginate, Pel, and Psl. *Frontiers in Microbiology*, **2**, pp. 167.

FREDHEIM, E.G.A., FLÆGSTAD, T., ASKARIAN, F. and KLINGENBERG, C., 2015. Colonisation and interaction between *S. epidermidis* and *S. aureus* in the nose and throat of healthy adolescents. *European journal of clinical microbiology & infectious diseases*, **34**(1), pp. 123-129.

FRY, L., BAKER, B.S., POWLES, A.V., FAHLEN, A. and ENGSTRAND, L., 2013. Is chronic plaque psoriasis triggered by microbiota in the skin? *British journal of dermatology (1951)*, **169**(1), pp. 47-52.

FRYKBERG, R.G. and BANKS, J., 2015. Challenges in the Treatment of Chronic Wounds. *Advances in Wound Care*, **4**(9), pp. 560-582.

- FUCHS, E., 2008. Skin stem cells: rising to the surface. *The Journal of Cell Biology*, **180**(2), pp. 273-284.
- FUJIWARA, K., MATSUKAWA, A., OHKAWARA, S., TAKAGI, K. and YOSHINAGA, M., 2002. Functional Distinction between CXC Chemokines, Interleukin-8 (IL-8), and Growth Related Oncogene (GRO) $\alpha$  in Neutrophil Infiltration. *Laboratory investigation*, **82**(1), pp. 15-23.
- FYHRQUIST, N., MUIRHEAD, G., PRAST-NIELSEN, S., JEANMOUGIN, M., OLAH, P., SKOOG, T., JULES-CLEMENT, G., FELD, M., BARRIENTOS-SOMARRIBAS, M., SINKKO, H., VAN DEN BOGAARD, E.H., ZEEUWEN, P.L.J.M., RIKKEN, G., SCHALKWIJK, J., NIEHUES, H., DÄUBENER, W., ELLER, S.K., ALEXANDER, H., PENNINO, D., SUOMELA, S., TESSAS, I., LYBECK, E., BARAN, A.M., DARBAN, H., GANGWAR, R.S., GERSTEL, U., JAHN, K., KARISOLA, P., YAN, L., HANSMANN, B., KATAYAMA, S., MELLER, S., BYLESJÖ, M., HUPÉ, P., LEVI-SCHAFFER, F., GRECO, D., RANKI, A., SCHRÖDER, J.M., BARKER, J., KERE, J., TSOKA, S., LAUERMA, A., SOUMELIS, V., NESTLE, F.O., HOMEY, B., ANDERSSON, B. and ALENIUS, H., 2019. Microbe-host interplay in atopic dermatitis and psoriasis. *Nature Communications*, **10**(1), pp. 4703.
- GALLE, M., CARPENTIER, I. and BEYAERT, R., 2012. Structure and Function of the Type III Secretion System of *Pseudomonas aeruginosa*. *Current Protein & Peptide Science*, **13**(8), pp. 831-842.
- GALLO, R.L. and NAKATSUJI, T., 2011. Microbial Symbiosis with the Innate Immune Defense System of the Skin. *Journal of Investigative Dermatology*, **131**(10), pp. 1974-1980.
- GALLUCCI, R.M., SLOAN, D.K., HECK, J.M., MURRAY, A.R. and O'DELL, S.J., 2004. Interleukin 6 Indirectly Induces Keratinocyte Migration. *Journal of Investigative Dermatology*, **122**(3), pp. 764-772.
- GALLUCCI, R.M., SIMEONOVA, P.P., MATHESON, J.M., KOMMINENI, C., GURIEL, J.L., SUGAWARA, T. and LUSTER, M.I., 2000. Impaired cutaneous wound healing in interleukin-6-deficient and immunosuppressed mice. *The FASEB Journal*, **14**(15), pp. 2525-2531.
- GARDINER, M., VICARETTI, M., SPARKS, J., BANSAL, S., BUSH, S., LIU, M., DARLING, A., HARRY, E. and BURKE, C.M., 2017. A longitudinal study of the diabetic skin and wound microbiome. *PeerJ*, **5**.
- GARDNER, S.E., HILLIS, S.L., HEILMANN, K., SEGRE, J.A. and GRICE, E.A., 2013. The neuropathic diabetic foot ulcer microbiome is associated with clinical factors. *Diabetes*, **62**(3), pp. 923-930.
- GHAZIZADEH, M., 2007. Essential Role of IL-6 Signaling Pathway in Keloid Pathogenesis. *Journal of Nippon Medical School*, **74**(1), pp. 11-22.
- GILLITZER, R. and GOEBELER, M., 2001. Chemokines in cutaneous wound healing. *Journal of leukocyte biology*, **69**(4), pp. 513-521.

GLATTHARDT, T., CAMPOS, J.C.D.M., CHAMON, R.C., DE SÁ COIMBRA, T.F., ROCHA, G.D.A., DE MELO, M.A.F., PARENTE, T.E., LOBO, L.A., ANTUNES, L.C.M., DOS SANTOS, K.R.N. and FERREIRA, R.B.R., 2020. Small Molecules Produced by Commensal *Staphylococcus epidermidis* Disrupt Formation of Biofilms by *Staphylococcus aureus*. *Applied and environmental microbiology*, **86**(5).

GONZALEZ, A.C.D.O., COSTA, T.F., ANDRADE, Z.D.A. and MEDRADO, A.R.A.P., 2016. Wound healing - A literature review. *Anais Brasileiros de Dermatologia*, **91**(5), pp. 614-620.

GOSAIN, A. and DIPIETRO, L.A., 2004. Aging and Wound Healing. *World journal of surgery*, **28**(3), pp. 321-326.

GÖTZ, F., PERCONTI, S., POPELLA, P., WERNER, R. and SCHLAG, M., 2013. Epidermin and gallidermin: Staphylococcal lantibiotics. *International journal of medical microbiology*, **304**(1), pp. 63-71.

GOUNANI, Z., ŞEN KARAMAN, D., VENU, A.P., CHENG, F. and ROSENHOLM, J.M., 2020. Coculture of *P. aeruginosa* and *S. aureus* on cell derived matrix - An in vitro model of biofilms in infected wounds. *Journal of Microbiological Methods*, **175**, pp. 105994.

GRAFFUNDER, E.M. and VENEZIA, R.A., 2002. Risk factors associated with nosocomial methicillin-resistant *Staphylococcus aureus* (MRSA) infection including previous use of antimicrobials. *Journal of antimicrobial chemotherapy*, **49**(6), pp. 999-1005.

GRELLNER, W., GEORG, T. and WILSKE, J., 2000. Quantitative analysis of proinflammatory cytokines (IL-1 $\beta$ , IL-6, TNF- $\alpha$ ) in human skin wounds. *Forensic science international*, **113**(1), pp. 251-264.

GRICE, E.A., KONG, H.H., CONLAN, S., DEMING, C.B., DAVIS, J., YOUNG, A.C., BOUFFARD, G.G., BLAKESLEY, R.W., MURRAY, P.R., GREEN, E.D., TURNER, M.L. and SEGRE, J.A., 2009. Topographical and Temporal Diversity of the Human Skin Microbiome. *Science (New York, N.Y.)*, **324**(5931), pp. 1190-1192.

GRICE, E.A., KONG, H.H., RENAUD, G., YOUNG, A.C., BOUFFARD, G.G., BLAKESLEY, R.W., WOLFSBERG, T.G., TURNER, M.L. and SEGRE, J.A., 2008. A diversity profile of the human skin microbiota. *Genome Research*, **18**(7), pp. 1043-1050.

GRICE, E.A. and SEGRE, J.A., 2011. The skin microbiome. *Nature Reviews. Microbiology*, **9**(4), pp. 244-253.

GRICE, E.A. and DAWSON, T.L., 2017. Host–microbe interactions: *Malassezia* and human skin. *Current Opinion in Microbiology*, **40**, pp. 81-87.

GRISHIN, A.V., KRIVOZUBOV, M.S., KARYAGINA, A.S. and GINTSBURG, A.L., 2015. *Pseudomonas aeruginosa* Lectins As Targets for Novel Antibacterials. *Acta Naturae*, **7**(2), pp. 29-41.

GRÖNE, A., 2002. Keratinocytes and cytokines. *Veterinary Immunology and Immunopathology*, **88**(1-2), pp. 1-12.

GROSSMAN, R.M., KRUEGER, J., YOURISH, D., GRANELLI-PIPERNO, A., MURPHY, D.P., MAY, L.T., KUPPER, T.S., SEHGAL, P.B. and GOTTLIEB, A.B., 1989. Interleukin 6 is Expressed in High Levels in Psoriatic Skin and Stimulates Proliferation of Cultured Human Keratinocytes. *Proceedings of the National Academy of Sciences - PNAS*, **86**(16), pp. 6367-6371.

GUAN, J., LIANG, C. and PARK, A.Y., 2007. In vitro scratch assay: a convenient and inexpensive method for analysis of cell migration in vitro. *Nature protocols*, **2**(2), pp. 329-333.

GUEST, J.F., AYOUB, N., MCILWRAITH, T., UCHEGBU, I., GERRISH, A., WEIDLICH, D., VOWDEN, K. and VOWDEN, P., 2015. Health economic burden that wounds impose on the National Health Service in the UK. *BMJ Open*, **5**(12), pp. e009283.

GUEST, J.F., FULLER, G.W. and VOWDEN, P., 2020. Cohort study evaluating the burden of wounds to the UK's National Health Service in 2017/2018: update from 2012/2013. *BMJ open*, **10**(12), pp. e045253.

GUO, S. and DIPIETRO, L.A., 2010. Factors Affecting Wound Healing. *Journal of Dental Research*, **89**(3), pp. 219-229.

GURTNER, G.C., WERNER, S., BARRANDON, Y. and LONGAKER, M.T., 2008. Wound repair and regeneration. *Nature*, **453**(7193), pp. 314-321.

HAISMA, E.M., RIETVELD, M.H., BREIJ, A.D., DISSEL, J.T.V., GHALBZOURI, A.E. and NIBBERING, P.H., 2013. Inflammatory and Antimicrobial Responses to Methicillin-Resistant *Staphylococcus aureus* in an In Vitro Wound Infection Model. *PLOS ONE*, **8**(12), pp. e82800.

HALL, B.G., ACAR, H., NANDIPATI, A. and BARLOW, M., 2014. Growth Rates Made Easy. *Molecular Biology and Evolution*, **31**(1), pp. 232-238.

HALL, S., MCDERMOTT, C., ANOOPKUMAR-DUKIE, S., MCFARLAND, A., FORBES, A., PERKINS, A., DAVEY, A., CHESS-WILLIAMS, R., KIEFEL, M., ARORA, D. and GRANT, G., 2016. Cellular Effects of Pyocyanin, a Secreted Virulence Factor of *Pseudomonas aeruginosa*. *Toxins*, **8**(8), pp. 236.

HAN, A., ZENILMAN, J.M., MELENDEZ, J.H., SHIRTLIFF, M.E., AGOSTINHO, A., JAMES, G., STEWART, P.S., MONGODIN, E.F., RAO, D., RICKARD, A.H. and LAZARUS, G.S., 2011. THE

IMPORTANCE OF A MULTI-FACETED APPROACH TO CHARACTERIZING THE MICROBIAL FLORA OF CHRONIC WOUNDS. *Wound repair and regeneration : official publication of the Wound Healing Society [and] the European Tissue Repair Society*, **19**(5), pp. 532-541.

HANCOCK, R.E.W. and BRINKMAN, F.S.L., 2002. Function of *Pseudomonas* porins in uptake and efflux. *Annual review of microbiology*, **56**(1), pp. 17-38.

HÄNEL, K.H., CORNELISSEN, C., LÜSCHER, B. and BARON, J.M., 2013. Cytokines and the skin barrier. *International journal of molecular sciences*, **14**(4), pp. 6720.

HANNIGAN, G.D., MEISEL, J.S., TYLDSLEY, A.S., ZHENG, Q., HODKINSON, B.P., SANMIGUEL, A.J., MINOT, S., BUSHMAN, F.D. and GRICE, E.A., 2015. The Human Skin Double-Stranded DNA Virome: Topographical and Temporal Diversity, Genetic Enrichment, and Dynamic Associations with the Host Microbiome. *mBio*, **6**(5), pp. e01578-e01515.

HAUSER, A.R., 2009. The type III secretion system of *Pseudomonas aeruginosa*: infection by injection. *Nature reviews. Microbiology*, **7**(9), pp. 654-665.

HEILMANN, C., THUMM, G., CHHATWAL, G.S., HARTLEIB, J., UEKOTTER, A. and PETERS, G., 2003. Identification and characterization of a novel autolysin (Aae) with adhesive properties from *Staphylococcus epidermidis*. *Microbiology (Society for General Microbiology)*, **149**(10), pp. 2769-2778.

HERNÁNDEZ-QUINTERO, M., KURI-HARCUCH, W., GONZÁLEZ ROBLES, A. and CASTRO-MUÑOZLEDO, F., 2006. Interleukin-6 promotes human epidermal keratinocyte proliferation and keratin cytoskeleton reorganization in culture. *Cell and tissue research*, **325**(1), pp. 77-90.

HIRAKATA, Y., FURUYA, N., TATEDA, K., KAKU, M. and YAMAGUCHI, K., 1993. In vivo production of exotoxin A and its role in endogenous *Pseudomonas aeruginosa* septicemia in mice. *Infection and Immunity*, **61**(6), pp. 2468-2473.

HOFFMAN, L.R., DÉZIEL, E., D'ARGENIO, D.A., LÉPINE, F., EMERSON, J., MCNAMARA, S., GIBSON, R.L., RAMSEY, B.W. and MILLER, S.I., 2006. Selection for *Staphylococcus aureus* small-colony variants due to growth in the presence of *Pseudomonas aeruginosa*. *Proceedings of the National Academy of Sciences - PNAS*, **103**(52), pp. 19890-19895.

HORNA, G. and RUIZ, J., 2021. Type 3 secretion system of *Pseudomonas aeruginosa*. *Microbiological research*, **246**, pp. 126719.

HORNEF, M.W. and BOGDAN, C., 2005. The role of epithelial Toll-like receptor expression in host defense and microbial tolerance. *Journal of Endotoxin Research*, **11**(2), pp. 124-128.



HOU, K., WU, Z., CHEN, X., WANG, J., ZHANG, D., XIAO, C., ZHU, D., KOYA, J.B., WEI, L., LI, J. and CHEN, Z., 2022. Microbiota in health and diseases. *Signal transduction and targeted therapy*, **7**(1), pp. 135.

HUBBARD, A.K. and ROTHLEIN, R., 2000. Intercellular adhesion molecule-1 (ICAM-1) expression and cell signaling cascades. *Free radical biology & medicine*, **28**(9), pp. 1379-1386.

IBBERSON, C.B. and WHITELEY, M., 2020. The social life of microbes in chronic infection. *Current Opinion in Microbiology*, **53**, pp. 44-50.

IWASE, T., UEHARA, Y., SHINJI, H., TAJIMA, A., SEO, H., TAKADA, K., AGATA, T. and MIZUNOE, Y., 2010. *Staphylococcus epidermidis* Esp inhibits *Staphylococcus aureus* biofilm formation and nasal colonization. *Nature*, **465**(7296), pp. 346-349.

JACK, A.A., KHAN, S., POWELL, L.C., PRITCHARD, M.F., BECK, K., SADH, H., SUTTON, L., CAVALIERE, A., FLORANCE, H., RYE, P.D., THOMAS, D.W. and HILL, K.E., 2018. Alginate Oligosaccharide-Induced Modification of the lasI-lasR and rhlI-rhlR Quorum-Sensing Systems in *Pseudomonas aeruginosa*. *Antimicrobial agents and chemotherapy*, **62**(5).

JAMES, G.A., SWOGGER, E., WOLCOTT, R., PULCINI, E.D., SECOR, P., SESTRICH, J., COSTERTON, J.W. and STEWART, P.S., 2008. Biofilms in chronic wounds. *Wound Repair and Regeneration*, **16**(1), pp. 37-44.

JENKINS, C.E., SWIATONIOWSKI, A., ISSEKUTZ, A.C. and LIN, T., 2004. *Pseudomonas aeruginosa* Exotoxin A Induces Human Mast Cell Apoptosis by a Caspase-8 and -3-dependent Mechanism. *The Journal of biological chemistry*, **279**(35), pp. 37201-37207.

JENNINGS, L.K., DREIFUS, J.E., REICHHARDT, C., STOREK, K.M., SECOR, P.R., WOZNIAK, D.J., HISERT, K.B. and PARSEK, M.R., 2021. *Pseudomonas aeruginosa* aggregates in cystic fibrosis sputum produce exopolysaccharides that likely impede current therapies. *Cell reports (Cambridge)*, **34**(8), pp. 108782.

JNEID, J., CASSIR, N., SCHULDINER, S., JOURDAN, N., SOTTO, A., LAVIGNE, J. and LA SCOLA, B., 2018. Exploring the Microbiota of Diabetic Foot Infections With Culturomics. *Frontiers in cellular and infection microbiology*, **8**, pp. 282.

JOHNSON, B.Z., STEVENSON, A.W., PRÊLE, C.M., FEAR, M.W. and WOOD, F.M., 2020. The Role of IL-6 in Skin Fibrosis and Cutaneous Wound Healing. *Biomedicines*, **8**(5), pp. 101.

JOHNSON, T.R., GÓMEZ, B.I., MCINTYRE, M.K., DUBICK, M.A., CHRISTY, R.J., NICHOLSON, S.E. and BURMEISTER, D.M., 2018. The Cutaneous Microbiome and Wounds: New Molecular Targets to Promote Wound Healing. *International Journal of Molecular Sciences*, **19**(9),.

KABASHIMA, K., HONDA, T., GINHOUX, F. and EGAWA, G., 2019. The immunological anatomy of the skin. *Nature reviews. Immunology*, **19**(1), pp. 19-30.

KADAM, S., NADKARNI, S., LELE, J., SAKHALKAR, S., MOKASHI, P. and KAUSHIK, K.S., 2019. Bioengineered Platforms for Chronic Wound Infection Studies: How Can We Make Them More Human-Relevant? *Frontiers in Bioengineering and Biotechnology*, **7**.

KALAN, L.R., MEISEL, J.S., LOESCHE, M.A., HORWINSKI, J., SOAITA, I., CHEN, X., UBEROI, A., GARDNER, S.E. and GRICE, E.A., 2019. Strain and species level variation in the microbiome of diabetic wounds is associated with clinical outcomes and therapeutic efficacy. *Cell host & microbe*, **25**(5), pp. 641-655.e5.

KALGUDI, R., TAMIMI, R., KYAZZE, G. and KESHAVARZ, T., 2021. Quorum quenchers affect the virulence regulation of non-mucoid, mucoid and heavily mucoid biofilms co-cultured on cell lines. *Applied microbiology and biotechnology*, **105**(23), pp. 8853-8868.

KANG, D., KIRIENKO, D.R., WEBSTER, P., FISHER, A.L. and KIRIENKO, N.V., 2018. Pyoverdine, a siderophore from *Pseudomonas aeruginosa*, translocates into *C. elegans*, removes iron, and activates a distinct host response. *Virulence*, **9**(1), pp. 804-817.

KANG, D. and KIRIENKO, N.V., 2018. Interdependence between iron acquisition and biofilm formation in *Pseudomonas aeruginosa*. *Journal of microbiology (Seoul, Korea)*, **56**(7), pp. 449-457.

KAUANOVA, S., URAZBAYEV, A. and VOROBYEV, I., 2021. The Frequent Sampling of Wound Scratch Assay Reveals the "Opportunity" Window for Quantitative Evaluation of Cell Motility-Impeding Drugs. *Frontiers in cell and developmental biology*, **9**, pp. 640972.

KAWASUMI, A., SAGAWA, N., HAYASHI, S., YOKOYAMA, H. and TAMURA, K., 2012. Wound Healing in Mammals and Amphibians: Toward Limb Regeneration in Mammals. *Current topics in microbiology and immunology*. Berlin, Heidelberg: Springer Berlin Heidelberg, pp. 33-49.

KHAN, F., PHAM, D.T.N., OLOKETUYI, S.F. and KIM, Y., 2020. Regulation and controlling the motility properties of *Pseudomonas aeruginosa*. *Applied microbiology and biotechnology*, **104**(1), pp. 33-49.

KIM, J.H., RUEGGER, P.R., LEBIG, E.G., VANSCHALKWYK, S., JESKE, D.R., HSIAO, A., BORNEMAN, J. and MARTINS-GREEN, M., 2020. High Levels of Oxidative Stress Create a Microenvironment That Significantly Decreases the Diversity of the Microbiota in Diabetic Chronic Wounds and Promotes Biofilm Formation. *Frontiers in Cellular and Infection Microbiology*, **10**.

KIRKER, K.R., JAMES, G.A., FLECKMAN, P., OLERUD, J.E. and STEWART, P.S., 2012. Differential Effects of Planktonic and Biofilm MRSA on Human Fibroblasts. *Wound Repair and Regeneration*, **20**(2), pp. 253-261.

KIRKER, K.R., SECOR, P.R., JAMES, G.A., FLECKMAN, P., OLERUD, J.E. and STEWART, P.S., 2009. Loss of viability and induction of apoptosis in human keratinocytes exposed to *Staphylococcus aureus* biofilms in vitro. *Wound repair and regeneration: official publication of the Wound Healing Society [and] the European Tissue Repair Society*, **17**(5), pp. 690-699.

KLAUSEN, M., AAES-JØRGENSEN, A., MOLIN, S. and TOLKER-NIELSEN, T., 2003. Involvement of bacterial migration in the development of complex multicellular structures in *Pseudomonas aeruginosa* biofilms. *Molecular microbiology*, **50**(1), pp. 61-68.

KNAPP, C.C. and WASHINGTON, J.A., 1989. Evaluation of trehalose-mannitol broth for differentiation of *Staphylococcus epidermidis* from other coagulase-negative staphylococcal species. *Journal of Clinical Microbiology*, **27**(11), pp. 2624-2625.

KOLARSICK, P.A.J., KOLARSICK, M.A. and GOODWIN, C., 2011. Anatomy and Physiology of the Skin. *Journal of the Dermatology Nurses' Association*, **3**(4), pp. 203–213.

KOLLS, J.K., MCCRAY, P.B. and CHAN, Y.R., 2008. Cytokine-mediated regulation of antimicrobial proteins. *Nature reviews. Immunology*, **8**(11), pp. 829-835.

KONG, H.H., OH, J., DEMING, C., CONLAN, S., GRICE, E.A., BEATSON, M.A., NOMICOS, E., POLLEY, E.C., KOMAROW, H.D., MURRAY, P.R., TURNER, M.L. and SEGRE, J.A., 2012. Temporal shifts in the skin microbiome associated with disease flares and treatment in children with atopic dermatitis. *Genome Research*, **22**(5), pp. 850-859.

KONG, H.H. and SEGRE, J.A., 2017. The Molecular Revolution in Cutaneous Biology: Investigating the Skin Microbiome. *Journal of Investigative Dermatology*, **137**(5), pp. e119-e122.

KONG, H.H., 2011. Skin microbiome: genomics-based insights into the diversity and role of skin microbes. *Trends in Molecular Medicine*, **17**(6), pp. 320-328.

KORGAONKAR, A., TRIVEDI, U., RUMBAUGH, K.P. and WHITELEY, M., 2013. Community surveillance enhances *Pseudomonas aeruginosa* virulence during polymicrobial infection. *Proceedings of the National Academy of Sciences - PNAS*, **110**(3), pp. 1059-1064.

KOSTER, M.I. and ROOP, D.R., 2007. Mechanisms Regulating Epithelial Stratification. *Annual review of cell and developmental biology*, **23**(1), pp. 93-113.

KOSTYLEV, M., KIM, D.Y., SMALLEY, N.E., SALUKHE, I., GREENBERG, E.P. and DANDEKAR, A.A., 2019. Evolution of the *Pseudomonas aeruginosa* quorum-sensing hierarchy. *Proceedings of the National Academy of Sciences - PNAS*, **116**(14), pp. 7027-7032.

KROEZE, K.L., BOINK, M.A., SAMPAT-SARDJOEPERSAD, S.C., WAAIJMAN, T., SCHEPER, R.J. and GIBBS, S., 2012. Autocrine Regulation of Re-Epithelialization After Wounding by

Chemokine Receptors CCR1, CCR10, CXCR1, CXCR2, and CXCR3. *Journal of Investigative Dermatology*, **132**(1), pp. 216-225.

KUANG, Z., HAO, Y., WALLING, B.E., JEFFRIES, J.L., OHMAN, D.E. and LAU, G.W., 2011. *Pseudomonas aeruginosa* elastase provides an escape from phagocytosis by degrading the pulmonary surfactant protein-A. *PLoS ONE*, **6**(11), pp. e27091.

KUPPER, T.S., 1990. Immune and inflammatory processes in cutaneous tissues. Mechanisms and speculations. *The Journal of clinical investigation*, **86**(6), pp. 1783-1789.

LAI, Y., DI NARDO, A., NAKATSUJI, T., LEICHTLE, A., YANG, Y., COGEN, A.L., WU, Z., HOOPER, L.V., VON AULOCK, S., RADEK, K.A., HUANG, C., RYAN, A.F. and GALLO, R.L., 2009. Commensal bacteria regulate TLR3-dependent inflammation following skin injury. *Nature medicine*, **15**(12), pp. 1377-1382.

LANGENDONK, R.F., NEILL, D.R. and FOTHERGILL, J.L., 2021. The Building Blocks of Antimicrobial Resistance in *Pseudomonas aeruginosa*: Implications for Current Resistance-Breaking Therapies. *Frontiers in cellular and infection microbiology*, **11**, pp. 665759.

LAU, G.W., HASSETT, D.J., RAN, H. and KONG, F., 2004. The role of pyocyanin in *Pseudomonas aeruginosa* infection. *Trends in Molecular Medicine*, **10**(12), pp. 599-606.

LE MAUFF, F., RAZVI, E., REICHHARDT, C., SIVARAJAH, P., PARSEK, M.R., HOWELL, P.L. and SHEPPARD, D.C., 2022. The Pel polysaccharide is predominantly composed of a dimeric repeat of  $\alpha$ -1,4 linked galactosamine and N-acetylgalactosamine. *Communications biology*, **5**(1), pp. 502.

LEBRE, M.C., VAN DER AAR, A.M.G., VAN BAARSEN, L., VAN CAPEL, T.M.M., SCHUITEMAKER, J.H.N., KAPSENBERG, M.L. and DE JONG, E.C., 2007. Human Keratinocytes Express Functional Toll-Like Receptor 3, 4, 5, and 9. *Journal of Investigative Dermatology*, **127**(2), pp. 331-341.

LECLERCQ, R., CANTÓN, R., BROWN, D.F.J., GISKE, C.G., HEISIG, P., MACGOWAN, A.P., MOUTON, J.W., NORDMANN, P., RODLOFF, A.C., ROSSOLINI, G.M., SOUSSY, C.-., STEINBAKK, M., WINSTANLEY, T.G. and KAHLMETER, G., 2013. EUCAST expert rules in antimicrobial susceptibility testing. *Clinical Microbiology and Infection*, **19**(2), pp. 141-160.

LEE, J., WU, J., DENG, Y., WANG, J., WANG, C., WANG, J., CHANG, C., DONG, Y., WILLIAMS, P. and ZHANG, L., 2013. A cell-cell communication signal integrates quorum sensing and stress response. *Nature Chemical Biology*, **9**(5), pp. 339-343.

LEE, J. and ZHANG, L., 2015. The hierarchy quorum sensing network in *Pseudomonas aeruginosa*. *Protein & cell*, **6**(1), pp. 26-41.

LEONI, G., NEUMANN, P.-., SUMAGIN, R., DENNING, T.L. and NUSRAT, A., 2015. Wound repair: role of immune–epithelial interactions. *Mucosal Immunology*, **8**(5), pp. 959-968.

LI, D., WANG, W., WU, Y., MA, X., ZHOU, W. and LAI, Y., 2019. Lipopeptide 78 from *Staphylococcus epidermidis* Activates  $\beta$ -Catenin To Inhibit Skin Inflammation. *The Journal of immunology (1950)*, **202**(4), pp. 1219-1228.

LIAO, C., HUANG, X., WANG, Q., YAO, D. and LU, W., 2022. Virulence Factors of *Pseudomonas aeruginosa* and Antivirulence Strategies to Combat Its Drug Resistance. *Frontiers in cellular and infection microbiology*, **12**, pp. 926758.

LIN, J., CHENG, J., WANG, Y. and SHEN, X., 2018. The *Pseudomonas* Quinolone Signal (PQS): Not Just for Quorum Sensing Anymore. *Frontiers in Cellular and Infection Microbiology*, **8**.

LINDSAY, J.A. and RILEY, T.V., 1991. Susceptibility to desferrioxamine: a new test for the identification of *Staphylococcus epidermidis*. *Journal of medical microbiology*, **35**(1), pp. 45-48.

LIU, H. and FANG, H.H.P., 2002. Extraction of extracellular polymeric substances (EPS) of sludges. *Journal of biotechnology*, **95**(3), pp. 249-256.

LIU, J., YAN, R., ZHONG, Q., NGO, S., BANGAYAN, N.J., NGUYEN, L., LUI, T., LIU, M., ERFE, M.C., CRAFT, N., TOMIDA, S. and LI, H., 2015. The diversity and host interactions of *Propionibacterium acnes* bacteriophages on human skin. *The ISME Journal*, **9**(9), pp. 2116.

LIVAK, K.J. and SCHMITTGEN, T.D., 2001. Analysis of relative gene expression data using real-time quantitative PCR and the  $2^{-\Delta\Delta C(T)}$  method. *Methods (San Diego, Calif.)*, **25**(4), pp. 402-408.

LOESCHE, M., GARDNER, S.E., KALAN, L., HORWINSKI, J., ZHENG, Q., HODKINSON, B.P., TYLDSLEY, A.S., FRANCISCUS, C.L., HILLIS, S.L., MEHTA, S., MARGOLIS, D.J. and GRICE, E.A., 2017. Temporal Stability in Chronic Wound Microbiota Is Associated With Poor Healing. *Journal of investigative dermatology*, **137**(1), pp. 237-244.

LUQMAN, A., MUTTAQIN, M.Z., YULAIPI, S., EBNER, P., MATSUO, M., ZABEL, S., TRIBELLI, P.M., NIESELT, K., HIDAYATI, D. and GÖTZ, F., 2020. Trace amines produced by skin bacteria accelerate wound healing in mice. *Communications biology*, **3**(1), pp. 277.

MA, L., CONOVER, M., LU, H., PARSEK, M.R., BAYLES, K. and WOZNIAK, D.J., 2009. Assembly and Development of the *Pseudomonas aeruginosa* Biofilm Matrix. *PLoS Pathogens*, **5**(3), pp. e1000354.

MA, L., LU, H., SPRINKLE, A., PARSEK, M.R. and WOZNIAK, D.J., 2007. *Pseudomonas aeruginosa* Psl Is a Galactose- and Mannose-Rich Exopolysaccharide. *Journal of Bacteriology*, **189**(22), pp. 8353-8356.

MACHO, A.P., ZUMAQUERO, A., ORTIZ-MARTÍN, I. and BEUZÓN, C.R., 2007. Competitive index in mixed infections: a sensitive and accurate assay for the genetic analysis of *Pseudomonas syringae*-plant interactions. *Molecular Plant Pathology*, **8**(4), pp. 437-450.

MARQUEZ, B., 2005. Bacterial efflux systems and efflux pumps inhibitors. *Biochimie*, **87**(12), pp. 1137-1147.

MARTINON, F., MAYOR, A. and TSCHOPP, J., 2009. The inflammasomes: guardians of the body. *Annual Review of Immunology*, **27**, pp. 229-265.

MARTINOTTI, S. and RANZATO, E., 2019. Scratch Wound Healing Assay. *Epidermal Cells*. New York, NY: Springer US, pp. 225-229.

MASHBURN, L.M., JETT, A.M., AKINS, D.R. and WHITELEY, M., 2005. *Staphylococcus aureus* Serves as an Iron Source for *Pseudomonas aeruginosa* during In Vivo Coculture. *Journal of Bacteriology*, **187**(2), pp. 554-566.

MASUKO, T., MINAMI, A., IWASAKI, N., MAJIMA, T., NISHIMURA, S. and LEE, Y.C., 2005. Carbohydrate analysis by a phenol-sulfuric acid method in microplate format. *Analytical biochemistry*, **339**(1), pp. 69-72.

MCAULIFFE, O., ROSS, R.P. and HILL, C., 2001. Lantibiotics: structure, biosynthesis and mode of action. *FEMS microbiology reviews*, **25**(3), pp. 285-308.

MEDINA, G., JUÁREZ, K., VALDERRAMA, B. and SOBERÓN-CHÁVEZ, G., 2003. Mechanism of *Pseudomonas aeruginosa* RhlR Transcriptional Regulation of the rhlAB Promoter. *Journal of Bacteriology*, **185**(20), pp. 5976-5983.

MEISEL, J.S., SFYROERA, G., BARTOW-MCKENNEY, C., GIMBLET, C., BUGAYEV, J., HORWINSKI, J., KIM, B., BRESTOFF, J.R., TYLDSLEY, A.S., ZHENG, Q., HODKINSON, B.P., ARTIS, D. and GRICE, E.A., 2018. Commensal microbiota modulate gene expression in the skin. *Microbiome*, **6**(1), pp. 20.

MELTER, O. and RADOJEVIČ, B., 2010. Small colony variants of *Staphylococcus aureus* — review. *Folia microbiologica*, **55**(6), pp. 548-558.

MEMPEL, M., VOELCKER, V., KÖLLISCH, G., PLANK, C., RAD, R., GERHARD, M., SCHNOPP, C., FRAUNBERGER, P., WALLI, A.K., RING, J., ABECK, D. and OLLERT, M., 2003. Toll-Like Receptor Expression in Human Keratinocytes: Nuclear Factor  $\kappa$ B Controlled Gene Activation by *Staphylococcus aureus* is Toll-Like Receptor 2 But Not Toll-Like Receptor 4 or Platelet Activating Factor Receptor Dependent. *Journal of Investigative Dermatology*, **121**(6), pp. 1389-1396.

MENDOZA, R.A., HSIEH, J. and GALIANO, R.D., 2019. The Impact of Biofilm Formation on Wound Healing. *Wound Healing - Current Perspectives*.

- MERRITT, J.H., KADOURI, D.E. and O'TOOLE, G.A., 2005. Growing and analyzing static biofilms. *Current protocols in microbiology (Online)*, **Chapter 1**(1), pp. Unit 1B.1.
- MESTRALLET, G., ROUAS-FREISS, N., LEMAOULT, J., FORTUNEL, N.O. and MARTIN, M.T., 2021. Skin Immunity and Tolerance: Focus on Epidermal Keratinocytes Expressing HLA-G. *Frontiers in immunology*, **12**, pp. 772516.
- MEYER, J.-., 2000. Pyoverdines: pigments, siderophores and potential taxonomic markers of fluorescent *Pseudomonas* species. *Archives of microbiology*, **174**(3), pp. 135-142.
- MICHALSKA, M. and WOLF, P., 2015. *Pseudomonas* Exotoxin A: optimized by evolution for effective killing. *Frontiers in microbiology*, **6**, pp. 963.
- MICHEL, G., KEMÉNY, L., PETER, R.U., BEETZ, A., RIED, C., ARENBERGER, P. and RUZICKA, T., 1992. Interleukin-8 receptor-mediated chemotaxis of normal human epidermal cells. *FEBS letters*, **305**(3), pp. 241-243.
- MILES, A.A., MISRA, S.S. and IRWIN, J.O., 1938. The estimation of the bactericidal power of the blood. *The Journal of Hygiene*, **38**(6), pp. 732-749.
- MILHO, C., SILVA, M.D., ALVES, D., OLIVEIRA, H., SOUSA, C., PASTRANA, L.M., AZEREDO, J. and SILLANKORVA, S., 2019. Escherichia coli and Salmonella Enteritidis dual-species biofilms: interspecies interactions and antibiofilm efficacy of phages. *Scientific Reports*, **9**(1), pp. 1-15.
- MILLER, M.B. and BASSLER, B.L., 2001. Quorum Sensing in Bacteria. *Annual Review of Microbiology*, **55**(1), pp. 165-199.
- MISIC, A.M., GARDNER, S.E. and GRICE, E.A., 2014. The Wound Microbiome: Modern Approaches to Examining the Role of Microorganisms in Impaired Chronic Wound Healing. *Advances in Wound Care*, **3**(7), pp. 502-510.
- MITCHELL, G., SÉGUIN, D.L., ASSELIN, A., DÉZIEL, E., CANTIN, A.M., FROST, E.H., MICHAUD, S. and MALOUIN, F., 2010. *Staphylococcus aureus* sigma B-dependent emergence of small-colony variants and biofilm production following exposure to *Pseudomonas aeruginosa* 4-hydroxy-2-heptylquinoline-N-oxide. *BMC Microbiology*, **10**(1), pp. 33.
- MOHAMMADPOUR, M., BEHJATI, M., SADEGHI, A. and FASSIHI, A., 2013. Wound healing by topical application of antioxidant iron chelators: kojic acid and deferiprone. *International Wound Journal*, **10**(3), pp. 260-264.
- MOHAMMEDSAEED, W., MCBAIN, A.J., CRUICKSHANK, S.M. and O'NEILL, C.A., 2014. *Lactobacillus rhamnosus* GG Inhibits the Toxic Effects of *Staphylococcus aureus* on Epidermal Keratinocytes. *Applied and Environmental Microbiology*, **80**(18), pp. 5773-5781.

MORADALI, M.F., GHODS, S. and REHM, B.H.A., 2017. *Pseudomonas aeruginosa* Lifestyle: A Paradigm for Adaptation, Survival, and Persistence. *Frontiers in Cellular and Infection Microbiology*, **7**.

MORITA, Y., TOMIDA, J. and KAWAMURA, Y., 2014. Responses of *Pseudomonas aeruginosa* to antimicrobials. *Frontiers in Microbiology*, **4**, pp. 422.

MOSMANN, T., 1983. Rapid colorimetric assay for cellular growth and survival: Application to proliferation and cytotoxicity assays. *Journal of immunological methods*, **65**(1), pp. 55-63.

MULCAHY, L.R., ISABELLA, V.M. and LEWIS, K., 2014. *Pseudomonas aeruginosa* Biofilms in Disease. *Microbial ecology*, **68**(1), pp. 1-12.

MUNITA, J.M. and ARIAS, C.A., 2016. Mechanisms of antibiotic resistance. *Microbiology spectrum*, **4**(2).

MURRAY, J.L., CONNELL, J.L., STACY, A., TURNER, K.H. and WHITELEY, M., 2014. Mechanisms of synergy in polymicrobial infections. *Journal of Microbiology (Seoul, Korea)*, **52**(3), pp. 188-199.

MURRAY, P.J. and WYNN, T.A., 2011. Protective and pathogenic functions of macrophage subsets. *Nature Reviews Immunology*, **11**(11), pp. 723-737.

MURRAY, T.S. and KAZMIERCZAK, B.I., 2008. *Pseudomonas aeruginosa* Exhibits Sliding Motility in the Absence of Type IV Pili and Flagella. *Journal of Bacteriology*, **190**(8), pp. 2700-2708.

NAGAOKA, T., KABURAGI, Y., HAMAGUCHI, Y., HASEGAWA, M., TAKEHARA, K., STEEBER, D.A., TEDDER, T.F. and SATO, S., 2000. Delayed Wound Healing in the Absence of Intercellular Adhesion Molecule-1 or L-Selectin Expression. *The American journal of pathology*, **157**(1), pp. 237-247.

NAIK, S., BOULADOUX, N., LINEHAN, J.L., HAN, S., HARRISON, O.J., WILHELM, C., CONLAN, S., HIMMELFARB, S., BYRD, A.L., DEMING, C., QUINONES, M., BRENCHLEY, J.M., KONG, H.H., TUSSIWAND, R., MURPHY, K.M., MERAD, M., SEGRE, J.A. and BELKAID, Y., 2015. Commensal–dendritic-cell interaction specifies a unique protective skin immune signature. *Nature*, **520**(7545), pp. 104-108.

NAIK, S., BOULADOUX, N., SPENCER, S., HALL, J.A., DZUTSEV, A., HEIDI KONG, CAMPBELL, D.J., TRINCHIERI, G., SEGRE, J.A., BELKAID, Y., WILHELM, C., MOLLOY, M.J., SALCEDO, R., KASTENMULLER, W., DEMING, C., QUINONES, M., KOO, L. and CONLAN, S., 2012. Compartmentalized Control of Skin Immunity by Resident Commensals. *Science (American Association for the Advancement of Science)*, **337**(6098), pp. 1115-1119.



NAKATSUJI, T., CHEN, T.H., BUTCHER, A.M., TRZOSS, L.L., NAM, S., SHIRAKAWA, K.T., ZHOU, W., OH, J., OTTO, M., FENICAL, W. and GALLO, R.L., 2018. A commensal strain of *Staphylococcus epidermidis* protects against skin neoplasia. *Science advances*, **4**(2), pp. eaao4502.

NAKATSUJI, T., CHEN, T.H., NARALA, S., CHUN, K.A., TWO, A.M., YUN, T., SHAFIQ, F., KOTOL, P.F., BOUSLIMANI, A., MELNIK, A.V., LATIF, H., KIM, J., LOCKHART, A., ARTIS, K., DAVID, G., TAYLOR, P., STREIB, J., DORRESTEIN, P.C., GRIER, A., GILL, S.R., ZENGLER, K., HATA, T.R., LEUNG, D.Y.M. and GALLO, R.L., 2017. Antimicrobials from human skin commensal bacteria protect against *Staphylococcus aureus* and are deficient in atopic dermatitis. *Science translational medicine*, **9**(378), pp. eaah4680.

NAMVAR, A.E., BASTARAHANG, S., ABBASI, N., GHEHI, G.S., FARHADBAKHTIARIAN, S., AREZI, P., HOSSEINI, M., BARAVATI, S.Z., JOKAR, Z. and CHERMAHIN, S.G., 2014. Clinical characteristics of *Staphylococcus epidermidis*: a systematic review. *GMS hygiene and infection control*, **9**(3), pp. Doc23.

NATHWANI, D., RAMAN, G., SULHAM, K., GAVAGHAN, M. and MENON, V., 2014. Clinical and economic consequences of hospital-acquired resistant and multidrug-resistant *Pseudomonas aeruginosa* infections: a systematic review and meta-analysis. *Antimicrobial Resistance and Infection Control*, **3**(1), pp. 32.

NESTLE, F.O., DI MEGLIO, P., QIN, J. and NICKOLOFF, B.J., 2009. Skin immune sentinels in health and disease. *Nature Reviews Immunology*, **9**(10), pp. 679-691.

NEGUT, I., GRUMEZESCU, V. and GRUMEZESCU, A.M., 2018. Treatment Strategies for Infected Wounds. *Molecules (Basel, Switzerland)*, **23**(9), pp. 2392.

NGUYEN, A.V. and SOULIKA, A.M., 2019. The Dynamics of the Skin's Immune System. *International journal of molecular sciences*, **20**(8), pp. 1811.

NIEUWLAAT, R., MBUAGBAW, L., MERTZ, D., BURROWS, L.L., BOWDISH, D.M.E., MOJA, L., WRIGHT, G.D. and SCHÜNEMANN, H.J., 2021. Coronavirus Disease 2019 and Antimicrobial Resistance: Parallel and Interacting Health Emergencies. *Clinical infectious diseases*, **72**(9), pp. 1657-1659.

NOUVONG, A., AMBRUS, A.M., ZHANG, E.R., HULTMAN, L. and COLLER, H.A., 2016. Reactive oxygen species and bacterial biofilms in diabetic wound healing. *Physiological Genomics*, **48**(12), pp. 889-896.

O TOOLE, G.A., 2011. Microtiter Dish Biofilm Formation Assay. *Journal of Visualized Experiments*, (47).

OTTO, M., 2009. *Staphylococcus epidermidis* - the 'accidental' pathogen. *Nature reviews. Microbiology*, **7**(8), pp. 555-567.

OH, J., BYRD, A.L., DEMING, C., CONLAN, S., KONG, H.H. and SEGRE, J.A., 2014. Biogeography and individuality shape function in the human skin metagenome. *Nature*, **514**(7520), pp. 59-64.

OH, J., BYRD, A.L., PARK, M., KONG, H.H. and SEGRE, J.A., 2016. Temporal Stability of the Human Skin Microbiome. *Cell*, **165**(4), pp. 854-866.

OLENDER, A., BOGUT, A., MAGRYŚ, A. and TABARKIEWICZ, J., 2019. Cytokine Levels in the In Vitro Response of T Cells to Planktonic and Biofilm *Corynebacterium amycolatum*. *Polish Journal of Microbiology*, **68**(4), pp. 457-464.

OMAR, A., WRIGHT, J.B., SCHULTZ, G., BURRELL, R. and NADWORNY, P., 2017. Microbial Biofilms and Chronic Wounds. *Microorganisms*, **5**(1).

ORAZI, G. and O'TOOLE, G.A., 2017. *Pseudomonas aeruginosa* Alters *Staphylococcus aureus* Sensitivity to Vancomycin in a Biofilm Model of Cystic Fibrosis Infection. *mBio*, **8**(4).

O'TOOLE, G.A. and KOLTER, R., 1998. Flagellar and twitching motility are necessary for *Pseudomonas aeruginosa* biofilm development. *Molecular microbiology*, **30**(2), pp. 295-304.

PAHARIK, A.E., PARLET, C.P., CHUNG, N., TODD, D.A., RODRIGUEZ, E.I., DYKE, M.J.V., CECH, N.B. and HORSWILL, A.R., 2017. Coagulase-Negative Staphylococcal Strain Prevents *Staphylococcus aureus* Colonization and Skin Infection by Blocking Quorum Sensing. *Cell Host & Microbe*, **22**(6), pp. 746-756.e5.

PAIXÃO, L., RODRIGUES, L., COUTO, I., MARTINS, M., FERNANDES, P., DE CARVALHO, C.C.C.R., MONTEIRO, G.A., SANSONETTY, F., AMARAL, L. and VIVEIROS, M., 2009. Fluorometric determination of ethidium bromide efflux kinetics in *Escherichia coli*. *Journal of Biological Engineering*, **3**(1), pp. 18.

PALLET, R., LESLIE, L.J., LAMBERT, P.A., MILIC, I., DEVITT, A. and MARSHALL, L.J., 2019. Anaerobiosis influences virulence properties of *Pseudomonas aeruginosa* cystic fibrosis isolates and the interaction with *Staphylococcus aureus*. *Scientific Reports*, **9**(1), pp. 1-18.

PAMP, S.J. and TOLKER-NIELSEN, T., 2007. Multiple Roles of Biosurfactants in Structural Biofilm Development by *Pseudomonas aeruginosa*. *Journal of Bacteriology*, **189**(6), pp. 2531-2539.

PANG, Z., RAUDONIS, R., GLICK, B.R., LIN, T. and CHENG, Z., 2019. Antibiotic resistance in *Pseudomonas aeruginosa*: mechanisms and alternative therapeutic strategies. *Biotechnology advances*, **37**(1), pp. 177-192.

PARMELY, M., GALE, A., CLABAUGH, M., HORVAT, R. and ZHOU, W.-., 1990. Proteolytic inactivation of cytokines by *Pseudomonas aeruginosa*. *Infection and Immunity*, **58**(9), pp. 3009-3014.

PASSOS DA SILVA, D., MATWICHUK, M.L., TOWNSEND, D.O., REICHHARDT, C., LAMBA, D., WOZNIAK, D.J. and PARSEK, M.R., 2019. The *Pseudomonas aeruginosa* lectin LecB binds to the exopolysaccharide Psl and stabilizes the biofilm matrix. *Nature Communications*, **10**(1), pp. 2183.

PASTAR, I., STOJADINOVIC, O., YIN, N.C., RAMIREZ, H., NUSBAUM, A.G., SAWAYA, A., PATEL, S.B., KHALID, L., ISSEROFF, R.R. and TOMIC-CANIC, M., 2014. Epithelialization in Wound Healing: A Comprehensive Review. *Advances in Wound Care*, **3**(7), pp. 445-464.

PATRA, V., WAGNER, K., ARULAMPALAM, V. and WOLF, P., 2019. Skin Microbiome Modulates the Effect of Ultraviolet Radiation on Cellular Response and Immune Function. *iScience*, **15**, pp. 211-222.

PATRIQUIN, G.M., BANIN, E., GILMOUR, C., TUCHMAN, R., GREENBERG, E.P. and POOLE, K., 2008. Influence of quorum sensing and iron on twitching motility and biofilm formation in *Pseudomonas aeruginosa*. *Journal of Bacteriology*, **190**(2), pp. 662-671.

PESCI, E.C., PEARSON, J.P., SEED, P.C. and IGLEWSKI, B.H., 1997. Regulation of las and rhl quorum sensing in *Pseudomonas aeruginosa*. *Journal of Bacteriology*, **179**(10), pp. 3127-3132.

PETERSON, J., GARGES, S., GIOVANNI, M., MCINNES, P., WANG, L., SCHLOSS, J.A., BONAZZI, V., MCEWEN, J.E., WETTERSTRAND, K.A., DEAL, C., BAKER, C.C., DI FRANCESCO, V., HOWCROFT, T.K., KARP, R.W., LUNSFORD, R.D., WELLINGTON, C.R., BELACHEW, T., WRIGHT, M., GIBLIN, C., DAVID, H., MILLS, M., SALOMON, R., MULLINS, C., AKOLKAR, B., BEGG, L., DAVIS, C., GRANDISON, L., HUMBLE, M., KHALSA, J., LITTLE, A.R., PEAVY, H., PONTZER, C., PORTNOY, M., SAYRE, M.H., STARKE-REED, P., ZAKHARI, S., READ, J., WATSON, B. and GUYER, M., 2009. The NIH Human Microbiome Project. *Genome Research*, **19**(12), pp. 2317-2323.

PIIPPONEN, M., LI, D. and LANDÉN, N.X., 2020. The Immune Functions of Keratinocytes in Skin Wound Healing. *International journal of molecular sciences*, **21**(22), pp. 8790.

POOLE, K., 2005. Aminoglycoside resistance in *Pseudomonas aeruginosa*. *Antimicrobial agents and chemotherapy*, **49**(2), pp. 479-487.

PRICE, L.B., LIU, C.M., FRANKEL, Y.M., MELENDEZ, J.H., AZIZ, M., BUCHHAGEN, J., CONTENTE-CUOMO, T., ENGELHALER, D.M., KEIM, P.S., RAVEL, J., LAZARUS, G.S. and ZENILMAN, J.M., 2011. Macroscale spatial variation in chronic wound microbiota: a cross-sectional study. *Wound Repair and Regeneration: Official Publication of the Wound Healing Society [and] the European Tissue Repair Society*, **19**(1), pp. 80-88.

- PRINCE, T., MCBAIN, A.J. and O'NEILL, C.A., 2012. Lactobacillus reuteri Protects Epidermal Keratinocytes from *Staphylococcus aureus*-Induced Cell Death by Competitive Exclusion. *Applied and Environmental Microbiology*, **78**(15), pp. 5119-5126.
- PROCTOR, R.A., VON EIFF, C., KAHL, B.C., BECKER, K., MCNAMARA, P., HERRMANN, M. and PETERS, G., 2006. Small colony variants: a pathogenic form of bacteria that facilitates persistent and recurrent infections. *Nature reviews. Microbiology*, **4**(4), pp. 295-305.
- PROKSCH, E., BRANDNER, J.M. and JENSEN, J., 2008. The skin: an indispensable barrier. *Experimental Dermatology*, **17**(12), pp. 1063-1072.
- QIN, S., XIAO, W., ZHOU, C., PU, Q., DENG, X., LAN, L., LIANG, H., SONG, X. and WU, M., 2022. *Pseudomonas aeruginosa*: pathogenesis, virulence factors, antibiotic resistance, interaction with host, technology advances and emerging therapeutics. *Signal transduction and targeted therapy*, **7**(1), pp. 199.
- RASHID, M.H. and KORNBERG, A., 2000. Inorganic polyphosphate is needed for swimming, swarming, and twitching motilities of *Pseudomonas aeruginosa*. *Proceedings of the National Academy of Sciences - PNAS*, **97**(9), pp. 4885-4890.
- REICHHARDT, C., JACOBS, H.M., MATWICHUK, M., WONG, C., WOZNIAK, D.J. and PARSEK, M.R., 2020. The Versatile *Pseudomonas aeruginosa* Biofilm Matrix Protein CdrA Promotes Aggregation through Different Extracellular Exopolysaccharide Interactions. *Journal of bacteriology*, **202**(19).
- RENNEKAMPFF, H.-., HANSBROUGH, J.F., WOODS, V.J., DORE, C., KIESSIG, V. and SCHRÖDER, J.-., 1997. Role of melanoma growth stimulatory activity (MGSA/gro) on keratinocyte function in wound healing. *Archives of Dermatological Research*, **289**(4), pp. 204-212.
- RIDIANDRIES, A., TAN, J.T.M. and BURSILL, C.A., 2018. The Role of Chemokines in Wound Healing. *International Journal of Molecular Sciences*, **19**(10), pp. 3217.
- RODRIGUES, M., KOSARIC, N., BONHAM, C.A. and GURTNER, G.C., 2019. Wound Healing: A Cellular Perspective. *Physiological reviews*, **99**(1), pp. 665-706.
- ROHDE, H., FRANKENBERGER, S., ZÄHRINGER, U. and MACK, D., 2010. Structure, function and contribution of polysaccharide intercellular adhesin (PIA) to *Staphylococcus epidermidis* biofilm formation and pathogenesis of biomaterial-associated infections. *European journal of cell biology*, **89**(1), pp. 103-111.
- RUFF, W.E., GREILING, T.M. and KRIEGEL, M.A., 2020. Host–microbiota interactions in immune-mediated diseases. *Nature reviews. Microbiology*, **18**(9), pp. 521-538.

RUFFIN, M. and BROCHIERO, E., 2019. Repair Process Impairment by *Pseudomonas aeruginosa* in Epithelial Tissues: Major Features and Potential Therapeutic Avenues. *Frontiers in Cellular and Infection Microbiology*, **9**, pp. 182.

RUTHERFORD, S.T. and BASSLER, B.L., 2012. Bacterial Quorum Sensing: Its Role in Virulence and Possibilities for Its Control. *Cold Spring Harbor Perspectives in Medicine*, **2**(11),.

RYDER, C., BYRD, M. and WOZNIAK, D.J., 2007. Role of polysaccharides in *Pseudomonas aeruginosa* biofilm development. *Current opinion in microbiology*, **10**(6), pp. 644-648.

SABATÉ BRESCÓ, M., HARRIS, L.G., THOMPSON, K., STANIC, B., MORGENSTERN, M., O'MAHONY, L., RICHARDS, R.G. and MORIARTY, T.F., 2017. Pathogenic Mechanisms and Host Interactions in *Staphylococcus epidermidis* Device-Related Infection. *Frontiers in Microbiology*, **8**, pp. 1401.

SACHDEVA, C., SATYAMOORTHY, K. and MURALI, T.S., 2022. Microbial Interplay in Skin and Chronic Wounds. *Current clinical microbiology reports*, **9**(3), pp. 21-31.

SADIKOT, R.T., BLACKWELL, T.S., CHRISTMAN, J.W. and PRINCE, A.S., 2005. Pathogen-Host Interactions in *Pseudomonas aeruginosa* Pneumonia. *American journal of respiratory and critical care medicine*, **171**(11), pp. 1209-1223.

SAINT-CRIQ, V., VILLERET, B., BASTAERT, F., KHEIR, S., HATTON, A., CAZES, A., XING, Z., SERMET-GAUDELUS, I., GARCIA-VERDUGO, I., EDELMAN, A. and SALLENAVE, J., 2018. *Pseudomonas aeruginosa* LasB protease impairs innate immunity in mice and humans by targeting a lung epithelial cystic fibrosis transmembrane regulator–IL-6–antimicrobial–repair pathway. *Thorax*, **73**(1), pp. 49-61.

SANDOVAL-MOTTA, S. and ALDANA, M., 2016. Adaptive resistance to antibiotics in bacteria: a systems biology perspective. *Wiley interdisciplinary reviews. Systems biology and medicine*, **8**(3), pp. 253-267.

SANMIGUEL, A. and GRICE, E.A., 2015. Interactions between host factors and the skin microbiome. *Cellular and molecular life sciences : CMLS*, **72**(8), pp. 1499-1515.

SANTAJIT, S., SEESUAY, W., MAHASONGKRAM, K., SOOKRUNG, N., AMPAWONG, S., REAMTONG, O., DIRAPHAT, P., CHAICUMPA, W. and INDRAWATTANA, N., 2019. Human single-chain antibodies that neutralize *Pseudomonas aeruginosa*-exotoxin A-mediated cellular apoptosis. *Scientific Reports*, **9**(1), pp. 14928-15.

SASS, G., NAZIK, H., PENNER, J., SHAH, H., ANSARI, S.R., CLEMONS, K.V., GROLEAU, M., DIETL, A., VISCA, P., HAAS, H., DÉZIEL, E. and STEVENS, D.A., 2018. Studies of *Pseudomonas aeruginosa* mutants indicate pyoverdine as the central factor in inhibition of *Aspergillus fumigatus* biofilm. *Journal of bacteriology*, **200**(1), pp. 345.

SCALISE, A., BIANCHI, A., TARTAGLIONE, C., BOLLETTA, E., PIERANGELI, M., TORRESETTI, M., MARAZZI, M. and DI BENEDETTO, G., 2015. Microenvironment and microbiology of skin wounds: the role of bacterial biofilms and related factors. *Seminars in Vascular Surgery*, **28**(3), pp. 151-159.

SCHAUBER, J. and GALLO, R.L., 2008. Antimicrobial peptides and the skin immune defense system. *The Journal of allergy and clinical immunology*, **122**(2), pp. 261-266.

SCHAUBER, J. and GALLO, R.L., 2007. Expanding the Roles of Antimicrobial Peptides in Skin: Alarming and Arming Keratinocytes. *Journal of Investigative Dermatology*, **127**(3), pp. 510-512.

SCHUSTER, M., LOSTROH, C.P., OGI, T. and GREENBERG, E.P., 2003. Identification, Timing, and Signal Specificity of *Pseudomonas aeruginosa* Quorum-Controlled Genes: a Transcriptome Analysis. *Journal of Bacteriology*, **185**(7), pp. 2066-2079.

SCHUSTER, M. and PETER GREENBERG, E., 2006. A network of networks: Quorum-sensing gene regulation in *Pseudomonas aeruginosa*. *International journal of medical microbiology*, **296**(2), pp. 73-81.

SECOR, P.R., JAMES, G.A., FLECKMAN, P., OLERUD, J.E., MCINNERNEY, K. and STEWART, P.S., 2011. *Staphylococcus aureus* Biofilm and Planktonic cultures differentially impact gene expression, mapk phosphorylation, and cytokine production in human keratinocytes. *BMC Microbiology*, **11**, pp. 143.

SEVERN, M.M. and HORSWILL, A.R., 2022. *Staphylococcus epidermidis* and its dual lifestyle in skin health and infection. *Nature reviews. Microbiology*.

SHERRY L. KUCHMA, ALBERT SIRYAPORN, GEORGE A. O'TOOLE, ZEMER GITAI and FREDERICK M. AUSUBEL, 2014. Surface attachment induces *Pseudomonas aeruginosa* virulence. *Proceedings of the National Academy of Sciences - PNAS*, **111**(47), pp. 16860-16865.

SEN, C.K., 2021. Human Wound and Its Burden: Updated 2020 Compendium of Estimates. *Advances in wound care (New Rochelle, N.Y.)*, **10**(5), pp. 281-292.

SEN, C.K., ROY, S., MATHEW-STEINER, S.S. and GORDILLO, G.M., 2021. Biofilm Management in Wound Care. *Plastic and reconstructive surgery (1963)*, **148**(2), pp. 275-288e.

SIDDIQUI, A.R. and BERNSTEIN, J.M., 2010. Chronic wound infection: Facts and controversies. *Clinics in Dermatology*, **28**(5), pp. 519-526.

SIMPSON, C.L., PATEL, D.M. and GREEN, K.J., 2011. Deconstructing the skin: cytoarchitectural determinants of epidermal morphogenesis. *Nature Reviews Molecular Cell Biology*, **12**(9), pp. 565-580.

SOBERÓN-CHÁVEZ, G., GONZÁLEZ-VALDEZ, A., SOTO-ACEVES, M.P. and COCOTL-YAÑEZ, M., 2021. Rhamnolipids produced by *Pseudomonas*: from molecular genetics to the market. *Microbial Biotechnology*, **14**(1), pp. 136-146.

SORG, H., TILKORN, D.J., HAGER, S., HAUSER, J. and MIRASTSCHISKI, U., 2017. Skin Wound Healing: An Update on the Current Knowledge and Concepts. *European Surgical Research*, **58**(1-2), pp. 81-94.

STACY, A. and BELKAID, Y., 2019. Microbial guardians of skin health. *Science (American Association for the Advancement of Science)*, **363**(6424), pp. 227-228.

STONER, S.N., BATY, J.J. and SCOFFIELD, J.A., 2022. *Pseudomonas aeruginosa* polysaccharide Psl supports airway microbial community development. *The ISME Journal*, **16**(7), pp. 1730-1739.

STREMPEL, N., NEIDIG, A., NUSSER, M., GEFFERS, R., VIEILLARD, J., LESOUHAITIER, O., BRENNER-WEISS, G. and OVERHAGE, J., 2013. Human Host Defense Peptide LL-37 Stimulates Virulence Factor Production and Adaptive Resistance in *Pseudomonas aeruginosa*. *PLOS ONE*, **8**(12), pp. e82240.

STROBER, W., 2001. Trypan blue exclusion test of cell viability. *Current protocols in immunology*, **Appendix 3**, pp. Appendix 3B.

SUGAWARA, E., NESTOROVICH, E.M., BEZRUKOV, S.M. and NIKAIDO, H., 2006. *Pseudomonas aeruginosa* Porin OprF Exists in Two Different Conformations. *The Journal of biological chemistry*, **281**(24), pp. 16220-16229.

SUGIMOTO, S., IWAMOTO, T., TAKADA, K., OKUDA, K., TAJIMA, A., IWASE, T. and MIZUNOE, Y., 2013. *Staphylococcus epidermidis* Esp Degrades Specific Proteins Associated with *Staphylococcus aureus* Biofilm Formation and Host-Pathogen Interaction. *Journal of Bacteriology*, **195**(8), pp. 1645-1655.

SUN, E., LIU, S. and HANCOCK, R.E.W., 2018. Surfing Motility: a Conserved yet Diverse Adaptation among Motile Bacteria. *Journal of bacteriology*, **200**(23).

SUN, Y., SMITH, E., WOLCOTT, R. and DOWD, S.E., 2013. Propagation of anaerobic bacteria within an aerobic multi-species chronic wound biofilm model. *Journal of Wound Care*, **18**(10), pp. 426-431.

TANKERSLEY, A., FRANK, M.B., BEBAK, M. and BRENNAN, R., 2014. Early effects of *Staphylococcus aureus* biofilm secreted products on inflammatory responses of human epithelial keratinocytes. *Journal of inflammation (London, England)*, **11**(1), pp. 17.

TANNE, J.H., 2022. Covid-19: Antimicrobial resistance rose dangerously in US during pandemic, CDC says. *BMJ (Online)*, **378**, pp. o1755.

TAYLOR, L., 2021. Covid-19: Antimicrobial misuse in Americas sees drug resistant infections surge, says WHO. *BMJ (Online)*, **375**, pp. n2845.

TENOVER, F.C., 2006. Mechanisms of Antimicrobial Resistance in Bacteria. *The American journal of medicine*, **119**(6), pp. S3-S10.

THI, M.T.T., WIBOWO, D. and REHM, B.H.A., 2020. Pseudomonas aeruginosa Biofilms. *International journal of molecular sciences*, **21**(22), pp. 8671.

THOM, S.M., HOROBIN, R.W., SEIDLER, E. and BARER, M.R., 1993. Factors affecting the selection and use of tetrazolium salts as cytochemical indicators of microbial viability and activity. *Journal of Applied Bacteriology*, **74**(4), pp. 433-443.

THURLOW, L.R., HANKE, M.L., FRITZ, T., ANGLE, A., ALDRICH, A., WILLIAMS, S.H., ENGBRETSSEN, I.L., BAYLES, K.W., HORSWILL, A.R. and KIELIAN, T., 2011. *Staphylococcus aureus* biofilms prevent macrophage phagocytosis and attenuate inflammation in vivo. *Journal of immunology (Baltimore, Md. : 1950)*, **186**(11), pp. 6585-6596.

TIELKER, D., HACKER, S., LORIS, R., STRATHMANN, M., WINGENDER, J., WILHELM, S., ROSENAU, F. and JAEGER, K., 2005. *Pseudomonas aeruginosa* lectin LecB is located in the outer membrane and is involved in biofilm formation. *Microbiology (Society for General Microbiology)*, **151**(5), pp. 1313-1323.

TOGNON, M., KÖHLER, T., LUSCHER, A. and VAN DELDEN, C., 2019. Transcriptional profiling of *Pseudomonas aeruginosa* and *Staphylococcus aureus* during in vitro co-culture. *BMC genomics*, **20**(1), pp. 30.

TOMASEK, J.J., GABBIANI, G., HINZ, B., CHAPONNIER, C. and BROWN, R.A., 2002. Myofibroblasts and mechano-regulation of connective tissue remodelling. *Nature Reviews Molecular Cell Biology*, **3**(5), pp. 349-363.

TRIZNA, E.Y., YARULLINA, M.N., BAIDAMSHINA, D.R., MIRONOVA, A.V., AKHATOVA, F.S., ROZHINA, E.V., FAKHRULLIN, R.F., KHABIBRAKHMANOVA, A.M., KURBANGALIEVA, A.R., BOGACHEV, M.I. and KAYUMOV, A.R., 2020. Bidirectional alterations in antibiotics susceptibility in *Staphylococcus aureus*—*Pseudomonas aeruginosa* dual-species biofilm. *Scientific reports*, **10**(1), pp. 14849.

TURNBAUGH, P.J., LEY, R.E., HAMADY, M., FRASER-LIGGETT, C.M., KNIGHT, R. and GORDON, J.I., 2007. The human microbiome project. *Nature*, **449**(7164), pp. 804-810.

URIBE-ALVAREZ, C., CHIQUETE-FÉLIX, N., CONTRERAS-ZENTELLA, M., GUERRERO CASTILLO, S., PEÑA, A. and URIBE-CARVAJAL, S., 2016. *Staphylococcus epidermidis*: metabolic adaptation and biofilm formation in response to different oxygen concentrations. *Pathogens and disease*, **74**(1), pp. ftv111.



VALENTIN, J.D.P., STRAUB, H., PIETSCH, F., LEMARE, M., AHRENS, C.H., SCHREIBER, F., WEBB, J.S., VAN DER MEI, H.C. and REN, Q., 2022. Role of the flagellar hook in the structural development and antibiotic tolerance of *Pseudomonas aeruginosa* biofilms. *The ISME Journal*, **16**(4), pp. 1176-1186.

VANDEPLASSCHE, E., SASS, A., LEMARCQ, A., DANDEKAR, A.A., COENYE, T. and CRABBÉ, A., 2019. In vitro evolution of *Pseudomonas aeruginosa* AA2 biofilms in the presence of cystic fibrosis lung microbiome members. *Scientific Reports*, **9**(1), pp. 1-14.

VERBANIC, S., SHEN, Y., LEE, J., DEACON, J.M. and CHEN, I.A., 2020. Microbial predictors of healing and short-term effect of debridement on the microbiome of chronic wounds. *npj Biofilms and Microbiomes*, **6**(1), pp. 1-11.

VOGGU, L., SCHLAG, S., BISWAS, R., ROSENSTEIN, R., RAUSCH, C. and GÖTZ, F., 2006. Microevolution of Cytochrome bd Oxidase in Staphylococci and Its Implication in Resistance to Respiratory Toxins Released by *Pseudomonas*. *Journal of bacteriology*, **188**(23), pp. 8079-8086.

VUONG, C., VOYICH, J.M., FISCHER, E.R., BRAUGHTON, K.R., WHITNEY, A.R., DELEO, F.R. and OTTO, M., 2004. Polysaccharide intercellular adhesin (PIA) protects *Staphylococcus epidermidis* against major components of the human innate immune system. *Cellular microbiology*, **6**(3), pp. 269-275.

WANG, J., WANG, C., YU, H., DELA AHATOR, S., WU, X., LV, S. and ZHANG, L., 2019. Bacterial quorum-sensing signal IQS induces host cell apoptosis by targeting POT1–p53 signalling pathway. *Cellular microbiology*, **21**(10), pp. e13076-n/a.

WANKE, I., STEFFEN, H., CHRIST, C., KRISMER, B., GÖTZ, F., PESCHEL, A., SCHALLER, M. and SCHITTEK, B., 2011. Skin Commensals Amplify the Innate Immune Response to Pathogens by Activation of Distinct Signaling Pathways. *Journal of Investigative Dermatology*, **131**(2), pp. 382-390.

WEBBER, M.A. and PIDDOCK, L.J.V., 2003. The importance of efflux pumps in bacterial antibiotic resistance. *Journal of antimicrobial chemotherapy*, **51**(1), pp. 9-11.

WERNER, S. and GROSE, R., 2003. Regulation of Wound Healing by Growth Factors and Cytokines. *Physiological Reviews*, **83**(3), pp. 835-870.

WERTHÉN, M., HENRIKSSON, L., JENSEN, P.Ø, STERNBERG, C., GIVSKOV, M. and BJARNSHOLT, T., 2010. An in vitro model of bacterial infections in wounds and other soft tissues. *APMIS: acta pathologica, microbiologica, et immunologica Scandinavica*, **118**(2), pp. 156-164.

WHITCHURCH, C.B., TOLKER-NIELSEN, T., RAGAS, P.C. and MATTICK, J.S., 2002. Extracellular DNA Required for Bacterial Biofilm Formation. *Science (American Association for the Advancement of Science)*, **295**(5559), pp. 1487.

WILDER, C.N., DIGGLE, S.P. and SCHUSTER, M., 2011. Cooperation and cheating in *Pseudomonas aeruginosa*: the roles of the las, rhl and pqs quorum-sensing systems. *The ISME Journal*, **5**(8), pp. 1332-1343.

WILGUS, T.A., ROY, S. and MCDANIEL, J.C., 2013. Neutrophils and Wound Repair: Positive Actions and Negative Reactions. *Advances in Wound Care*, **2**(7), pp. 379-388.

WILLIAMS, I.R. and KUPPER, T.S., 1996. Immunity at the surface: homeostatic mechanisms of the skin immune system. *Life Sciences*, **58**(18), pp. 1485-1507.

WILLIAMS, M.R., COSTA, S.K., ZAMELA, L.S., KHALIL, S., TODD, D.A., WINTER, H.L., SANFORD, J.A., O'NEILL, A.M., LIGGINS, M.C., NAKATSUJI, T., CECH, N.B., CHEUNG, A.L., ZENGLER, K., HORSWILL, A.R. and GALLO, R.L., 2019. Quorum sensing between bacterial species on the skin protects against epidermal injury in atopic dermatitis. *Science translational medicine*, **11**(490), pp. eaat8329.

WOLCOTT, R., COSTERTON, J.W., RAOULT, D. and CUTLER, S.J., 2013. The polymicrobial nature of biofilm infection. *Clinical Microbiology and Infection*, **19**(2), pp. 107-112.

WOLCOTT, R.D., HANSON, J.D., REES, E.J., KOENIG, L.D., PHILLIPS, C.D., WOLCOTT, R.A., COX, S.B. and WHITE, J.S., 2016. Analysis of the chronic wound microbiota of 2,963 patients by 16S rDNA pyrosequencing. *Wound Repair and Regeneration*, **24**(1), pp. 163-174.

WRIGHT, G.D., 2005. Bacterial resistance to antibiotics: Enzymatic degradation and modification. *Advanced drug delivery reviews*, **57**(10), pp. 1451-1470.

WU, Y., CHENG, N. and CHENG, C., 2019. Biofilms in Chronic Wounds: Pathogenesis and Diagnosis. *Trends in Biotechnology*, **37**(5), pp. 505-517.

XIA, X., LI, Z., LIU, K., WU, Y., JIANG, D. and LAI, Y., 2016. Staphylococcal LTA-Induced miR-143 Inhibits *Propionibacterium acnes*-Mediated Inflammatory Response in Skin. *Journal of Investigative Dermatology*, **136**(3), pp. 621-630.

XIAO, T., YAN, Z., XIAO, S. and XIA, Y., 2020. Proinflammatory cytokines regulate epidermal stem cells in wound epithelialization. *Stem cell research & therapy*, **11**(1), pp. 1-232.

XU, H. and LI, H., 2019. Acne, the Skin Microbiome, and Antibiotic Treatment. *American Journal of Clinical Dermatology*, **20**(3), pp. 335-344.

YANEZ, D.A., LACHER, R.K., VIDYARTHI, A. and COLEGIO, O.R., 2017. The Role of Macrophages in Skin Homeostasis. *Pflugers Archiv: European journal of physiology*, **469**(3-4), pp. 455-463.

YANG, Y., QU, L., MIJAKOVIC, I. and WEI, Y., 2022. Advances in the human skin microbiota and its roles in cutaneous diseases. *Microbial cell factories*, **21**(1), pp. 1-176.

YOUNG, V.B., 2017. The role of the microbiome in human health and disease: an introduction for clinicians. *BMJ*, **356**, pp. j831.

ZHANG, Y., REN, S., LI, H., WANG, Y., FU, G., YANG, J., QIN, Z., MIAO, Y., WANG, W., CHEN, R., SHEN, Y., CHEN, Z., YUAN, Z., ZHAO, G., QU, D., DANCHIN, A. and WEN, Y., 2003. Genome-based analysis of virulence genes in a non-biofilm-forming *Staphylococcus epidermidis* strain (ATCC 12228). *Molecular microbiology*, **49**(6), pp. 1577-1593.

ZHENG, Y., HUNT, R.L., VILLARUZ, A.E., FISHER, E.L., LIU, R., LIU, Q., CHEUNG, G.Y.C., LI, M. and OTTO, M., 2022. Commensal *Staphylococcus epidermidis* contributes to skin barrier homeostasis by generating protective ceramides. *Cell host & microbe*, **30**(3), pp. 301-313.e9.

ZULFAKAR, S.S., WHITE, J.D., ROSS, T. and TAMPLIN, M.L., 2012. Bacterial attachment to immobilized extracellular matrix proteins in vitro. *International Journal of Food Microbiology*, **157**(2), pp. 210-217.

ZULIANELLO, L., CANARD, C., KÖHLER, T., CAILLE, D., LACROIX, J. and MEDA, P., 2006. Rhamnolipids Are Virulence Factors That Promote Early Infiltration of Primary Human Airway Epithelia by *Pseudomonas aeruginosa*. *Infection and Immunity*, **74**(6), pp. 3134-3147.